Prostate Cancer Exosomes Differentiate BM-MSCs into Pro-Angiogenic and Pro-Invasive Myofibroblasts

Thesis presented for the degree of Philosophiae Doctor

Ridwana Chowdhury

Institute of Cancer and Genetics

School of Medicine

Cardiff University

2015

Declaration

This work has not been submitted in substance for any other degree or award at this or any other university or place of learning, nor is being submitted concurrently in candidature for any degree or other award.

Signed …… (candidate) Date ……..

STATEMENT 1

This thesis is being submitted in partial fulfilment of the requirements for the degree of PhD

Signed …… (candidate) Date ……

STATEMENT 2

This thesis is the result of my own independent work/investigation, except where otherwise stated.

Other sources are acknowledged by explicit references. The views expressed are my own.

Signed …… (candidate) Date ……

STATEMENT 3

I hereby give consent for my thesis, if accepted, to be available online in the University's Open Access repository and for inter-library loan, and for the title and summary to be made available to outside organisations.

Signed …… (candidate) Date ……

STATEMENT 4: PREVIOUSLY APPROVED BAR ON ACCESS

I hereby give consent for my thesis, if accepted, to be available online in the University's Open Access repository and for inter-library loans **after expiry of a bar on access previously approved by the Academic Standards & Quality Committee.**

Signed …… (candidate) Date ……

Dedication

This thesis is dedicated to my parents whose constant support, guidance and inspiration gave me the strength to succeed.

Acknowledgement

First and foremost, I offer my sincerest gratitude to my supervisor Dr Aled Clayton, for the patient guidance, encouragement and advice he has provided throughout my time as his student. I have been extremely lucky to have a supervisor who cared so much about my work and responded to my questions and queries so promptly.

I would also like to thank my co-supervisor Prof Malcom Masson and all the members of the Cancer Research Wales Laboratories; Dr Zsuzanna Tabi, Dr Lisa Spary, Dr Joanne Welton, Dr Saly Al-Taei and Mr Hossein Navabi, who have given me ample of advice which have contributed to this study. In particular I owe a debt of gratitude to Dr Jason Webber, a valuable mentor who taught me so much, provided many suggestions and assistance in experiments. Completing this work would have been all the more difficult if it were not for the generation of Rab27a knock down cell lines by Dr Jason Webber and Professor Wen Jiang's group at Cardiff University.

In my daily work I have been blessed with a friendly and cheerful group of fellow students and colleagues. The humour from Mark Gurney, Vincent Young, Chi Poo Lei and Alex Cook, as well as the great company from Jessy Evans and Edel Brown which has provided a much needed form of escape from my studies and deserve a huge thanks for helping me keep things in perspective. A special thanks for my great friend Josephine Salimu, as it has been her unwavering support, mentally and physically, throughout which made my PhD endurable.

I would like to thank Cancer Research Wales and the Cardiff University, Institute of Cancer and Genetics, not only for providing funding which allowed me to undertake this research, but also for giving me the opportunity to attend conferences and meet so many interesting people.

Finally, I thank my parents for their unconditional support throughout all my studies. I must also express my gratitude for the encouragement and patience from both my sisters, Rehnuma and Ruhaima and my cousins Sabera and Eima who experienced all of my ups and downs of my research.

Summary

The reactive stroma in prostate cancer is predominantly composed of myofibroblasts, which are thought to be required for tumour progression. Bone-marrow derived mesenchymal stem cells (BM-MSCs) are known to migrate into the tumour and are one of the many potential precursors of myofibroblasts. The factors secreted by cancer cells which may drive myofibroblastic differentiation of MSC, however are poorly understood. The aim of this thesis was to explore for the first time, the impact of TGF-β1 expressing exosomes (nano-sized vesicles) secreted by prostate cancer cells in directing the differentiation of BM-MSCs and subsequently the functions of exosome differentiated BM-MSCs.

Exosomes isolated from prostate cancer cells skewed BM-MSCs away from differentiating into adipocytes, and instead towards alpha-smooth muscle actin (α-SMA) positive myofibroblasts. BM-MSCs treated with exosomes exhibited enhanced secretion of VEGF-A, HGF and had an altered transcript profile with heightened matrix metalloproteinases (MMP-1, -3 and -13).

Impairing the secretion of exosomes by Rab27a knockdown or depleting exosomes from prostate cancer cells culture media by high speed ultracentrifugation, attenuated myofibroblastic differentiation of BM-MSCs, demonstrating exosomes as the key driving factor for this. Furthermore, differentiation of BM-MSCs into myofibroblasts was dependent on exosomally tethered TGF-β1, however BM-MSCs treated with soluble TGF-β1 at the same dose, failed to obtain the same myofibroblastic phenotype.

The exosome-differentiated MSCs enhanced endothelial and cancer cell proliferation and migration, supported endothelial vessel formation and promoted tumour cell invasion into peri-tumoural matrix *in vitro*.

In conclusion, this study reports prostate cancer exosomes expressing TGF-β1, to dominantly modulate the fate of BM-MSCs, generating cells with tumour promoting myofibroblastic traits.

Publications and Presentations

Peer-Reviewed Publications

Webber, JP., Spary, LK., Chowdhury, R., Jiang, WG., Steadman, R., Wymant, J., Jones, AT., Kynaston, H., Mason, MD., Tabi, Z and Clayton, A. 2014. **Differentiation of tumour-promoting stromal myofibroblasts by cancer exosomes.** *Oncogene* Vol.34 (3): pp.290-302

Chowdhury, R., Webber, JP., Gurney, M., Mason, MD., Tabi, Z and Clayton, A. 2015. **Cancer exosomes trigger mesenchymal stem cell differentiation into pro-angiogenic and pro-invasive myofibroblasts.** Oncotarget Vol.6 (2): pp.715-734

Presentations

Presentations to learned societies: International Conferences

Chowdhury, R. Webber, J. Mason, M. Tabi, Z and Clayton, A. **The role of prostate cancer exosomes in mesenchymal stem cell differentiation.** World Stem Cell Summit (WSCS). San Antonio, Texas, USA. Poster Presentation (12/2014)

Chowdhury, R. **Prostate cancer exosomes skew BM-MSC differentiation away from adipocytes and instead towards myofibroblasts.** International Society of Extracellular Vesicles (ISEV) Conference. Rotterdam, Netherlands. Poster Presentation (04/2014)

Chowdhury, R. Webber, J. Mason, M. Tabi, Z and Clayton, A. **Prostate cancer exosomes alter the fate of BM-MSCs differentiation.** International Society for Extracellular Vesicles. Boston, USA. Poster Presentation (04/2013).

Presentations to learned societies: National Conferences

Chowdhury, R. Webber, J. Mason, M. Tabi, Z and Clayton, A. **Prostate cancer exosomes differentiate mesenchymal stem cells into pro-angiogenic myofibroblasts.** UK Extracellular Vesicle Forum (UKEV). Royal Veterinary College, London. Poster presentation; *Best poster prize awarded* (12/2014)

Chowdhury, R. Webber, J. Mason, M. Tabi, Z and Clayton, A. **Prostate cancer exosomes skew MSC differentiation away from adipocytes and towards tumour- promoting myofibroblasts.** Society of Extracellular Vesicles. Royal Veterinary College, London, UK. Poster Presentation (12/2013)

Local Presentations (Cardiff):

Chowdhury, R. Webber, J. Mason, M. Tabi, Z and Clayton, A. **Differentiation of pro-angiogenic and pro-invasive myofibroblasts by prostate cancer exosomes.** Institute of Cancer and Genetics, Cardiff University. Poster Presentation; *Best poster prize awarded* (08/2014)

Chowdhury, R**. Cancer exosomes differentiate BM-MSCs into tumour-promoting myofibroblast-like cells.** Speaking of Science Conference, Cardiff University. Oral Presentation (05/2014)

Chowdhury, R. Webber, J. Mason, M. Tabi, Z and Clayton, A. **Cancer exosomes alter the fate of mesenchymal stem cells.** Stem Cell Conference, Cardiff University, Cardiff. Poster Presentation (01/2014)

Chowdhury, R. **Prostate cancer exosomes skew MSC differentiation away from adipocytes and into myofibroblasts-like cells.** 28th Annual Postgraduate Research Day, Cardiff University. Oral Presentation (11/2013)

Chowdhury, R. **Prostate Cancer Exosomes can differentiate mesenchymal stem cells into tumour supporting cells**. Speaking of Science Conference, Cardiff University. Oral Presentation (05/2013)

Chowdhury, R. Webber, J. Mason, M. Tabi, Z and Clayton, A. **Cancer exosomes differentiate MSCs into α-SMA positive myofibroblast-like cells**. Cancer Research Wales Symposium, SWALEC stadium, Cardiff. Poster Presentation; *Best poster prize awarded* (03/2013)

Chowdhury, R. Webber, J and Clayton, A. **Cancer exosomes can alter the fate of MSCs.** Cancer Research Wales Open Day, Velindre Cancer Centre, Cardiff. Poster Presentation (01/2013)

Chowdhury, R. Webber, J. Mason, M. Tabi, Z and Clayton, A. **Cancer exosomes impair the adipogenic differentiation of BM-MSCs**. 27th Annual Postgraduate Research Day, Cardiff University. Poster Presentation (11/2012)

Chowdhury, R. Webber, J. Mason, M. Tabi, Z and Clayton, A. **Prostate cancer exosomes and the fate of mesenchymal stem cells.** Institute of Cancer and Genetics. Cardiff University. Oral Presentation (10/2012)

Table of Contents

List of figures and tables

Abbreviations

α-SMA	Alpha smooth muscle actin
ANXA1	Annexin-1
ADT	Androgen-deprivation therapy
AGT	Angiotensinogen
ANOVA	Analysis of variance
BCA	Bicinchoninic acid
BCL-2	B cell lymphoma 2
BM-MSCs	Bone- marrow mesenchymal stem cells
BMP	Bone morphogenetic protein
BPH	Benign prostate hyperplasia
BSA	Bovine serum albumin
CCL2	Chemokine ligand-2
CK	Cytokeratin
CM	Cell-conditioned media
D_2O	Deuterium oxide
DAPI	4’,6-diamidino-2-phenylindole
DMEM	Dulbecco’s modified Eagle’s medium
DRE	Digital rectal examination
EBM-2	Endothelial growth basal medium-2
ECM	Extracellular matrix
EEA-1	Early endosome antigen-1
EGF	Epidermal growth factor
ELISA	Enzyme linked Immunosorbent assay
ESCRT	Endosomal sorting complex required for transport
FACS	fluorescence-activated cell sorting
FBS	Fetal bovine serum
FGF	Fibroblast growth factor
GAPDH	Glyceraldehyde 3-phosphate dehydrogenase
GD-2	Ganglioside-2
GVHD	Graft versus host disease

HA	Hyaluronic acid
HBSS	Hanks' balanced salt solution
HGF	Hepatocyte growth factor
HSPG	Heparan sulphate proteoglycan
HUVEC	Human umbilical vein endothelial cell
IBMX	3-isobutyl-1-methylxanthine
IGF-1	Insulin-like growth factor-1
IHC	Immunohistochemistry
IL	Interleukin
INHBE	Inhibin beta E
ISCT	International society of cellular therapy
ITGB8	Integrin beta-8
LAMP	Lysosomal-associated membrane protein
LAP	Latency associated protein
LTBP	Latent TGF-β binding protein
MAPK	Mitogen-activated protein kinase
MI	Myocardial infarction
miRNA	Micro ribonucleic acid
MMP	Matrix metalloproteinase
MUC-1	Mucin-1
MV	Microvesicle
MVB	Multivesicular body
NTA	Nanoparticle tracking analysis
OI	Osteogenesis imperfecta
PBS	Phosphate buffered saline
PCa	Prostate cancer
PDGF	Platelet-derived growth factor
PD-ECGF	Platelet derived endothelial cell growth factor
PGE_2	Prostaglandin E_2
PIN	Prostatic intraepithelial neoplasia
PSA	Prostate specific antigen
PSCA	Prostate specific cancer antigen

qPCR	Quantitative polymerase chain reaction
SDF-1	Stromal derived factor-1
SEM	Standard error of mean
shRNA	Small hairpin ribonucleic acid
siRNA	Small interfering ribonucleic acid
SSEA-4	Stage specific embryonic antigen-4
TEM	Transmission electron microscopy
TGF-β1	Transforming growth factor beta one
TIMP	Tissue inhibitor of metalloproteinase
TRUS	Trans-rectal ultra sound
U/ml	Units per millilitre
uPA	Urokinase-type plasminogen activator
v/v	Volume per volume
VEGF-A	Vascular endothelial growth factor-A
w/v	Weight per volume

Chapter 1: Introduction

1.1 Prostate cancer

1.1.1 Aetiology and risk factors

Prostate cancer (PCa) is now the most common cancer in men in the UK, where more than 41,700 men are diagnosed each year (NICE 2009). The risk factors for developing PCa are not well understood but age and family history have been reported as risk factors. A study carried out over 8 countries including the UK showed that men over 75yrs had higher incidence than men under 50yrs (Hsing *et al.* 2000). Family history is also a risk factor for PCa, in which, hereditary PCa is estimated to account for 5-10% of all cases of PCa. Both meta-analysis studies and cohort-based studies have discovered that patients who have 2 or more relatives with PCa have a 2-3 fold higher risk of developing PCa in comparison to men with no family history (Zeegers *et al.* 2003; Carter *et al.* 1992; Cannon *et al.* 1982; Kiciński *et al.* 2011). Although the reason for this difference in risk is unknown, possible hypotheses have included X-linked or recessive inheritance.

Furthermore, there is a world-wide disparity between ethnicity and the incidence of PCa. The risk of developing PCa was found to be highest among African-Americans, who were 2 or 3 times more likely to develop PCa than Caucasians. In contrast, the lowest risk was found amongst native Japanese and Chinese (Moul *et al.* 1995; Stanford *et al.* 1999). Therefore race may also be a risk factor for PCa development. However this may be biased due to the availability and differences of screening and diagnosis methods among different countries (Altekruse *et al.* 2010; Bunker *et al.* 2002; Ross *et al*. 1998). Nevertheless, the variation of PCa development between the different races may be real and the differences may arise due to both inherited genes and environmental factors. Such environmental factors include diet, where Southeast Asian men typically consume soy products which contain PCa protective agent called phytoestrogen and this may contribute to the low risk of PCa among the Southeast Asian population (Barnes *et al.* 2001: Goetzl *et al.* 2007). Thus along with major risk factors such as age and family history, the world-wide disparity in the incidence rates of PCa, suggests that environmental factors such as dietary agents may also affect the risk of PCa development.

1.1.2 Diagnosis and Treatment

Prostate cancer has similar symptoms to other problems of the prostate, such as prostatitis and benign prostate hyperplasia (BPH) which is a non-cancerous enlargement of the prostate. Therefore, discrimination between these conditions are challenging (Xue *et al.* 2015), and accurate diagnosis is essential, as different treatments are required.

Diagnosis

The methods used for PCa detection is testing for abnormally high levels of prostate specific antigen (PSA) in serum as well as rectal examination and prostatic ultrasonography. PSA is a glycoprotein, specifically secreted by prostate epithelial cells and all men have PSA in their blood, which increases with age (Catalona *et al.* 1991; Oesterling *et al.* 1993). Men under 60yrs of age have PSA level of 3ng/ml which increases to 4ng/ml by age of 60 and a further increase to 5ng/ml for men in their 70's and over (Punglia *et al.* 2003). A result higher than these values but less than 10ng/ml are usually due to benign prostatic hyperplasia (BPH). PSA levels of more than 10ng/ml can also be caused by BPH but are more likely to be caused by PCa (Punglia *et al.* 2003). The PSA test is still a commonly used approach for detecting PCa but is very insensitive as a study revealed around 15% of men with normal PSA level, actually have PCa, whereas 60% of men with abnormally high PSA levels do not have PCa after further investigations (Thompson *et al.* 2004). The PSA test, thus cannot solely diagnose PCa, as it only indicates a problem with the prostate, which may be due to BPH, prostatitis or infections of the prostate (McConnell *et al.* 1994; Selley *et al.*1997; Azab *et al.* 2012).

The digital rectal examination (DRE) involves the back surface of the prostate being felt for an oversized prostate or any hard lumpy area which may suggest PCa. DRE has high specificity, as false negative test results are rare (Hoogendam *et al.* 1999) and so a combinational use of PSA test and DRE increases the overall rate of PCa detection, compared to either test alone (Carroll *et al.* 2001; Catalona *et al.* 1994; Bretton *et al.* 1994). The DRE is however, not very sensitive, as examination can miss early stages of the disease. Hence the diagnosis of PCa is further examined by taking a biopsy using the trans-rectal ultra sound (TRUS) needle biopsy. This procedure involves insertion of an

ultrasound probe containing needle through the rectum and the probe helps guide the needle to the prostate for tissue sample collection. The sample can then be histologically examined. Biopsy is the most accurate way of finding out whether PCa is present in the prostate gland and for classifying the stage of the cancer, if present. Samples from two areas are graded from 1-5, and the number of grades are added to give a Gleason score between 2- 10. A higher score indicates the cancerous tissues is more aggressive and has a worse prognosis than those with lesser scores (Cimitan *et al.* 2015; Szot *et al.* 2014; Heidenreich *et al.* 2008). Since the location of cancer is not known, TRUS examinations have a low sensitivity, because the needle may sample a non-cancerous area, missing the cancerous lesion, resulting in a lot of "false negatives" (Catalona *et al.* 1994). Therefore, "false negatives" should not rule out cancer completely as the samples collected may have been from a non-cancerous region. Even though TRUS is more reliable than a PSA test, TRUS is not recommended as the primary screening test for PCa because of its low sensitivity. Prostatic biopsy is only considered when the PSA levels are high or DRE indicates possible PCa. Overall, the combination of PSA test, rectal examination, with ultrasonography is the better method for diagnosis of PCa than either one test alone.

Current Treatments

The treatment of PCa aims to prevent death and disability whilst minimising intervention-related complications. Treatment for PCa depends on the combination of the PSA level, age and Gleason score and every treatment is considered individually for men with PCa. Furthermore, cancers that are small and retained in the prostate gland (known as localised prostate cancer) may require different treatments to that of cancers that have metastasised to secondary sites (known as advanced prostate cancer) (Kupelian *et al.* 2004). The main treatments include surgery, radiotherapy and hormone therapy.

Men with good health with localised PCa can have it removed by surgery known as radical prostatectomy (Murphy *et al.* 1994; Onik *et al*. 1993). Surgery is restricted to men with good health as there are some risk such as blood loss and infection (Gao *et al*. 2013) which may be detrimental to men with poor health. Another major problem which can

arise post-surgery is impotency and so radical prostatectomy may not be the best approach for treatment of PCa. Low level of PSA can be measured to ensure treatment has been successful. If PSA starts to rise again, the patient may require other treatments such a radiotherapy and hormone therapy.

Radiotherapy is a better option for men who are not fit or well enough for surgery. Radiation can be used to treat localised PCa, but may also be suitable for advanced PCa. Patients can undergo external radiation therapy, which involves exposure of high-energy X-rays directed to the prostate gland from outside the body (Zelefsky *et al.* 2002). This attenuates tumour growth by damaging the cancer cells. Alternatively, patients can be treated using a 3D conformal radiotherapy (3D-CRT). With this procedure, the radiation beam matches the shape of the prostate. This helps prevent damage to the surrounding tissues, thus reducing the side effects (Zelefsky *et al.* 1998). A newer and better approach is the intensity modulated radiotherapy (IMRT), where the beam of radiation matches the size, shape and position of the prostate. Intensity of the radiation beam can also be controlled so that the region of the prostate where cancer cells are accumulated will get a higher dose in comparison to the outer regions where cancer cells are lower. Additionally, the risk of side effects, such as bowel, urinary and erection problems are usually lower with IMRT than 3D-CRT (Zelefsky *et al.* 2002). Another option is the internal radiation therapy, also known as brachytherapy (Langley and Liang 2004), which involves implantation of radioactive seeds into the tumour in the prostate gland or at secondary sites. The radiation from the seeds kills the tumour cells (Peinemann *et al.* 2011; Langley and Liang 2004), however the side effects are similar to others, such as urinary, bowel and erectile complication (Chen *et al.* 2006). Lastly, palliative radiotherapy is suitable for advanced PCa, as a large area of the body is treated with radiation in one go and can also provide some relief from bone pain for example.

Testosterone is an androgen hormone with multiple functions, one of which is the requirement for the development and function of the male reproductive system. In aggressive cancer, testosterone accelerates tumour growth (Xiao *et al.* 2003). Therefore orchiectomy was a popular surgical option to remove the testicles where testosterone is mainly released from. Orchiectomy reduces testosterone level by 90-95%, whilst the

rest was produced by the adrenal glands. Alternatively, androgen derived therapy using anti-androgen agents can be used instead to keep testosterone levels low (Shore *et al.* 2013). Androgen-deprivation therapy (ADT) along with the surgery was shown to obtain maximal androgen blockage resulting in a greater survival, in comparison to patients who underwent surgery but had no hormone therapy, over 5 years of assessment in randomised trials (Schmitt *et al.* 2000). Additionally the requirement of any further treatment declined at 5yrs, thus combinational treatment with hormone therapy and surgery are beneficial (Schmitt *et al.* 2000). However ADT can increase adverse effects such as stroke (Azoulay *et al.* 2011) and reduction in cognitive function (Nelson *et al.* 2008; Jamadar *et al.* 2012) and so must be taken with consideration. ADT is very effective in tumour regression, however such treatment results in the recurrence of highly aggressive and metastatic PCa that is androgen independent, making it more difficult to treat (Menon and Walsh 1979; Isaacs and Coffey 1981).

PCa patients may undergo chemotherapy which utilises drugs like mitoxantrone, cabazitaxel and docetaxel, to reduce the tumour size and halt tumour progression (Bahl *et al.* 2013; Collins *et al.* 2006; Serpa Neto *et al.* 2011). However it is not the primary line of treatment for patients at early stage. It is offered to patients with advanced or metastatic PCa patients who are not responding to hormone therapy (Doyle-Lindrud *et al.* 2012; Colloca *et al.* 2010). This is because there are serious side effects, such as bleeding, bowel problems and infection, and so it is recommended that the patient is healthy and fit for consideration of chemotherapy (Tipton *et al.* 2007; Husson *et al.* 2011). Despite the advances in diagnosis and treatment, the majority of patients with metastatic disease are incurable. Therefore, it remains important to understand the cellular biology and molecular mechanisms involved in tumour growth and metastasis, which may allow us to identify new targets to prevent disease progression.

1.2 Cancer Associated Stroma

The prostate is composed of two compartments, an epithelial compartment which includes the secretory exocrine glands and the surrounding connective tissue stroma. Interactions between the stroma and epithelium are required for the normal development and function of the prostate (Sun *et al.* 2009). However the interaction has also been reported to play a crucial role in the development and progression of tumours and tumour metastasis (Orimo *et al.* 2005; Giannoni *et al.* 2010). Most therapeutics, however are targeted towards the cancer cells, but the stroma is also an important player in tumour progression and so targeting the stroma may be an effective therapeutic approach for treating cancer.

1.2.1 The reactive stroma

The stroma of the prostate is heterogeneous and consists of endothelial cells, fibroblasts, immune cells, nerve cells, smooth muscle cells and mesenchymal stem cells. The smooth muscle cells are the major stromal cell type in the normal prostate (Grossfeld *et al.* 1998). However, in prostate carcinoma, the neoplastic cells are surrounded by an altered stromal tissue, called the “desmoplastic reactive” tissue, but are also referred to as the reactive stroma. This reactive stroma is altered in comparison to the normal stroma, in which the interstitial smooth muscle cells are displaced by α-smooth muscle actin and vimentin positive myofibroblasts (Tuxhorn *et al.* 2002) as shown in figure 1.1. Prostatic intraepithelial neoplasia (PIN) is considered as a precursor of PCa, because the frequency and incidence of PIN was found to be greater in men with PCa than without (Sakr *et al.* 1994; Sakr *et al.* 1999). However, similar observations by pre-neoplastic myofibroblasts are also seen in PIN. Therefore stromal changes are not secondary to tumour development, rather it can occur hand in hand with epithelial changes in PCa.

Stromal changes from healthy to diseased stroma

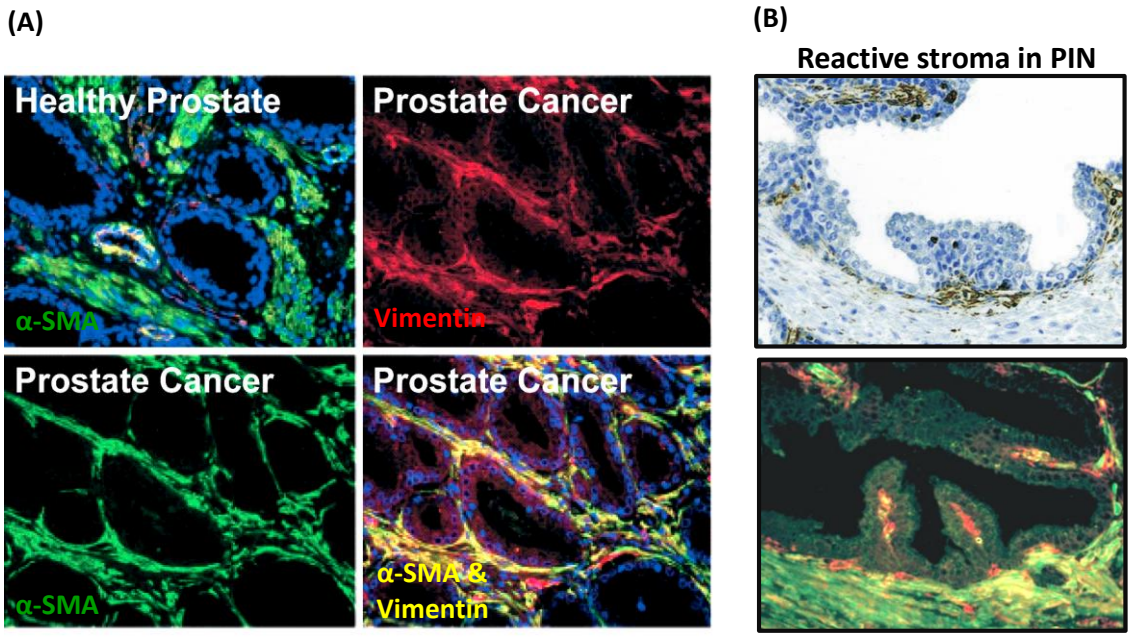

Figure 1.1: Smooth muscle cells are replaced by myofibroblasts.
Healthy and cancerous prostatic specimen obtained from radical prostectomy were dual-labelled with α-SMA (green) and vimentin (red) and analysed by immunofluorescence. The healthy stroma contains co-localisation (yellow) of α-SMA and vimentin only at the blood vessel walls. Increased co-localisation of α-SMA and vimentin, indicative of myofibroblasts was observed in the stroma of cancerous prostate. DAPI used to stain nuclei (blue). (A). Immunostaining of vimentin was observed in stromal cells adjacent to PIN (brown) (top). Dual-labelling of fluorescence antibodies against α-SMA (green) and vimentin (red) were used to identify myofibroblasts (co-localisation; yellow) (bottom) adjacent to the PIN (B) X 400
Source: *Tuxhorn et al. 2002*

1.2.2. Tumour associated myofibroblasts

There are multiple potential cellular precursors of myofibroblasts, such as pericytes, smooth muscle cells (Rajkumar *et al.* 2005), fibroblasts (Hinz 2007; Desmouliére *et al.* 1993), epithelial cells, endothelial cells, circulating fibrocytes (Abe *et al.* 2001; Direkze *et al*. 2003), adipose tissue derived cells and mesenchymal stem cells (McAnulty *et al.* 2007; Őstman and Augsten 2009; Micallef *et al.* 2012). The myofibroblastic differentiation of fibroblasts has been studied the most, especially in the realm of granulation during wound healing, as illustrated in figure 1.2. Firstly, the fibroblasts evolves into proto-myofibroblasts which are characterised by the formation of β and γ cytoplasmic actins (Hinz *et al.* 2001; Kapanci *et al.* 1992). The stimuli to trigger this process is not very well understood, but mechanical tension has been shown to generate proto-myofibroblasts from the fibroblasts (Tomasek *et al.* 2002). Secondly, the proto-myofibroblasts are stimulated to develop into differentiated myofibroblasts in response to transforming growth factor-β1 (TGF-β1) and extracellular matrix (ECM) components like ED-A fibronectin and mechanical stress (Tomasek *et al.* 2002). The differentiated myofibroblasts are characterised by the neoexpression of α-smooth muscle actin (Darby *et al.* 1990; Ronnov-Jessen *et al.* 1996) and the incorporation of α-SMA into stress fibres provides contractile features of myofibroblastic cells (Hinz *et al.* 2001).

Functionally, the differentiated myofibroblasts can generate a greater contractile force than the proto-myofibroblasts for matrix remodelling. This is reflected by higher organisation of α-SMA stress fibres to the extracellular fibronectin fibrils via focal adhesion complexes (figure 1.2) (Dugina *et al.* 2001; Singer *et al.* 1984). Due to this connection the myofibroblasts possesses a mechanotransduction system where the force generated by the actin stress fibres can be transmitted to the surrounding ECM (Burridge and Chrzanowska-Wodnicka 1996). Once the original structure of the ECM is reconstituted at the wound site, the myofibroblasts may undergo apoptosis (Hata *et al.* 2013) or may revert back into fibroblasts (Darby *et al.* 2014), but the latter has not been clearly demonstrated. Nevertheless, myofibroblasts are more likely to undergo apoptosis and be cleared by macrophages.

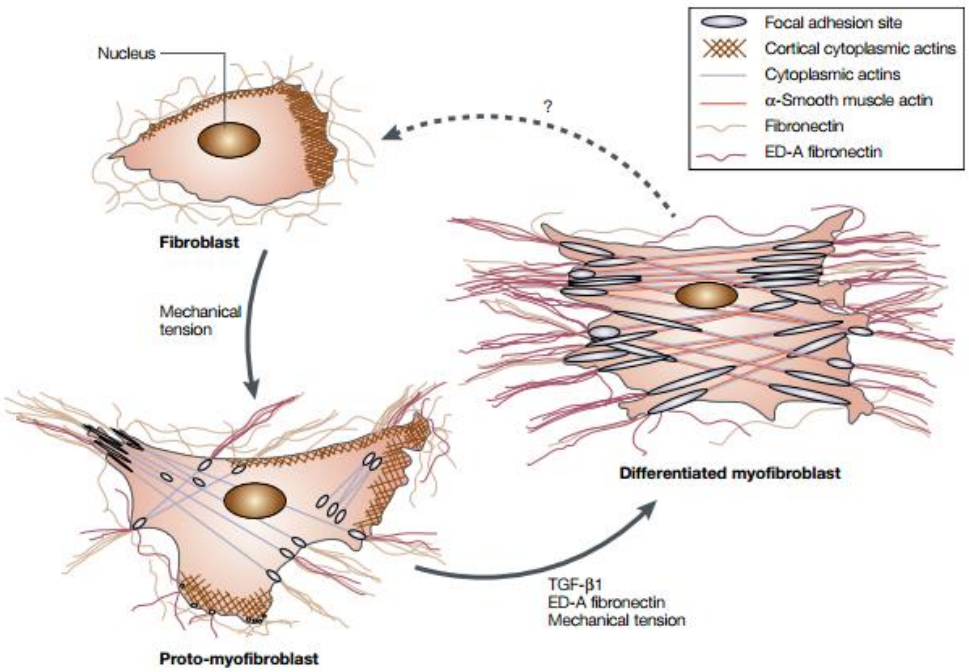

Figure 1.2: Myofibroblast differentiation from resting fibroblasts at wound sites
Under mechanical stress, fibroblasts can differentiated into proto-myofibroblasts, which form cytoplasmic actin-containing stress fibres that terminate in focal adhesion complexes. Proto-myofibroblasts also express and organise cellular fibronectin, including ED-A fibronectin and these proto-myofibroblasts. Transforming growth factor-β1 (TGF-β1) can increase the expression of ED-A fibronectin and both factors, along with mechanical stress, can stimulate the proto-myofibroblasts to modulate into differentiated myofibroblasts. The differentiated myofibroblasts are characterised by the de-novo expression of α-smooth muscle actin in more extensively developed stress fibres. Once tissue-healing is complete, myofibroblasts may undergo apoptosis or revert back into a myofibroblasts but the mechanism behind this is unknown.
Source: *Gabbiani et al. 2003*

1.2.3 Tumour associated myofibroblasts promote cancer progression

Alterations of the stroma during tumorigenesis has led researchers to assess the role of stromal-epithelial interactions with regard to tumour progression. In one experiment, myofibroblasts taken from invasive breast cancer patients, promoted the growth of breast carcinoma cells *in vivo*, to a much greater extent than that of normal mammary fibroblasts taken from the same patients (Orimo *et al*. 2005). In another experiment, myofibroblasts, taken from human prostate tumours, or fibroblasts taken from benign prostate hyperplasia (BPH) were administered with immortalised non-tumourigenic prostate epithelial cells in mice and tumour growth was assessed (figure 1.3). Tissue recombinants of myofibroblasts with the epithelial cells strikingly enhanced growth by 500 times in comparison to fibroblasts with the epithelial cells (Olumi *et al*. 1999). Therefore stromal activation, resulting in enhanced myofibroblasts is recognised as a rate limiting step in tumour progression. Furthermore, there is a clear correlation between the extent of stromal changes and the clinical prognosis of various cancers. One example is a study conducted amongst 60 breast cancer patients with known prognosis. Immunohistochemical (IHC) analysis of biopsies revealed, patients with metastatic breast cancer to be significantly abundant in α-SMA expressing myofibroblasts in comparison to patients with non-invasive breast cancer (Yamashita *et al.* 2012). In another study, the stroma from prostate cancer patients after radical prostatectomy for clinically localised PCa was analysed by IHC, revealing a significant correlation between the myofibroblast phenotype and the length of disease-free period. Therefore, in PCa patients who have identical Gleason score, the intensity of stroma changes i.e. the increase in myofibroblast phenotype could identify patients with a higher risk of PCa relapse (Tomas *et al.* 2010). Similarly, the use of myofibroblasts as an independent prognostic factor has been shown in various other cancers including oesophageal adenocarcinoma, oral squamous carcinoma, colorectal cancer and pancreatic cancer (Underwood *et al.* 2015; Marsh *et al.* 2011; Surowiak *et al.* 2007; Tsujino *et al.* 2007; De Monte *et al.* 2011) emphasising the importance of the stroma in directing and influencing disease outcomes.

Myofibroblasts exert tumour promoting functions by enhancing proliferation of the cancer cells, most likely in a hepatocyte growth factor (HGF)-dependent manner as

shown in hepatocellular carcinoma (Jia *et al* 2013), prostate carcinoma (Olumi *et al* 1999) and breast carcinoma (Surowiak *et al* 2006). Myofibroblasts have also been shown to support tumour progression by enhancing angiogenesis, tumour migration and invasion.

Angiogenesis

Angiogenesis is the formation of new capillaries from pre-existing blood vessels and is essential for the growth and progression of the tumour (Reinhart-King 2008). Capillaries are a monolayer of endothelial cells, creating a semi-permeable barrier between the blood and the surrounding tissue, for the exchange of nutrients and waste products to and from the tumour cells (Reinhart-King 2008; Eliceiri and Cheresh 2001). Tumourigenic tissues exhibit abnormally high blood vessel densities in comparison to non-tumourigenic tissues (Olumi *et al.* 1999; Kamoun *et al.* 2010; Yang *et al.* 2005). Additionally, the blood vessels were reported to increase during early tumour formation (Kamoun *et al.* 2010), indicating their importance in tumour growth.

For angiogenesis to occur, endothelial cells migrate from pre-existing blood vessels, proliferate and reorganise with vascular smooth muscle cells and pericytes to form a new capillary network (Davis and Senger 2005; Lamalice *et al.* 2007). The process of angiogenesis is regulated by a balance between anti- and pro- angiogenic agents. Examples of pro-angiogenic factors are vascular endothelial growth factor-A (VEGF-A), fibroblast growth factor (FGF), hepatocyte growth factor (HGF) and platelet derived growth factor (PDGF) (Lamalice *et al.* 2007; Bouïs *et al.* 2006). Tumour promoting myofibroblasts have been reported to secrete pro-angiogenic factors such as VEGF-A and HGF which may aid angiogenesis at tumour sites (Webber *et al.* 2014; Orimo *et al*. 2001).

Myofibroblasts may have the capacity to induce endothelial recruitment into the tumour site and hence support angiogenesis for tumour progression. This assumption was based on studies where myofibroblasts from breast cancer stroma were able to mobilise endothelial cells *in vitro* in a Boyden transwell chamber (Orimo *et al.* 2005). In contrast non-cancerous stromal cells such as fibroblasts failed to recruit the endothelial

cells. The mobilisation of endothelial cells were reported to be dependent on the chemokine, stromal derived growth factor-1 (SDF-1) secreted by myofibroblasts, as shown using SDF-1 blocking experiments (Orimo *et al.* 2005). Furthermore, administration of anti-SDF-1 neutralising antibody into nude mice with breast cancer cells admixed with myofibroblasts greatly reduced tumour growth *in vivo* (Orimo *et al.* 2005) and this may be due to the lack of recruitment of endothelial cells into the tumour site required for angiogenesis. In addition, co-culturing of diseased stromal cells from the prostate with endothelial cells promoted vessel-like structure formation *in vitro* (Webber *et al.* 2014). The diseased stromal cells were identified to be α-SMA positive, indicating a myofibroblast phenotype. Therefore myofibroblasts promote tumour progression at least in part by enhancing formation of vessels.

Tumour invasion and metastasis

The ability of cancer cells to move and invade, allows the escape of cells from the primary tumour site to a distant site to form a secondary tumour. Myofibroblasts are abundantly present at the invasive front of primary tumours, such as in colon cancer *in vivo* (De Wever *et al.* 2004) and are thus speculated to play a role in supporting tumour invasion. *In vitro* studies demonstrate myofibroblasts promote tumour cell invasion. For example, conditioned medium (CM) from myofibroblasts obtained from colon cancer and squamous carcinoma were found to promote invasion of the colon and squamous cancer cells, respectively in a collagen gel matrix (De Wever *et al.* 2004; Cat *et al.* 2006). In contrast, CM from standard culture media or from non-cancerous fibroblasts from healthy stroma of the same patients failed to support tumour cell invasion. Furthermore, lowering the amount of myofibroblasts, reduced the invasive capacity of tumour cells (Cat *et al.* 2006), thus the invasion of cancer cells can be directed by myofibroblasts.

Myofibroblasts have increased secretion of hepatocyte growth factor (HGF) in comparison to their precursors, such as the fibroblasts. Blocking experiments revealed tumour cell invasion to be partially dependent on HGF (De Wever *et al.* 2004). There are additional factors such as matrix metalloproteinases (MMPs) which may also be involved in promoting tumour cell invasion. MMPs are enzymes which are used by cells

to break down structural proteins within the ECM such as collagen, laminin, elastin and fibronectin (Sternlicht and Werb 2001). Conditioned medium (CM) of myofibroblasts derived from breast cancer contained higher levels of MMP-1 than that of normal fibroblasts (Boire *et al.* 2005). Similarly, myofibroblasts from prostate cancer were found to have elevated MMP-2 expression (Giannoni *et al.* 2010). Blocking experiments revealed MMP-1 is required for the motility of breast cancer cells and MMP-2 for the motility of prostate cancer cells in a Boyden transwell chamber (Boire *et al.* 2005; Giannoni *et al.* 2010). Therefore myofibroblasts provide components to support the motility and invasive capacity of the cancer cells, which are required for tumour metastasis. Giannoni and group (2010) have observed prostate cancer cells to metastasise to the lung when admixed with myofibroblasts in a xenograft model. This spontaneous metastasis was not observed, however, when prostate cancer cells were injected in mice alone or with fibroblasts from healthy stroma. Even though myofibroblasts are essential elements involved in promoting metastasis, the paracrine factors involved are, however poorly understood.

Various studies, have shown that in comparison to normal fibroblasts, tumour associated myofibroblasts secrete high levels of soluble factors such as insulin-like growth factor-1 (IGF-1), epidermal growth factor (EGF), vascular endothelial growth factor- A (VEGF-A), HGF and interleukin-6 (IL-6), as shown using ELISA, immunohistochemistry and qPCR analysis (Webber *et al.* 2014; Orimo *et al.* 2001; Cat *et al.* 2006). These factors may participate in tumour progression by stimulating tumour cell proliferation, angiogenesis, tumour cell invasion and metastasis, making myofibroblasts essential for tumours to progress. Hence understanding the mechanisms involved in the generation of myofibroblasts is of great importance if we are to ever devise therapeutic approaches to target this rate-limiting step in disease progression.

Tumour associated myofibroblasts support tumour growth

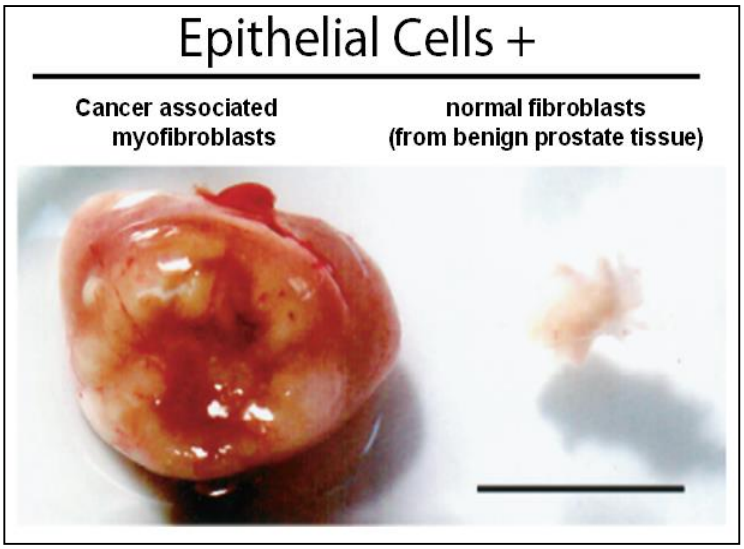

Figure 1.3: Tumour associated myofibroblasts enhance tumour growth.
Image shows the gross appearance of tissue recombinants harvested after 85 days of growth in nude mice. Myofibroblasts (taken from prostate cancer) administered with prostate epithelial cells weighed 1250mg (Left hand side). Normal fibroblasts (taken from BPH) administered with prostate epithelial cells weighed 10mg (Right hand side). Scale bar; 1cm
Source: *Olumi et al. 1999*

1.3 Transforming Growth Factor-β

1.3.1 TGF-β1 within the reactive stroma

The Transforming Growth Factor-β1 (TGF-β1) is a member of the TGF-β superfamily of cytokines. There are three isoforms of TGF-β (-1, -2 and -3) and the TGF-β1 isoform has been the most widely studied in the context of myofibroblastic differentiation. The mRNA and protein for TGF-β1 is overexpressed in many types of human cancers, including colon cancer (Coffey *et al.* 1986) and breast cancer tissues (Barette-Lee *et al.* 1990) in comparison to the normal colon and breast tissues, respectively. Overexpression of TGF-β1 is also observed in human prostate cancer tissues, in comparison to the normal prostate tissue or BPH (Eastham *et al.* 1995; Gerdes *et al.* 1998). Additionally, rat prostate cancer cells genetically manipulated to overexpress TGF-β1 enhanced tumour size by 50% and produced a more extensive metastatic disease *in vivo*, in comparison to the un-manipulated tumour cells (Steiner and Barrack 1992). Therefore TGF-β1 is believed to be an essential factor for tumour progression.

Similar to fibrosis at wound sites, TGF-β1 from cancer cells has been reported to drive the differentiation of stromal fibroblasts into myofibroblasts as characterised by the *de-novo* expression of α-SMA expression. Such examples are seen in squamous cell carcinoma (Lewis *et al.* 2004) and prostate cancer (Tuxhorn *et al.* 2001). Moreover, blocking TGF-β1 signalling via the TGF-β1 neutralising antibody or inhibiting the TGF-β1 receptor (Alk-5), resulted in attenuation of fibroblasts differentiating into α-SMA positive myofibroblasts (Tuxhorn *et al.* 2001; Webber *et al.* 2010). Therefore TGF-β1 is important for directing the differentiation of fibroblasts into myofibroblasts.

1.3.2 TGF-β1 signalling pathway

TGF-β1, a polypeptide homodimer is secreted by cells as a large latent complex, consisting of dimeric propeptides called latency associated protein (LAP), which are bound to the latent TGF-β binding protein (LTBP) (Gerdes *et al.* 1998). LTBP contain multiple epidermal-growth-factor-like repeats as well as unique domains containing eight cysteine residues (8-cys domains). Immunoblotting of the protein complexes indicated that the third 8-Cys repeat of LTBP binds covalently to the LAP region of the TGF-β1 (Saharinen *et al.* 1996). Additionally, disulphide linkages are formed between

the cysteine residues of LAP and cysteine residues in the LTBP (Saharinen *et al.* 1996). Due to this interaction, the TGF-β is incapable of interacting with the TGF-β receptors as shown by multi-light scattering mass measurements (Shi *et al.* 2011).

Cleavage of the bond between the LAP and LTBP is required for activation of TGF-β (Annes *et al.* 2003) and this can be accomplished by proteases, integrins, thrombospondin, heat and pH (Wipff and Hinz 2008; Lyons *et al.* 1988), most of which are found to be up-regulated in response to injury. Once activated, TGF-β1 triggers a downstream signalling pathway as illustrated in figure 1.4. Activated TGF-β1 binds to the serine/threonine kinase domain of the TGF-β receptor II (TGF-βR II), which in turn phosphorylates the TGF-β receptor I (TGF-βR I) as it forms a receptor complex with it (Roberts 1999). Additionally, TGF-β1 may also be presented to the TGF-β receptor II by the accessory protein, betaglycan (also known as TGF-β receptor III) or endoglin (De Crescenzo *et al.* 2003; Midgley *et al.* 2013; Guerrero-Esteo *et al.* 2002). The activation of TGFβRI phosphorylates members of the Smad family, in particular the receptor-activated Smad protein (R-SMAD) such as SMAD-2 and SMAD-3. The phosphorylated SMAD-2 or SMAD-3 forms a heterodimeric complex with Co-Smad (SMAD-4) which then translocates into the nucleus and interacts with Smad-binding elements (SBE) in the DNA to regulate transcription of target genes and thus the synthesis of proteins such as α-SMA. Therefore the active form of TGF-β1 has the capacity to differentiate stromal cells into α-SMA positive myofibroblasts. Various studies use the TGF-βR I (Alk-5), inhibitor called SB43152 to block the receptor and hence the corresponding downstream signalling, to investigate the TGFβ-SMAD dependent pathway involved in the differentiation of cells into α-SMA positive myofibroblasts (Webber *et al.* 2010; Gu *et al.* 2012).

The accessory proteins which deliver TGF-β1, can also modify the cellular response to TGF-β1, for example overexpression of endoglin in fibroblasts, suppressed Smad-3 dependent activity (Leask *et al.* 2002). Another experiment showed the suppression of Smad 3 via genetic manipulation repressed the generation of α-SMA expressing myofibroblast in response to TGF-β1 (Gu *et al.* 2007). In a similar experiment, suppression of Smad 2 activity (phsophorylation) caused by inhibition of TGF-βR I (Nyati

et al. 2011) attenuated myofibroblastic differentiation of fibroblasts (Webber *et al.* 2010). Thus myofibroblast differentiation is dependent on Smad 2 and 3 activity.

Recently, fibroblast-to-myofibroblast differentiation in response to TGF-β1 was shown to be dependent on the polysaccharide hyaluronan (HA) (Webber e*t al.* 2009) via the epidermal growth factor receptor (EGFR) and CD44 (Midgley *et al.* 2013). The EGFR and CD44, however, also triggers downstream mitogen-activated protein kinase (MAPK) and calcium-calmodulin kinase II activation (Ito *et al.* 2004; Midgley *et al.* 2013). In addition, knock down of these receptors, abrogates HA and attenuates the downstream MAPK signalling and myofibroblastic differentiation (Midgley *et al.* 2013). Thus other pathways independent of the Smad signalling, such as MAPK are also involved in the myofibroblastic differentiation process (Hashimoto *et al.* 2001; Hough *et al.* 2012).

TGF-β Signalling Pathway

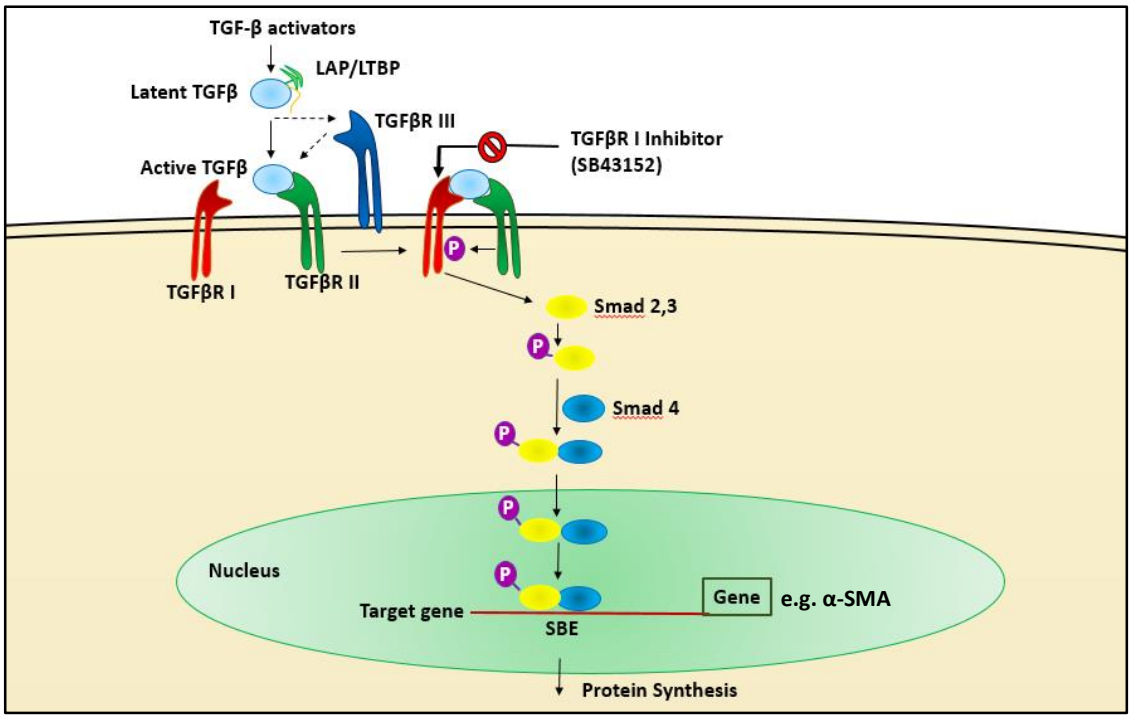

Figure 1.4: The TGF-β driven pathway involved in myofibroblastic differentiation.
Latent TGF-β is activated by the dissociation of LAP from LTBP in response to certain activators. Active TGF-β may bind to TGFBR II directly or with the aid of TGFβ-III (betaglycan). TGFβRII in turn phosphorylates TGFβRI, by forming heterodimerisation of the receptors. TGFβRI can phosphorylate receptor-associated Smads (R-Smads), such as Smad-2 and Smad-3. The phosphorylated Smad-2,-3 forms a complex with Smad-4, a co-Smad, which translocates into the nucleaus and binds to Smad Binding Element (SBE) which can influence the transcription of target genes and thus the synthesis of target proteins. SB43152 can bind to the Alk-5 TGFβRI and inhibit the downstream TGF-β pathway.
Source: Adapted from *Saharinen et al. 1996; De Crescenzo et al. 2003; Shi et al. 2011*

1.4 Exosome Biology

Exosomes are a distinct population of membranous nanovesicles of endocytic origin, ranging in a size from 30-150nm in diameter. They used to be regarded as "cellular debris" but are now seen as important communicating tools. They were first described to be released by rat reticulocytes maturing into red blood cells (Harding *et al.* 1984, 1983; Johnston *et al.* 1987; Pan *et al.* 1985). Secretion of exosomes were later, noted in other cells such as B-cells (Raposo *et al.* 1996), dendritic cells (Zitvogel *et al.* 1998), platelets (Heijnen *et al.* 1999), T cells (Peters *et al.* 1991; Denzer *et al.* 2000) and tumour cells (Wolfers *et al.* 2001). Over the past few years, exosomes have been demonstrated to play roles fundamental to cancer and other diseases and thus study of exosomes has become of great interest.

1.4.1 Characteristics of exosomes

Studying the biology of exosomes is technically challenging due to many reasons such as their small size, variation in molecular composition and confusion in their terminology, resulting in exosomes being referred to as microvesicles and vice versa. Nevertheless, exosomes possess characteristic biophysical and biochemical properties, for example they have a diameter of 30-150nm, as shown by immuno-electron microscopy and Nanoparticle Tracking Analysis (NTA) (Escola *et al.* 1998; Sokolova *et al.* 2011; Sharma *et al.* 2010) and have a buoyant density in sucrose of 1.1-1.2g/mL (Raposo *et al.* 1996).

The protein content of exosomes has been extensively examined from various tumour cells such as breast cancer (Koga *et al.* 2005), colorectal cancer (Choi *et al.* 2007), mammary adenocarcinoma (Wolfers *et al.* 2001), mesothelioma (Hegmans *et al.* 2004) and brain tumour (Graner *et al.* 2009). Furthermore, the exosomes studied have been isolated from cancer cell supernatants as well as diseased biological fluids, including blood-plasma (Caby *et al.* 2005), urine (Gonzales *et al.* 2009; Nilsson *et al*. 2009) and pleural effusions (Andre *et al.* 2002). The exosome composition has been assessed using methods such as western blotting, flow cytometry and immuno-electron microscopy but mass spectrometry (MS) is the most widely used tool to study the protein content of exosomes. In comparison to the early mass spectrometry (MS) used for peptide mapping (Théry *et al.* 1999 and 2001), newer MS-based proteomic tools generate peptide

sequence information by time of flight (TOF/TOF) which are better due to their higher sensitivity, resolution and mass accuracy and hence assigning a protein identification can be done with much greater confidence. Thus the advances in MS has significantly improved the depth of exosomal proteome coverage (Simpson *et al.* 2008). From the vast published and unpublished studies the proteins, lipids and RNAs found in exosomes have been catalogued in the ExoCarta, an online database (http://www.exocarta.org). Additionally, the purification method and characterisation properties are noted on the ExoCarta so that the researchers can assess the quality of the exosome preparations to that of their corresponding data shown (Mathivanan *et al.* 2012).

From the ExoCarta database, exosomes in general have been revealed to contain membrane and cytosol components associated with their endosomal origin and exosome biogenesis. Some of which are illustrated in figure 1.5, such as the Rab proteins, annexins (Mears *et al.* 2004), tetraspanins (CD9, CD81 and CD63) (Théry *et al.* 2002; Escola *et al.* 1998), ALIX, TSG101 and heat shock proteins (HSC70 and HSP90) (Théry *et al.* 2002). Most exosomes also contain MHC Class I molecules (Blanchard *et al*. 2002; Wolfers *et al*. 2001) and lysosomal markers LAMP1 and LAMP2 (Denzer *et al.* 2000). Some cancer cell-derived exosomes express certain cytokines and growth factors, such as TNFα in melanoma derived exosomes (Soderberg *et al.* 2007) and TGF-β in brain, mesothelioma and prostate cancer exosomes (Graner *et al*. 2009; Clayton *et al.* 2007; Webber *et al*. 2010). Apart from proteins, constituents of lipidic membrane like cholesterol and ceramide are also enriched in exosomes (Trajkovic *et al.* 2008; Subra *et al.* 2007; Wubbolts *et al.* 2003). Studies have also shown exosomes to contain both mRNA and miRNA (Valadi *et al.* 2007; Taylor and Gercel-Taylor 2008; Skog *et al.* 2008). The most common proteins found amongst exosomes are ALIX, TSG101 and tetraspanins (CD9, CD63 and CD81) and are routinely used as positive markers for exosome identification using antibody based techniques such as ELISA and western blot.

Exosomes also possess some distinct sets of proteins associated with their cell of origin. For example, antigen presenting cells such as dendritic cells and B-lymphocytes are enriched in MHC Class I and II, tetraspanins (CD9, CD63 and CD81) and co-stimulatory molecules CD80 and CD86, indicating exosomes from antigen presenting cells contain

the cellular machinery required to induce a potent T-cell response (Raposo *et al.* 1996; Zitvogel *et al.* 1998; Théry *et al.* 1999, 2001; Clayton *et al.* 2001; Heijnen *et al.* 1999). In numerous cancer cell studies, the tumour-associated proteins and miRNA content in the cells were similarly expressed in their corresponding exosomes, thus exosomes may provide a cell-type signature for diagnostic purposes (Mathivanan *et al.* 2010; Skog *et al.* 2008; Rabinowits *et al.* 2009; Taylor and Gercel-Taylor 2008; Andre *et al.* 2002; Huber *et al.* 2005). All these studies, demonstrate the complexity of exosomal vesicles and hence their potential diverse roles as mechanistic component involved in cell-to-cell communication.

Molecular composition of exosomes

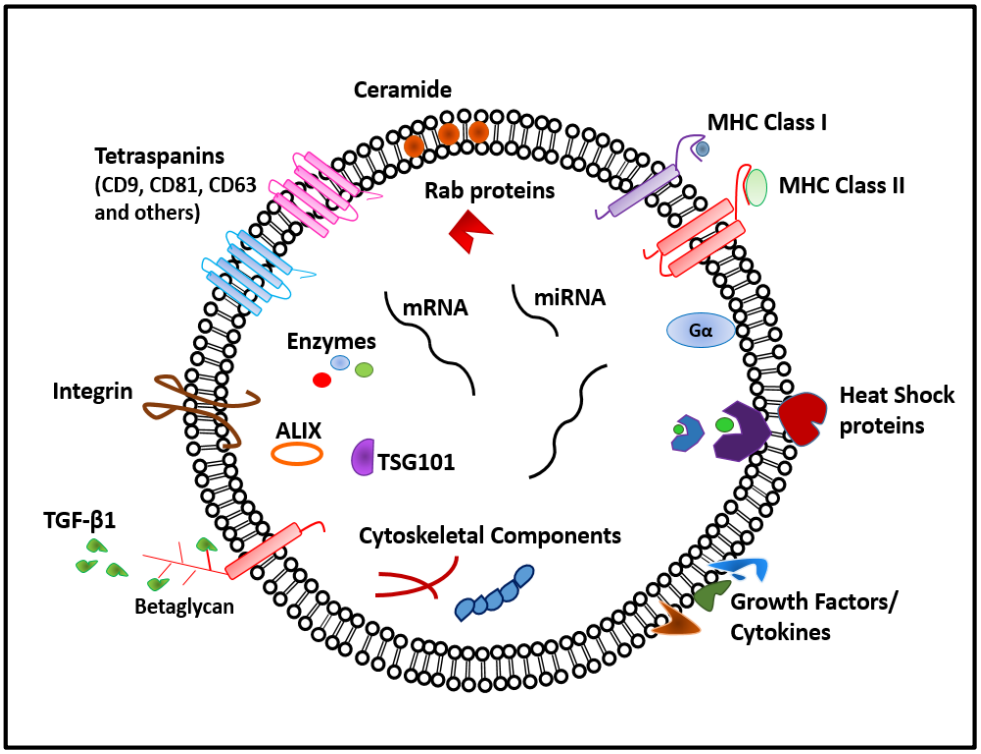

Figure 1.5: Schematic representation of the some of the components found on an exosome. Exosomes are membrane-bounded vesicles containing various transmembrane proteins including integrins, tetraspanins (CD9, CD81, CD63), MHC molecules, heat shock proteins, growth factors and cytokines. Exosomes also encapsulate MVB-associated proteins (ALIX and TSG101), enzymes, Rab proteins, cytoskeletal components as well as mRNA and miRNA.
Source: Adapted from *Raposo et al 1996; Zitvogel et al 1998; Thery et al 1999; Clayton et al 2001;* Wolfers *et al*. 2001; Graner *et al*. 2009; Clayton *et al.* 2007; Subra *et al.* 2007; Wubbolts *et al.* 2003; Valadi *et al.* 2007 *Webber et al. 2010*

1.4.2 Exosome biogenesis and the endogenous control of their secretion

The biogenesis and secretion of exosomes involves various molecules and is schematically summarised in figure 1.6. Early studies using pulse chase and immuno-electron microscopy revealed exosomes to be contained within endosomal compartments, known as multivesicular bodies (MVBs) (also referred to as multivesicular endosomes) which then fuse to the plasma membrane to release pre-formed vesicles as exosomes. The generation of exosomes, corresponding to the intraluminal vesicles (ILVs) in the MVBs involves the cargo clustering at the endosomal limiting membrane, the formation of inward budding of the vesicle and its release into the MVB. Many studies carried out in yeast revealed the endosomal sorting complex required for transport (ESCRT) family to be involved in the formation of MVBs. The ESCRTs proteins are grouped into 4 complexes (ESCRT-0, -I, -II and -III) plus accessory proteins and are recruited to the endosome in an ordered manner. The ESCRT-0 is responsible for the cargo recognition and clustering in an ubiquitin-dependent manner (Katzmann *et al.* 2003). ESCRT-0 also recruits ESCRT-I components (such as TSG101), which in turn recruits members of the ESCRT-II. Both the ESCRT-I and ESCRT-II induce the inward budding of vesicles (Katzmann *et al.* 2001). ESCRT-III is then recruited along with the accessory proteins which drive vesicular scission, as well as the disassembly and recycling of the ESCRT complexes (Babst *et al.* 2002; Katzmann *et al.* 2001; Jouvenet *et al.* 2011).

Likewise, in eukaryotic cells such as MHC class II expressing HeLa cells, RNA interference (RNAi) was used to target different components of the ESCRT machinery, revealing exosome biogenesis and secretion to be dependent on various components of the ESCRT. For example, silencing of HRS and STAM (ESCRT-0 members) reduced exosome secretion as noted by reduction of MHC class II, CD63 and particle concentration, measured by fluorescence-activated cell sorting (FACS), western blotting and Nanoparticle Tracking Analysis (NTA) (Colombo *et al.* 2013). Similarly, silencing of TSG101 (ESCRT-I member) reduced exosome secretion and modified protein content of exosomes as evidenced by increased number of exosomes being negative for CD63 and MHC class II, suggesting TSG101 is required for targeting these cargos into exosomes in

HeLa cells. Thus interfering with the components of the ESCRT machinery lowers exosome secretion and modifies their protein composition.

The ESCRT-III accessory protein, ALIX has been reported to promote the inward budding of vesicles in MVBs by its interaction with heparan sulphate proteoglycan (HSPG) syndecan-1 and the cytoplasmic adaptor syntenin (Baietti *et al.* 2012). Depletion of ALIX using siRNA, did not affect exosome secretion but increased the amount of MHC class II expressed on the cells and subsequently on their exosomes. Silencing of ALIX, also lowered the level of CD63 and HSP70, indicating that ALIX may also control the protein composition of the exosomes (Colombo *et al.* 2013). Once inward budding of vesicles is complete, the ESCRT complexes require energy to dissociate from the endosomal membrane and this energy is provided by the ESCRT-III accessory protein ATPase Vps4 (Babst *et al*. 2011).

Inhibiting ESCRT components does not completely block the formation MVBs (Stuffers *et al*. 2009) thus other molecules independent of the ESCRT machinery maybe involved such as lipids and tetraspanins. Sphingolipids such as ceramide, are synthesised by an enzyme called neutral sphingomyelinase (nSMase) which converts sphingomyelin to ceramide. Ceramide is proposed to facilitate membrane invagination of exosomes into MVBs and exosome secretion, as the inhibition of nSMase attenuated the biogenesis and the release of exosomes from glial cells (Trojkovic *et al.* 2008). Other studies have also reported the release of miRNA containing vesicles (presumed to be exosomes) to be dependent on ceramide (Iguchi *et al.* 2010; Kosaka *et al.* 2010). Specific lipids such as cholesterol are also enriched in exosomes from human dendritic cells (Laulagnier *et al.* 2004) and oligodendroglia cells (Strauss *et al.* 2010). Drug-induced inhibition of cholesterol reduced the secretion of exosomes, thus cholesterol may be involved in exosome release. Tetraspanins expressed on exosomes may also play a role in the biogenesis and secretion of exosomes. Silencing CD63 using siRNA impaired vesicle formation by melanocytes, as noted by reduction of ILV numbers within the MVBs in comparison to the control melanocytes (Van Niel *et al.* 2011). CD81 is also enriched in internal vesicles of MVBs (Escola *et al.* 1998) and the depletion of CD81 using RNAi did not affect the size nor the amount of exosomes released from lymphoblasts, as

determined by electron microscopy and the Nanoparticle Tracking Analysis (Perez-Hernandez 2013). However, proteomics analysis of exosomes from CD81 deficient cells, revealed an altered protein profile with reduced CD19 and CD20 in comparison to exosomes from the wild type cells. Therefore, CD81 plays a role in regulating the protein composition of exosomes (Perez-Hernandez 2013), emphasising exosome biogenesis and secretion are regulated by both ESCRT-dependent and independent components.

Mechanisms that drive trafficking of MVBs to the plasma membrane involves the Rab family of small GTPase proteins. In a leukaemia cell line (K562), time-lapse confocal microscopy revealed GFP-labelled Rab11 to dock MVBs containing transferrin receptor and HSC70 expressing exosomes to the plasma membrane in a Ca^{2+}-dependent manner (Savina *et al.* 2005). Furthermore, screening for GTPase in proteolipid protein (PLP)-rich exosomes from oligodendroglia cells revealed Rab35 to be the most abundant GTPase and the knock down of Rab35 impaired the secretion of exosomes-containing PLP and ALIX, resulting in the accumulation of PLP within the endosomes (Hsu *et al*. 2010; Frühbeis *et al*. 2013). Furthermore, Rab27a and Rab27b were observed to regulate exosome secretion in HeLa cells, in particular Rab27a, where knock down of Rab27a resulted in accumulation of endosomes within the cells (Ostrowski *et al.* 2010). The involvement of Rab27a in exosome secretion was later confirmed in other cancer cell lines such as melanoma (Peinado *et al.* 2012), breast cancer (Zheng *et al.* 2013) and prostate cancer (Webber *et al.* 2014). In these studies, depletion of Rab27a resulted in a reduction of exosomes within the conditioned media as determined by NTA, immunoblotting and protein quantification.

The fusion of the MVBs with the plasma membrane to release vesicles may require soluble NSF Attachment Protein Receptor (SNARE) complexes, as shown in various models of lysosome secretion (Rao *et al.* 2004; Proux-Gillardeaux 2004). Immunofluorescence revealed, the vesicle-SNARE (v-SNARE) protein, VAMP-7 localised on the lysosomes, to interact with the target-SNARE (t-SNARES) such as syntaxin-4 and SNAP-23 on the plasma membrane, inducing fusion of the vesicle to the cell membrane (Rao *et al.* 2004). Additionally, the inhibition of VAMP-7 or SNAP-23, reduced the secretion of lysosomes, thus lysosome secretion is dependent on SNARE complexes

(Proux-Gillardeaux 2004). Whether the same interaction occurs with MVBs containing exosomes has not been thoroughly explored. Nevertheless, a study using a leukaemia cell line noted depletion of VAMP-7 to cause accumulation of enlarged MVBs containing acetylcholinesterase-exosomes close to the cell membrane, suggesting the fusion of MVB with the plasma membrane was abrogated (Fader *et al.* 2009). Thus the SNARE proteins are important for the release of exosomes.

An alternate view of exosome release in certain cell types such as T cells is the direct budding of nanovesicles, referred to as exosome-like vesicles from the plasma membrane (Booth *et al.* 2006). The co-localisation of exosomal and endosomal molecules such as CD81, CD63, TSG101 and ATPase Vps4 at certain locations of the plasma membrane of Jurkat T cells were capable of outward vesicular budding. This indicates that certain regions of the plasma membrane contain elements which can permit exosome biogenesis and the outward budding of vesicles. Taken together, the biogenesis and secretion of exosomes is complex and the mechanism involved may differ among different cell types.

Biogenesis and secretion of exosomes

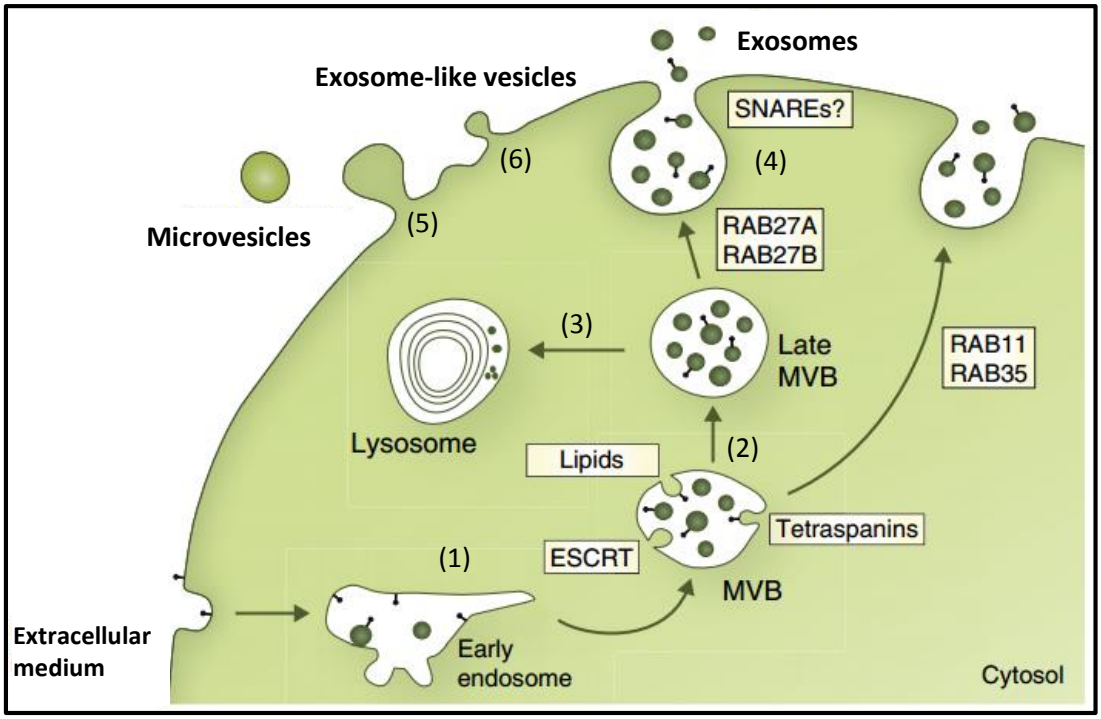

Figure 1.6: Schematic representation of the origin and secretion of exosomes.
Exosomes are endosomal in origin (1), as they are generated in multivesicular bodies (MVBs) (2). The formation of MVBs has been shown to require ESCRT proteins, lipids (ceramide) and tetraspanins, but the role of these molecules in exosome biogenesis are unclear. The MVBs can either fuse with the lysosomes for degradation (3) or fuse with the plasma membrane to secrete exosomes into the extracellular milieu (4). Several Rab proteins (Rab11, Rab27 and Rab25) are known to be involved in trafficking MVB to the plasma membrane. The final step of exosome secretion, i.e the fusion of MVBs with the plasma membrane most probably requires the SNARE proteins, but is still unclear. Large vesicles such as microvesicles bud directly from the plasma membrane (5). Some studies report nanovesicles referred to as exosome-like vesicles to also possess the capacity to bud directly from the plasma membrane (6).
Source: *Adapted from Kowal et al. 2014 and Booth et al. 2006*

1.4.3 Exogenous regulators of exosome secretion

The secretion of exosomes is found to be up-regulated in cancer. For example, women with ovarian cancer have a greater level of circulating tumour-derived exosomes, in comparison to those with benign or age-matched healthy volunteers. Additionally, exosome concentration was found to increase with a more aggressive stage of ovarian cancer (Taylor and Gercel Taylor 2008). Similarly, circulating tumour exosomes were significantly increased in patients with adenocarcinoma in comparison to those without adenocarcinoma (control) (Rabinowits *et al.* 2009). There are many factors involved in the regulation of exosome secretion. Environmental factors such as stress can enhance exosome secretion via activation of p53 (Yu *et al.* 2006). Furthermore, a hypoxic tumour phenotype in breast cancer cell lines enhanced the release of exosomes (King *et al.* 2012). This hypoxic response may be driven by hypoxia-induced factor (HIF-1α) as manipulating the cancer cells with HIFα siRNA attenuated the enhanced release of exosomes, when the cells were cultured under hypoxic conditions *in vitro.*

Various agents can also regulate exosome secretion. The Ca^{2+} ionophore, A23187 increased exosome secretion by B lymphoblast cells in a dose-dependent manner (Clayton *et al.* 2001). Other studies also reported exosome release to be induced in a Ca^{2+}-dependent manner (Blott *et al.* 2002; Savina *et al.* 2003). Another ionophore, monensin (an Na^{2+}/H^{+} exchanger) was also found to increase exosome secretion by the cells, possibly in a Ca^{2+}-dependent manner as noted by accumulation of Ca^{2+} in endosomes of leukaemia cells (Savina *et al.* 2003). Likewise, lymphoblastoid T cells treated with monensin or A23187 increased exosome release in a dose-dependent manner, as noted by enhanced particle concentration measured by NTA and correlated with increased exosome associated proteins ALIX, TSG101, MHC class I (Soo *et al*. 2012; Powis *et al.* 2011). However, the Ca^{2+} ionophore, A23187 is known to induce vesicle release from the plasma membrane (Heijnen *et al.* 1999) and these vesicles may also express proteins similar to those found on exosomes and so analysis should be taken with caution. Nevertheless, some of these studies, analysed exosomal vesicles after isolation using a linear sucrose gradient (which will be discussed in more detail later), to obtain highly pure exosomal preparations (free from other non-exosomal components)

for analysis. This suggests that the response to calcium flux is genuinely exosomal and not due to a membrane-blebbing phenomenon.

A recent study reported heparanase, an endoglycosidase to increase exosome secretion in myeloma cancer cells. To demonstrate this, the cancer cells were manipulated to express high or low levels of heparanase. Cells with abundant heparanase had a 6-fold higher amount of total exosomes secreted in the culture media, in comparison to the cancer cells with low levels of heparanase, as confirmed by western blotting against exosome-associated proteins, NTA and electron microscopy (Thompson *et al.* 2013). Heparanase cleaves heparan sulphate proteoglycan (HSPG) and so exosome secretion may be dependent on a specific structural feature of HSPG once exposed after cleavage. Furthermore, exosome biogenesis is dependent on the assembly of a complex consisting of syndecan-1, cytoplasmic domain syntenin and ALIX as mentioned earlier (Baietti *et al.* 2012). The addition of heparanase to glioma cells was found to increase syndecan-1 within endosomes (Gingis-Velitski *et al.* 2004). Thus, heparanase may regulate the localisation of syndecan-1 and hence promote exosome biogenesis. Lastly, exosomes released by cells have been reported to possess a negative feedback loop on exosome release by the cell and thus regulating the amount of exosome being secreted. The negative feedback regulation was also found to be tissue specific as the addition of exosomes from one cell type had no effect on the exosome secretion by another cell type (Riches *et al*. 2014). Collectively, these studies suggest various factors are involved in the regulation of exosome secretion by the cell.

1.4.4 Methods for exosome isolation

Exosomes have been isolated from cell culture medium or biological fluids in several ways based on the characteristic properties of exosomes. The most widely used method is differential centrifugation involving incremental increase in centrifugal forces, as shown in figure 1.7A, to remove cellular debris and large particles. After this centrifugation step, some researchers include filtration, using a 0.22µm membrane filters (Admyre *et al.* 2003). This helps remove any fragments and vesicles larger than 200nm. Very few researchers also use 0.1µm membrane filters (Ji *et al.* 2008) to eliminate large vesicles. However, this is not ideal for viscous fluids, as the filters can

become easily blocked, resulting in the loss of exosomes. The final step of ultracentrifugation at around 100,000 x g for 1h or longer is used to pellet the exosomal vesicles which can then be further washed with PBS at ~100,000 x g to obtain an exosomal pellet, relatively free of non-exosomal components (Raposo *et al.* 1996; Escola *et al.* 1998; Zitvogel *et al.* 1998). However, an absolute separation of exosomes and non-exosomal components is impossible by this method alone.

For further purification the exosomal pellet can be centrifuged through flotation on a continuous sucrose gradient (0.25M to 2M sucrose) or iodixanol gradient (Opti-Prep^{TM}) at 100,000 x g for around 15h or longer (figure 1.7B). This method separates molecules based on their density, where the exosomes equilibrate at around 1.1-1.2g/mL (Raposo *et al.* 1996; Tauro *et al.* 2012; Kalra *et al.* 2013). This approach results in a homogenous size population of vesicles, and eliminates contaminants such as protein aggregates and other non-exosomal components. However, the density-gradient is a complex and time-consuming process. Furthermore, this procedure was found to result in a variable recovery of exosomes from the starting amount as measured by the levels of MHC Class II expression on biological fluids containing MHC Class II positive exosomes before and after isolation using a continuous sucrose gradient (Lamparski *et al.* 2002). To overcome this perceived problem, Lamparski and group (2002) developed a rapid method with high exosome recovery, which is based on ultracentrifugation of culture media or biological fluids containing exosomes using a 30% sucrose/deuterium oxide (D_2O) cushion at 100,000 x g for 1h or longer, as shown in figure 1.7C. The cushion has a density of 1.210g/cm^3, where the exosomes float in. The cushion containing exosomes is collected and washed at the same high speed with PBS to obtain a purer exosome preparation. Therefore, ultracentrifugation using the sucrose cushion is a suitable method of rapid exosome purification and has been used as part of an isolation protocol to complete phase 1 clinical trials for melanoma and lung cancer studies (Lamparski *et al.* 2002; Morse *et al.* 2002).

Even though the density gradient approach obtains exosomes of good purity, it fails to isolate exosomes from contaminants such as high density lipoprotein (HDL) which have overlapping densities to that of exosomes (Thery *et al.* 2001). Thus isolation of exosomes

from bodily fluids such as the plasma is a challenge due to the highly abundant presence of HDL. To overcome this, Size Exclusion Chromatography (SEC) can be used, which isolates exosomes based on their size (Böing *et al.* 2014) and claims to separate exosomes from HDL. SEC such as the sepharose CL-2B resin, contains heterogeneous sepharose beads with numerous pores of varying sizes, resulting in sequential elution of vesicles size fractions which can be collected. This approach, however, is very time-consuming to complete each run, including the set-up of the column, elution time and column washing. This limits the use of SEC for high-throughput exosome isolation and makes processing multiple samples difficult.

A more simple and rapid approach for isolating exosomes is the use of immuno-affinity capture of exosomes by magnetic beads (Clayton *et al.* 2001). This involves low speed centrifugation at 200 x g and 2000 x g to remove cells and cellular debris. Thereafter, culture media or biological fluids containing exosomes are incubated for 24h with Dyna beads coated with antibodies directed against proteins exposed on exosomes membrane (Clayton *et al.* 2001; Rabesandratana *et al*. 1998; Wubbolts *et al.* 2003). Therefore it is a method of isolating exosomes without the need for ultracentrifugation. Using this method, antibodies against tumour specific proteins, has been used to isolate HER-2 expressing breast cancer exosomes (Koga *et al.* 2005) and A33-expressing colon cancer cell derived exosomes (Ritter *et al*. 1997; Mathivanan *et al.* 2010). Since biological fluids such as the plasma highly abundant in proteins and lipoproteins, the use of affinity-capture magnetic beads for exosomes isolation, lowers the chances of co-isolation of plasma protein components, which can otherwise co-sediment with exosomes at high centrifugation forces using the ultracentrifugation method (Kalra *et al.* 2013). Additionally, the affinity-capture method allows isolation of exosomes from culture media containing exosomes from fetal bovine serum (FBS) which can also co-sediment with exosomes prepared using ultracentrifugation. However, as well as benefits of this affinity-capture procedure, there are some disadvantages, such as the choice of exosome marker is a key issue. For example, MHC class I can be used to isolate MHC class I positive exosomes, however MHC Class I is also shed from plasma membrane as a soluble molecule, hence decreasing the efficiency of exosomes being captured (Théry *et al.* 2006). Even though capturing exosomes based on their expression

of a chosen protein is advantageous in many ways, it is noted that this approach may only isolate a subpopulation exosomes which are positive for the protein selected for exosome isolation (Théry *et al.* 2006). Thus the outcome from this may not represent the exosome population as a whole. Taken together, this method is ideal for routine use as an analytical tool to assess the phenotype of exosomes. However, this method limits the study of the biology of exosomes due to possible loss of function during the release of exosomes from the beads. Also many groups claim the method to be poorly efficient in the context of biological fluids and is inappropriate for isolation of large amount of exosomes as the beads may be fully saturated with exosomes

The most recent methods developed for exosome isolation are commercialised kits of polymer-based precipitation, such as the Exo-Quick™ (Systems Biosciences), Total Exosome Isolation Kit (LifeTechnologies) and ExoSpin (Cell Guidance Systems). The biological sample containing exosomes are added along with the ExoQuick™ solution or other commercial reagents and spun at low speed centrifugation (10,000-20,000 x g), resulting in an exosome pellet. This method is quick and requires no ultracentrifugation or syringes such as those required for density gradient or column chromatography. Whilst these kits are less user intensive, the components claimed to be exosomes using reagents such as the Exo-Quick™, however have been poorly characterised and have been previously reported to also precipitate non-exosomal contaminants (Oosthuyzen *et al.* 2013). Thus, it may not be an ideal method for studying exosome composition and function as these specimens will contain significant contaminants, and potentially alter the vesicles structure.

Depending on factors such as source of exosomes, yield of exosome recovery and time required for exosome isolation, dictates the methods of choice to use. Ultimately, it is the sucrose cushion which is the gold standard for exosome isolation as it can isolate large quantities of exosomes over small period of time in comparison to other methods. It should also be noted that depending on the exosome isolation procedure, exosome preparations may have contaminants to various extent with other extracellular vesicles or RNA protein complexes, dramatically affecting the outcome of downstream analysis. Therefore, assessing the purity of exosome preparations are of critical importance to

demonstrate for example the outcome from experiments are due to properties of exosomes and not the contaminants. One way to assess purity is to measure the particle to protein ratio (P:P ratio) of the exosomal sample using the nanosight and a colourimetric assay for particle and protein concentration measurement, respectively (Webber and Clayton 2013). Introduction of contaminants results in a low P:P ratio, confirming that a higher P:P ratio, indicates a purer exosome preparation. Using this approach, exosomes isolated via the sucrose cushion method exhibited a much higher purity of exosomes preparation, in comparison to the traditional simple pellet and wash ultracentrifugation method. Therefore, the sucrose cushion method is robust and provides isolation of very pure exosomes and this is the approach employed in this thesis.

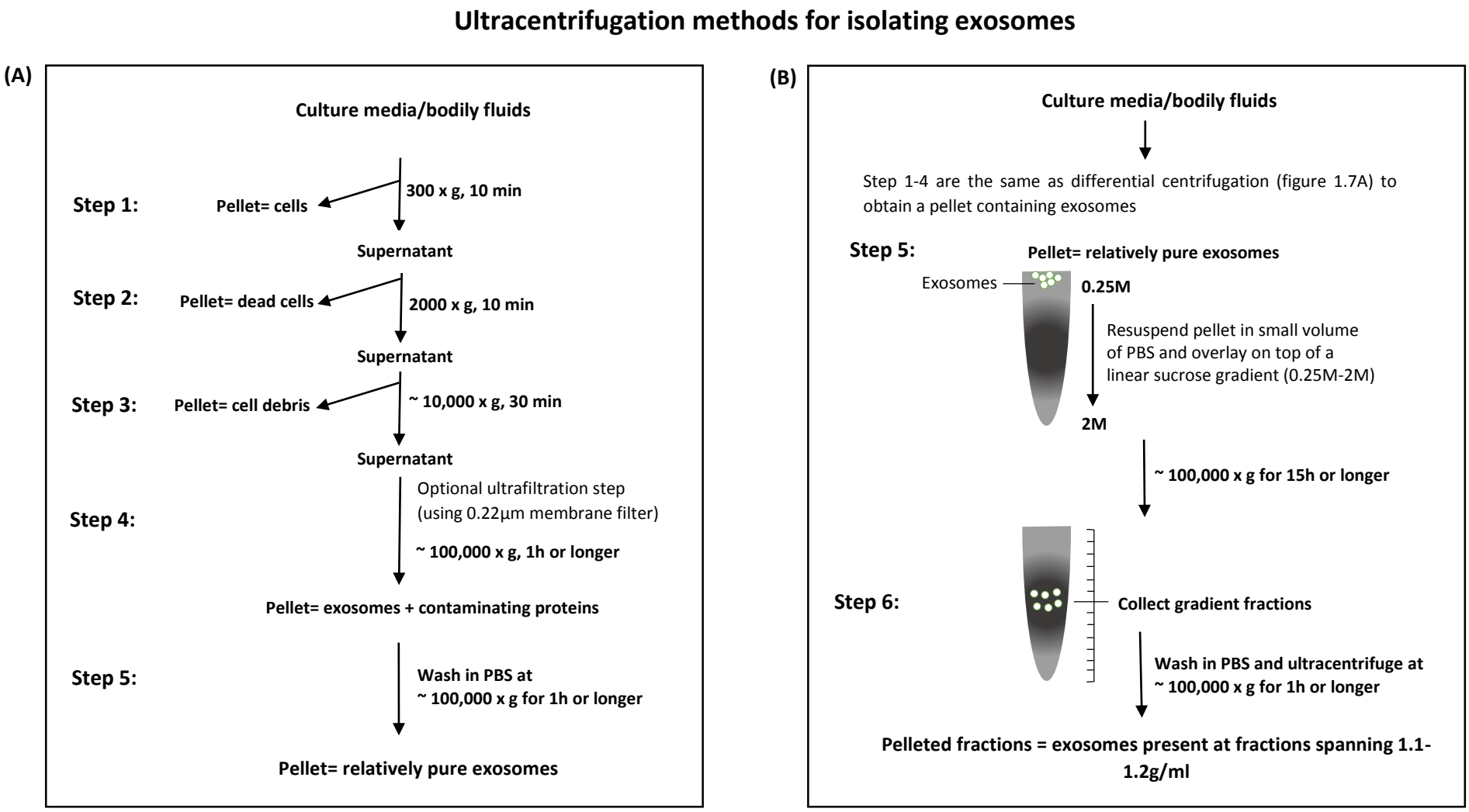

Figure 1.7: Diagram illustrates the steps involved for isolating exosomes using simple pellet and wash ultracentrifugation and the continuous sucrose gradient method. Flow chart shows the steps (1-5) involved for obtaining a relatively pure exosome pellet (A) which can be further purified by floatation on a continuous sucrose gradient at a density range of 1.1-1.2g/mL (B).
Source: *Raposo et al. 1996; Théry et al. 2006*

Ultracentrifugation methods for isolating exosomes

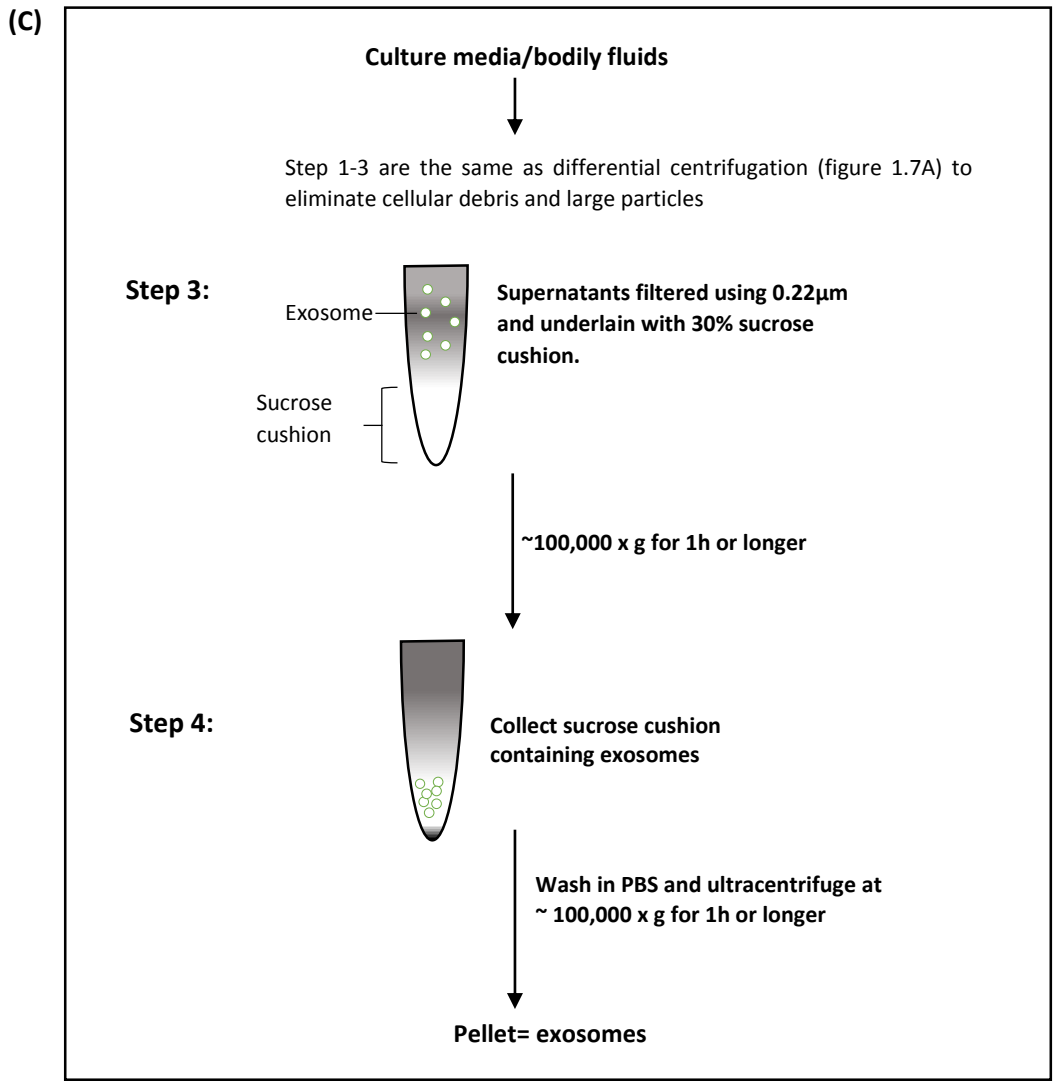

Figure 1.7 continued: Diagram illustrates the steps involved for isolating exosomes using the 30% sucrose/D_2O cushion method. Step 1-3 is the same as the simple pellet and wash method (A) to remove cellular debris and large particles from the exosome containing sample. The exosome containing media is ultracentrifuged with a sucrose cushion to collect exosomes and the cushion is washed thereafter to obtain a highly pure exosome pellet (C).
Source: *Lamparski et al. 2002*

1.4.5 Function of exosomes in cancer

Exosomes are known to exhibit similar function to that of their parent cell, for example, exosomes from antigen presenting cells such as B cells, are enriched in MHC Class II and have been demonstrated to be functional in antigen presentation, leading to the stimulation of T cell proliferation *in vitro* (Raposo *et al.* 1996). In cancer, exosomes can play an important role in cell-to-cell communication and appear to effect target cells by stimulating them directly by surface expressed ligands or by transferring molecules between cells.

Exosomes and immune response

Cancer derived exosomes are known to present tumour-specific antigens on their surface such as HER-2 in breast cancer exosomes and Mart-1 in melanoma derived exosomes and so cancer derived exosomes can exert an anti-tumorigenic effect via aiding cross-presentation. Melanoma derived exosomes have been reported to deliver Mart-1 to antigen presenting dendritic cells for cross-presentation to cytotoxic T lymphocytes (CD8+ T cells) via MHC Class I molecules (Andre *et al.* 2002). The activated T cells triggers an anti-tumour response and hence the suppression of tumour growth *in vivo* (Wolfers *et al.* 2001). In addition, some studies have demonstrated exosomes from human pancreas and colon cancer to express heat shock protein 70 (Hsc-70) which stimulates the cytotoxic activity of NK cells, resulting in NK-mediated apoptosis of the tumour cells (Gastpar *et al.* 2005; Lv *et al.* 2012). Taken together, tumour-derived exosomes can inhibit tumour progression by promoting both adaptive and innate immune responses.

From numerous studies, however, tumour exosomes have been reported to exert immunosuppressive functions. The immune escape of tumour cells is one of the critical factors in preventing cancer destruction by the immune system. One such way that the tumour derived exosomes achieve this is by their induction of apoptosis of CD8+ T cells (cytotoxic T-cells). Exosomes from melanoma and prostate cancer cells express Fas-Ligand (CD95L) which induced apoptosis of Fas positive CD8+ T cells in a dose-dependent manner (Andreola *et al.* 2002; Abusamra *et al.* 2005). Furthermore, blocking FasL abrogated this apoptotic effect by the tumour exosomes (Abusamra *et al.* 2005). Similar

apoptotic property of exosomal vesicles was reported in colorectal cancer cells (Huber *et al.* 2005) and ovarian cancer patients. Another way tumour derived exosomes act on the immune system in favour of the tumour cells is by blocking the proliferation and IL-2 mediated activation of natural killer (NK) cells (Liu *et al.* 2006). Other studies have shown cancer derived exosomes to inhibit myeloid differentiation into dendritic cells (DCs) and instead differentiate myeloid cells into immunosuppressive cells (Valenti *et al.* 2006; Yu *et al.* 2007; Xiang *et al.* 2009). The mechanisms behind this however, are not well understood, but exosome driven inhibition of monocyte differentiation into DCs *in vitro* correlated with an increased level of IL-6 and phosphorylated Stat3 in the monocyte cells (Yu *et al.* 2006). Furthermore, in an IL-6 knock out murine model, tumour exosomes were less effective at inhibiting monocyte differentiation towards DCs and addition of recombinant IL-6 to with tumour exosomes in the IL-6 knockout mice restored the tumour exosome mediated inhibition of DC differentiation. Thus exosomes may induce enhanced secretion of IL-6 by monocytes, which is partially involved in inhibition of DC generation from monocytes (Yu *et al.* 2006). In addition, the impairment of monocyte to DC differentiation has been reported to be mediated by TGF-β and prostaglandin-E2 (PGE2) expressed on exosomes (Valenti *et al.* 2006; Xiang *et al*. 2009). Neutralisation of TGF-β and PGE2 expressed on breast cancer exosomes reverses tumour exosome mediated inhibition of DC differentiation and subsequently promotes tumour growth *in vivo* (Xiang *et al.* 2009). Therefore cancer-derived exosomes direct escape from immune surveillance.

From the range of different studies, tumour derived exosomes have therefore been revealed to have contradicting roles in cancer; exosomes may exert an anti-tumour response as well as triggering an immunosuppressive function. The conflict of the role exosomes play in tumour progression may be due to the fact exosomes from various cancers possess different phenotypes and hence differences in function are observed.

Drug-resistance

Cancer exosomes may support drug resistance and in this way help the tumour to progress. Ovarian cancer cells which were resistant to the chemotherapy drug cisplatin (CDDP) were noted to release significantly more exosomes than cancer cells sensitive to

chemotherapy. Thus cancer cells were speculated to release large amounts of exosomes in order to export the drug CDDP out of the cell (Safaei *et al.* 2005). Furthermore, the breast cancer cell line MCF-7 was manipulated to become insensitive to the chemotherapy agents (adriamycin or docetaxel). These drug-resistance cancer cells were found to spread their resistance traits, using exosomes to residual cancer cells which were not drug-resistant (Levchenko *et al.* 2005; Li *et al.* 2013). Pre-treatment of exosomes with RNase failed to make the recipient cancer cells resistant to the drugs, therefore the resistance traits may be exosomal RNA dependent (Chen *et al.* 2014). It should be noted however, exosomal RNA content are entrapped within the exosomal vesicle (Valadi *et al.* 2007) and so are protected from degradation by RNase. Hence, in these observations, the RNA components being characterised for their role in drug resistance are of extracellular RNA and not associated with exosomes (Grange *et al.* 2011). Taken together cancer cells can use exosomes to become insensitive to drugs and may also use exosomes to transfer their resistance traits to other cells to make them resistant too.

Angiogenesis

Angiogenesis is essential for tumour growth and some studies demonstrate tumour derived exosomes to support angiogenesis. Exosomes express tetraspanins which have multiple function such as B and T cell activation, adhesion and motility of cells (Levy and Shoham 2005; Tarrant *et al*. 2003; Wright *et al.* 2004), but the tetraspanin CO-029 (Tspan8) has also been implicated to play a role in angiogenesis. Tspan8 was found to be over-expressed in some tumour cells such as pancreatic cancer cells which correlated with significantly increased amount of angiogenesis in mice. Tspan8 positive exosomes promoted angiogenesis by favouring endothelial cell branching *in vitro* (Gesierich *et al.* 2006). A study showed fluorescently labelled Tspan8 containing exosomes from rat adenocarcinoma cells to be internalised by endothelial cells, resulting in up-regulation of several angiogenesis related genes and proteins in endothelial cells such as urokinase plasminogen activator (uPA), vascular endothelial growth factor receptor (VEGFR), von Willebrand factor (vWF) and other factors. These changes correlated with enhanced endothelial proliferation, migration and endothelial branching (Nazarenko *et al.* 2010). Furthermore, exosomal vesicles from glioblastoma were observed to deliver mRNA to

endothelial cells which are subsequently translated to protein and promoted tubule formation of the endothelial cells (Skog *et al.* 2008). Similarly, exosomes from colorectal cancer and leukaemia were found to promote endothelial proliferation and tubule formation *in vitro* (Hong *et al.* 2009). The transfer of miRNA-92a from exosomes to endothelial cells in particular, significantly decreased the expression of the adhesion molecule integrin α5, resulting in enhancement of endothelial cell migration and tubule formation (Umezu *et al.* 2013). Therefore tumour exosomes can act as a means to delivering proteins and genetic information to endothelial cells to promote angiogenesis and consequently tumour growth.

1.4.6 Role of cancer secreted exosomes expressing TGF-β1 in reactive stroma generation

Tumour associated myofibroblasts are known to support the progression of tumours (Kalluri and Zeisberg 2006; Kucharzewska *et al.* 2013; Tuxhorn *et al.* 2002). Recently TGF-β positive exosomes secreted from cancer cells such as mesothelioma, and some PCa cell lines (DU145 and PC3) have been shown to differentiate normal fibroblasts (lung origin) into myofibroblasts, as characterised by *de-novo* onset of α-SMA expression organised into stress fibres, similar to that of an equal dose of exogenous TGF-β1 (Webber *et al.* 2010). In contrast exosomes secreted from some cancer cell lines such as CaCo2 (a colorectal cancer), MCF-1 (breast cancer) or LnCap (prostate cancer) with low or undetectable levels of TGF-β1 failed to differentiate fibroblasts into α-SMA expressing myofibroblasts (Webber *et al.* 2010). Thus exosome-associated TGF-β1 was speculated to be involved in the myofibroblastic differentiation. Blocking TGF-β1 signalling revealed the differentiation of fibroblast-to-myofibroblasts to be dependent on exosome-associated TGF-β1 by triggering signalling through the SMAD-dependent pathway (Webber *et al.* 2010)

Further phenotypic analysis revealed major differences in myofibroblasts generated by soluble TGF-β1 (sTGF-β1) or TGF-β1 positive exosome induced fibroblasts. Such differences are elevation of proteins associated with angiogenesis including HGF, VEGF-A FGF-2 and uPA in exosomal induced generation of myofibroblasts and these effects were inhibited by blocking TGF-β signalling. Additionally, exosome-generated myofibroblasts promoted endothelial migration and vessel-like structure formation in a

TGF-β1 dependent manner. Soluble TGF-β1 generated myofibroblasts on the other hand, failed to produce this pro-angiogenic function. Apart from lung derived fibroblasts, exosomes also differentiated non-cancerous stromal cells from the prostate to become pro-angiogenic akin to the diseased stroma cells *in vitro*. Furthermore, exosome generated myofibroblasts enhanced tumour *growth in vivo* in comparison to the sTGF-β1 generated myofibroblasts or tumour cells rendered deficient in the secretion of exosomes via Rab27aKD (Webber *et al.* 2014). Thus TGF-β1 associated exosomes from cancer cells educate the stromal fibroblasts to become tumour-promoting, but whether exosomes can influence other precursor cells of myofibroblasts, such as mesenchymal stem cells has not been thoroughly explored.

1.5 Mesenchymal Stem Cells

Apart from fibroblasts, another precursor of myofibroblasts are bone-marrow derived mesenchymal stem cells (Mishra *et al.* 2008), which have been reported to home to tumour sites and once there, the MSCs may support tumour progression (Shinagawa *et al.* 2010). Thus studying the fate of MSCs differentiation at the tumour sites may help understand MSCs contribution to the tumour stroma.

1.5.1 Origin

The human bone marrow (BM) is a spongy, complex tissue at the centre of bones. Their main job is to produce blood cells and is composed of two distinct but independent compartments; the hematopoietic and the stromal compartment. The stromal compartment consists of a heterogeneous population of cells, such as fibroblasts, mesenchymal stem cells (MSCs), macrophages, endothelial cells, adipocytes, osteoblasts and osteoclasts which provides the structural and physiological support for hematopoietic cells (Krebsbach *et al.* 1999).

Mesenchymal stem cells (MSCs) are adult stem cells with the capacity of self-renewal and trilineage differentiation into adipocytes, chondrocytes and osteoblasts. They were first isolated from the bone marrow (BM) of guinea pigs in 1976 by Friedenstein and colleagues on the basis of their properties of adherence to plastic, spindle-shaped morphology and formation of fibroblasts colonies (Friedenstein *et al.* 1976). MSCs can also be isolated from various tissues such as the umbilical cord blood (Bieback *et al.* 2004), synovium (Orbay *et al.* 2012) and adipose tissue (Fraser *et al.* 2006). Isolation and expansion of BM-MSCs involves the aspiration of BM from the iliac crest and thereafter MSCs are isolated by Ficoll-density gradient centrifugation. The cells are seeded on plastic plates and MSCs which show plastic adherence expand whilst other cells are washed off (Pittenger *et al.* 1999). Only 0.001 to 0.01% of the cells isolated from the BM using the density gradient were in fact MSCs (Pittenger *et al.* 1999). In contrast, MSCs isolated from adipose tissue using liposuction and the gradient method, obtained 500 times more MSCs in comparison to the BM (Fraser *et al.* 2006; Kitagawa *et al.* 2006). Thus there are far more MSCs in the adipose tissue but it is the BM-derived MSCs that

are the most frequently investigated cell type and are often designated as the gold standard MSC source for studying MSC biology.

1.5.2 Classifications of MSCs: lack of stringent MSC definition

Researchers use different approaches to characterise MSCs, making it difficult to compare and contrast study outcomes. To solve this problem, the International Society of Cellular Therapy (ISCT) has set a minimal criterion for defining MSCs. Firstly, the MSCs must be plastic adherent when maintained in standard culture conditions. Secondly, the MSCs must express a varied repertoire of cell surface markers, such as CD44, CD73, CD90, CD105 and must be negative for hematopoietic markers CD14 and CD45. Thirdly and most importantly, MSCs must differentiate into osteoblasts, adipocytes and chondrocytes *in vitro* when cultured with the appropriate stimuli (Dominici *et al.* 2006). Unfortunately, the current definition suggested by the ISCT is incapable in distinguishing MSCs to other stromal cells such as fibroblasts, as they also express similar molecular repertoire (Alt *et al.* 2011; Gang *et al.* 2007). Fibroblasts do not differentiate into osteoblasts, adipocytes and chondroblasts under the same conditions. However, fibroblasts are known to have a degree of plasticity and can for example be driven to differentiate towards possessing adipocytic features (Feldon *et al.* 2006; Kuriyan *et al.* 2013). Therefore one of the obstacles to MSC research is the lack of unique markers for MSC identification. This makes it a challenge to identify MSCs as a contributor within the reactive stroma at tumour sites.

Recently, the glycoprotein, stage specific embryonic antigen 4 (SSEA-4) and ganlioside-2 (GD-2) which are usually found to be expressed in embryonic stem cells have also been discovered to be expressed in the BM-derived and adipose-derived MSCs, respectively (Gang *et al.* 2007; Martinez *et al.* 2007). Additionally, GD-2 expression was absent in foreskin fibroblasts. Even though, the function of these antigens are not very well understood, SSEA-4 and GD-2 may be associated with a multipotent function and hence may be able to distinguish MSCs from other stromal cell types. Furthermore, MSCs isolated from different sources share considerable degree of overlap in their surface expression profile, but they are known to have variations in the pattern and level of expressions at different times of culture. For example, adipose-derived MSCs initially

express CD34 but this marker is lost after culturing over time (Djouad *et al.* 2005). Other than variation in expression level of cell surface markers, there are currently no unique markers for absolute discrimination of MSCs according to their tissue of origin and from other stromal cell types.

1.5.3 Multipotent differentiation capacity

MSCs can self-renew and have the capacity to differentiate into a variety of tissue types of mesodermal lineages such as osteoblasts (Ogura *et al.* 2004), adipocytes (Qian *et al*. 2010) and chondrocytes (Song *et al.* 2007) when cultured under appropriate conditions. The osteogenic differentiation of MSC is divided in three stages. The first is MSC proliferation for around 4 days, followed by early cell differentiation which can take up to 14 days. The early osteogenic differentiation is characterised by the transcription and protein expression of alkaline phosphatase (Aubin *et al.* 2001) and the expression of collagen type I (Quarles *et al.* 1992). The final stage from days 14-28 results in a full osteogenic differentiation as observed by a high expression of osteopontin and osteocalcin and the deposition of calcium and phosphate (Huang *et al.* 2007; Hoemann *et al.* 2009). Similarly the adipogenic differentiation, characterised by the formation of lipid droplets and the chondrogenic differentiation identified by cartilage-specific extracellular matrix (such as aggrecan and collagen type II), take around 21 days to complete (Pittenger *et al.* 1999; Barry *et al.* 2001). Therefore the differentiation of MSCs into another cell type is a slow process.

The differentiation of MSCs *in vitro* are totally dependent on culture conditions. Growth factors, such as the TGF-β family are essential for chondrogenic differentiation, and TGF-β along with dexamethasone, an anti-inflammatory steroid molecule are required for the osteogenic differentiation (Mackay *et al.* 1998; Jaiswal *et al.* 1997; Barry *et al.* 2001). Whereas MSCs differentiate into adipocytes when cultured with dexamethasone, isobutyl methyl xanthine, insulin and indomethacin (Pittenger *et al.* 1999). Thus there are some overlaps in culture conditions for the tri-lineage differentiation pathway of MSCs.

1.5.4 MSCs as a therapeutic tool

The biological properties of MSCs provides beneficial use as therapeutic tools for various medical conditions.

Multi-lineage differentiation capacity

The multipotent capacity of MSCs has led to their use in regenerative medicine such as tissue engineering, where MSCs have been used in bone and cartilage repair, in osteogenesis imperfecta (OI) and osteoarthritis, respectively (Horwitz *et al.* 1999; Gupta *et al.* 2012). Due to their regenerative and their multi-lineage differentiation capacity, MSCs are also an attractive candidate for cardiovascular repair. Preclinical trials have shown MSCs to engraft and improve cardiac repair after administration (Zhang *et al.* 2006; Jiang *et al.* 2006; Nagaya *et al.* 2005). Furthermore, a randomized pilot study has shown patients with acute myocardial infarction (MI) who received BM-MSCs to have an improved cardiac function in comparison to those who received standard saline as controls (Chen *et al.* 2004). Following this study, MSCs have been used to treat both acute and chronic MI, with significant improvements in cardiac function (Yang *et al.* 2010).

Immunosuppressive property

MSCs are immunosuppressive, but the mechanisms behind this are still being investigated. Many studies report MSC-mediated immunosuppression via inhibition of immune cells such as T cells (Di Nicola *et al.* 2002; Bartholomew *et al.* 2002; Glennie *et al.* 2005; Augello *et al.* 2005 and Le Blanc *et al.* 2003) where increasing the dose of MSCs resulted in a greater decline in T-cell proliferation (Bartholomew *et al.* 2002). Furthermore, production of molecules by the MSCs, such as indoleamine 2,3-dioxygenare (IDO) and nitric oxide were up-regulated following cross-talk with T-cells, resulting in the inhibition of T cell proliferation (Meisel *et al.* 2004; Maby-El Hajjami *et al.* 2009; Sato *et al.* 2007). Additionally, MSCs secretion of prostaglandin E_2 (PGE_2) suppressed the differentiation of monocytes to dendritic cells, another immune cell type which are responsible for antigen presentation to T-cells (Aggarwar and Pittenger 2005; Németh *et al.* 2009; Spaggiari *et al.* 2009). Therefore various secreted factors by the MSCs provide an anti-immune response.

Based on the immunosuppressive property of MSCs, they have been proposed as a treatment for autoimmune diseases such as graft-versus-host disease (GVHD). GVDH is a severe inflammatory condition that results from immune-mediated attack of recipient tissues by donor T cells following an allogeneic transplantation for the treatment of malignant and non-malignant disorders (Vianello and Dazzi 2008). The clinical efficacy of MSCs in acute GVDH was first observed in a 9-year old boy with acute GVHD (Le Blanc *et al.* 2004). The patient, who was unresponsive to other therapies, showed a complete response after receiving donor MSCs. Following this pilot study, MSC treatment has been studied extensively in steroid-refractory/acute GVDH (Le Blanc *et al.* 2004; Fang *et al.* 2006; Le Blanc *et al.* 2008; Wu *et al.* 2011).

Delivery vehicles

Gene therapy involves the introduction of functional genes into the body and human BM-MSCs has been an attractive cellular vehicle for gene delivery applications because of their capacity for multi-lineage differentiation and *ex vivo* cell expansion. This makes it possible to greatly broaden the spectrum of diseases for which MSCs could provide therapeutic benefit. Gene therapy has been used to engineer MSCs, by the use of lentiviral vectors to enable MSCs to augment their own natural production of a specific desired protein or to produce proteins outside of their native repertoire (Morizono *et al.* 2003).

Using such approaches, MSCs can be used for cancer gene therapy due to their inherent migratory abilities toward tumours (Wang *et al.* 2009). MSCs have been genetically modified to overexpress various anticancer genes, such as interleukins (ILs), interferons (IFNs) and prodrugs which are anti-tumorigenic (Gao *et al.* 2010; Seo *et al.* 2011; Studeny *et al.* 2002; Ren *et al.* 2008; Miletic *et al.* 2007; Cavarretta *et al.* 2010). Even though preclinical models using gene-modified MSCs for the treatment of cancer have been well studied, clinical trials utilising engineered MSCs for cancer therapy have not yet been reported. Prior to clinical use the safety of MSC administration needs to be thoroughly explored, even though MSC administration has not yet shown any major adverse events.

Collectively, the multi-lineage differentiation capacity and immunosuppressive property of MSCs provides various beneficial functions in tissue engineering and regenerative medicine.

1.5.5. Migratory property: MSCs can migrate at tumour sites

One of the most remarkable but least understood finding is the ability of MSC to migrate from the bone marrow (BM) or peripheral blood into damaged tissues. Systemic administration of MSCs in mice and in patients demonstrated that MSCs migrate to sites of injury or disease where they enhance wound healing (Fu *et al.* 2009; Wu *et al.* 2007) or support tissue regeneration, for example in patients with myocardial infarction (Kawada *et al.* 2004). Multiple studies have used fluorescent dyes to show that BM-MSCs home to and contribute to the tumour stroma such as the colon, breast and prostate cancer (Shinagawa *et al.* 2010; Quante *et al.* 2011; Jung *et al.* 2013). However, for MSCs to reach their target tissues, they must be able to cross the endothelial barrier twice: once to enter and then again to leave the vascular system.

Transmigration

One of the first attempts to show transendothelial migration of MSC was by Schmidt *et al* (2006) who utilised isolated mouse heart perfusions with gold-labelled MSCs. Electron microscopy detected abolishment of tight cell-cell contacts in-between the endothelial cells upon MSC contact. In a later study using human lung and cardiac endothelial cells, time-lapse and confocal microscopy demonstrated MSCs expressing the cognate receptor very late antigen-4 (VLA-4) specifically binds to the adhesion molecule, vascular cell adhesion molecule-1 (VCAM-1) on endothelial cells. This resulted in a split between the endothelial cells, allowing MSCs to develop cell contacts and integrate across the endothelial layer (Teo *et al.* 2012; Schmidt *et al.* 2006; Steingen *et al.* 2008 and Matsushita *et al.* 2011).

Factors involved in MSC migration and invasion

Inflammatory cytokines have been suggested to mobilise MSCs from the bone marrow, as the concentration of cytokines increases during injury and other disease processes, which coincides with increase in MSCs within the circulation (Hong *et al.* 2009; Wang *et al.* 2008). Tumour-associated myofibroblasts secrete stromal-derived growth factor-1 (SDF-1) and matrix metalloproteinase (MMPs) proteolytic enzymes which may be involved in homing of

MSCs (Hong *et al.* 2009; Klopp *et al.* 2007; Orimo *et al.* 2005), but have not been investigated thoroughly *in vitro* or *in vivo*.

The invasion of MSCs into the surrounding tissues requires MSCs to penetrate the basement membrane that separates the endothelium from the tumour stroma. The basement membrane is a specialised form of extracellular matrix (ECM) consisting of collagen fibres, laminin and proteoglycans. For MSCs to overcome this barrier and recruit into the stroma, pronounced secretion of MMP-2 by MSCs, in response to inflammatory cytokines (TGF-β1, IL-1β and TNF-α), has been reported to play a key role in the degradation of the ECM *in vitro* (Reis *et al.* 2007). Furthermore, silencing the enzyme using RNA interference, impaired their supportive function in promoting MSC invasion. Therefore, MMP-2 supports the invasion of MSCs and other MMPs as well as growth factors which have not been investigated as thoroughly, may also be involved.

1.5.6 MSCs at the tumour site

Anti-tumorigenic

Some studies have shown MSCs which home to the tumour site, have an anti-tumorigenic effect. For example, intravenously injected MSCs migrated to kaposi's sarcoma (KS) *in vivo* and inhibited tumour growth in a dose-dependent manner (Khakoo *et al.* 2006). Examination of the interaction between the MSCs and KS were explored in a co-culture system *in vitro*. MSCs were found to inhibit the activation of the protein kinase, Akt, which is a critical mediator of KS tumour cell proliferation and survival (Khakoo *et al.* 2006). Similar anti-tumorigenic effect of MSCs were observed with hepatoma model *in vivo* (Qiao *et al.* 2008), again possibly through an anti-proliferative effect on the tumour cells. Furthermore, MSCs in a mouse melanoma model *in vivo* inhibited tumour growth, most likely via inhibition of angiogenesis. Assessment of the interaction of MSCs and endothelial cells *in vitro* revealed MSC-mediated apoptosis of the endothelial cells in a dose-dependent manner and hence destruction of capillary formation (Otsu *et al.* 2009). The MSC-mediated apoptosis, was associated with the production of MSC-derived reactive oxygen species (ROS), as the anti-oxidant NAC attenuated the increased release of MSC-derived ROS and hence reduced the damage to the capillary formation. Together, these results indicate that MSCs potentially possess cytotoxic properties and can supress angiogenesis and hence inhibit tumour growth.

Pro-tumorigenic

Whether or not MSCs themselves exhibit an anti-tumorigenic effect is still controversial as a lot of studies report MSCs to promote tumorigenesis and metastasis in various cancer models such as colon, breast, pancreatic and skin cancer *in vivo* (Djouad *et al.* 2003; Karnoub *et al.* 2007; Zhu *et al.* 2006; Direkze *et al.* 2004; Quante *et al.* 2011). MSCs mixed with weakly metastatic human breast carcinoma cells in a mice, increased the metastatic abilities of cancer cells into the lung (Karnoub *et al.* 2007). Inhibition of the chemokine, CCL5 protein expression using short hairpin (sh)RNA revealed the MSC-induced metastasis was dependent on CCL5 released from MSCs and not from the cancer cells (Karnoub *et al.* 2007). Furthermore, MSCs *in vitro* exhibited immunosuppressive property, as shown by their inhibitory effect on T-cell proliferation in a dose-dependent manner. This immunosuppressive effect of MSCs was shown to increase tumour growth when MSCs were co-injected with melanoma cells in mice, in comparison to the administration of tumour cells alone (Djouad *et al.* 2003). These studies, therefore suggest MSCs to provide factors to support migration and escape from the immune system and hence aids tumour progression.

Moreover, studies have reported MSCs to contribute to the tumour stroma as α-SMA positive myofibroblasts. One such studies revealed approximately 25% of α-SMA positive myofibroblasts in pancreatic tumours to be green fluorescent protein (GFP)-labelled donor-derived BM-MSCs (Direkze *et al.* 2004). Similar was also observed in a gastric cancer mice model (Quante *et al.* 2011; Gu *et al.* 2012), confirming that MSCs do contribute to the tumour stroma as myofibroblasts. Furthermore, these myofibroblasts were found to still hold the capacity to differentiate into adipocytes and osteoblasts once isolated from the gastric cancer stroma *in vivo* and cultured under the appropriate conditions (Quante *et al.* 2011). This indicates that MSCs still retain their multi-potency function after myofibroblastic differentiation.

1.5.7 Cancer exosomes may be involved in MSC differentiation into myofibroblast-like cells

Human BM-MSCs cultured with breast cancer conditioned media differentiated into α-SMA positive myofibroblast-like cells and promoted tumour growth *in vivo* (Mishra *et al.* 2008). However, the molecular factors secreted by the cancer cells, responsible for driving this particular differentiation programme remain incompletely understood. Similar to our observation with fibroblasts (Webber *et al.* 2010), some recent studies have pointed a potential role of cancer cell secreted exosomes in driving the myofibroblastic differentiation of MSCs. Such experiments reveal, exosomes from gastric cancer and breast cancer to differentiate human umbilical cord derived and adipose derived MSCs into α-SMA positive myofibroblasts, respectively (Gu *et al.* 2012; Cho *et al.* 2012). However, these experiments failed to successfully show the mechanism involved in this exosome-driven differentiation. Exosome treated MSCs were noted to have a small increase in phosphorylated SMAD-2/3 in comparison to the untreated MSCs and this effect was reduced with the TGF-β receptor inhibitors, indicating a TGFβ-SMAD dependent pathway may be involved, similar to that of exosome-mediated fibroblast-to-myofibroblast differentiation. However, whether the breast and gastric cancer exosomes express TGF-β and whether the expression of α-SMA stress fibres in the differentiated MSCs are attenuated by the blockage of TGF-β signalling was not shown. Thus the mechanism involved in the exosome-mediated generation of myofibroblasts from MSCs remains unknown. Furthermore the current studies lack information regarding the time and dose of exosome required to differentiate MSCs into α-SMA positive myofibroblasts. An important aspect, which has yet to be investigated, is the phenotype and function of myofibroblasts derived from MSCs exposed to exosomes. We know that α-SMA does not define the tumour promoting features of myofibroblasts, as α-SMA positive myofibroblasts generated from fibroblasts induced by cancer exosomes or sTGF-β have distinctive functions, in which the exosome generated fibroblasts are tumour-promoting (Webber *et al.* 2014). Thus a lot is unknown regarding the differentiation of MSCs into myofibroblasts and subsequently their role, if any in tumour progression.

1.5.8 Study Aims

In this thesis, we address the hypothesis that prostate cancer exosomes expressing TGF-β1 exert an influence on BM-MSCs, capable of modulating their differentiation towards tumour-promoting stromal cells.

In order to investigate this, the major aims of the thesis are to:

1. Assess the phenotype of BM-MSCs, following their exposure to prostate cancer exosomes expressing TGF-β1.
2. Investigate the effect of exosome-differentiated BM-MSCs in modulating the behaviours of endothelial and tumour cells.

Chapter 2: Materials and methods

2.1. Culture of human cells

2.1.1 Monolayer culture

Prostate cancer DU145 or PC3 cell lines were purchased from ATCC and the cells were expanded into bioreactor flasks (Integra, Nottingham, UK). The cells were cultured in RPMI 1640 (Lonza, Wokingham, UK), supplemented with penicillin (100 U/ml) and streptomycin (100 µg/ml) and 10% foetal bovine serum (FBS). Bovine derived exosomes were removed from FBS by ultracentrifugation at 100,000 g for 24h, followed by filtration through 0.2 µm and then 0.1 µm vacuum filters, (Millipore, Watford, UK). For some experiments DU145 rendered deficient in Rab27a using a ribozyme or the lentiviral shRNA knockdown method, were used (Webber *et al.* 2014). Human bone marrow MSCs were purchased from Promocell and expanded according to the supplier's instructions using Promocell culture media, with their supplement mixture. For differentiation experiments the expansion culture medium was replaced by DMEM-low glucose (Lonza) with 10% MSC-optimised FBS (also rendered exosome depleted as above). All experiments were conducted with early passage MSC (up to passage 5). Adult lung fibroblasts (Coriell Institute for Medical Research, USA) were cultured in DMEM/F12 (Lonza) containing penicillin/streptomycin and 10% exosome depleted FBS (Life technologies). Human umbilical vein endothelial cells (HUVEC) were purchased from Lonza, and maintained using the EBM2-bullet kit. For functional assays, these additional growth factor supplements were withdrawn for the duration of the experiments.

2.1.2 Bioreactor flasks for prostate cancer cell lines

DU145 or PC3 cells were seeded into bioreactor flasks (Integra, Nottingham, UK), and maintained at high density culture for exosome production. These flasks have two compartments; a cellular compartment and a nutrient medium compartment (figure 2.1) which are separated by a semi-permeable membrane. The membrane provides exchange of nutrients from medium to the cells and removal of waste products from the cells, into the outer compartment. The exosomes secreted by the cancer cells are retained in the cellular compartment (can hold up to volume of 20ml). Since the cells are maintained at higher density compared to T75cm^2 flasks, exosomes can therefore be purified from small volumes at high yields in comparison to T75cm^3 culture flasks. The exosome yields from bioreactor flasks can be 8-10 times greater than traditional T75cm^3 culture flasks (Mitchell *et al.* 2008).

The culture media (CM) from bioreactor flasks containing prostate cancer cells were removed and replaced with fresh media on a weekly basis. The CM from prostate cancer cells containing

exosomes (from the cellular compartment) were centrifuged at 400 g, 4°C for 10 min, followed by and additional spin at 2000 g for 15 min to remove dead cells and cellular debris. The supernatant was collected and filtered using a 0.22µm filter (MILLEX GP Filter), to remove any remaining debris and larger vesicles. The supernatant was stored at -80°C until required for exosome purification.

Bioreactor flask

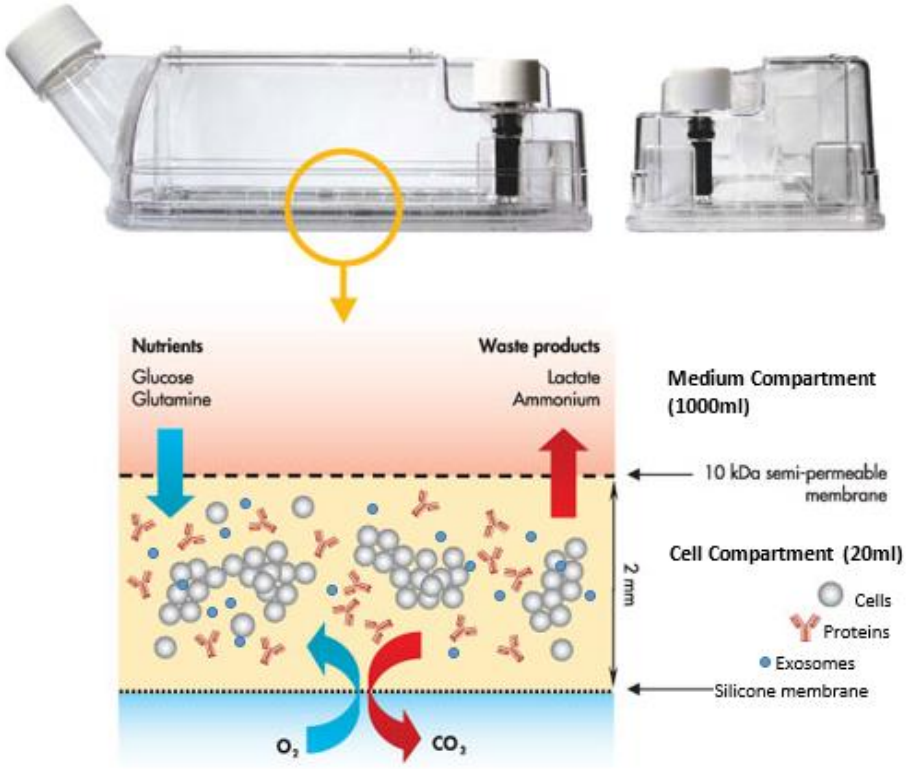

Figure 2.1*:* **Bioreactor flask.**
The cell compartment containing exosomes are separated from the medium compartment by a 10kDa semi-permeable membrane. The membrane allows a continuous diffusion of nutrients and waste products between the two compartments. The silicone membrane at the base of the cell compartment ensures an efficient gas transfer.
Source: *Adapted from Integra CELLine™ website*

2.2 Isolation and characterisation of exosomes

2.2.1 Continuous sucrose gradient

To characterise exosomes based on their classical density range of 1.1-1.2 g/ml, the continuous sucrose gradient was used. To do this, pre-cleared DU145 and PC3 conditioned media (CM) stored at -80^{o}C were defrosted at 37^{o}C. The CM were centrifuged at 120,000 x g for 40 min (4^{o}C) in a fixed-angle TLA110 rotor using Optima max ultracentrifugation (Beckman Coulter) to obtain an exosomal pellet. The pellet was resuspended in a small volume of PBS (200µl) and overlaid on top of a continuous sucrose gradient (0.2M-2.5M) in a polyallomer centrifuge tube (Beckman Coulter). The continuous sucrose gradient was produced using a gradient maker, consisting of two chambers (Hoefer S614, GE BioScience). One chamber was filled with 0.2M sucrose solution and the second chamber with 2.5M sucrose solution. The exosome-loaded gradient was ultracentrifuged (using the Optima-Max ultracentrifuge) at 210,000 x g with a swing out rotor (MLS-50) for 18h at 4^{o}C. Additionally, a second gradient was made to provide a balance during the spin.

Fractions of 330µl were collected carefully from the top to the bottom of the gradient, in which a total of 14-15 fractions were obtained. The refractive index of each fraction and from this, the density was calculated as described previously (Raposo *et al.* 1996), using the conversion table provided by Beckman Coulter- the relationship between density and refractive index is linear.

2.2.2 Sucrose cushion method

For all experiments, unless otherwise stated, the exosomes were isolated from their conditioned medium (CM) using the sucrose cushion method which is a much shorter technique for isolating exosome in comparison to using the continuous sucrose gradient. The sucrose cushion method involved defrosting the pre-cleared DU145 or PC3 CM which were stored at -80^{o}C. The CM underwent ultracentrifugation at 10,000 g for 1.5h 4^{o}C as an additional clearing step (Optima LE80K Ultracentrifuge, Beckman Coulter, High Wycombe, UK). The CM was underlain with a 4ml cushion of 30% Sucrose/ deuterium oxide (D_2O) (density of 1.2g/ml), and subjected to ultracentrifugation at 100,000 g (with a SW32 rotor, Beckman Coulter) for 2h at 4^{o}C. Around 2ml of centre most part of the

sucrose cushion was collected and washed by dilution in excess PBS and spinning at an additional 100,000 g using a fixed angle rotor to obtain an exosome pellet (70Ti rotor, Beckman Coulter). The exosome pellet was resuspended in 50-150µl PBS and stored at -80^{o}C until required for experimental use. Thus in total, exosomes have been frozen and thawed twice before their use in experimental studies.

The protein concentration of the exosome sample was evaluated using the microBCA protein assay (Thermo Scientific, Loughborough, UK). A standard curve was performed by serial dilution of 2000µg/ml BSA to 0µg/ml. Exosome samples were diluted 1:8 with PBS and absorbance values were extrapolated from the standard curve to calculate the protein concentration. Unless stated otherwise, purified DU145 exosomes and PC3 exosomes were used in BM-MSC differentiation experiments at a dose of 150µg/ml and 75 µg/ml respectively which is equivalent to a dose of 1ng/ml sTGF-β1 as described previously (Clayton *et al.* 2007; Webber *et al.* 2010).

2.2.3 Nanoparticle Tracking Analysis

The Nanoparticle Tracking Analysis (NTA) visualises and analyses nanometre particles in liquids from 10-2000nm. The size of the particles are related to the rate of Brownian motion, temperature and the viscosity of the liquid. Each exosome preparation was taken and particle counts and size distribution was determined using NTA (NanoSight Ltd, Amesbury, UK). The instrument was configured with a 488nm LM14 laser module and a high sensitivity digital camera system (OrcaFlash2.8, Hamamatsu C11440, NanoSight Ltd, Amesbury, UK). Six replicate videos of 30s were taken at 25^{o}C, with samples under controlled flow (with the syringe pump speed set to 80), and batch-analysed using NTA-software (version 2.3), with the minimal expected particle size set to automatic, and camera sensitivity set at 14-16 and detection thresholds set to 1-3, to reveal small particles. Samples were diluted in clinical water, free of particles (Fresenius Kabi, Runcorn, UK) to a concentration between $2x10^{8}$ and $9x10^{8}$ particles/ml within the linear range of the instrument. Prior to analysis of exosomal samples, 100nm standard latex beads were tested as a control to confirm the NTA measurements are accurate.

The estimated purity of exosomal samples was determined using particle to protein ratio (P:P) (P/µg) as described previously (Webber and Clayton 2013). The protein and particle concentration were measured by the BCA assay and Nanosight, respectively and used to calculate the P:P ratio. Webber and Clayton's study (2013) involved the isolation of exosomes using different methods with or without incremental doses of contamination.

This led them to propose an arbitrary threshold, in which ratios greater than $3x10^{10}$ P/µg are of high purity, ratios of 2×10^9 to 2×10^{10} P/µg represent low purity and ratios below 1.5×10^9 P/µg are unpure. In this thesis, these arbitrary thresholds were used to estimate the purity of exosomal preparations.

2.2.4 Cryo-Transmission Electron Microscopy

The morphology of exosomes were examined using a cryo-transmission electron microscopy (cryo-TEM) in collaboration with Dr. Georgi Lalev (Cardiff University). DU145 and PC3 exosome pellets purified using the 30% sucrose/D_2O cushion method were resuspended in PBS (at a dilution of 1:10,000). 1µl of the exosomal sample was applied onto a carbon grid (JEOL) and blotted with filter paper to remove excess fluid. The specimen grid was then rapidly plunged into liquid ethane that has been pre-cooled to liquid nitrogen temperature (-175^{o}C) to prevent the formation of ice crystals. The specimen grid was transferred into a cryo holder and inserted into the JEM-2100 LaB 6 cryo-TEM (JEOL, Peabody, MA, USA) to view nano-sized particles present within the sample using the JEOL TEMography^{TM} software system. This method currently remains incompletely optimised at Cardiff University, and this is ongoing and being undertaken by the group.

2.2.5 Microplate-immuno-phenotype assay

Purified exosomes were diluted in PBS and immobilised onto high protein binding ELISA strips (Fisher) at a dose of 1µg/well and incubated overnight at 4^{o}C. The exosome wells were washed 3 times using PBS, to remove unbound particles. Following 2h blocking (1% BSA/PBS w/v), primary monoclonal antibodies (mAbs) were added at 2µg/ml, for 1h at RT, including; anti-CD9 (R&D Systems), CD81, CD63 (Serotec), MHC Class-I (eBioscience), PSCA (Santa Cruz), GAPDH and isotype (IgG1 and IgG2b) control (eBiosystems). After

washing wells with 0.1% BSA/PBS (w/v) the primary mAbs were detected by goat anti-mouse biotinylated antibody (Perkin Elmer) (diluted in 0.1% BSA/PBS (w/v) in a 1:5000 dilution) for 1h RT. Signal was assessed by adding Europium-streptavidin conjugate (Perkin Elmer), for 40min at RT. The wells were washed 6 times and enhancement solution (Perkin Elmer) added for 10min and signal assessed by time-resolved fluorimetry on a Wallac Victor-II multi-label plate reader (Perkin Elmer).

2.2.6 Cell lysates and western blotting

Lysates of exosomes (purified from the sucrose cushion) or whole cells ($1x10^6$ cells) were prepared by resuspending in RIPA buffer containing 1X protease inhibitor cocktail (Santa Cruz). To remove insoluble materials, the samples were centrifuged at 10,000 g for 10 min (4^oC), split into aliquots and stored at -80^oC. Protein concentration was determined by Bradford protein assay (BioRad, Hertfordshire, UK).

Cell lysates (10µg) and exosomes (10µg) were boiled in SDS sample buffer (Invitrogen), either reducing with the addition of 20mM Dithiothreitol (DTT) or under non-reducing conditions. Samples as well as molecular weight markers (Precision Plus Protein™ Standards, Invitrogen) were subjected to electrophoresis for 1h on NuPAGE precast 4%-20% Bis-Tris gradient gels (Invitrogen). The gels were run using 1x NuPAGE MOPS SDS running buffer (Invitrogen) and Invitrogen PowerEase™ 500 power supply. Proteins were transferred to a methanol-activated PVDF membrane (GE Healthcare) using 25mM Tris, 192mM glycine (both Sigma) and a BioRad Mini Trans-Blot Electrophoretic Transfer Cell (BioRad Laboratories Inc, Hemel Hempstead, UK). The tank was kept cool by placing on ice with BioIce cooling unit in the tank and the blots were run for 1.5h at a constant 80V. The membranes were blocked in PBS containing 0.5% (w/v) Tween-20 (Sigma) and 3% (w/v) non-fat powdered milk. Membranes were probed with antibodies including TSG101, ALIX, LAMP-1, Calnexin (Santa Cruz), 5T4 (gift from Oxford Biomedica UK Limited), MHC Class I (Clone HC-10; gift from Dr E Wang from Cardiff University) and GAPDH (Bio Chain) at 1µg/ml for 1h at RT. After membranes were washed 3x for 5min in 0.5% Tween20 in PBS and incubated with goat anti-mouse-HRP conjugate (Santa Cruz), bands were detected using X-ray film (GE Healthcare, Buckinghamshire, UK) and a chemiluminescence reagent (Super Signal West Pico, Thermo Scientific).

2.2.7 TGF-β1 ELISA

Quantification of TGF-β1 was performed using the DuoSet ELISA Development System (R&D Systems). A serial dilution of TGF-β1 standard from 2000pg/ml to 0pg/ml was prepared in 0.1% BSA in PBS to generate a seven point standard curve. Different doses of prostate cancer exosomes (1µg, 5µg, 10µg and 15µg) were prepared in 0.1% BSA in PBS. To activate latent TGF-β1 to the immunoreactive form detectable by the Quantikine TGF-β1 immunoassay, the exosome samples (100ul each sample) were acid activated using 20µl of 1N HCL, vortexed and incubated for 10min at RT. The acidified samples were then neutralised by adding equal volume (20µl) of 1.2N NaOH/0.5M HEPES. 1N HCL (100mL) was prepared by adding 8.33mL of 12N HCL to 91.67mL deionised water. 1.2N NaOH/0.5M HEPES (100mL) was prepared by adding 12mL of 10N NaOH and 11.9g of HEPES to 75mL deionised water. The pH was measured after neutralisation to ensure pH was within 7.2-7.6. Once neutralised the standards and samples were added to the 96 microplate strips (100ul/well), covered with adhesive strips and incubated for 2h at RT (The samples were run in triplicates). The wells were aspirated and washed three times using 1x Delfia buffer (PerkinElmer) and TGF-β detection antibody (biotinylated goat anti-human at 300ng/ml) diluted in 0.1% BSA in PBS, was added to the wells, covered and incubated for another 2h at RT.

The plate was aspirated and washed again using Delifa buffer x 3 and streptavidin-conjugated europium in Delfia assay buffer (PerkinElmer) (1:1000) was added to the wells and incubated for 45 min at RT. The microplate was aspirated and washed x6 using Delfia wash buffer and enhancement solution (PerkinElmer) added for 5 min and signal measured using time resolved fluorimetry on the Wallac Victor 2 (PerkinElmer). The absorbance values were extrapolated from the standard curve to calculate the TGF-β1 concentration of the sample.

2.3 BM-MSC Differentiation

2.3.1 Growth Arrest

Prior to all experiments, BM-MSCs were growth-arrested in serum-free medium for 24h to allow cell cycle synchronisation. To do this, the Promocell culture media with supplement mix was removed via aspiration and the cells were washed using serum-free DMEM-low glucose to remove any residual FBS. Fresh serum-free medium (DMEM-low glucose) was then added to the cells for 24h. In all experiments, unless otherwise stated, the cells were cultured in DMEM (low-glucose) with 1% FBS, as BM-MSCs become senescent with long term serum deprivation.

2.3.2 Adipogenic Differentiation

6 x 10^4 BM-MSCs or lung fibroblasts were cultured in wells of a 24 well plate and once confluent the cells were given adipogenic induction medium (DMEM containing insulin, dexamethasone, indomethacin and IBMX) as described (Pittenger *et al.* 1999). In addition soluble recombinant human TGF-β1 (1ng/ml) or DU145 exosomes (150µg/ml) was added along with the induction medium to some wells. Fresh adipogenic induction medium was given every 2-3 days over a period of 21 days, with the exception of day 7 and day 15, in which maintenance medium (DMEM with only insulin and FBS) was given. After 21 days of differentiation, adipocytes were fixed in 4% (w/v) paraformaldehyde (ebioscience) and lipid droplets stained with Oil Red O Solution and counterstained with haematoxylin solution (both from Chemicon International, Ternecula, US).

2.3.3 Myofibroblastic Differentiation

BM-MSCs were cultured in 8 well chamber slides or 24 well plates with Promocell culture media with supplement mixture and once 70% confluent, the cells were growth-arrested for 24h. The cells were then stimulated with 150µg/ml of DU145 exosomes or 75µg/ml of PC3 exosomes or the equivalent of sTGF-β1 (1ng/ml) (added in DMEM 1% exosome-depleted FBS) for 14 days. In some experiments this was done in the presence of a neutralising TGF-β antibody at 10µg/ml (R&D Systems), or an inhibitor of the Alk-5 TGF-β receptor-1 (SB431542) at 10µM (Sigma, Dorset, UK). In other experiments, BM-MSCs were also cultured in conditioned media of normal or exosome-deficient DU145 cells (by either ultracentrifugation or Rab27a knock down using the ribozyme silencing method).

For kinetics and dose experiments, BM-MSCs were exposed to 150µg/ml over different time points (day 0, 3, 6, 9 and 14) or BM-MSCs exposed to variable exosome doses (0-300µg/ml). The cells were stained for α-SMA and the proportion of positive cells were manually counted across 6 microscopic fields and triplicate treatments unless stated otherwise.

2.4 Characterisation and phenotyping of cells

2.4.1 Light microscopy and immunohistochemistry

Light microscopy was used to examine the general morphology of cells *in vitro*. DU145, PC3, fibroblasts, myofibroblasts and BM-MSCs in 75cm^3 or 25cm^3 culture flasks, at 70-100% confluence were viewed under phase-contrast using a Zeiss AxoiVert 40 CFL microscope (Carl Zeiss Ltd, Welwyn Garden City, UK). Images were captured using the Canon Powershot G6 digital camera and Canon utilities remote capture (v.2.7.5.27).

For indirect immunofluorescence analysis, the monolayer of DU145 and PC3 cells were seeded at 20,000 cells/well in the wells of 8 chambered cover glass slides (Fisher) and incubated until ~70% confluent. Similarly, stromal cells such as fibroblasts, myofibroblasts, as well as untreated, TGF-β1 or exosome treated BM-MSCs were cultured in chamber slides. The cells were gently washed 3x in pre-warmed phosphate buffered saline (PBS) (Lonza) and fixed in fresh ice-cold acetone: methanol (1:1 v/v) (Fisher Scientific) for 5 min and allowed to completely air dry at room temperature. The cells were washed with PBS and blocked for 1.5h at room temperature (RT) in 1% Bovine serum albumin (BSA) (R&D Systems) in Hanks' balanced salt solution (HBSS) (Sigma). The cells were washed 3 times using 0.1% BSA/HBSS (w/v) and were then stained with unconjugated anti-mouse monoclonal antibodies (shown in table 2.1) at 1µg/ml (in 0.1% BSA/HBSS w/v) for 1h at RT. The cells were washed 3 times again and goat- anti mouse secondary antibody (Alexa-488) at 10µg/ml was applied (Invitrogen) for 40 min at RT, in the dark. Following another 3 washes, the cells were counterstained with 4',6-diamidino-2-phenylindole (DAPI) (14.3mM) (Invitrogen) diluted 1:50,000 in 0.1% BSA/HBSS (w/v) for 10 min, followed by 3 further washes and the cells were visualised by wide-field fluorescence (AxioVert, Zeiss).

2.4.2 Phenotypic assessment by flow cytometry

Stromal cells were seeded in 6-well plates at 80,000 cells/well. Once confluent, cells were harvested using accutase (Promocell) and centrifuged to obtain cell pellets which was then resuspended in PBS to form a homogenous suspension. The resuspended cell pellets were incubated on ice with directly conjugated antibodies (Table 2.2) at doses of 5-20µl/test (as recommended by the supplier) for 1h. Matched isotype controls included

as negative controls. Resuspended cell pellets which were incubated with unconjugated antibodies for 1 hr such as GD-2 (BD Bioscience) were detected using Alexa-488 labelled goat-anti-mouse secondary antibody (1:200 from Invitrogen) for 40 min and then washed in PBS. Cells were analysed using a FACScanto cytometer (Beckton Dickinson, Oxford, UK).

Antibodies used for immunohistochemistry

Primary antibody against:	Target protein details	Source	Final concentration
CK-7 (IgG1)	Epithelial cytoskeletal protein	Santa Cruz	1µg/ml
CK-8 (IgG1)	Epithelial cytoskeletal protein	Santa Cruz	1µg/ml
CK-19 (IgG1)	Epithelial cytoskeletal protein	Santa Cruz	1µg/ml
α-Tubulin (IgG2a)	Cytoskeletal component	Santa Cruz	1µg/ml
CD9 (IgG2b)	Tetraspanin	R&D Systems	1µg/ml
CD81 (IgG1)	Tetraspanin	R&D Systems	1µg/ml
CD63 (IgG1)	Tetraspanin	R&D Systems	1µg/ml
PSCA (IgG1)	Prostate stem cell antigen	Santa Cruz	1µg/ml
MUC-1 (IgG1)	Tumour-associated antigen	Santa Cruz	1µg/ml
α-SMA (IgG2a)	Myofibroblast marker	Santa Cruz	1µg/ml
EEA-1 (IgG1)	Early endosome marker	Santa Cruz	1µg/ml
LAMP-2 (IgG1)	Glycoprotein	Santa Cruz	1µg/ml
MMP-1 (IgG1)	Enzyme	Santa Cruz	1µg/ml
MMP-3 (IgG1)	Enzyme	Santa Cruz	1µg/ml
MMP-13 (IgG1)	Enzyme	Santa Cruz	1µg/ml
SerpinA-1 (IgG1)	Serine protease Inhibitor	Santa Cruz	1µg/ml
CD31 (IgG1)	Endothelial cell marker	Santa Cruz	1µg/ml
IgG1	Isotype control	ebioscience	1µg/ml
IgG2a	Isotype control	ebioscience	1µg/ml
IgG2b	Isotype control	ebioscience	1µg/ml

Table 2.1: List of antibodies used to assess phenotype of cells by indirect immunohistochemistry. Matched isotype controls were included as negative controls.

Antibodies for phenotypic analysis by flow cytometry

Primary antibody against:	Target protein details	Source	Final concentration
SSEA-4 FITC (IgG3)	Cell surface glycosphingolipids	R&D Systems	10µl/test
Unconjugated GD-2 (IgG2a)	Disganglioside	BD Bioscience	10µg/ml
CD146 FITC (IgG2a)	Cell adhesion molecule	Biolegend	10µg/ml
CD44 PE (IgG1)	Cell surface glycoprotein	BD	20µl/test
CD90 PE (IgG1)	(Thy-1) cell surface molecule	eBioscience	20µl/test
CD105 APC (IgG1)	(Endoglin) Cell surface glycoprotein	eBioscience	5µl/test
CD73 PE (IgG1)	Cell surface molecule	BD Pharmingen	20µl/test
CD14 APC (IgG1)	Haematopoietic marker	eBioscience	5µl/test
CD45 PE-Cy5 (IgG1)	Haematopoietic marker	eBioscience	20µl/test
FITC (IgG2a)	Isotype control	BD Phosflow	20µl/test
APC (IgG1)	Isotype control	eBioscience	20µl/test
PE (IgG1)	Isotype control	eBioscience	5µl/test
PE Cy5 (IgG1)	Isotype control	BD Pharmingen	5µl/test
FITC (IgG3)	Isotype control	eBioscience	10µl/test

Table 2:2: List of antibodies used to assess phenotype of cells by fluorescence-activated cell sorting (FACS). Matched isotype controls were included as negative controls.

2.4.3 Enzyme-Linked Immunosorbent Assay (ELISA)

The quantity of VEGF-A or HGF present in cell conditioned media (CM) of BM-MSCs was assayed using the DuoSet ELISA system (R&D Systems). The manufacturer's instructions were followed, in which the VEGF-A or HGF capture antibody at a dose of 1µg/ml (mouse anti-human against VEGF-A or HGF) were added to a 96-well microplate (Greiner) at 100µl per well and incubated overnight at room temperature (RT). Unbound antibody was removed by aspiration and the wells were washed 3 times with Delfia wash buffer (1X diluted in water) (Perkin Elmer, Cambridge, UK). Thereafter, blocking buffer was added to the wells (1% BSA in PBS) for 1 hour, followed by the addition of a serial dilution of recombinant human VEGF-A and HGF standards (diluted in 0.1% BSA in PBS) starting from 2000pg/ml or 8000pg/ml, respectively to 0pg/ml, to create a seven point standard curve.

Secondly, the CM from the BM-MSCs was normalised for cell count and lightly spun using the bench centrifuge to remove any large cellular debris. Since the protein concentration is unknown, the CM was diluted at a high and low range (1:2 and 1:6) in 0.1% BSA in PBS and applied to the wells and incubated for 2h at RT. The wells were aspirated and washed and VEGF-A or HGF detection antibody (biotinylated goat anti-human antibody against VEGF-A or HGF) at 50ng/ml or 200ng/ml, was added respectively for 2h at RT. After another aspiration and wash step, the colourimetric HRP-based detection antibody recommended by the manufacturer was substituted for streptavidin-conjugated Europium diluted in Delfia assay buffer in a 1:1000 dilution (both from PerkinElmer) and applied to wells for 45 min, at RT. Lastly, the microplate was washed 6x using the Delfia wash buffer and enhancement solution (PerkinElmer) added for 5 min and signal measured using time resolved fluorimetry on the Wallac Victor 2 (PerkinElmer). The absorbance values were extrapolated from the standard curve to calculate the VEGF-A or HGF protein concentration of the sample.

2.4.4 PCR Fibrosis Array

RNA Extraction

In order to examine potential differences in the phenotype of differentiated BM-MSCs following exosome or sTGF-β1 treatment, a PCR fibrosis array was used. To do this, firstly

the cellular RNA of the untreated or treated BM-MSCs cultured in 6-well plates was extracted at day 3 using 1ml Tri-Reagent per well (Sigma-Aldrich). Thereafter 200µl chloroform was added to the samples and was mixed by inverting the sample several times in eppendorf tubes. The samples were incubated on ice for 5 min to allow separation of the aqueous and phenol phases and centrifuged at 12,000 x g for 20min at 4^0C. The colourless aqueous layer containing RNA was removed and mixed with an equal volume of ice-cold isopropanol and incubated at -20^0C for 24h. The samples were again centrifuged at 12,000 x g for 20min at 4^oC, to wash away the isopropanol and the pellets were washed in ice-cold 75% ethanol (v/v) by inversion and centrifuged again at 12,000 x g for 20min at 4^0C. This step was repeated again and thereafter, the RNA pellets were air dried at RT and dissolved in 20µl H_2O.

Determining the RNA concentration

The RNA sample was diluted (1:50) in RNAse free H_2O (1µl RNA in 49µl H_2O) and the Nanodrop 2000 Spectrophotometer (Thermo Scientific, Loughborough, UK) was used to obtain a ratio of absorbance measured at 260nm and 280nm. A ratio ≥1.7 was considered sufficiently pure RNA and used for analysis. The absorbance at 260 was used to calculate the RNA concentration as shown below. The extinction coefficient for RNA is 40 and the dilution factor of samples were 1:50.

[RNA] (µg/ml)= Absorbance$_{260}$ x dilution factor x extinction coefficient

Reverse Transcription

Total RNA (0.5µg) was reverse transcribed using the RT^2 First Strand Kit (Qiagen, Manchester, UK) to generate complementary DNA (cDNA). Reverse transcription was carried out in a final volume of 10ul per reaction containing 0.5µg of RNA, 4µl of 5x Buffer BC3, 1µl Control P2, 2µl PE3 Reverse Transcriptase Mix and 3µl RNAse- free H_2O. 10µl genomic DNA elimination mix was added to each RNA sample (each reaction) and samples were then reverse transcribed using the StepOne Plus Real-Time PCR System thermocycler (Life Technologies). This involved sample incubation at 42^0C for 15min, followed by incubation at 95^0C for 5 min. 91µl RNase-free H_2O was added to the cDNA sample and stored at -20^0C.

Quantitative Polymerase Chain Reaction (q-PCR)

The Polymerase Chain Reaction (PCR) component mix contained cDNA synthesis reaction (102µl), RNase-free water (1248µl) and 2x RT^2 SYBR Green Mastermix containing the HotStart DNA Taq Polymerase (1350µl) which was required for amplification. The mixture was prepared in a 5ml tube and vortexed. 25µl of the PCR mix was added per well of a RT^2 Profiler 96-well plate array covering 84 transcripts of known association with fibrosis (table 2.3) (Qiagen). The RT^2 Profiler Array was performed as biological triplicates for each treatment condition; the untreated, TGF-β1 treated and exosome treated BM-MSCs (9 arrays in total). The array also contained 5 housekeeping genes (β-actin, β-2-microglobulin, GAPDH, HPRT1 and RPLP0), a genomic DNA control, reverse-transcription controls and positive PCR controls. The PCR array plates were sealed with an Optical adhesive film (Qiagen) and centrifuged at 1000 g for 1 min at room temperature to remove bubbles. Amplification was carried out using the StepOne Plus Real-Time PCR System thermocycler (Life Technologies) which involved a cycle at 95^0C for 10min, so that the HotStart DNA Taq polymerase is activated, followed by 40 cycles at 95^0C for 15s and 60^0C for 1min.

The comparative Ct method was used for relative transcript quantification against the average ΔCt derived from the internal controls (β-actin, β-2-microglobulin, GAPDH, HPRT1 and RPLP0). Data was analysed using the ABI StepOnePlus software (Version 2.0 supplied by Applied Biosystems) and the data as presented as volcano plots with a p-value threshold of <0.05 and a fold-change threshold of ±3.

Human Fibrosis PCR Array

Pro-Fibrotic:	ACTA2 (α-SMA), AGT, CCL11 (Eotaxin), CCL2 (MCP-1), CCL3 (MIP-1a), CTGF, GREM1, IL13, IL13RA2, IL4, IL5, SNAI1 (Snail)
Anti-Fibrotic:	BMP7, HGF, IFNG, IL10, IL13RA2
Extracellular Matrix & Cell Adhesion:	
ECM Components;	COL1A2, COL3A1
Remodelling Enzymes;	LOX, MMP1 (Collagenase 1), MMP13, MMP14, MMP2 (Gelatinase A), MMP3, MMP8, MMP9 (Gelatinase B), PLAT (tPA), PLAU (uPA), PLG, SERPINA1 (a1-antitrysin), SERPINE1 (PAI-1), SERPINH1, TIMP1, TIMP2, TIMP3,TIMP4
Cellular Adhesion;	ITGA1, ITGA2, ITGA3, ITGAV, ITGB1, ITGB3, ITGB5, ITGB6, ITGB8
Inflammatory Cytokines & Chemokines:	CCL11 (Eotaxin), CCL2 (MCP-1), CCL3 (MIP-1a), CCR2, CXCR4, IFNG, IL10, IL13, IL13RA2, IL1A, IL1B, IL4, IL5, ILK, TNF
Growth Factors:	AGT, CTGF, EDN1, EGF, HGF, PDGFA, PDGFB, VEGFA
Signal Transduction:	
TGF-β Superfamily;	BMP7, CAV1, DCN, ENG (EVI-1), GREM1, INHBE, LTBP1, SMAD2, SMAD3, SAMD4, SMAD6, SMAD7, TGFB1, TGFB2, TGFB3, TGFBR1 (ALK5), TGFBR2, TGIF1, THBS1, THBS2
Transcription Factors;	CEBPB, JUN, MYC, NFKB1, SP1, STAT1, STAT6
Epithelial-to-Mesenchymal Transition:	AKT1, BMP7, COL1A2, COL3A1, ILK, ITGAV, ITGB1, MMP2 (Gelatinase A), MMP3,MMP9,SERPINE1 (PAI-1), SMAD2, SNAI1 (Snail), TGFB1, TGFB2, TGFB3, TIMP1
Others:	BCL2, FASLG (TNFSF6)

Table 2:3: The Human Fibrosis PCR Array profiles the expression of 84 key genes involved in dysregulation tissue remodelling during repair and healing of wounds or at tumour sites. The array contains genes encoding ECM remodelling enzymes, TGFβ signalling molecules and inflammatory cytokines as well as additional genes important for fibrosis.

2.4.5 TaqMan gene PCR

The selected transcripts (MMP-1, MMP-3, MMP-13, SerpinA-1, AGT) from the PCR fibrosis array were verified using TaqMan PCR gene expression assays. In addition, the mRNA level of Rab27a in PCa cells was also evaluated using this method. Firstly the RNA was extracted and measured the same way as mentioned above, but the RT and amplification step were different and explained below.

Reverse Transcription

Reverse transcription was performed using the random primer method in a final volume of 20µl per reaction containing 1µg of RNA of the sample, 2µl of 10x reverse transcription buffer, 0.8µl of 25mM deoxynucleotide triphosphate (dNTPs) (mixed nucleotides of dATP, dCTP, dGTP and dTTP), 2µl of 10x reverse transciption random primers, 1µl of Multiscribe^{TM} reverse transcriptase and 1µl of RNase Inhibitor. A negative control was included, which was H_2O substituted for the Multiscribe^{TM} reverse transcriptase (all from Applied Biosystems). The samples were reverse transcribed using the StepOne Plus Real-Time PCR System thermocycler which involved incubation at 25^0C for 10min to allow the primers to anneal to the RNA. The primers were then extended using the reverse transcriptase in the presence of dNTPs at 37^0C for 2hr, generating cDNA. The cDNA was then heated at 85^0C for 5s to deactivate the RT. The cDNA samples were stored at -20^0C.

Quantitative Polymerase Chain Reaction (q-PCR)

The q-PCR was carried out in a final volume of 20µl per reaction containing 1µl of sample cDNA, 10µl x2 of PCR TaqMan Master Mix, 8µl H_2O, 1µl primer + probe (primer of MMP-1, MMP-3, MMP-13, SerpinA-1, AGT, Rab27a and GAPDH) (Qiagen). A negative control was prepared using H_2O substituted for the cDNA. The PCR amplification was performed using the Step One Plus Thermocycler, involving a cycle of 95^{o}C for 1s, and 60^{o}C for 20s for 40 cycles.

The comparative C_T method was used for relative quantification of gene expression. The C_T (threshold cycle where amplification is in the linear range of the amplification curve) for the standard reference gene (GAPDH) was subtracted from the target gene C_T to

obtain the ΔC_T for each sample. The expression of the target gene in experimental samples relative to expression in control samples was calculated:

Relative expression = 2 - (ΔCT 1)-ΔCT(2))

The $\Delta C_T(1)$ is the mean ΔC_T value calculated for the experimental samples, and $\Delta C_T(2)$ is the mean ΔC_T value calculated for the control samples (GAPDH). The data was analysed using the ABI StepOnePlus software (Version 2.0 supplied by Applied Biosystems).

2.5 Rab27a knock down

Exosomes secretion is regulated by Rab27a GTPase (Ostrowski *et al.* 2010) and hence the knock down of Rab27a in DU145 cells, is expected to negatively influence exosome secretion. Our Rab27a^{KD} was achieved through collaboration with Prof Wen Jiang (Department of surgery and tumour biology, Cardiff University) who have routinely established the ribozyme method for gene silencing and the DU145$^{Control\ Vector}$ and DU145^{Rab27aKD} cells were used for some experiments in this thesis (Oncotarget, 2014). However during my study the more stable lentiviral approach was developed by our group and cells obtained by this approach were used in the later part of the studies. The two different methods for Rab27a^{KD} are described below.

2.5.1 Ribozyme silencing method

One way to silence genes is by the use of ribozymes. Ribozymes are catalytic RNA molecules used to inhibit gene expression by cleaving to the mRNA molecules via Watson-Crick base pairing, and so silencing the genes by preventing translation, as shown in figure 2.2A (Xiet *et al.* 1997; Dorsett and Tuschl 2004). Cleavage by ribozyme also requires divalent ions, such as magnesium and ribozymes are short enough to be chemically synthesised or transcribed from a vector, allowing a continuous production of ribozymes within the transfected cells (Dorsett and Tuschl 2004).

Rab27a knock down using the ribozyme silencing method was carried out by a collaborator, Prof Wen Jiang (Jiang *et al.* 2006). This involved designing a hammerhead ribozyme transgene targeting human Rab27a using Zukers RNA mfold programme (Zuker *et al.* 2003) and synthesised by Sigma-Aldrich. These were subsequently cloned in mammalian pEF6/V5 vector, amplified in E.coli and uptake of vector verified by their resistance of ampicillin (100µg/ml). 1 x 10^6 DU145 cells were transfected with the vectors using electroporation and cells which had taken up the vector were selected based on their resistant to blasticidin (5µg/ml). DU145$^{Control\ Vector}$ (carrying the empty vector pEF6/V5) and two DU145^{Rab27aKD} attempts were made, named Rab27aKD2 and Rab27aKD3. The cells were cultured in RPMI 10% FBS containing blasticidin at a high dose of 5µg/ml for 1 week and thereafter the dose of blasticidin was reduced to 0.5µg/ml. The knockdown of Rab27a was confirmed by qPCR. For functional

experiments, blasticidin was not used. Such experiments included the collection of conditioned media from the DU145$^{\text{Control Vector}}$ or DU145$^{\text{Rab27aKD}}$ cells to treat BM-MSCs and the use of these mutated cells for the xenograft experiment to assess tumour growth.

2.5.2 shRNA lentiviral method

Gene silencing was also carried out using a short hairpin RNA (shRNA) which is a sequence of RNA that makes a tight hairpin turn that can be used to silence target gene expression via RNA interference (RNAi). RNAi is a biological process in which RNA molecules inhibits gene expression by causing destruction of specific mRNA molecules. shRNA was in these studies delivered using lentiviral vectors as shown in figure 2.2B. Once the vector has integrated into the host genome, the shRNA are transcribed in the nucleus and the resulting shRNA are exported out of the nucleus and processed by Dicer (ribonuclease) and loaded into the RNA-induced silencing complex (RISC). This complex cleaves the target mRNA and thus represses translation of the mRNA, resulting in target gene silencing.

For my studies, the DU145$^{\text{NM Control}}$ (transduced with a non-mammalian control shRNA) and DU145$^{\text{Rab27aKD}}$ cells used, were previously generated by Dr Jason Webber. The DU145 cells were plated in a 48-well flat-bottomed plates at 18,000 cells/well, in exosome-depleted media. At day 1, the cells were infected with lentiviral particles (MOI=10) in the presence of Hexadimethrine bromide (8mg/ml). At day 2, Puromycin (1.25mg/ml) was added and media was changed at day 5 and Rab27a knockdown was verified using qPCR. The cells were cultured in the presence of Puromycin for a further 6 passages prior to experimental use, such as the spheroid models to assess cellular invasion and growth.

Gene Silencing

(A)

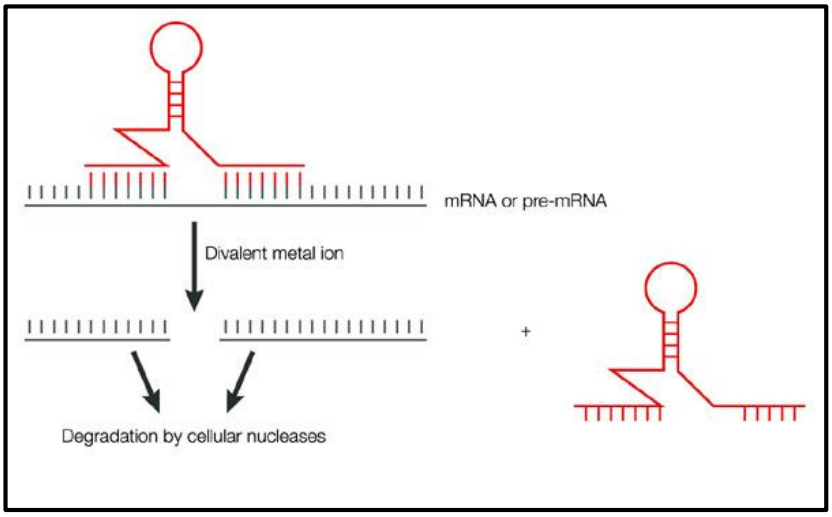

(B)

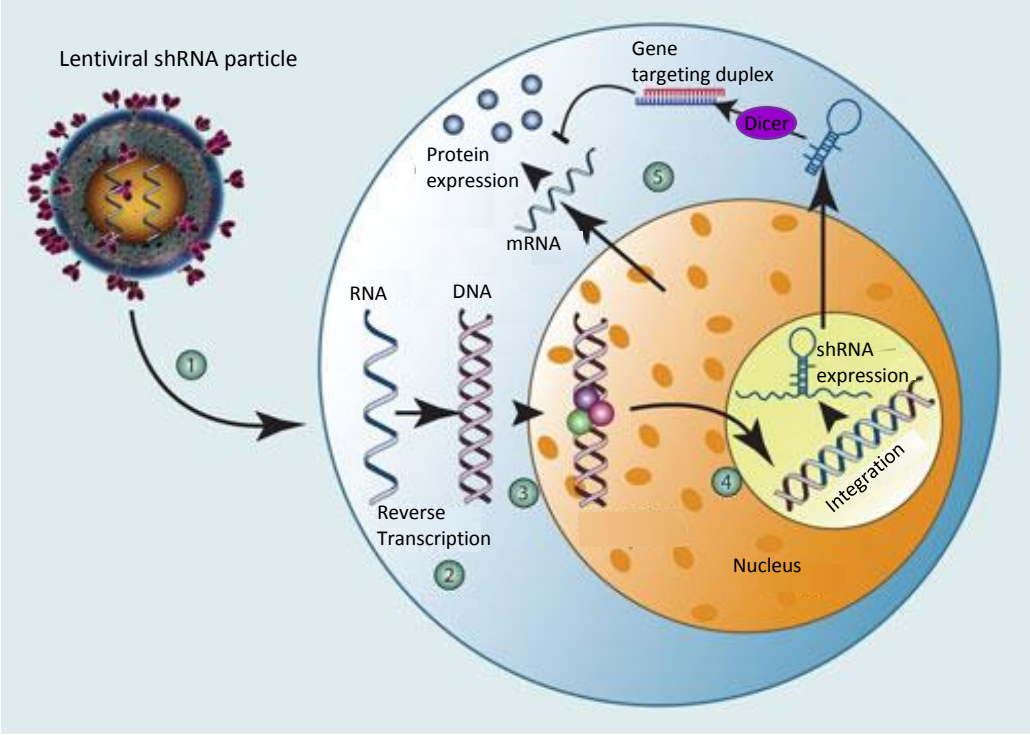

Figure 2.2: Rab27a knockdown via the ribozyme silencing and the lentivrival shRNA method. Ribozymes can be directly introduced into the cell using the mammalian pEF6/V5 vector. The hammerhead ribozyme has two arms which bind to and degrade the mRNA by cleaving via hydrolysis of the phosphodiester backbone of the mRNA and thus prevent mRNA translation into a protein (A). Lentiviral vectors can be used to stably deliver viral genome into the cytoplasm where they are reverse-transcribed (2). The DNA intermediate is imported into the nucleus (3) where it is stably integrated into the host genome (4). The silencing construct is then constitutively expressed and processed into shRNAs that forms a complex using Dicer and cleaves target mRNA, preventing its translation into proteins (5) (B).
Source: *Adapted from Dorsett and Tuschl 2004 and ThermoScientic website*

2.6 Functional experiments

2.6.1 Proliferation

Endothelial cells or prostate cancer (PCa) cells were seeded at $1x10^4$ cells/ml and cultured for 24h in growth-factor free conditions prior to stimulations. BM-MSCs were pre-treated for 4d with exosomes (150µg/ml) or sTGF-β1 (1ng/ml) and conditioned media (CM) was harvested and centrifuged at 400 g to remove cellular debris. BM-MSCs CM normalised for cell count was added to endothelial cells or PCa cells at a ratio of 1:1 (v:v) with EBM2-medium or RPMI media, and incubated for 6 or 3 days respectively. Endothelial and PCa cells were harvested using accutase or trypsin, respectively (Lonza) and the cellular pellet obtained after centrifugation at 400 g for 7min was resuspended in 100µl PBS (original volume) and diluted in Guava ViaCount reagent (at 1:3 and 1:10 dilutions) for 5 min at RT and cell number and viability was measured using the Guava EasyCyte flow cytometer (Millipore). The ViaCount assay distinguishes viable and non-viable cells based on differential permeabilities of two DNA-binding dyes in the Viacount reagent; the nuclear dye which only stains nucleated cells and a viability dye which brightly stains dying cells. Debris are excluded from the results based on negative staining with the nuclear dye. The cell counts and viability measurements of the original sample (corrected for dilution) were performed in triplicates.

2.6.2 Motility

Prior to the assessment of cell motility, a confluent monolayer of endothelial cells or tumour cells in 24 well plates were cultured for 24h in growth-factor free conditions. The confluent monolayer was subject to a single vertical scratch using a 200µl pipette tip. The wells were gently washed with PBS and BM-MSC CM was added as above, and wells were microscopically monitored up to 24hr. The width of the scratch in duplicate wells was measured at 4 points for each well, using Image-J (National Institutes of Health, Bethesda, MD, USA) and the rate of monolayer recovery plotted as relative to the original scratch width (% closure), as described previously (Webber *et al.* 2014).

2.6.3 Tubule formation assay

Formation of endothelial tubules was performed as described previously (Webber *et al.* 2014), with endothelial cells (20,000/well) added in triplicate to monolayers of BM-MSCs that had been previously treated with exosomes or sTGF-β1 for 4 days. After a further 6 days of culture, structures formed by endothelial cells were visualised by immunofluorescent labelling of CD31 (SantaCruz). The total area occupied by CD31-positive structures was quantified using the free-hand selection tool in Image-J to calculate the area occupied by stained cells in each well. Data shows the average from triplicate wells per treatment, and are representative of three such experiments.

2.6.4 Spheroid generation for invasion and growth assessment

Spheroids were generated in poly (2-hydroxyethyl methacrylate) (poly-HEMA) (Sigma, Dorset, UK) coated 96-well "u"-bottom plates. To do this, 20mg/ml poly-HEMA solution was made in pre-warmed 95% ethanol (diluted in H_2O) and the mixture was vortexed to solubilise the poly-HEMA. 150µl of the solution was added to the wells of a 96-well plate and allowed to evaporate in the hood overnight. A second coat was applied and again evaporated for 24h. To generate tumour cell and BM-MSC heterotypic spheroids, tumour cells ($DU145^{NM}$ or $DU145^{Rab27aKD}$ using the shRNA lentiviral knockdown method) were incubated alone or together with BM-MSCs at a ratio of 4 tumour cells: 1 MSC in the poly-HEMA plates and was centrifuged at 1000rpm for 10min (15 spheroids were generated for each condition). The total cell seeding was of $1x10^4$ cells per well and the medium used consisted of 1:1 ratio (v/v) or RPMI and DMEM (low glucose) in 10% FBS. After 4 days, the cells had established 3D-spheroidal structures.

Growth assessment

The spheroids were cultured in a 1:1 ratio of RPMI: DMEM 10% FBS and every other day, 50% of the culture media was replaced by fresh media. Over a 20d period, spheroid volume was measured every 4 days. Image J was used to measure the radius of the spheroid as shown below;

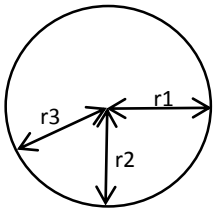

The radius measurement was used to estimate spheroid volume using the formula: $\mathbf{(4/3)\pi_{r1r2r3}}$.

Invasion assay

To evaluate potential changes in invasive behaviour of the cells, spheroids were transferred to fresh uncoated 96 well plates and Matrigel^{TM} (Corning, Flintshire, UK) was added (100µl/well). The matrigel basement membrane matrix consists of laminin, collagen type IV, heparan sulphate proteoglycan and entactin. After setting of the Matrigel^{TM} at 37^0C for 30min, medium was added and the wells monitored microscopically for 4 days thereafter. To estimate the magnitude of invasion out from the spheroid, the free-hand selection tool in Image-J was used to draw the circumference of the central sphere. This was subtracted from the circumference of the region occupied by invading cells. This gives an approximation of the area of the Matrigel^{TM} invaded by cells, as it does not take account of the volume aspect of the 3D culture, and is likely therefore to underestimate the true differences across the treatments.

2.6.5 Xenotransplantation for tumour growth assessment

With the aid of Dr Jason Webber and collaboration with Prof Wen Jiang and group (Cardiff University), tumour growth was assessed *in vivo*, in the presence of BM-MSCs with exosome proficient or exosome deficient DU154 tumour cells (using ribozyme method of Rab27a knockdown). Suspensions (100ml) containing 600,000 DU145 cells and 150,000 BM-MSCs in 3mg/ml Matrigel were sub-cutaneously injected into both flanks of 4 to 6 week old athymic nude mice (CD-1; Charles River Laboratories, Kent, UK). There were a total 5 groups (DU145$^{\text{Control Vector}}$ only, DU145$^{\text{Rab27aKD}}$ only, DU145$^{\text{Control Vector}}$ with BM-MSCs, DU145$^{\text{Rab27aKD}}$ with BM-MSCs and BM-MSCs only). There were 6 mice per group, except the BM-MSC only controls (the negative control), where only 3 mice were used. Tumour size was measured weekly over 28 days, using an external caliper to measure the height and width of the tumour. Tumour volume was calculated; tumour volume (mm^3) = 0.523 x $width^2$ x length. Animals were treated humanely in accordance with UK Home Office code of practice and the United Kingdom Coordinating Committee on Cancer Research (UKCCCR) guidelines (Workman *et al.* 2010). At the experimental end point or severity limits, the mice were dispatched humanely under the schedule 1 (Scientific Procedures) Act 1986, involving the exposure to carbon dioxide.

Chapter 3: Isolation and characterisation of prostate cancer exosomes

3.1 Isolation and characterisation of prostate cancer exosomes

The prostate cancer (PCa) cell lines chosen for this study are DU145 and PC3 because they are commonly used for the study of prostate cancer as these are well characterised (Alimirah *et al.* 2006; Clayton *et al.* 2007; Webber *et al.* 2010; Tai *et al.* 2011; Perkel *et al.* 1990). In addition, unlike LnCap (a PCa cell line), DU145 and PC3 cells are known to produce TGF-β1 bearing exosomes (Webber *et al.* 2010) which are under investigation in this thesis for their role in BM-MSC differentiation.

A high quality isolation method for exosomes, followed by characterisation and identification of these vesicles are crucial, to enable one to distinguish exosomes from other non-exosomal vesicles or cellular debris from within the cell secretome. This will also demonstrate that the experimental outcome are due to exosomes and not the contaminants. I will describe two gold standard methods to isolate exosomes form prostate cancer cells, based on their biophysical properties. These are the continuous sucrose gradient (Raposo *et al.* 1996; Caby *et al.* 2005; Nilsson *et al.* 2009) and the 30% sucrose cushion method (Lamparski *et al.* 2002), both of which utilise the floatation property of exosomes to isolate them.

To characterise the exosomes isolated from PCa cell lines (DU145 and PC3), we assessed the biophysical and phenotypic nature of the vesicles. The morphology of PCa exosomes was examined using cryo-Transmission Electron Microscopy. Validation of exosomal markers was performed on purified exosomes using a microplate-immuno-phenotype assay or western blotting for a range of exosomal related proteins including tetraspanins, ALIX, TSG101 as well as for proteins not expressed on exosomes, such as calnexin, an endoplasmic reticulum marker. The purity of exosomes was assessed based on the particle to protein ratio using the Nanosight and a colourimetric (BCA) assay for particle and protein concentration measurement, respectively (Webber and Clayton 2013). PCa derived exosomes have been shown to express TGF-β1 which is involved in the differentiation of fibroblasts into myofibroblasts (Webber *et al.* 2010). To test if exosomal TGF-β1 have an effect on MSC differentiation, TGF-β1 expression on exosomes from DU145 and PC3 will be quantified here using TGF-β1 ELISA.

3.1.1 Characterisation of prostate cancer cell lines

For my studies, PCa cell lines (DU145 and PC3) were bought new from ATCC, in which the DU145 and PC3 cells were derived from the brain and bone metastatic site, respectively. The prostatic epithelium consist mainly of luminal and basal cells (Wang *et al.* 2001) and hence the morphology and phenotype of the carcinoma cells were evaluated to confirm if they appeared as epithelial cells prior to their expansion in bioreactor flasks. In addition the expression of tumour associated proteins and proteins commonly enriched in exosomes were examined.

The monolayer of DU145 and PC3 epithelial cells were evaluated by phase contrast microscopy (figure 3.1), revealing both cell lines to be plastic adherent and exhibiting polygonal shape in appearance. This morphology agreed with other reports of prostate epithelial cells (Hayward *et al.* 2001; Lang *et al.* 2001). The PCa cell lines also appeared to grow without contact inhibition and formed overlapping cell layers after reaching confluence.

The phenotype of PCa cell lines was assessed by immunofluorescence staining for a variety of epithelial markers. Cytokeratins (CKs) such as CK-7, CK-8 and CK-19 are intermediate filaments used to characterise epithelial cells (Wang *et al.* 2001; Lang *et al.* 2001). Other common characteristics of epithelial cells are the presence of microtubules, such as α-tubulin (Soucek *et al.* 2006; Husain and Harrod 2011). Here, both the DU145 and PC3 cells were strongly positive for CK-7, CK-8 and α-tubulin (figure 3.2A). Therefore, the epithelial phenotype of DU145 and PC3 here agreed with the published literature (Nagle *et al.* 1987; Wang *et al.* 2001).

The expression of tetraspanins (CD9, CD81 and CD63) which are commonly found in exosomes (Lamparski *et al.* 2002; Rapaso *et al.* 1996; Escola *et al.* 1998; Heijnen *et al.* 1999) were assessed among the PCa cell lines using immunofluorescence. Heterogeneous population of DU145 and PC3 cells were positive for CD9. Additionally, the majority of the PCa cells were positive for CD81 and CD63 (figure 3.2B). These findings were similar to published literature on the expression of tetraspanins in PCa cells (Zvereff *et al.* 2007; Liu 2000). As a negative control, DU145 and PC3 cells were

stained for the non-epithelial marker, α-SMA, and as expected both PCa cell lines were negative for this cytoskeletal protein (figure 3.2B). This suggests the DU145 and PC3 cells are epithelial in nature with no mixed population containing myofibroblast or smooth muscle cells, from the stromal compartment of the prostate.

DU145 and PC3 cell lines were also assessed for the presence of tumour-associated Mucin-1 (MUC-1) and prostate stem cell antigen (PSCA). The expression of the glycoprotein, MUC-1 is usually found on the apical surface of epithelial cells (Brayman *et al.* 2004), but is overexpressed in many carcinomas such as breast and lung cancer (Lacunza *et al.* 2010; Yao *et al.* 2011). In the context of prostate cancer, MUC-1 was expressed in DU145 and to a lesser extent in PC3 cells (Joshi *et al.* 2009). Here, a heterogeneous population of DU145 and PC3 cells were also positive for MUC-1 (figure 3.2C). Furthermore, the name of PSCA is inaccurate as it is not a stem cell marker nor is it expressed exclusively by the prostate cells but is found to be overexpressed in prostate carcinoma cells (Reiter *et al.* 1998; Bargäo Santos and Patel 2014; Taeb *et al.* 2014). In agreement with these reports, DU145 and PC3 cells were strongly positive for PSCA (figure 3.2C). In summary, the morphology and phenotype of PCa cell lines are indeed epithelial cells in nature consistent with the literature. They also express proteins that are found to be overexpressed by many cancer cells, giving us an indication of what we might expect to find on PCa exosomes.

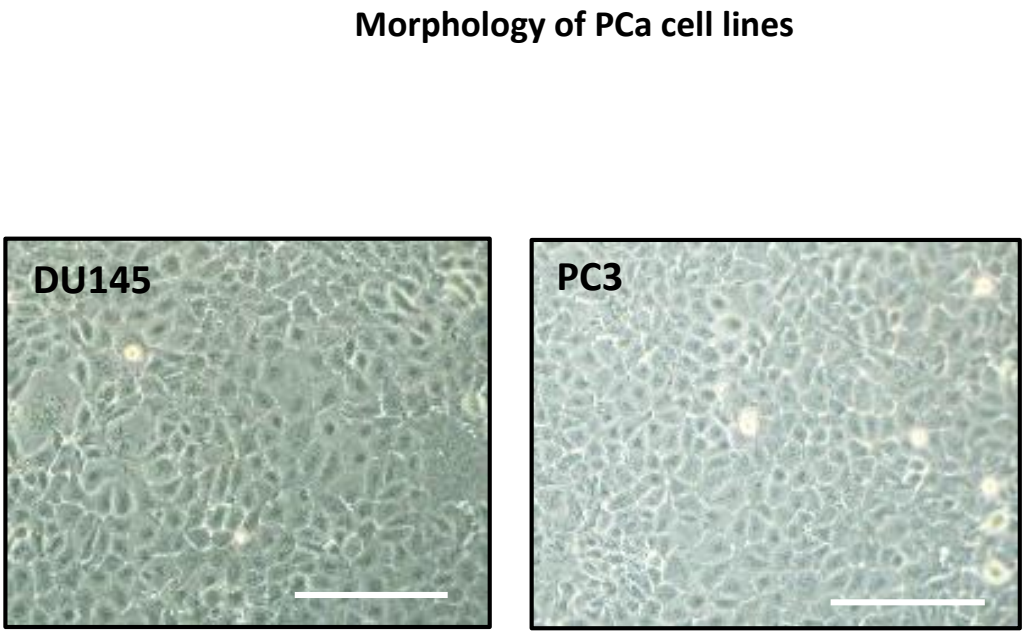

Figure 3.1: DU145 and PC3 have a cobblestone morphology.
Monolayer of live-prostate cancer cells (DU145 and PC3) were imaged using phase-contrast microscopy to confirm the cobblestone morphology of the epithelial cells. Scale bar 100µm.

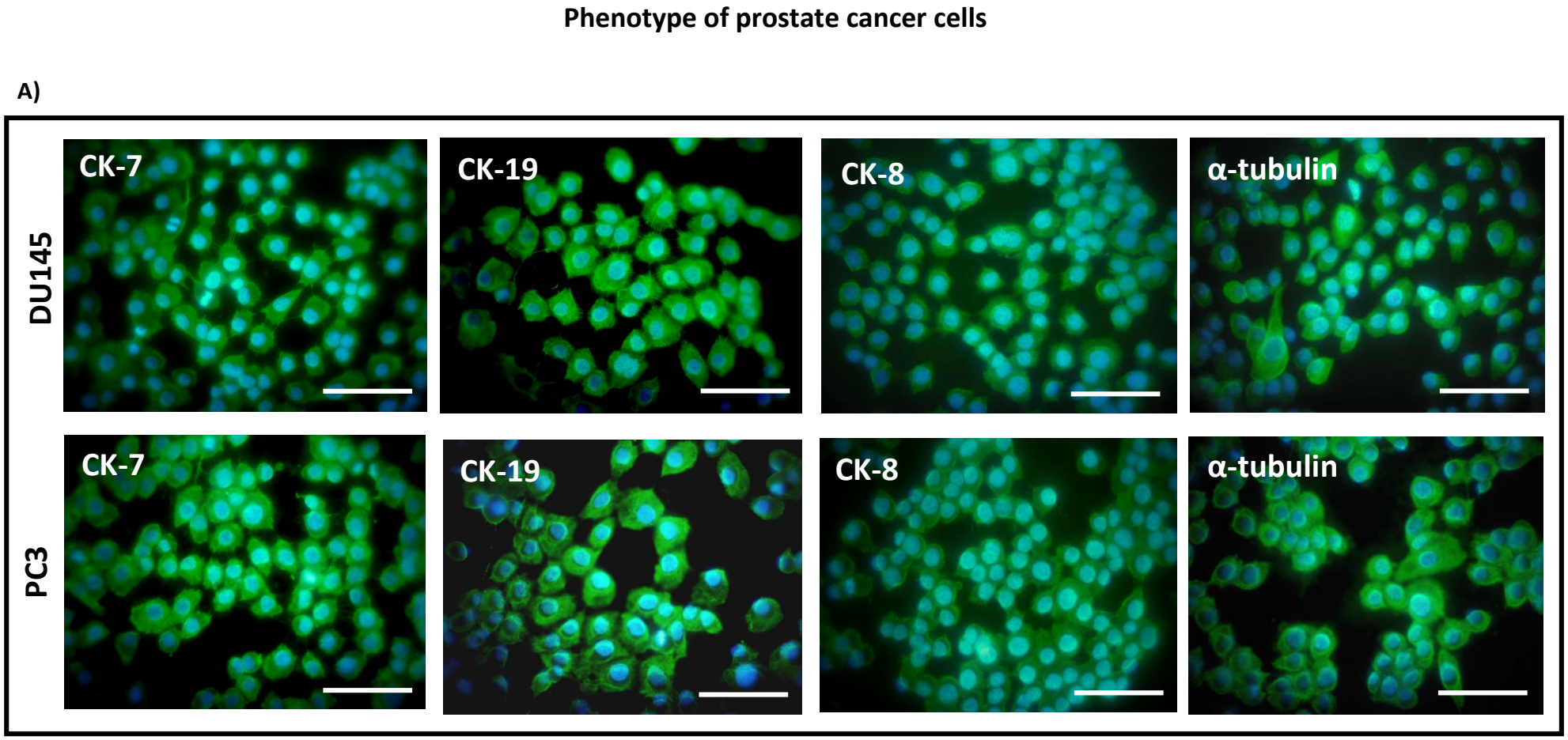

Figure 3.2: DU145 and PC3 cells have an epithelial phenotype. DU145 and PC3 cells were fixed and stained with antibodies against cytokeratin-7, -19 and -8 and α-tubulin followed by goat anti-mouse FITC secondary antibody (green). The cells were additionally stained with DAPI (blue). Scale bar 100µm (A).

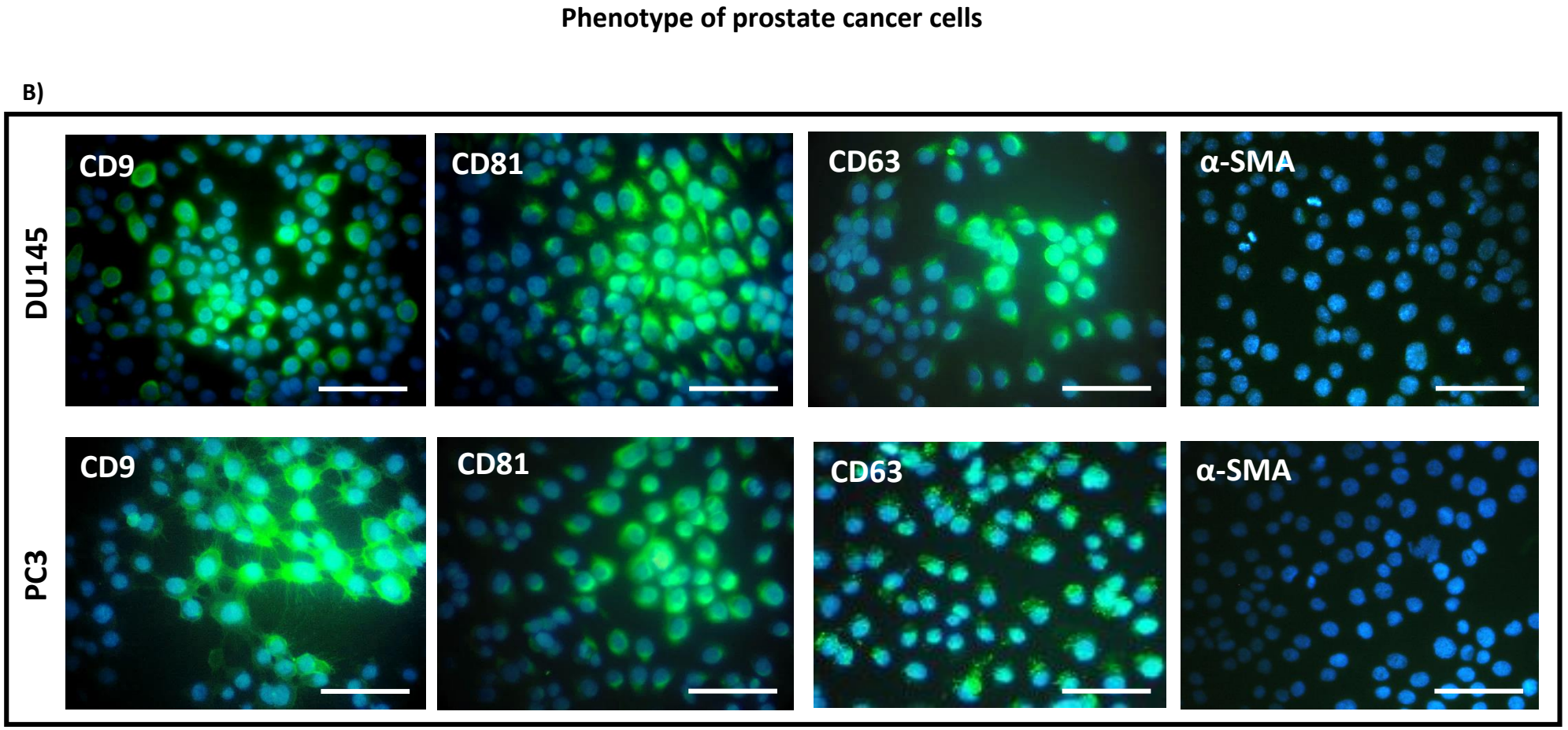

Figure 3.2 Continued*:* DU145 and PC3 cells were fixed and stained with antibodies against tetraspanins (CD9, CD81 and CD63) and α-SMA followed by goat anti-mouse FITC secondary antibody (green). The cells were additionally stained with DAPI (blue). Scale bar 100µm (B).

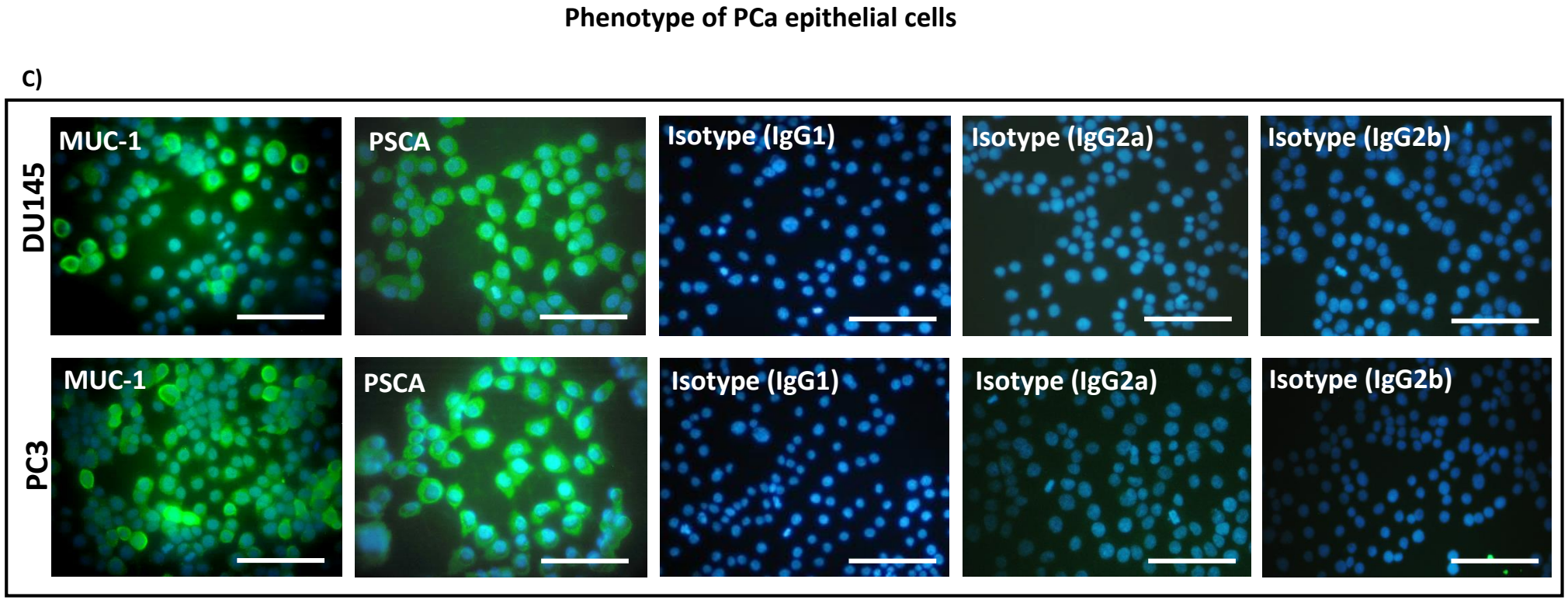

Figure 3.2 Continued: DU145 and PC3 cells were fixed and stained with antibodies against MUC-1 and PSCA followed by goat anti-mouse FITC secondary antibody (green). The cells were additionally stained with DAPI (blue). IgG isotype controls were also included. Scale bar 100µm (C).

3.1.2 Flotation of vesicles on continuous sucrose gradient

Spinning exosomal samples on a continuous sucrose gradient as mentioned in materials and methods, is a commonly used analytical tool to isolate exosomes, based on their flotation property (Raposo *et al.* 1996; Escola *et al.* 1998). A total of fifteen fractions was collected from a continuous sucrose gradient overlaid with DU145-exosome and fourteen fractions collected from gradient overlaid with PC3-exosomes. The refractive index (RI) of the individual fractions was measured using an automatic refractometer and the RI was then used to calculate the density of the fractions using a conversion table provided by Beckman Coulter. A serial increase in density with increasing fraction number was revealed (figure 3.3A and 3.3D). DU145 exosomes were predicted to be present at fractions 7-10 and PC3 exosomes were predicted to be present in fractions 5-10, as these fractions span the classical density range for exosomes at 1.1-1.2g/ml (Raposo *et al.* 1996).

The Nanoparticle Tracking Analysis (NTA) revealed the number of nanoparticles per fractions (figure 3.3B and 3.3E), in which the early DU145 fractions (1-4) and PC3 fractions (1-3) was extremely low in particle count ($<3x10^{11}$ counts/ml) and so were no longer subjected to any further analysis. With regard to the continuous sucrose gradient containing DU145 exosomes, the numbers of particles were found to increase by 28 fold from fraction 5 to fraction 9 and thereafter the particle count gradually decreased to low levels. Similarly with the continuous sucrose gradient containing PC3 exosomes, the particles increased from fraction 4 to fraction 8 by 13-fold and particle counts decreased thereafter. Thus, the majority of nanoparticles were concentrated within the density range of 1.1-1.2g/ml, agreeing with the literature (Raposo *et al.* 1996; Escola *et al.* 1998).

To characterise purified vesicles as exosomes, the fractions were subjected to western blotting using antibodies against the multivesicular endosome associated proteins (TSG101 and ALIX). Positive staining for the TSG101 in fractions spanning the exosomal density range was observed, with no staining at the hypo or hyper dense region of the gradient. Maximal staining was found within fractions 8 and fraction 9 from the DU145-continuous sucrose gradient (figure 3.3C) which contained the most particles. ALIX was found to be only expressed within fraction 9 and 10. Similarly with the PC3-continous

sucrose gradient, positive staining for TSG101 was found in fractions 5-9 and positive ALIX staining at fractions 5-10, with maximal staining at fractions 8 where the highest particle counts resided (figure 3.3F). Therefore the commonly used proteins for defining a vesicle as exosomes, ALIX and TSG101 are only found to stain fractions at exosomal density range of 1.1-1.2g/ml and so exosomes must be present in these fractions.

DU145 exosomes isolated using a continuous sucrose gradient

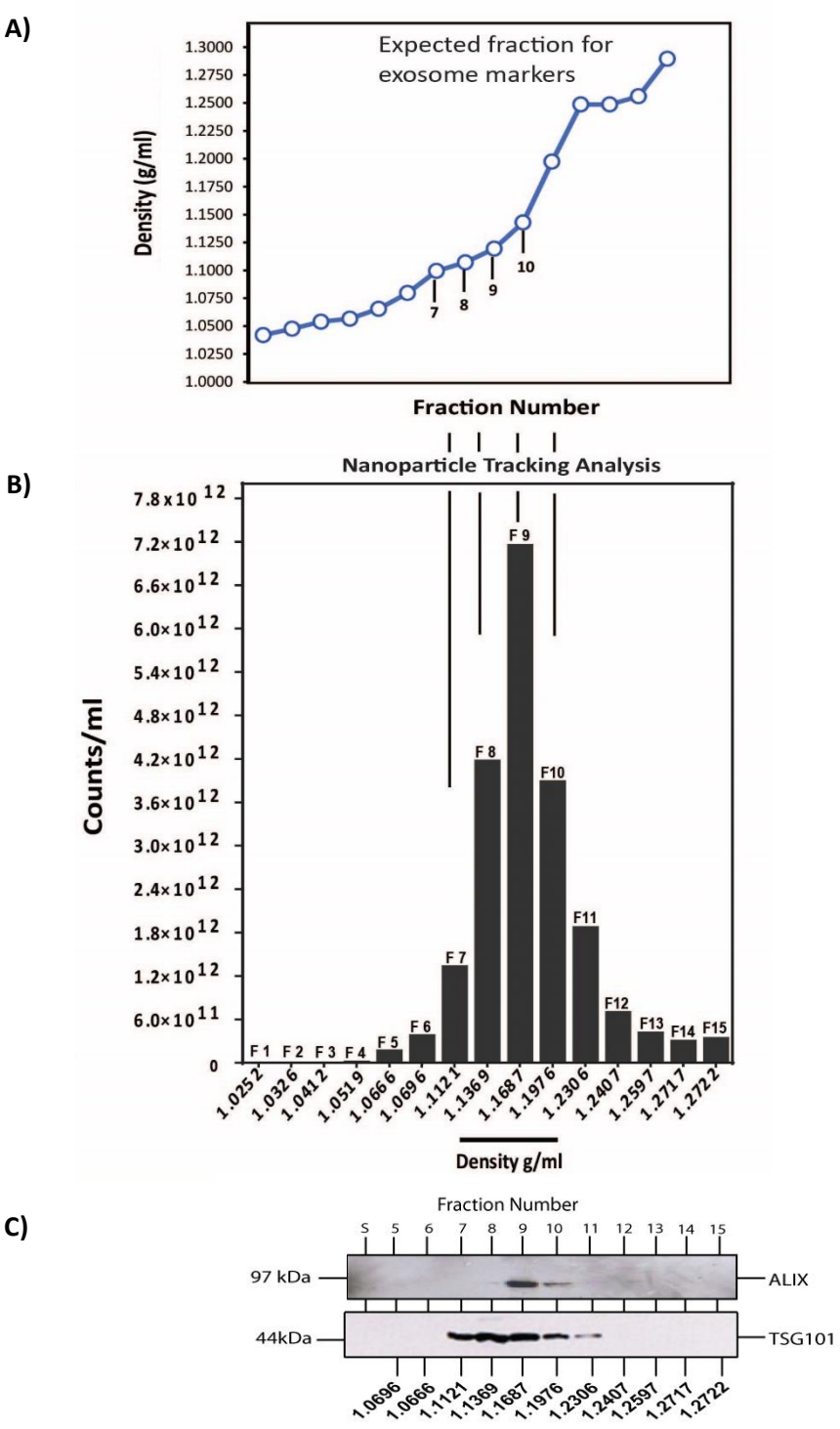

Figure 3.3: DU145 exosomes float at density of 1.1-1.2g/ml.
DU145 exosomal pellet centrifuged at 120,000 x g was overlaid on a sucrose gradient (0.2M-2M) and spun at 210,000 x g at 4^0C overnight. Fractions (1-15) were collected and density of each fraction calculated using refractometry and density conversion table. Fractions 7-10 are predicted to contain exosomes (A). Fractions (1-15) were analysed by nanoparticle tracking analysis (NTA), showing peak nanoparticle concentration at fraction 9 (B). Fractions 5-15 was analysed by western blot for exosomal markers (TSG101 and ALIX). Marker lane (ML) included for identifying the molecular weight of the antibody (C).

PC3 exosomes isolated using a continuous sucrose gradient

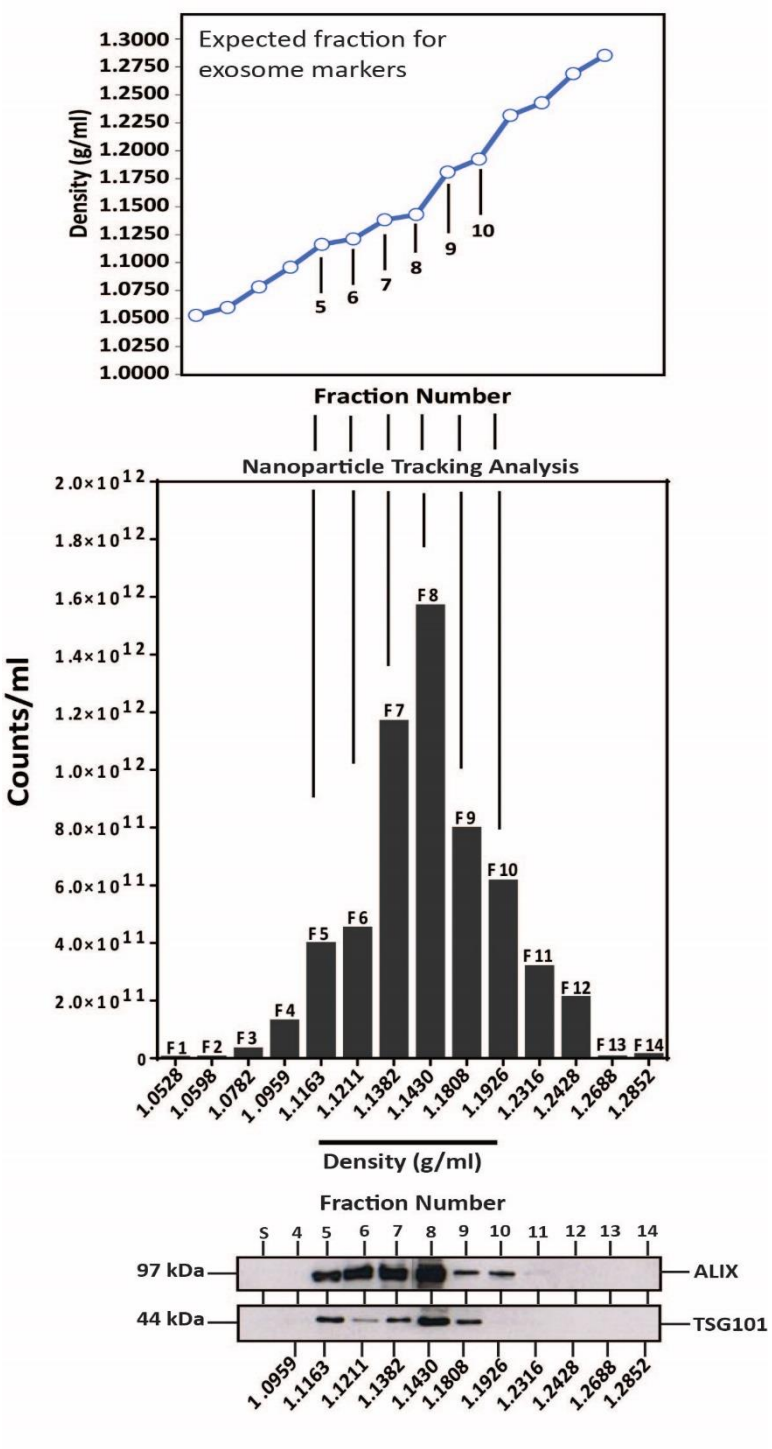

Figure 3.3 continued: PC3 exosomes float at density of 1.1-1.2g/ml.
PC3 exosomal pellet was overlaid on a sucrose gradient, in the same manner as with the DU145 exosomes. Fractions (1-14) were collected and density of each fraction was calculated, in which fractions 5-10 are predicted to contain exosomes (D). Fractions (1-14) were analysed by NTA, showing peak nanoparticle concentration at fraction 8 (E). Fractions 4-14 were analysed by western blot for exosomal markers (TSG101 and ALIX). Marker lane (ML) included for identifying the molecular weight of the antibody (F).

3.1.3 Exosomes purified by the sucrose cushion method.

Isolation of exosomes using a continuous sucrose gradient is a good method to characterise exosomes but it is a long process (>18h) and results in variable recovery of the starting amount of exosomes (Lamparski *et al.* 2002). Thus it is not ideal as a routine use of isolating exosomes for experimental use. Instead the sucrose cushion is a rapid method for isolating exosomes of high yield (Lamparski *et al.* 2002). This method involves ultracentrifugation of cell conditioned media (CM) with a 30% sucrose/D_2O cushion to capture exosomes based on their buoyant density in sucrose of 1.1-1.2g/ml. The cushion containing exosomes was collected and underwent a PBS wash at high speed, resulting in an exosomal pellet which was then characterised.

Firstly, the morphology of DU145 and PC3 exosome pellets were examined using cryo-transmission electron microscopy (TEM) in collaboration with Dr. Georgi Lalev (Cardiff University). To do this, the exosomal pellets were resuspended in PBS and placed onto carbon grids and were then rapidly plunged into liquid ethane at liquid nitrogen temperature to prevent formation of ice crystals. The grid containing exosomal sample was viewed under cryo-TEM, revealing rounded structure of vesicles with thick outer boundary, suggesting the possibility of the lipid bilayer (figure 3.4). The diameter of the DU145 and PC3 exosomes agrees with the classical diameter range of exosomes at 30-100nm found by others (Raposo *et al.* 1996; Escola *et al.* 1998; Sokolova *et al.* 2011; Sharma *et al.* 2010; Welton *et al.* 2010).

Secondly, the phenotype of DU145 and PC3 exosomes was examined using a microplate-immuno-phenotype assay, in which the exosomes were coated on plates overnight and were assessed for their surface expression of proteins commonly found in exosomes, such as the tetraspanins (CD9, CD81 and CD63). Our data demonstrated, exosomes from both PCa cell lines express tetraspanins (figure 3.5A), in which the DU145 exosomes have a 2-fold greater expression of CD9 and CD81 in comparison to the PC3 exosomes ($P<0.001$). Furthermore, DU145 and PC3 derived exosomes express CD63 but to a lesser extent than that of the other tetraspanins. The expression of cytosolic protein, glyceraldehyde-3-phosphatedehrogenase (GAPDH) and PSCA was also assessed, revealing DU145 and PC3 exosomes to exhibit positive expression of GAPDH and a low

expression level (<7 x10^5 TRF) for PSCA. Therefore the PCa exosomes express proteins commonly found to be present in exosomes by other researchers (Lamparski *et al.* 2002; Théry *et al.* 1999; Escola *et al.* 1998) as well as proteins that are found in cells they originate from.

To ensure that a particular protein is specifically enriched in exosomes, one successful approach is to compare proteins from exosomes and from whole cell lysates (CL) prepared from the parent cells on the same gel. Cell lysates and exosomes from DU145 and PC3 were compared by western blotting with a range of antibodies. This allowed us to compare the relative expression of known exosome markers, such as MVE markers (TSG101 and ALIX), 5T4 a tumour associated marker and MHC Class I, in exosomes compared to whole cell lysates (figure 3.5B). These were highly enriched in exosomes from both PCa cell lines. LAMP-1 (lysosomal-associated membrane protein-1), a glycoprotein expressed within the lysosomal compartment was found to be positively expressed in DU145 and PC3 exosomes, at a similar level to that of their parent cell. In contrast, the endoplasmic reticulum protein, calnexin was only stained in cell lysates. The expression of the cytosolic marker, GAPDH were found in both exosomes and cell lysates, as expected. The phenotype of exosomes analysed here agree with the literature (Raposo *et al.* 1996; Lamparski *et al.* 2002; Escola *et al.* 1998).

Using Nanoparticle Tracking Analysis (NTA), the majority of the nanovesicles within the PCa vesicular pellet isolated from the sucrose cushion had a diameter of 79nm and 85nm, from the DU145 and PC3 cells respectively (figure 3.6 and 3.7). This finding agrees with the cryo-TEM data presented here and by previous studies, in that exosome have a diameter within the range of 30-100nm (Raposo *et al.* 1996; Sokolova *et al.* 2011; Escola *et al.* 1998). Furthermore, there are no large particles present (>400nm), concluding that there are no microvesicles or other large form of cellular participate present.

Estimating the purity of exosomes isolated, aids researchers to carry out routine quality control tests. The purity of exosomes can be measured based on the particle to protein ratio (P:P) using the nanosight and a colourimetric (BCA) assay for particle

(nanovescicles) and protein concentration measurement respectively, as described by Webber and Clayton (2013). A recent study has shown that introducing protein contaminants into the exosome preparation, resulted in a reduced P:P ratio in comparison to the exosome sample with no contamination. The decrease in P:P ratio correlated with increased dose of protein contamination. Thus pure exosome preparations exhibit higher particle to protein ratio (Webber and Clayton 2013).

Furthermore, their study showed conditioned media (CM) containing exosomes from PCa bioreactor flasks had a low P:P ratio (3.7 x 10^8 P/µg). Whereas pelleting and wash purification of exosomes increased the P:P ratio (2 x 10^{10}P/µg). Isolating purer exosomes, using the sucrose cushion method further enhanced this P:P ratio (3.4 x 10^{10} P/µg). From these outcomes, Webber and Clayton (2013) proposed arbitrary thresholds, in which ratios greater than 3 x10^{10} P/µg are of high purity, ratios of 2 x 10^9 to 2 x 10^{10} P/µg represent low purity and ratios below 1.5 x 10^9 P/µg are unpure. Using these thresholds, in this particular exosome preparation, the DU145 and PC3 exosomes isolated using the sucrose cushion had a P:P ratio of 4.00 x 10^{10} and 2.97 x 10^{10} P/µg respectively, and are therefore of high purity (figure 3.6 and 3.7). The quality control threshold has been used routinely on exosomes prepared from the 30% sucrose cushion, some of which are shown in table 3.1. The majority of exosomes passed the quality threshold and are used for experimental studies. The exosomal vesicles that are unpure (<1.5 x 10^9 P/µg), due to issues during the purification (i.e. not collecting the sucrose cushion in a clean manner) are discarded. In summary, exosomes isolated from PCa cells using the sucrose cushion method are of good purity and largely free from non-exosomal proteins.

Morphology of exosomal vesicles from prostate cancer cells

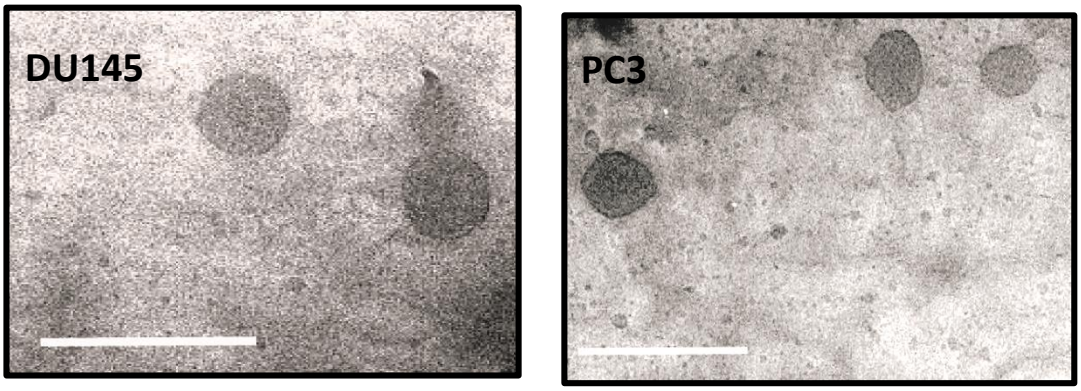

Figure 3.4: DU145 and PC3 exosomes are circular and less than 100nm in diameter. DU145 and PC3 exosome pellet was resuspended in PBS (1:10000) and applied to a holey carbon grid. The exosomal specimen grid was then rapidly plunged into liquid ethane at (-196^{o}C to -210^{o}C) and viewed under cryo-transmission electron microscopy (Cryo-TEM), confirming the rounded structure of exosomal vesicles with a diameter <100nm. Scale bar; 100nm.

Characterisation of DU145 and PC3 derived exosomes from the sucrose cushion method

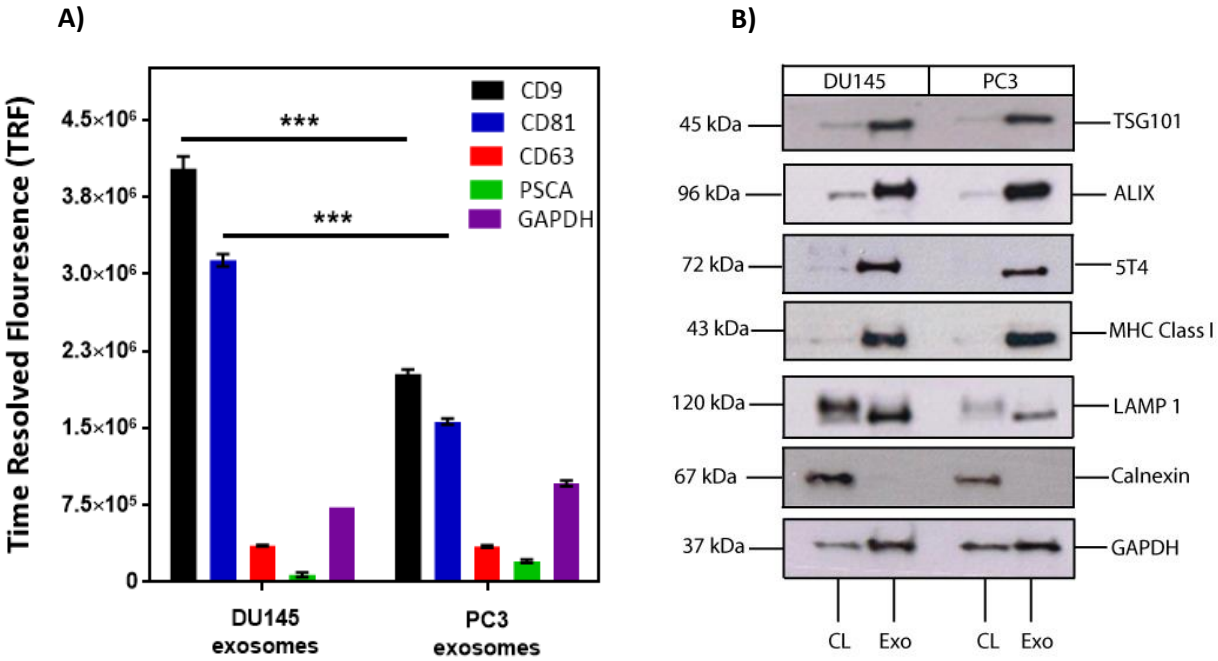

Figure 3.5: Exosomes from DU145 and PC3 cells express exosome-associated proteins. Exosomes from DU145 and PC3 cells were captured onto high protein binding ELISA plates (1µg/well) and analysed for the expression of tetraspanins (CD9, CD81, CD63) as well as expression of prostate stem cell antigen (PSCA) and GAPDH. Time resolved fluorescence (TRF) of the staining is shown with isotype subtraction (A). One-Way ANOVA with Tukey's multiple comparison test ***=P≤0.001. Cell lysates (10µg) and exosomes (10µg) from DU145 and PC3 were compared by western blot using a range of antibodies (TSG101, ALIX, 5T4, MHC Class I, Calnexin and GAPDH (B).

A)

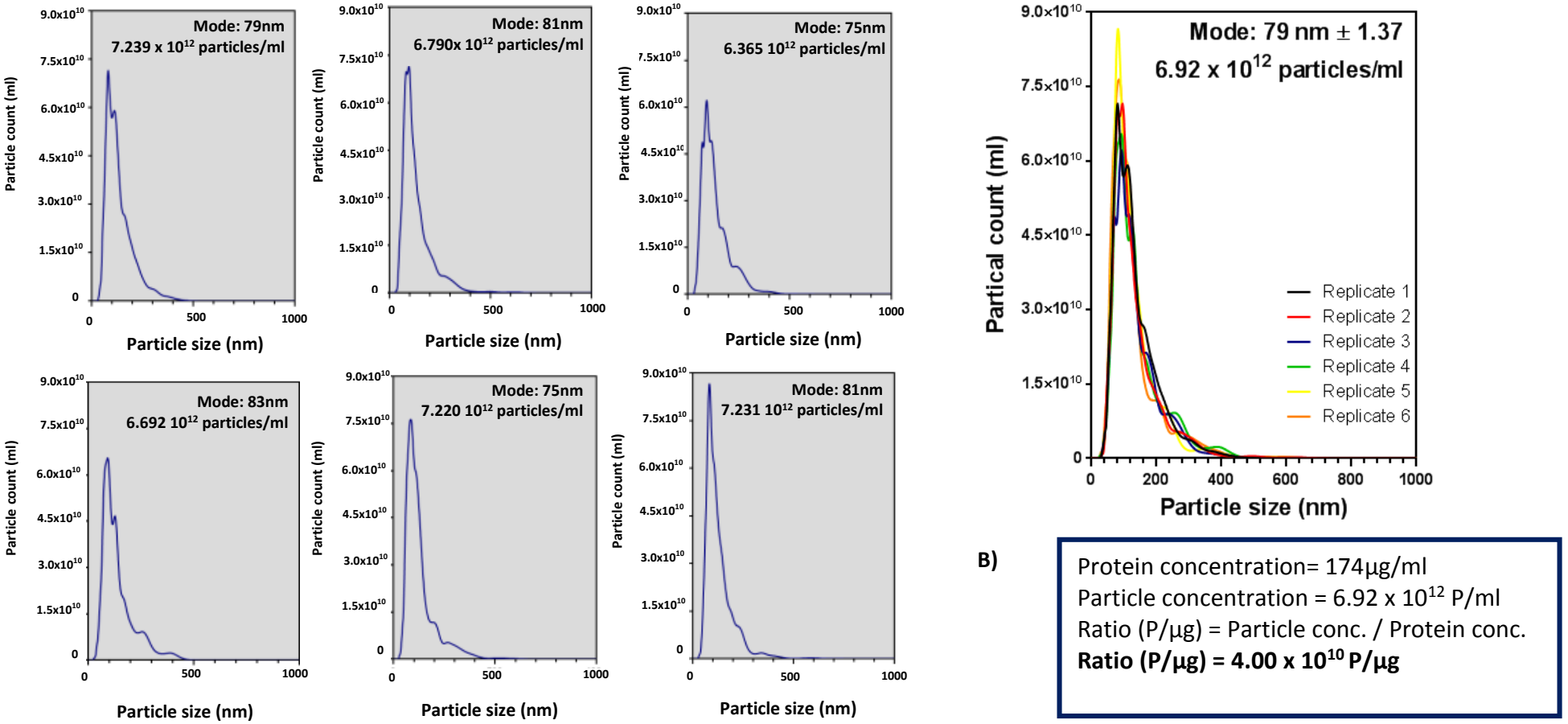

B)

Protein concentration= 174µg/ml
Particle concentration = 6.92 x 10^{12} P/ml
Ratio (P/µg) = Particle conc. / Protein conc.
Ratio (P/µg) = 4.00 x 10^{10} P/µg

Figure 3.6: Exosomes isolated from DU145 cells using the sucrose cushion are of high purity. The particle concentration (P/ml) and diameter of DU145-exosomes isolated using the 30% sucrose cushion was measured using Nanoparticle Tracking Analysis (NTA). 6 replicate measurements were carried out and overlaid to show the consistency across the repeat measurements (A). BCA assay was used to calculate the protein concentration (µg/ml) of the exosomes. The purity of exosomes were assessed by the particle: protein ratio (B).

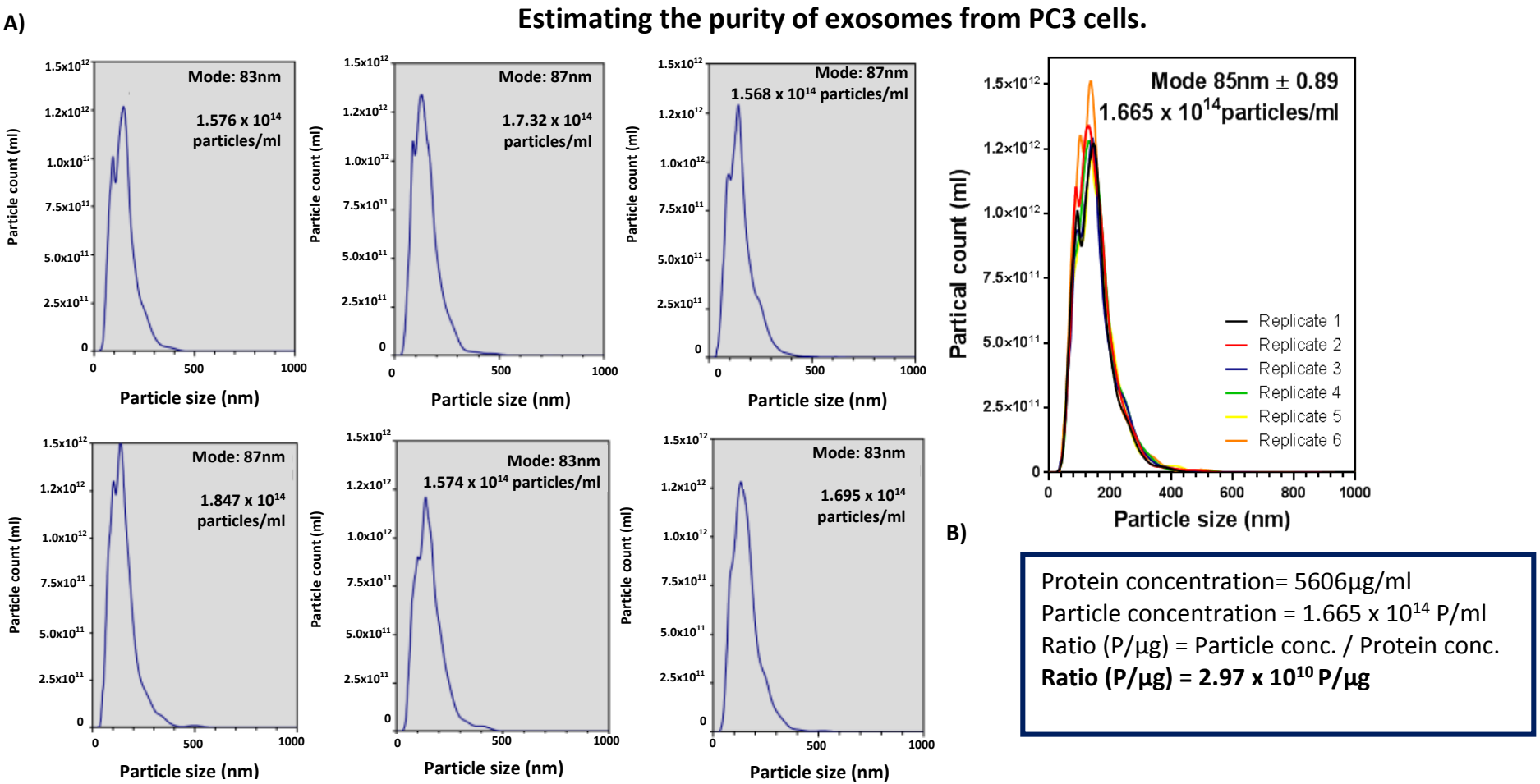

Protein concentration= 5606µg/ml
Particle concentration = 1.665 x 10^{14} P/ml
Ratio (P/µg) = Particle conc. / Protein conc.
Ratio (P/µg) = 2.97 x 10^{10} P/µg

Figure 3.7: **Exosomes isolated from PC3 cells using the sucrose cushion are of high purity.** The particle concentration (P/ml) and diameter of PC3-exosomes isolated using the 30% sucrose cushion was measured using Nanoparticle Tracking Analysis (NTA). 6 replicate measurements were carried out and overlaid to show the consistency across the repeat measurements (A). BCA assay was used to calculate the protein concentration (µg/ml) of the exosomes. The purity of exosomes were assessed by the particle: protein ratio (B).

Routine quality control of exosome preparations

Date	Exosome source	Protein concentration (µg/ml)	Particle concentration (Particles/ml)	Ratio (P/µg)	Quality Control
07/03/12	DU145	605	7.27×10^{12}	1.20×10^{10}	**PASS**
30/7/13	PC3	2271	2.33×10^{12}	1.03×10^{9}	**FAIL**
20/08/12	DU145	1097	3.95×10^{13}	3.6×10^{10}	**PASS**
08/09/13	DU145	3696	3.25×10^{13}	8.79×10^{9}	**PASS**
02/06/13	PC3	513	4.8×10^{12}	9.36×10^{9}	**PASS**
03/10/13	PC3	4301	1.64×10^{14}	3.8×10^{10}	**PASS**
11/09/13	DU145	6390	1.86×10^{13}	2.91×10^{9}	**PASS**
09/10/13	PC3	4006	3.18×10^{13}	9.43×10^{9}	**PASS**
09/10/13	DU145	2372	3.95×10^{11}	1.66×10^{8}	**FAIL**
10/10/13	DU145	1905	1.2×10^{14}	6.30×10^{10}	**PASS**
18/10/13	Du145	10273	2.51×10^{14}	2.44×10^{10}	**PASS**
01/11/13	DU145	1927	6.73×10^{13}	3.49×10^{10}	**PASS**
16/11/13	DU145	689	4.23×10^{12}	6.14×10^{9}	**PASS**
17/11/13	DU145	4549	1.78×10^{13}	3.91×10^{9}	**PASS**
30/01/14	PC3	1393	1.71×10^{13}	1.23×10^{10}	**PASS**
14/03/14	DU145	3518	3.86×10^{13}	1.09×10^{10}	**PASS**
11/02/14	DU145	6875.7	1.05×10^{14}	1.53×10^{10}	**PASS**
17/01/14	DU145	1762	4.25×10^{13}	2.41×10^{10}	**PASS**
30/01/14	PC3	1404	1.71×10^{13}	1.22×10^{10}	**PASS**
14/02/14	DU145	3518	3.86×10^{13}	1.09×10^{10}	**PASS**
26/03/14	DU145	4240	1.48×10^{14}	3.49×10^{10}	**PASS**
23/7/14	DU145	13898	8.24×10^{11}	5.93×10^{7}	**FAIL**
30/07/14	PC3	2271	2.33×10^{12}	1.09×10^{9}	**FAIL**
13/8/14	DU145	7281	2.20×10^{12}	3.02×10^{8}	**FAIL**
30/06/14	PC3	4322	1.53×10^{14}	3.54×10^{10}	**PASS**

Table 3.1: Quality of exosomes prepared from the sucrose cushion. Protein and particle concentration of exosomes were measured using Nanoparticle Tracking Analysis and BCA assay, respectively, to calculate the particle: protein ratio. Exosomal samples isolated with a particle: protein ratio of ≥2 x 10^9 (P/µg) passes the arbitrary quality threshold (as proposed by Webber and Clayton 2013).

3.1.4 Quantification of exosomal TGF-β1 expression

My thesis will be focusing on the biological function of exosomal TGF-β1 on the fate of bone marrow mesenchymal stem cell (BM-MSC) differentiation. The focus on TGF-β1 was brought about from its importance in the induction of fibroblast differentiation into myofibroblasts (Tuxhorn *et al.* 2002). Furthermore, exosomes from mesothelioma and PCa cells have been shown to express TGF-β1 (Clayton *et al.* 2007; Webber *et al.* 2010). Here, different doses of exosomes from DU145 and PC3 cells were evaluated for the expression of TGF-β1 using the TGF-β1 ELISA (figure 3.8). The exosomal samples were prepared prior to running the assay by acid-activating the latent TGF-β1 to the immunoreactive form (using HCL) which can be detected by the TGF-β1 immunoassay. A good linear response was observed with increasing dose of exosomes and the TGF-β1 levels. A consistent expression of the active form of TGF-β1 was observed among the exosome samples, in which 7pg of TGF-β1 was expressed per µg of DU145 exosomes and 14pg of TGF-β1 expressed per µg of PC3 exosomes. Therefore, TGF-β1 is found to be expressed on the exosome surface, with PC3-derived exosomes expressing double the amount of TGF-β1 in comparison to the DU145 derived exosomes. Knowing the quantity of TGF-β1 expressed on exosomes will allow equivalent dose of both exosomal TGF- β1 and soluble TGF-β1 to be used for comparison when assessing their effects on fate of MSC differentiation.

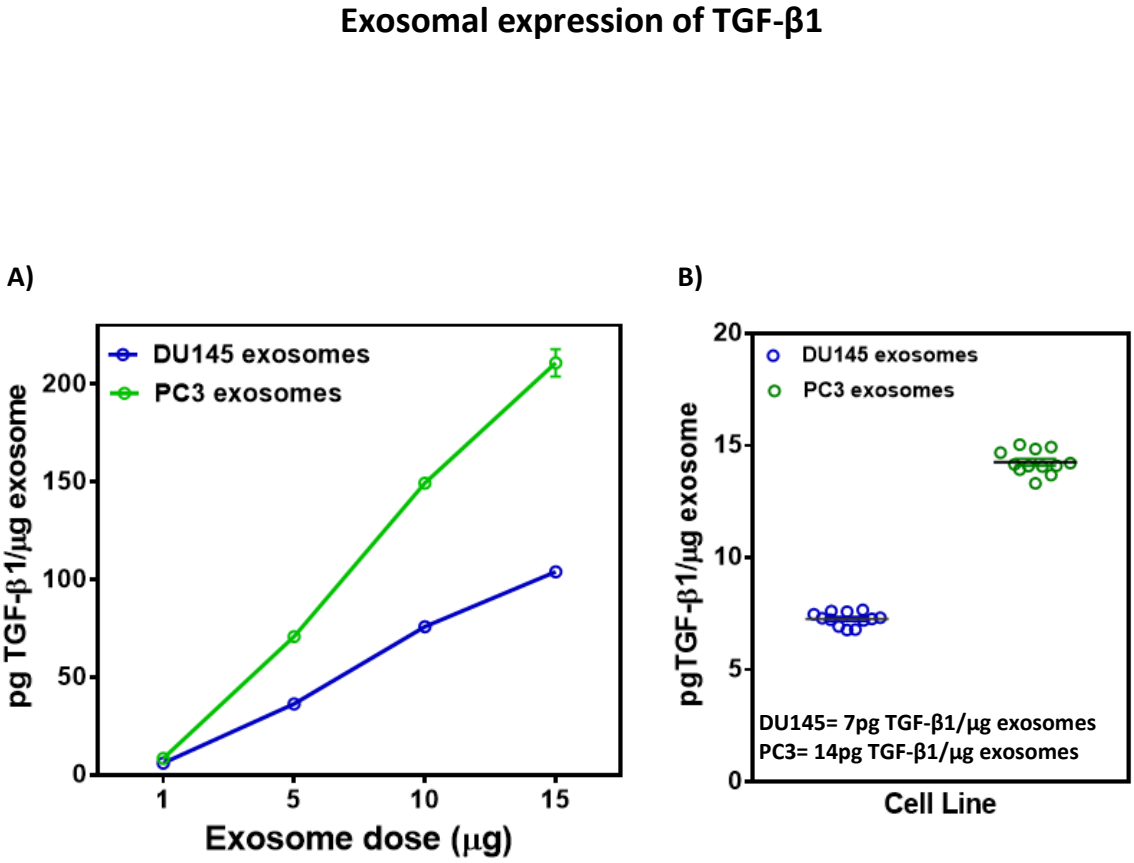

Figure 3.8: TGF-β1 are expressed more in PC3 exosomes than the DU145 exosomes
Different doses of DU145 and PC3 exosomes (1μg, 5μg, 10μg and 15μg) in triplicates were subjected to acid activation and the expression of active TGF-β1 were measured using TGF-β1 ELISA (A). From these multiple preparations, the TGF-β1 concentration per μg of exosomes was plotted (B).

3.2 Discussion

In this chapter, the PCa cell lines, DU145 and PC3 have been confirmed to be epithelial by their cobblestone appearance, and the repertoire of CK expression revealed the DU145 and PC3 cells to exhibit classical luminal epithelial features, such as the expression of CK-7, CK-8 and CK-19. The PCa cells lacked the expression of α-SMA and so there was no stromal cells such as myofibroblasts or smooth muscle cells. In addition the DU145 and PC3 are heterogeneously positive for tumour-associated proteins MUC-1, which are found to be overexpressed in many cancers such as breast, lung and also prostate cancer (Lacunza *et al.* 2010; Yao *et al.* 2011). DU145 and PC3 also exhibit prostate specific marker, PSCA, which is known to be specifically expressed in prostate epithelial cells and overexpressed in PCa cells (Reiter *et al.* 1998; Bargão Santos *et al.* 2014; Taeb *et al.* 2014). Tetraspanins are commonly found in exosomes from various cell types (Lamparski *et al.* 2002; Rapaso *et al.* 1996; Escola *et al.* 1998; Heijnen *et al*. 1999). Our data has shown DU145 and PC3 cells to heterogeneously express tetraspanins CD9, CD81 and CD63. These findings were akin to other reports of expression of tetraspanins found in PCa cells (Zvereff *et al.* 2007; Liu *et al.* 2000). Some studies demonstrate exosomes to be akin to their parental cells (Bharathiraja *et al.* 2014) and if so, assessing the phenotype of PCa cells here, may indicate the phenotypic nature of their respective exosomes.

PCa exosomes can be isolated using the continuous sucrose gradient method, where PCa cells have been demonstrated to secrete exosomes which float in fractions which span the classical exosomal densities of 1.1-1.2g/ml. These fractions contained the greatest number of nanoparticles and the strongest staining for exosome-associated proteins such as ALIX and TSG101. Thus the biophysical and biochemical properties of PCa exosomes agree with that of exosomes from other cancer cell lines (Raposa *et al.* 1996; Escola *et al.* 1998; Heijnen *et al.* 1999).

Exosomes purified from DU145 and PC3 cells using the sucrose cushion method revealed them to be rounded. However, the structural features of the vesicles, such as the lipid bilayer could not be visualised clearly. This is due to the lack of optimisation of factors such as sample preparation, sample loading onto the carbon grid, surface charge on

carbon support films and thickness of ice, all of which affects the performance and resolution of imaging (Cho *et al.* 2013; Grassucci *et al.* 2007). We couldn't yet optimise the procedure as the Cryo-TEM is a new instrument at the School of Optometry (Cardiff University). PCa exosomes were a monodisperse population, in which the majority of the vesicles were less than 100nm in diameter, as shown by the cryo-TEM and the NTA, which agrees with most publications (Webber and Clayton 2013; Sheldon *et al.* 2010). The Nanosight performs a size analysis of particles in fluid phase, as opposed to fixed and dehydrated samples used in other methods such as traditional (non-cryo) electron microscopy and hence may give a truer representation of exosomes in their natural state. There were no large particles of more than 400nm, demonstrating an absence of non-exosomal components, such as apoptotic cellular material, in the size range of 500nm in diameter or more. Microplate-immuno-phenotype assay revealed exosomes express tetraspanins and low levels of PSCA and so have some resemblance to their parental cells. Western blot demonstrated exosomes to be of good quality as they were enriched in exosomal markers with respect to whole cell lysates and levels of non exosomal calnexin was barely detectable. Furthermore, using the particle to protein ratio as proposed by Webber and Clayton (2013) showed the majority of exosomes isolated using the sucrose cushion method to be of high purity. More recent methods have been established for exosome isolation, such as the use of sepharose 2B column (Rabinowits *et al.* 2009; Sokolova *et al.* 2011) and exosome immunocapture plates. In addition, commercial methods such as the Exo-spin (Cell Guidance), exosome isolation kit (Life Technologies) and the ExoQuick method which utilises the total exosome isolation reagent, claim to precipitate exosomes from cell culture CM (System Biosciences). However, these methods are still yet to be standardized, and do not always generate exosomes of typical characteristics and purity, and the methods have not been thoroughly tested, especially in the context of P:P ratio. Therefore utilising the sucrose cushion method was justified by their results and we kept to this method for the remainder of the thesis, as this is a more rapid method than the continuous sucrose gradient technique for isolating exosomes.

Lastly, in this chapter TGF-β1 has been demonstrated to be expressed on the surface of both DU145 and PC3 exosomes, with PC3 expressing double the amount of TGF-β1 to

that of PC3 exosomes. Previous studies report TGF-β1 to be expressed on exosomes by various cell types (Clayton *et al.* 2007; Cai *et al.* 2012; Xiang *et al.* 2009) and in agreement with the data presented here, similar levels of TGF-β1 expression were reported on DU145 and PC3 cells (Webber *et al.* 2010). Furthermore, TGF-β1 expression on exosomes do differ among the different PCa cell lines. For example, PC3 and DU145 were both found to express TGF-β1 whereas LnCap, (another PCa cell line) had very low levels of TGF-β1 (Webber *et al.* 2010). Since soluble TGF-β1, as well as exosomal TGF-β1 are known to be involved in the myofibroblastic differentiation of stromal cells (Tuxhorn *et al.* 2002; Webber *et al.* 2010), PCa exosomes expressing TGF-β1 are hypothesised to differentiate BM-MSCs into myofibroblast-like cells. By knowing the quantity of TGF-β1 on exosomes, equivalent dose of exosomes, matched to the sTGF-β dose can be used to investigate the effect they have on the fate of BM-MSC differentiation.

Chapter 4: Characterisation of stromal cells

4.1 Characterisation of MSC, fibroblasts and myofibroblasts

Bone-marrow derived MSCs (BM-MSCs) are well-known to possess powerful tissue reparative and protective mechanisms, such as their capacity to differentiate into various mesenchymal tissues and their immunosuppressive property. This makes BM-MSCs attractive for treatment of different diseases (Fujita *et al.* 2015; Fortier and Smith 2008). Despite these advantageous MSC traits, BM-MSCs have been recently demonstrated to migrate to tumour stroma sites (Shinagawa *et al.* 2010; Khakoo *et al.* 2006) and conflicting reports exist, demonstrating MSCs to either promote (Djouad *et al.* 2003; Zhu *et al.* 2006; Karnoub *et al.* 2007) or suppress tumour growth (Qiao *et al.* 2008; Khakoo *et al.* 2006). BM-MSCs under the influence of cancer cells CM have been noted to differentiate into myofibroblast-like cells (Mishra *et al.* 2008). Recently TGF-β1 positive exosomes from cancer cells have been shown to differentiate fibroblasts into tumour-promoting myofibroblasts (Webber *et al.* 2014). Thus, in this thesis we will be focusing on the fate of BM-MSC differentiation in response to PCa derived TGF-β1 bearing exosomes.

Before using BM-MSCs in our experimental studies, BM-MSCs have been rigorously characterised to confirm they are genuine MSCs and not a mixed population of other stromal cell types, such as macrophages, endothelial cells, hematopoietic cells and fibroblasts found within the BM. Freidenstein (1976) was the first to isolate and expand BM-MSCs and noted them to be plastic adherent with an elongated spindle-shaped morphology. Further adaptation from this, the International Society for Cellular Therapy (ISCT) set a minimal criteria for defining MSC, which state that in addition to MSCs being plastic adherent, they must express surface antigens; CD73, CD105, CD90 and must be negative for hematopoietic antigens (CD14 and CD45). The function of these molecules on BM-MSCs are not well defined, but CD73 is an ecto-5'-nucleotidase known to support MSC migration (Ode *et al.* 2011), whereas CD105, is a TGF-β receptor III, which plays a role in TGF-β signalling during MSC chondrogenic differentiation (Barry *et al.* 1999). In contrast, the exact function of CD90 is less well defined and has been proposed to have a role in the stromal adherence of CD34+ cells (Craig *et al.* 1993). The last criteria set by the ISCT, is that MSCs must also be able to differentiate into multi-lineage pathways, such as adipocytes, chondrocytes and osteocytes when cultured under appropriate

conditions (Dominici *et al.* 2006). This criteria is followed by scientists carrying out MSC research, but unfortunately, one of the obstacles with MSC research remains to be the lack of unique markers for MSC identification. The cell surface markers suggested by the ISCT is incapable in distinguishing MSCs from stromal cells such as fibroblasts (Kundrotas, 2012), and so identifying MSC as a contributor to the activated stroma at cancer sites is a challenge.

4.1.1 Morphology and phenotypic characterisation of BM-MSCs, fibroblasts and myofibroblasts

The morphology and phenotype of BM-MSCs were compared to other stromal cell types that are found within the tumour stroma such as fibroblasts and myofibroblasts. Any differences will help define BM-MSCs and may potentially aid in demonstrating their relative proportion within the activated stroma. Commercially purchased naïve BM-MSCs from healthy donors were used. With regard to fibroblasts, and myofibroblasts, normal adult diploid fibroblasts (AG02262 from Coriell Institute) of lung origin were used as they represent a typical fibroblasts exhibiting appropriate mesenchymal markers and are non-transformed and become senescent after approximately ten population doubling. In addition, the majority of these fibroblasts can differentiate into myofibroblasts under the control of TGF-β1 and have been widely used in the study of exosome controlled differentiation (Webber *et al.* 2010; Webber *et al.* 2014).

The BM-MSCs were plastic adherent and morphological evaluation by phase-contrast microscopy revealed the cells to possess a rounded cell body with long and thin cell processes (figure 4.1A) which agree with published literature (Martinez *et al.* 2007). However, evaluation of fibroblasts and myofibroblasts (generated from fibroblasts treated with sTGF-β1 over 72h) also exhibited a similar cell shape. Therefore morphology fails to distinguish the BM-MSCs from fibroblasts and myofibroblasts. This led us to assess the phenotype of the cells by immunofluorescence staining for alpha smooth muscle actin (α-SMA), a well-known myofibroblast marker. Unlike myofibroblasts, BM-MSCs and fibroblasts do not constitutively express α-SMA (Figure 4.1B) thus α-SMA cannot distinguish between these two cell types.

The surface-phenotype of BM-MSCs was analysed according to the classical ISCT criteria using flow cytometry. The majority of the BM-MSCs positively expressed the markers CD73, CD90 and CD105 and were negative for haematopoietic markers CD14 and CD45 (figure 4.2A). Thus the BM-MSCs well satisfied characteristics suggested by the ISCT. The phenotype of BM-MSCs was explored a little deeper, by evaluating the expression of other surface proteins such as CD44, CD146, SSEA-4 and GD-2. Previous studies have reported BM-MSCs to express CD44 (Spaeth *et al.* 2013; Yang *et al.* 2010), CD146

(Espagnolle *et al.* 2014) and the glycoprotein, stage-specific embryonic antigen-4 (SSEA-4) which are usually found in undifferentiated pluripotent human embryonic stem cells (Gang *et al.* 2007). Furthermore a study has reported ganglioside-2 (GD-2) a protein commonly found in embryonic stem cells to be expressed in adipose derived MSCs and absent in foreskin fibroblasts (Martinez *et al.* 2007), making it a potential marker to distinguish MSCs from fibroblasts. Here, we revealed all the BM-MSCs to highly express CD44 and likewise the majority of all the cells positively expressed SSEA-4 and GD-2 and to a lesser extent, CD146 (figure 4.2B). Fibroblasts and myofibroblasts were compared to this panel and found to display similar characteristics to the BM-MSCs (figure 4.2C). However, staining for SSEA-4 and GD-2 was absent or low in both fibroblasts and myofibroblasts ($P \leq 0.001$), demonstrating BM-MSCs are phenotypically distinct from other stromal cell types.

In our hands, SSEA-4 was exclusively expressed in BM-MSCs and not fibroblasts and myofibroblasts and so this antigen raised the possibility of detecting MSCs within the tumour stroma as well as tumour associated myofibroblasts of MSC origin. To test this, normal and prostate cancer stromal cells were obtained from the Wales Cancer Bank and the stromal cells were evaluated for the expression of SSEA-4 (figure 4.3). There was a 2% higher population of SSEA-4 positive cells found within the tumour stromal cells, in comparison to the normal prostatic stroma. This observation was not significant, but the data still indicates the presence of SSEA-4 positive cells within the prostate stroma, may indeed be MSCs

In summary, the morphology and phenotype of BM-MSCs to other stromal cells are similar, but α-SMA can identify myofibroblasts whilst SSEA-4 can uniquely distinguish BM-MSCs from fibroblasts and myofibroblasts and so this marker may enable us to track BM-MSCs as contributors to the tumour stroma. In this particular case, however, there is an insignificant increase in SSEA-4 positive cells in tumour stroma, suggesting little MSC contribution in the tumour stroma.

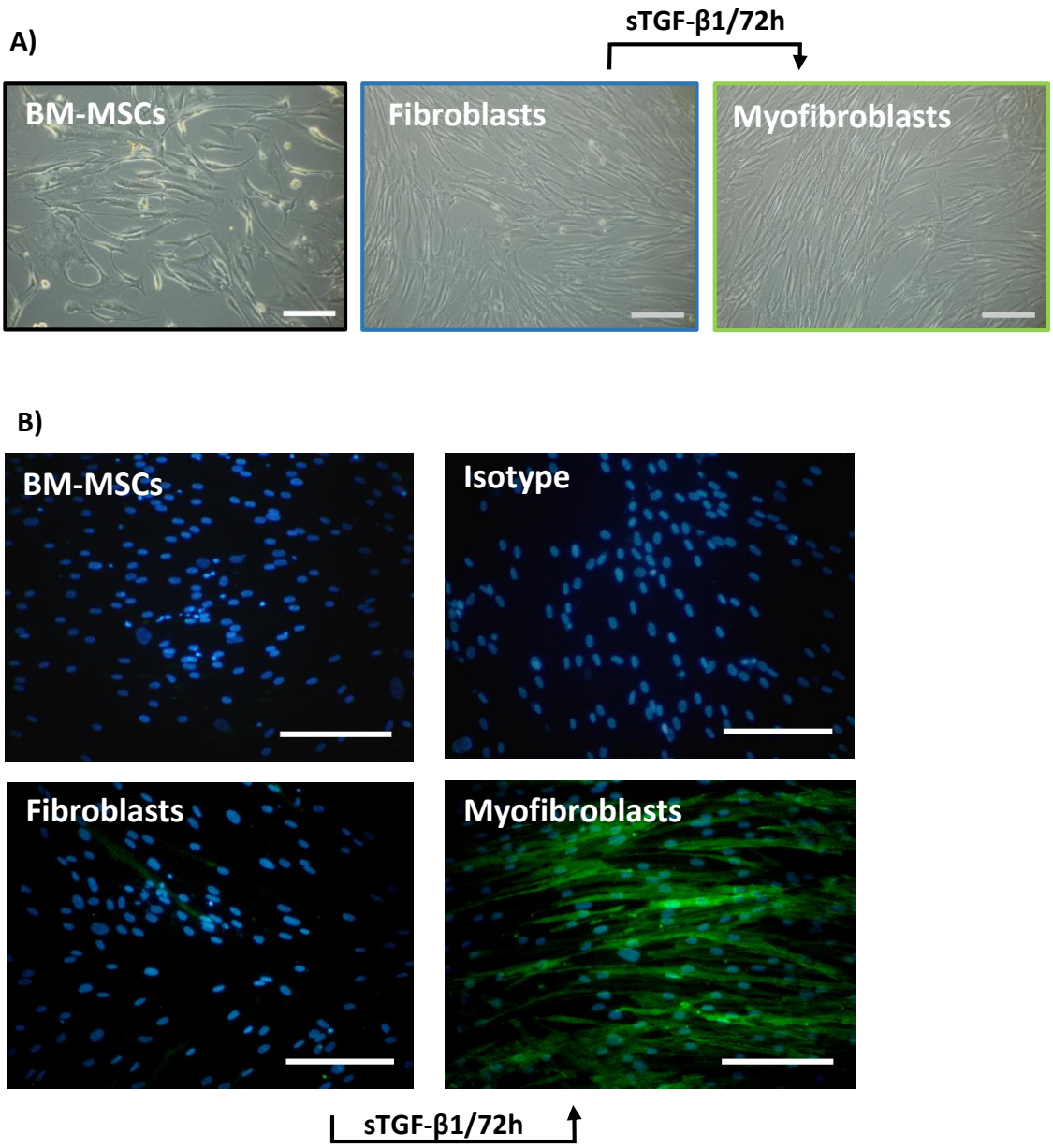

Figure 4.1: **BM-MSCs, fibroblasts and myofibroblasts are spindle-shaped but only the myofibroblasts express α-SMA**. The spindle-shaped appearance of BM-MSCs, fibroblasts and myofibroblasts (generated by treating fibroblasts with 1.5ng/ml sTGF-β1 for 72h) were imaged live *in vitro* using light microscopy under phase contrast. Scale bar 100µm (A). The stromal cells were fixed and immunofluorescently stained with monoclonal antibody against α-SMA, followed by goat anti-mouse FITC secondary antibody (green). The cell were additionally stained with DAPI (blue). IgG2a isotype control were also included. Scale bar 100µm (B).

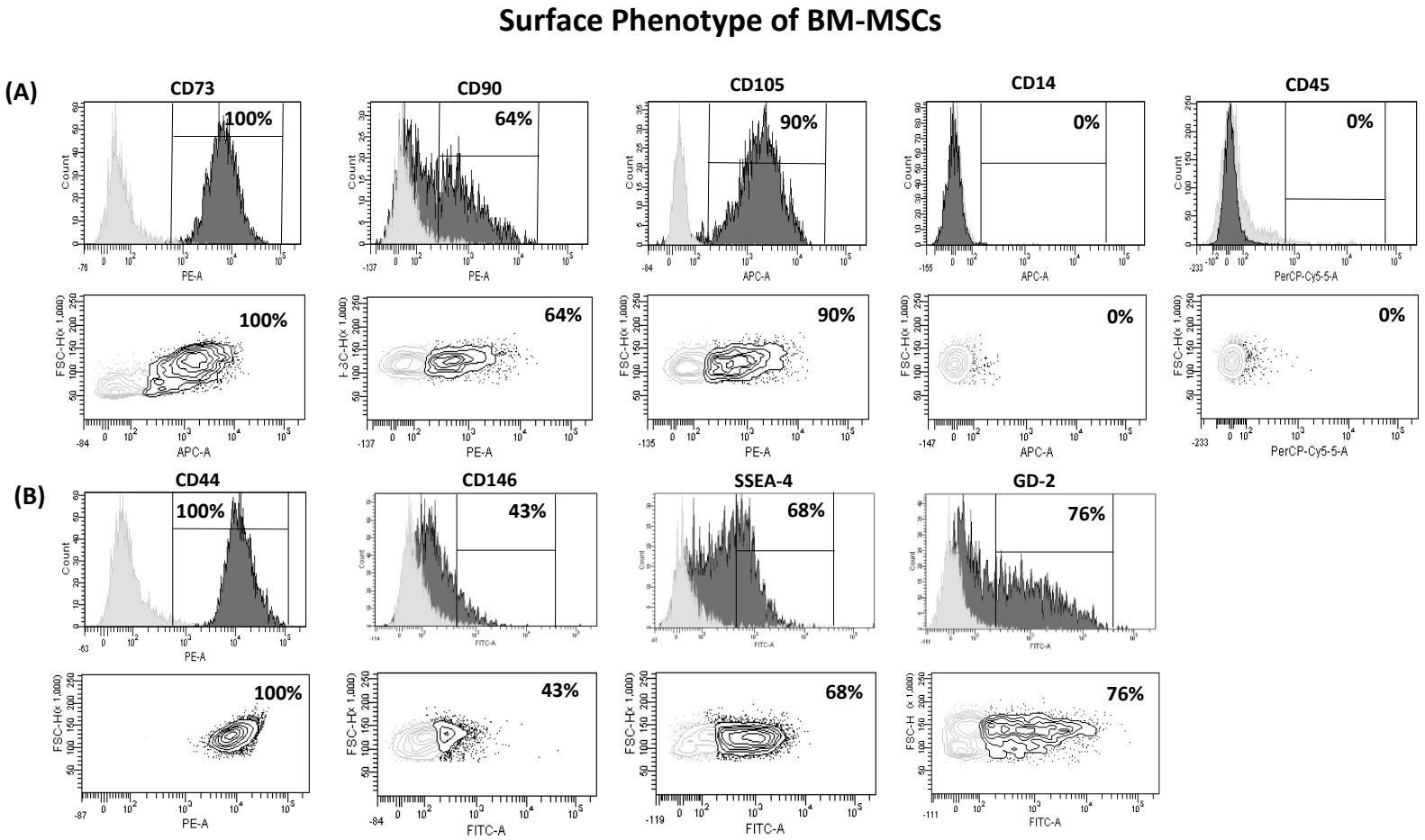

Figure 4.2: BM-MSCs express surface antigen suggested by the ISCT and also express CD44, CD146, SSEA-4 and GD-2. BM-MSCs were fixed and stained with conjugated antibodies against the ISCT suggested molecules; CD73, CD90, CD105, CD14, CD45, CD44 (A), as well as other cell surface molecules; CD146, SSEA-4, and GD-2 (B). Flow cytometric histograms show a positive shift in the cell surface molecules expression (black) from the isotype control (grey). No shift in CD14 and CD45 (black) are seen from the isotype (grey). Dot blot show the percentage of cells positive (black) for the specified marker (CD73, CD90, CD105, CD14, CD45, CD44, CD146, SSEA-4, and GD-2) in relation to the isotype control (grey).

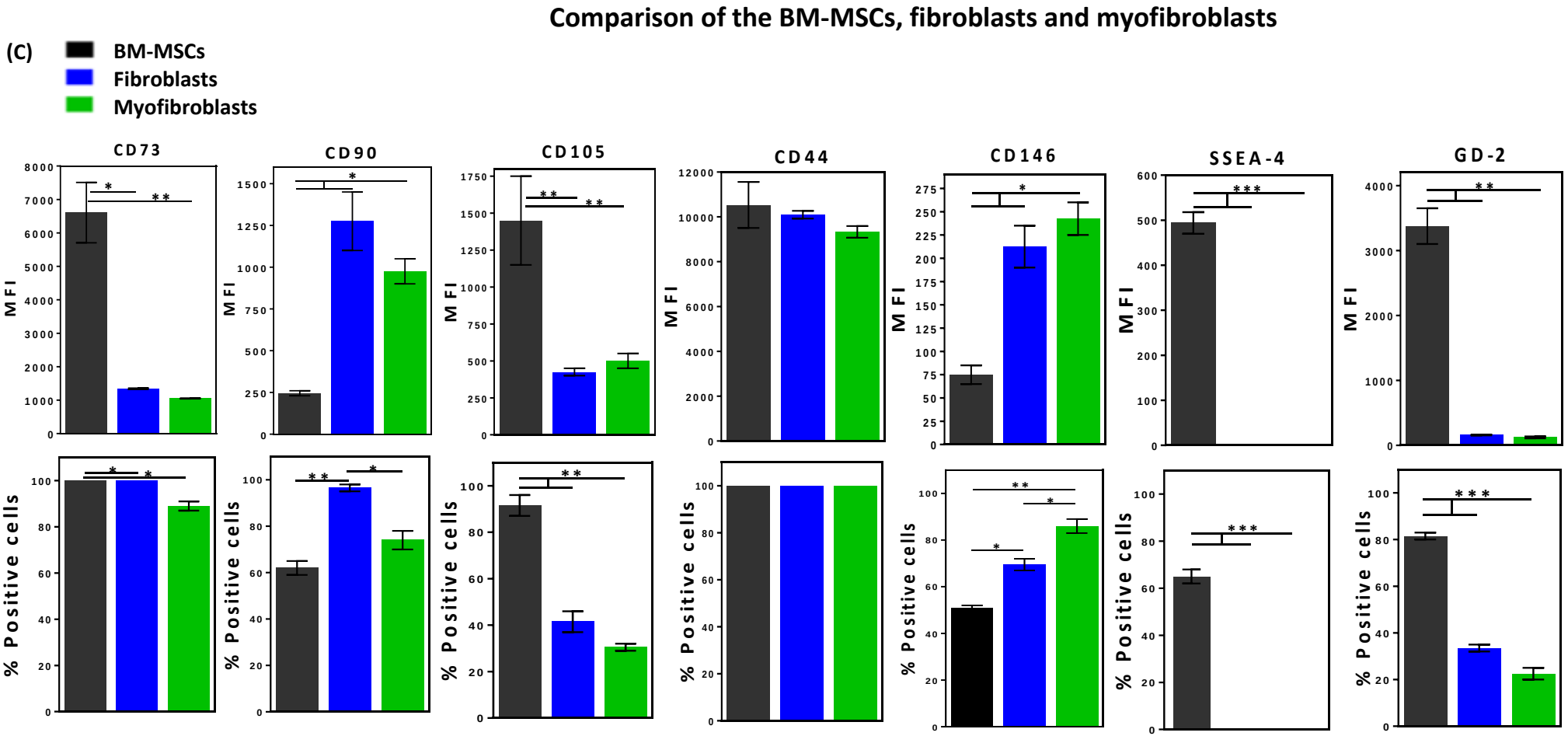

Figure 4.2 continued: BM-MSCs, fibroblasts and myofibroblast express similar cell surface molecules. Fibroblasts and myofibroblasts (fibroblasts treated with 1ng/ml sTGFb1 for 72h) were treated in the same manner as BM-MSC and summary data (bar) to compare various cell surface antigen expression among the three cell types; BM-MSCs (black), fibroblasts (blue) and myofibroblasts (green). Median Fluorescence Intensity (MFI) plotted after isotype subtraction (above) and percentage positive cells (below) are recorded ± SD of duplicates (C). Students T-test *P≤ 0.005, **P≤ 0.01 and ***P≤ 0.001.

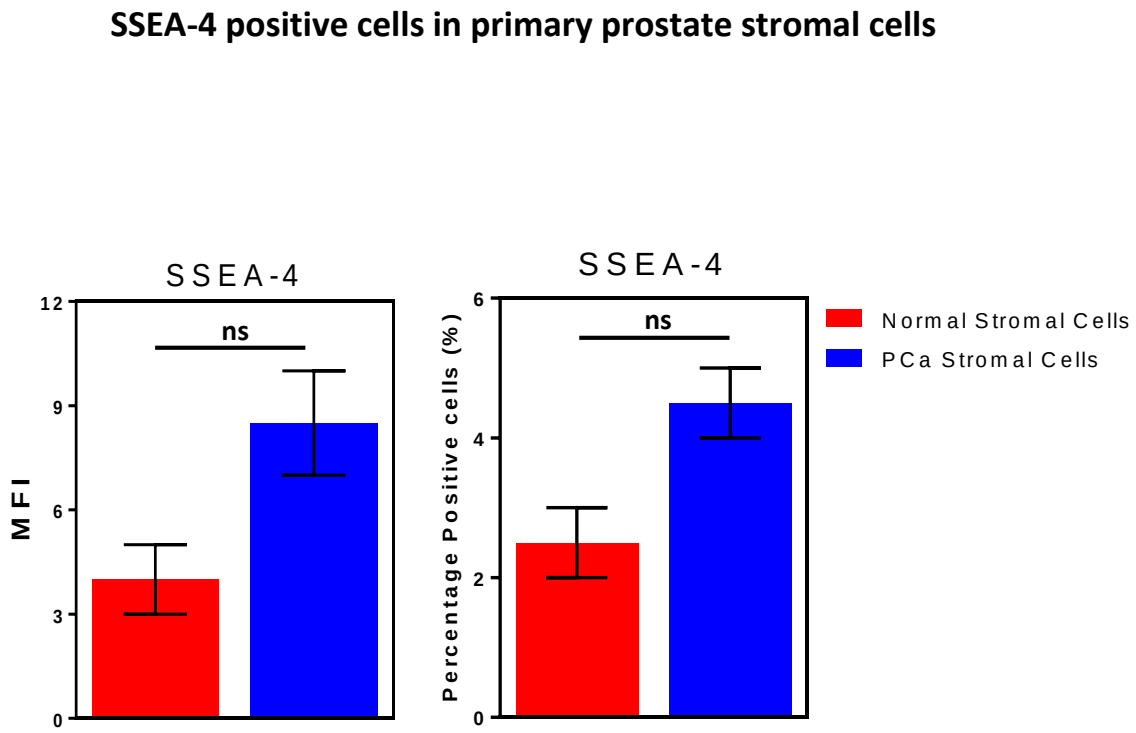

Figure 4.3: SSEA-4 positive stromal cells are found in the prostate. Normal and prostate cancer stromal cells were fixed and stained with FITC-conjugated monoclonal antibody against SSEA-4. Median Fluorescence Intensity (MFI) of cell surface expression of SSEA-4 plotted after isotype subtraction (right) and percentage positive cells (left) are shown with ± SD of duplicates. T-test: not significant.

4.1.2 Adipogenic differentiation of BM-MSCs and the response to DU145 exosomes

BM-MSCs have already been shown to differentiate into adipocytes, osteoblasts and chondrocytes according to the supplier. Nevertheless, we wanted to be certain this property of cells was real in our hands, by examining the ability of BM-MSCs to undergo at least one of the classical programmes of differentiation, focusing on adipogenesis in this case. BM-MSCs were cultured in the adipogenesis media (containing dexamethasone, IBMX, insulin and indomethacin) for a period of 21 days as described by Pittenger (1999). The BM-MSCs developed multiple lipid droplets within the cytosol, which stained intensely with Oil red O (figure 4.4A). Fibroblasts treated identically showed no signs of adipogenic differentiation. Therefore we have genuine MSCs that can be used for our planned investigations.

Since this thesis intends to examine the effect of PCa exosomes upon the fate of BM-MSC differentiation, we explored the impact of adding exogenous sTGF-β1 or TGF-β1 bearing exosomes from PCa cells to this adipogenic system. A dose of 1ng/ml of sTGF-β1 was used, as this is a common concentration known to induce MSC differentiation into various mesenchymal cell types such as vascular smooth muscle cells and chondrocytes (Guerrero *et al.* 2014; Motoyama *et al.* 2010). Furthermore, exosomes in the previous chapter were shown to contain around 7pg of TGF-β1 per µg of DU145 exosomes and this agreed with published literature (Webber *et al.* 2010; Clayton *et al.* 2007). Thus sTGF-β1 (at 1ng/ml) or DU145-exosomal TGF-β1 (150µg/ml) at a dose approximately equivalent to 1ng/ml TGF-β1 were added to some wells together with the adipogenic differentiation factors every 3 days throughout the 21 day experiment and the effect on adipogenesis was compared (figure 4.4B). To obtain quantification of the adipogenic differentiation, adipocyte were counted from a total of 10 microscopic fields from the different conditions (figure 4.4C). Evaluation under microscopy revealed either treatment of sTGF-β1 or exosomal TGF-β1 to result in significant ($P<0.001$) inhibition of the differentiation into adipocytes, by 96% and 87% respectively in comparison to the untreated adipogenic differentiation of BM-MSCs.

In addition, we examined whether BM-MSCs under the influence of PCa exosomes, differentiate to a myofibroblast-like phenotype. The BM-MSCs under the same

conditions as mentioned above were evaluated for the myofibroblastic marker, α-SMA by immunohistochemistry and proportion of α-SMA positive cells were quantified. BM-MSCs in standard (DMEM with 10% FBS) or adipogenesis media exhibited a low proportion of α-SMA positive cells (<7%) and this was not altered following sTGF-β1 treatment (figure 4.5A and B). In contrast more than 50% of the cells exhibited strong α-SMA expression following treatment with exosomes at a matched TGF-β1 dose as observed by filamentous stress fibres, which are not seen in other conditions. In summary BM-MSCs possess the ability to differentiate into adipocytes when cultured under appropriate conditions. However, this differentiation pathway is attenuated when either sTGF-β1 or PCa exosomes were added, indicating the potent strength of these factors, being able to override this differentiation programme. By evaluating α-SMA expression, it is clear that exosomes drive MSC differentiation into myofibroblast-like cells, although the response was heterogeneous. In contrast, α-SMA expression was not apparent with sTGF-β1 along with the adipogenesis media, therefore differentiation of BM-MSCs into myofibroblast-like cells may not be possible when stimulated with the soluble form of TGF-β1.

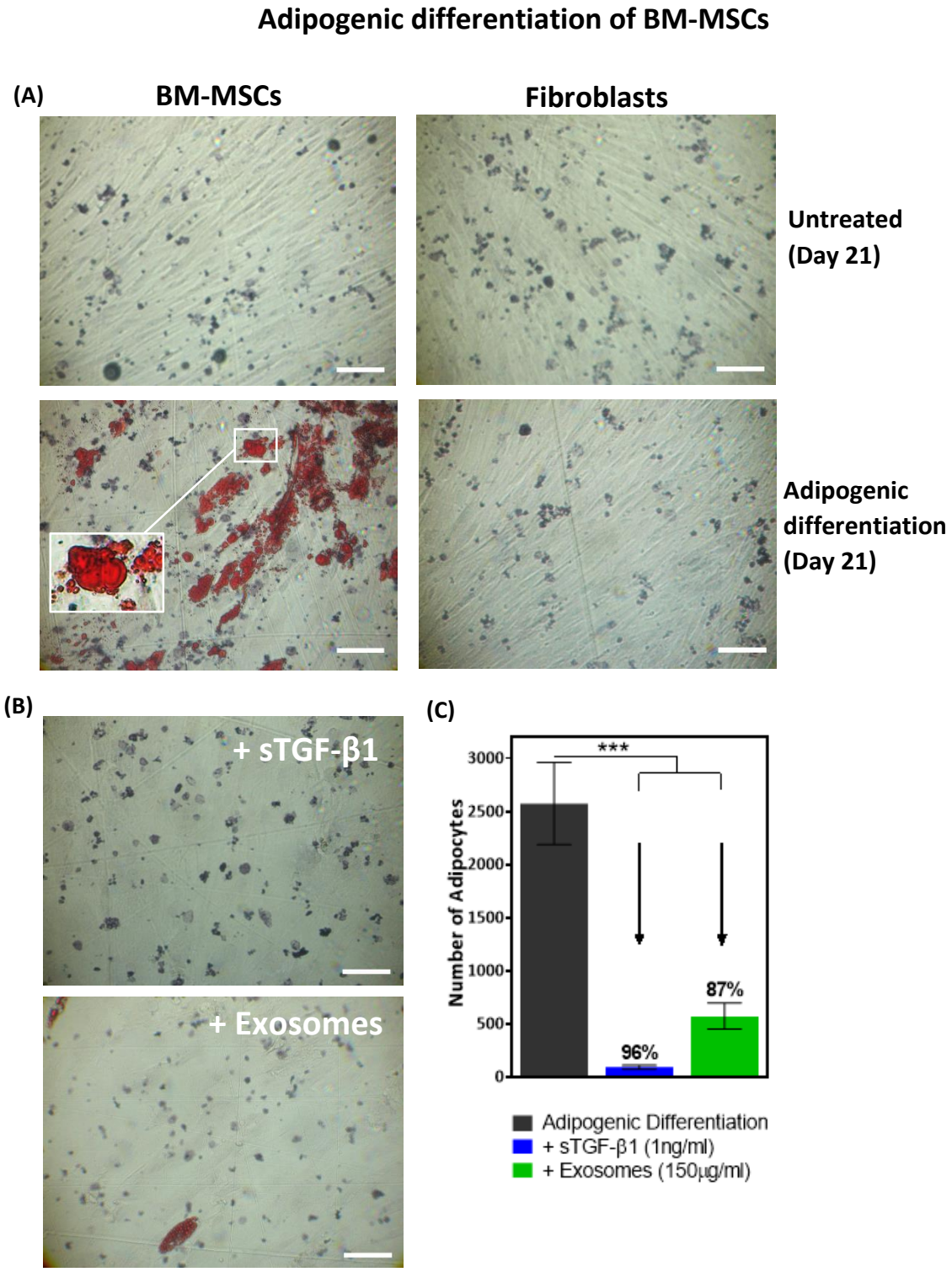

Figure 4.4: BM-MSCs have the capacity to differentiate into adipocytes and this differentiation is inhibited by either sTGF-β1 or PCa exosomes. BM-MSCs and fibroblasts cultured in standard media (top) or with the addition of adipogenic stimulants (bottom) for 21 days was stained for adipocytes using Oil Red O solution and nuclei was stained using haematoxylin (A). Selection from image showing clusters of Oil Red O-stained fat droplets in adipocytes (A, inset). During adipogenic differentiation, sTGF-β1 (1ng/ml) or DU145 exosomes (150µg/ml) were repeatedly added along with the adipogenic stimulants and the formation of Oil Red O positive adipocytes (black arrows) examined at day 21. Scale bar 100µm (B). Bars show the mean (±SD) number of adipocytes per field of view, from a total of 10 microscopic fields examined in duplicate wells per treatment and are representative of two independent experiments (C).***P≤0.001 One-way ANOVA with Tukey's post-test.

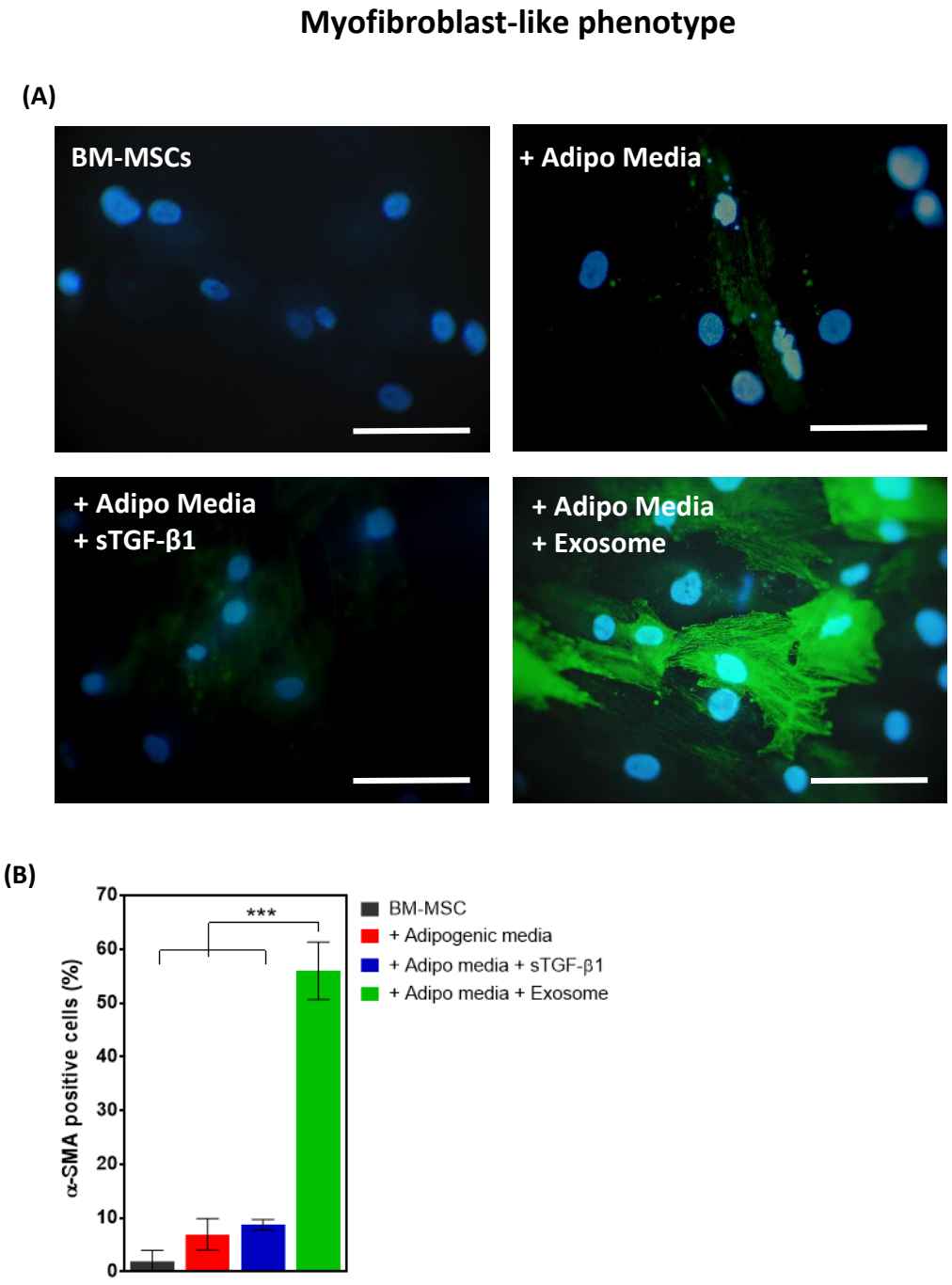

Figure 4.5: Presence of DU145 exosomes in the adipogenesis media trigger enhanced α-SMA expression in BM-MSCs. BM-MSCs were cultured in standard media or adipogenesis media (with or without sTGF-β1 (1ng/ml) or DU145 exosomes (150µg/ml) as depicted) over 21 days. The cells were stained for α-SMA (green) and DAPI (blue). Scale 100µm (A). Quantification of the proportion of α-SMA positive cells, from a total of 6 microscopic fields examined in duplicate wells per treatment, is shown (**B**). Representative of two independent experiments. ***P≤0.001 One-way ANOVA with Tukey's post-test.

4.2 Discussion

Our data fulfils ISCTs criteria for defining MSCs, as the cells were plastic adherent, spindle-shaped in appearance, expressed the cell surface molecules CD73, CD90, CD105 and were negative for the hematopoietic markers. Therefore, we have genuine MSCs which are not contaminated with hematopoietic cells or other stromal cells. In addition, we also demonstrated the expression of the protein CD44 on BM-MSCs, in agreement with previous studies (Spaeth *et al.* 2013; Yang *et al.* 2010). CD44 was demonstrated to facilitate MSC migration *in vitro* through the interaction with extracellular hyaluronan (Zhu *et al.* 2006), which may be crucial for recruitment of MSCs into wound and tumour sites. BM-MSCs also expressed GD-2, similar to that of adipose-derived MSCs (Martinez *et al.* 2007), but the function of GD-2 on MSCs is unknown. In addition, our data revealed a subpopulation of BM-MSCs to express CD146 and this heterogeneity was also noted by others (Tomin *et al.* 2011; Espagnolle *et al.* 2014; Russell *et al.* 2013). CD146 positive and negative BM-MSCs were found to express similar levels of CD73, CD90 and CD105 but under appropriate conditions, only the CD146 positive MSCs were committed towards a vascular smooth muscle lineage characterised by up-regulation of calponin-1 and the ability to contract collagen matrix (Espagnolle *et al.* 2014). Therefore there are subpopulations of BM-MSCs that are more prone to differentiate into certain cell types.

The panel of cell surface molecules used to characterise MSCs do not distinguish MSCs from fibroblasts and myofibroblasts as they also display similar characteristics. The presence of α-SMA stress fibres was able to distinguish myofibroblasts from the other two stromal cell types, but it remained difficult to discriminate between fibroblasts and BM-MSCs. Based on this reason, some researchers argue that MSCs and fibroblasts are identical (Hematti 2012). However, the SSEA-4 glycoprotein usually expressed in embryonic stem cells was also expressed on BM-MSCs (Gang *et al.* 2007) and here we confirm the value of SSEA-4 in distinguishing MSCs from fibroblasts and myofibroblasts in an unequivocal manner. SSEA-4 does not play critical roles in maintaining the pluripotency of embryonic cells (Brimble *et al.* 2007), but instead is related to the multipotency function, as only the MSCs expressing SSEA-4 exclusively exhibited the capacity to differentiate into the classical multi-lineage pathways *in vitro* (Rosu-Myles *et al.* 2013). Therefore the SSEA-4 subpopulation within the MSCs is indicated to truly

exhibit the multi-lineage capacity. Overall, it is a challenge to define MSCs in tissues, but SSEA-4 may be a definitive marker for MSCs which can help identify these cells *in situ*. Our data demonstrated an insignificance difference in SSEA-4 positive cells among the normal and prostatic stromal cell populations (taken from prostatectomy tissue). This may have been partly affected by the small sample size used for assessment which is taken into account by the t-test, resulting in a bigger p-value. Nevertheless, there was a small percentage of stromal cells from both normal and tumour prostate to be SSEA-4 positive, suggesting the presence of MSCs in prostatic stromal cell populations. However, the origin of SSEA-4 positive MSCs within the prostate stroma are unknown. It may be that SSEA-4 is also expressed on MSCs from other sources such as adipose tissue and SSEA-4 may also be expressed on cancer stem cells. In addition, whether SSEA-4 expression decreases once MSCs have migrated or differentiated requires investigation. A marker unique to BM-MSC, will enable us to track BM-MSCs as contributors to the tumour stroma.

The last criteria and arguably the most important for defining MSCs, is their functional multi-lineage differentiation capacity. Here we confirm that BM-MSCs can differentiate into adipocytes and the addition of sTGF-β1 or DU145 exosomes along with the adipogenesis media had the capacity to override the potent adipogenic differentiation programme. However, it was only the PCa exosomes that imposed a switch towards generating myofibroblast-like cells. TGF-β1 is a key cytokine driving the differentiation of MSCs into various mesenchymal cell types at the dose used in this study (1ng/ml). For example, MSCs treated with sTGF-β1 over 14 days can differentiate into vascular smooth muscle cells (Guerrero *et al.* 2014). In addition the presence of sTGF-β1 along with the adipogenic stimulants, dexamethasone can halt MSC differentiation towards adipocytes and drive the MSCs to differentiate into osteoblasts (Jaiswal *et al.* 1997; Bruder *et al.* 1997). Furthermore, 3-dimensional conformation of MSC aggregates with sTGF-β1, dexamethasone and insulin will undergo chondrogenic differentiation (Johnstone *et al.* 1998; Mackay *et al.* 1998; Lee *et al.* 2004b). Therefore sTGF-β1 within the adipogenesis media may drive MSCs to differentiate into mesenchymal cell types, other than the adipocytes or myofibroblasts.

Our data show that PCa exosomes can differentiate MSCs into myofibroblast-like cells, but whether this effect is solely dependent on PCa exosomes and not observed as a synergistic effect with other hormones present within the adipogenesis media requires investigation. DU145 and PC3 exosomes have been demonstrated to express high levels of latent TGF-β1, which can be presented to recipient cells in a biologically active manner (Webber *et al.* 2010). In addition, a distinct phenotype and function of myofibroblasts generated from fibroblasts using exosomes, in comparison to using sTGF-β1 has been shown (Webber *et al.* 2014). Thus, even though the interaction between exosomes and MSCs are not well understood, exosomal-TGFβ1 is believed to play a role in this myofibroblastic differentiation, and can be a focus for a mechanistic investigation. In addition the function of exosome-modified MSC in promoting tumour progression warrants further investigation.

Chapter 5: Differentiation of BM-MSCs

5.1 Direct effect of exosomes on MSC phenotype

In the previous chapter, prostate cancer exosomes within the adipogenesis media were shown to drive BM-MSC differentiation away from adipogenesis and towards a myofibroblast-like cells. Here, the direct effect of PCa exosomes on BM-MSCs differentiation will be explored.

5.1.1 Phenotypic changes of BM-MSCs in response to exosomes

To assess the fate of BM-MSC differentiation in response to PCa exosomes, the BM-MSCs were firstly growth arrested overnight once 70% confluent. Thereafter BM-MSCs were cultured in standard media (DMEM 1% exosome depleted FBS) alone or with a single stimulation with sTGF-β1 (1ng/ml) or exosomes from DU145 or PC3 cell lines at equivalent TGF-β1 dosage (150µg/ml or 75µg/ml, respectively) over a 14 day period. The BM-MSCs were fixed and phenotypic changes such as the expression of α-SMA were explored by immunohistochemistry. In addition, the percentage of positive cells were counted over six microscopic fields (figure 5.1 A,B), revealing BM-MSCs treated with sTGF-β1 to exhibit negligible change in α-SMA positive cells, compared to that of the untreated MSCs. Only the PCa exosomes (DU145 or PC3 derived) drove a significant elevation, in α-SMA positive cells, by a 6-fold increase in comparison to the untreated MSCs ($P \leq 0.01$). Importantly α-SMA protein was not simply elevated in these experiments but was present as organised stress-fibres; the onset of which is a key characteristic of myofibroblasts. Thus, unlike sTGF-β1, cancer exosomes differentiate the majority of BM-MSCs into α-SMA positive myofibroblast-like cells.

The level of pro-angiogenic growth factors such as VEGF-A and HGF secreted by the undifferentiated and differentiated BM-MSCs was also investigated, by measuring the quantity of these growth factors present within the BM-MSC conditioned medium (CM) which has been normalised to their cell number (figure 5.1C). There was around twice as much of VEGF-A found in MSC CM in the presence of exosomes ($P \leq 0.05$) in comparison to untreated MSC CM. Similarly, there was an elevated level of HGF ($P \leq 0.001$) in exosome-treated MSC CM in comparison to the untreated. In contrast, there was less HGF in the CM when BM-MSCs was treated with sTGF-β1. From this we

can conclude that exosomes and sTGF-β1 differentiate MSCs but towards different end points, as shown by the striking difference in phenotype and secretory profile.

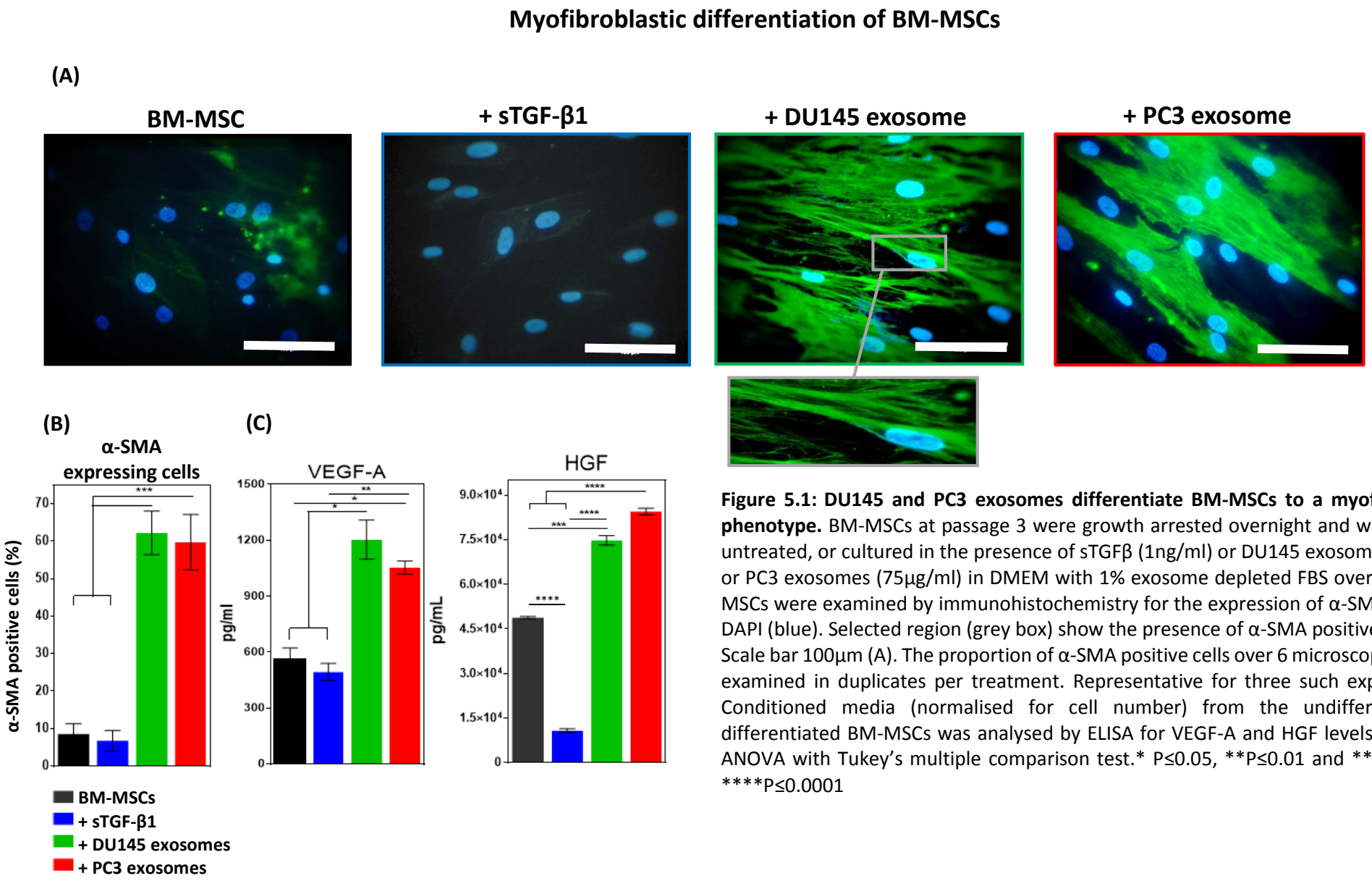

Figure 5.1: DU145 and PC3 exosomes differentiate BM-MSCs to a myofibroblast-like phenotype. BM-MSCs at passage 3 were growth arrested overnight and were either left untreated, or cultured in the presence of sTGFβ (1ng/ml) or DU145 exosomes (150ug/ml) or PC3 exosomes (75µg/ml) in DMEM with 1% exosome depleted FBS over 14 days. BM-MSCs were examined by immunohistochemistry for the expression of α-SMA (green) and DAPI (blue). Selected region (grey box) show the presence of α-SMA positive stress fibres. Scale bar 100µm (A). The proportion of α-SMA positive cells over 6 microscopic fields were examined in duplicates per treatment. Representative for three such experiments (B). Conditioned media (normalised for cell number) from the undifferentiated and differentiated BM-MSCs was analysed by ELISA for VEGF-A and HGF levels (C). One-way ANOVA with Tukey's multiple comparison test.* P≤0.05, **P≤0.01 and ***P≤0.001 and ****P≤0.0001

5.1.2 Dose and kinetics of MSC differentiation in response to DU145 exosomes

So far we know that PCa exosomes can differentiate BM-MSCs into myofibroblast-like cells. However the optimal dose and time of exosome exposure needed to generate myofibroblasts from BM-MSCs is not yet known. Most researchers use sTGFβ-1 at a dose of 1-1.5ng/ml to differentiate cells into myofibroblasts (Lewis *et al.* 2004; Lijnen *et al.* 2003; Jester *et al.* 1999). Likewise a single dose of 200µg/ml of PCa exosomes which was a matched-TGF-β1 dose to 1.5ng/ml sTGF-β1 induced fibroblasts to differentiate into α-SMA positive myofibroblasts after 72h (Webber *et al.* 2010). With regard to MSCs, Gu *et al.* (2012) treated umbilical cord derived MSCs with 800µg/mL of gastric cancer exosomes repeatedly every 3 days, over a 14 day period, resulting in α-SMA positive myofibroblast-like cells. In contrast to this high dose, as little as 4 or 20µg of breast cancer exosomes was used to investigate if adipose-derived MSCs differentiate into myofibroblasts, they did not however mention how long the MSCs were treated for. Nevertheless, low levels of α-SMA positive cells were observed but the actin stress fibres were not detected (Cho *et al.* 2012). Thus, exosomes at a very low dose was probably too weak to have an effect on MSC differentiation towards myofibroblast-like cells. In addition, in these cases, the expression level of TGF-β1 on exosomes was not known and even though both low and high range of exosome dose have been used to study myofibroblastic differentiation, the optimal dose and time of exosome exposure needed to generate myofibroblasts from BM-MSCs are not yet known.

Here, the kinetics of BM-MSC differentiation in response to PCa exosomes was tested by treating the BM-MSCs with a single dose of 150µg/ml DU145 exosomes over different time points (3d, 6d, 9d and 14d period). After each time point, α-SMA expression was assessed by immunohistochemistry and the proportion of α-SMA positive cells were counted. There was no spontaneous elevation of α-SMA in the untreated BM-MSCs. The kinetics of α-SMA onset was slower than we had expected, certainly slower than that for fibroblasts in which α-SMA peaks at around 3 days post-exosome stimulation (Webber *et al.* 2010). Here, there was no change in α-SMA status by day 3 for BM-MSCs, with changes only becoming apparent 6 days post exosome treatment but continuing steadily thereafter approaching 70% positivity with α-SMA stress fibres by day 14 (figure 5.2 A,B). The level of pro-angiogenic factors, VEGF-A and HGF secreted by the

exosomally-differentiated BM-MSCs were also measured using ELISA and compared to untreated and sTGF-β1 treated BM-MSCs. As expected, the secretion of these growth factors by the untreated BM-MSCs was low over 14 days and the VEGF-A level remained unchanged with sTGF-β1 treatment (figure 5.2C), agreeing with earlier observations. In contrast, elevated secretion of VEGF-A and HGF by exosome-treated BM-MSCs occurred, with peak elevation of VEGF and HGF secretion ($P \leq 0.001$) observed at day 8 and 6 respectively. Therefore, there was notable changes in the cells at time point's preceding the changes in the cytoskeleton (α-SMA), and so the response to exosomes is actually quick but takes two weeks to fully generate into myofibroblasts.

The impact of exosome dose on BM-MSC differentiation was examined, by treating BM-MSCs with DU145 exosomes at 75µg/ml, 150µg/ml or 300µg/ml for 14 days. The response to exosome treatment was dose dependent, with an approximately 3 fold elevation to around 30% of the population becoming α-SMA positive at 75µg/ml. This increased to around 75% with very high exosome doses of 300µg/ml (figure 5.3 A,B). When evaluating levels of pro-angiogenic factors secreted by the MSCs, there was no significant difference in VEGF-A concentration between the untreated and 75µg/ml exosome treated MSCs. However, a 4 fold increase in VEGF-A secretion was observed with 150µg/ml and this incremented further with 300µg/ml exosomes ($P \leq 0.0001$) (figure 5.3C). Similarly, HGF secretion by exosome-treated BM-MSCs was dose-dependent, as HGF secretion was elevated with increasing exosome-dose. In summary, our data show exosome-mediated MSC differentiation is time and dose-dependent.

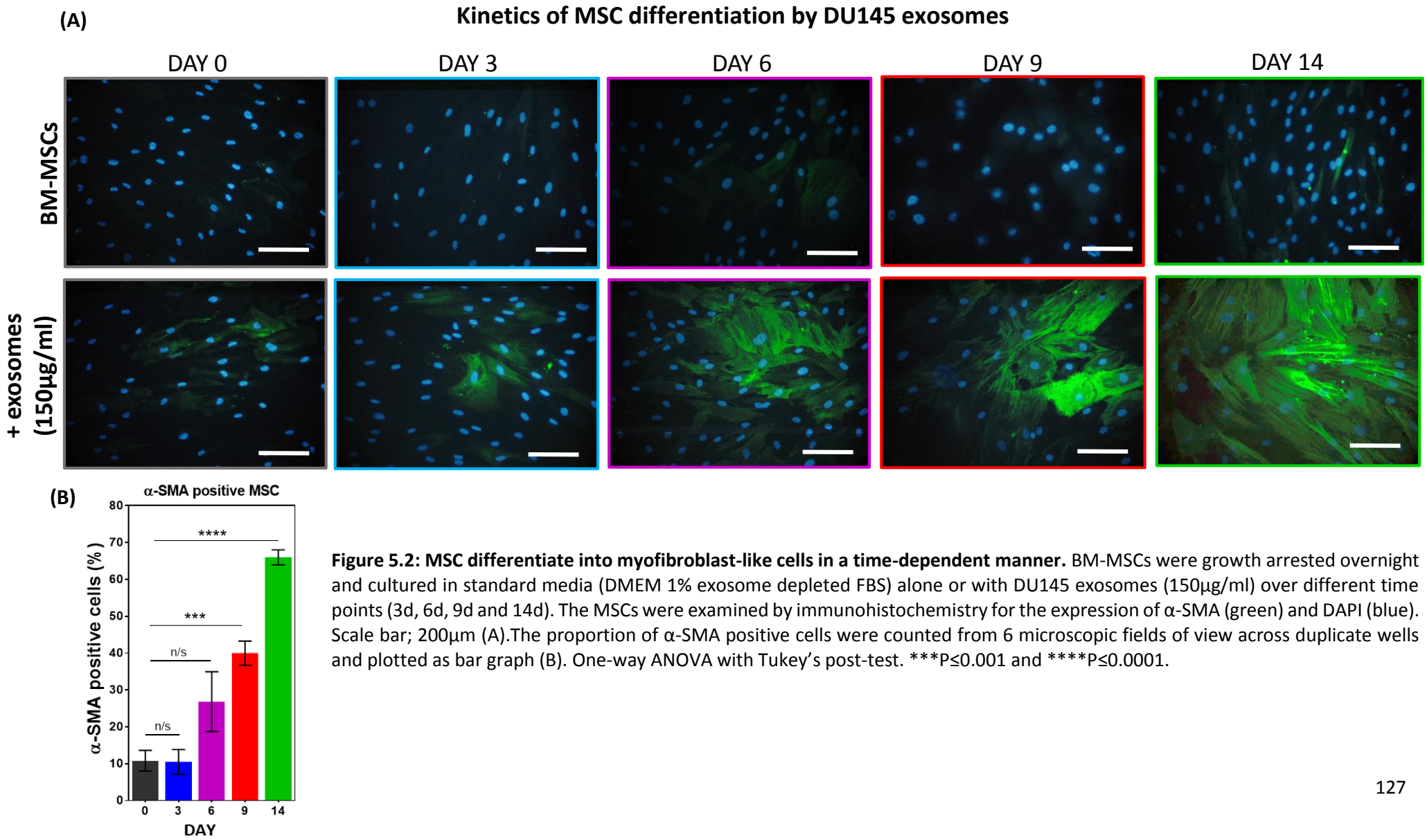

Figure 5.2: MSC differentiate into myofibroblast-like cells in a time-dependent manner. BM-MSCs were growth arrested overnight and cultured in standard media (DMEM 1% exosome depleted FBS) alone or with DU145 exosomes (150µg/ml) over different time points (3d, 6d, 9d and 14d). The MSCs were examined by immunohistochemistry for the expression of α-SMA (green) and DAPI (blue). Scale bar; 200µm (A).The proportion of α-SMA positive cells were counted from 6 microscopic fields of view across duplicate wells and plotted as bar graph (B). One-way ANOVA with Tukey's post-test. ***P≤0.001 and ****P≤0.0001.

Kinetics of MSC differentiation by DU145 exosomes

(C)

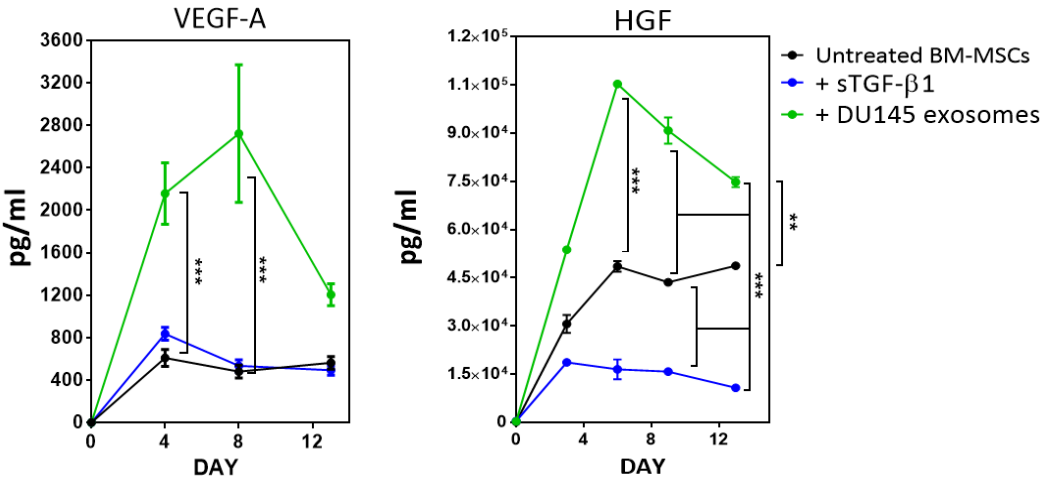

Figure 5.2 continued: MSC differentiate into myofibroblast-like cells in a time-dependent manner. Conditioned media (normalised for cell number) taken from BM-MSCs treated with sTGF-β1 or DU145 exosomes at specified time point, were analysed by ELISA for levels of VEGF-A or HGF (C). Two-way ANOVA with Benferroni post-test. * P≤0.05, **P≤0.01 and ***P≤0.001 (n=3).

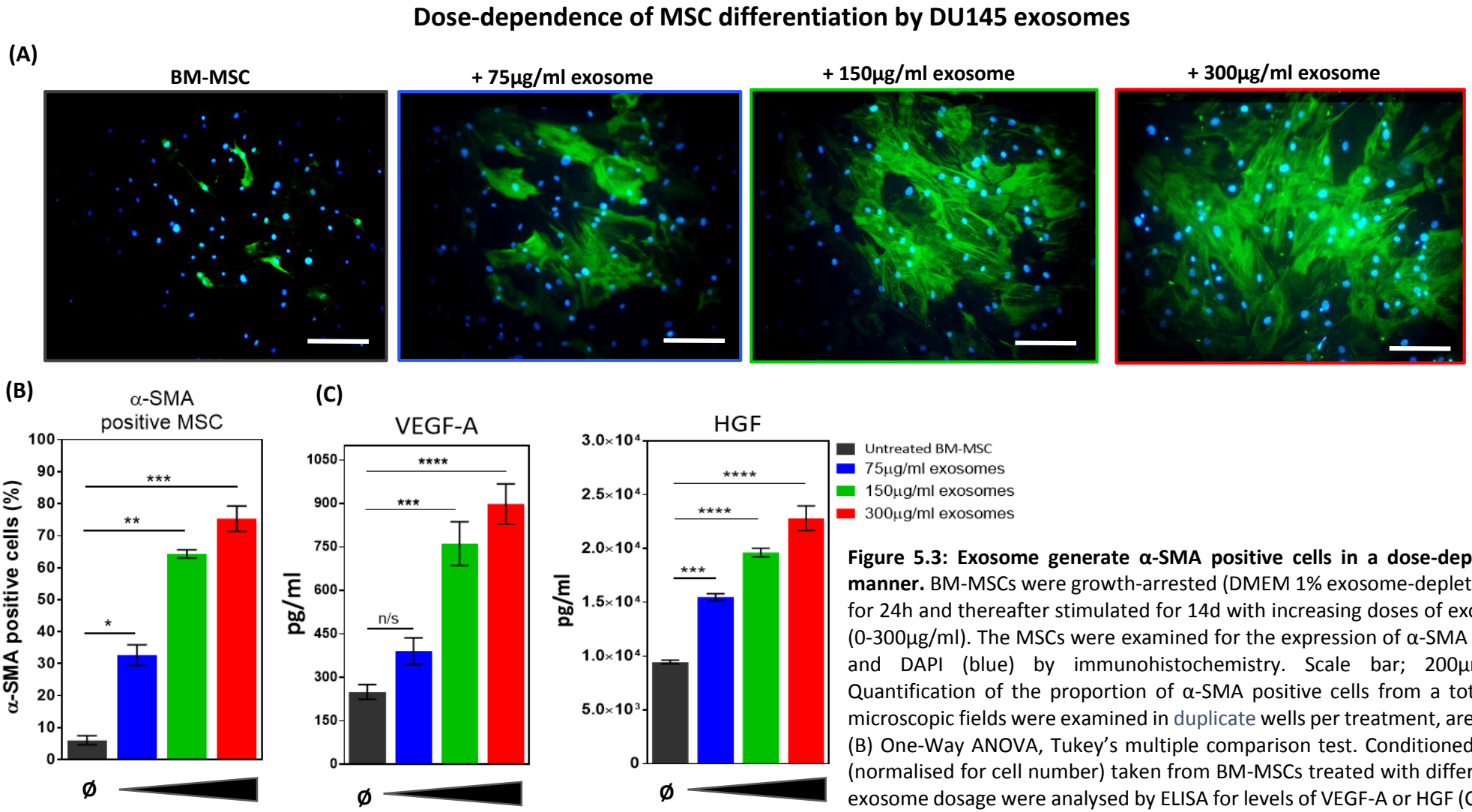

Figure 5.3: Exosome generate α-SMA positive cells in a dose-dependent manner. BM-MSCs were growth-arrested (DMEM 1% exosome-depleted FBS) for 24h and thereafter stimulated for 14d with increasing doses of exosomes (0-300µg/ml). The MSCs were examined for the expression of α-SMA (green) and DAPI (blue) by immunohistochemistry. Scale bar; 200µm (A). Quantification of the proportion of α-SMA positive cells from a total of 6 microscopic fields were examined in duplicate wells per treatment, are shown (B) One-Way ANOVA, Tukey's multiple comparison test. Conditioned media (normalised for cell number) taken from BM-MSCs treated with differentiate exosome dosage were analysed by ELISA for levels of VEGF-A or HGF (C). Two-way ANOVA with Benforri post-test. * P≤0.05, **P≤0.01, ***P≤0.001 and ****P≤0.0001.

5.2 The relative importance of exosomes, as a component of the cancer secretome, in driving MSC differentiation

The secretion of exosomes is regulated by Rab27a; a GTPase involved in the fusion of multivesicular endosomes containing exosomes to the plasma membrane, resulting in the release of exosomes (Ostrowski *et al.* 2010; Bobrie *et al.* 2012). Blockade of Rab27a has been shown to decrease the secretion of exosomes in many studies (Li *et al.* 2014; Bobrie *et al.* 2012; Ostrowski *et al.* 2010). Here, the secretion pathway of exosomes was interfered by Rab27a knock down in DU145 cells using the ribozyme silencing method, carried out by our group in collaboration with Prof Wen Jiang (Cardiff University). These DU145 Rab27a^{KD} cells were then used to test the exosome-dependency of BM-MSC differentiation.

5.2.1 Characterisation of Rab27a^{KD} DU145 cells

Two RAB27a^{KD} DU145 cell lines were generated using the ribozyme silencing method, referred to as RAB27a^{KD2} and RAB27a^{KD3}. Confirmation of the knock down of RAB27a was carried out using qPCR to show the relative quantitation (RQ) of the RAB27a mRNA (figure 5.4). In comparison to the DU145$^{Control\ Vector}$ cells, RAB27a mRNA level was reduced by 53% and 65% in DU145^{RAB27aKD2} and DU145^{RAB27aKD3}, respectively. Therefore DU145^{RAB27aKD3} had the lowest mRNA level of RAB27a. To investigate the effects of RAB27a silencing upon the endocytic tract, the DU145$^{Control\ Vector}$ and DU145^{RAB27aKD3} cells were stained for the early endosome antigen-1 (EEA-1) and lysosome associated membrane protein-2 (LAMP-2) and evaluated using immunohistochemistry. Given the association of exosomes with the late endocytic tract, it was predicted that there will be very little impact in the distribution of EEA-1 due to the silencing of RAB27a. As expected the knock down of RAB27a did not affect the localisation of EEA-1, as in both the control vector and RAB27a^{KD} cells, EEA-1 protein was found to be spread throughout the cell (figure 5.5A). Conversely, expression of LAMP-2, a marker of lysosomes and endosomes, became concentrated near the nuclei (principally where the late endosomes are located) (figure 5.5B). This cytopathic effect was also reported by Ostowski *et al.* (2010) when silencing RAB27a, and is suggestive of a failure to secrete LAMP-2 positive exosomes, with the cell having to concentrate this molecule into lysosomes possibly for degradation.

To observe whether knock down of RAB27a mRNA affected exosome secretion, the particle concentration was quantified. To do this, the conditioned media from the DU145 control vector and both the RAB27a^{KD} DU145 cells were collected, spun at 400g and 2000g to remove cells and cellular debris, and filtered to remove large non-exosomal particles. The media was normalised to cell count and then subjected to Nanoparticle Tracking Analysis, as mentioned in materials and methods. In comparison to the DU145$^{Control\ Vector}$ CM, the particle concentration within the DU145^{RAB27aKD2} CM and DU145^{RAB27aKD3} CM was reduced by 16.8% ($P<0.01$) and 67.3% ($P<0.0001$), respectively (figure 5.6A). This agreed well with the aforementioned decrease in cellular mRNA for RAB27a. Because the NTA method does not discriminate exosomes from other nano-particles, it was important to use other approaches to confirm these data. To confirm the loss of exosomes from RAB27a knock down, the CM from the control and RAB27a^{KD} cells were normalised to cell count and subjected to high speed ultracentrifugation (120,000g) to obtain a pellet, which should contain exosomes if any present. The resuspended pellet was stained for the exosome-associated proteins ALIX and GAPDH (figure 5.6B). As expected, DU145^{RAB27aKD2} had reduced ALIX staining in comparison to the control, whereas negligible amount of ALIX and GAPDH staining were seen in the DU145^{RAB27aKD3} sample. Our conclusion is that DU145^{RAB27aKD3} is the better knockdown and attenuates exosome secretion the most. From hereafter, DU145^{RAB27aKD2} was no longer used for analysis.

Another way to deplete exosomes from tumour cell conditioned media is by high speed ultracentrifugation at 120,000g as mentioned in materials and methods and as described above. Nanoparticle Tracking Analysis of the conditioned media revealed 91% reduction in nanoparticle concentration by this method, in comparison to the control tumour cell CM (pre-spin CM) (figure 5.7), indicating that the majority of the exosome particles can be removed by high speed ultracentrifugation. Therefore exosome deficient DU145 conditioned media can be produced by gene manipulation or directly by physical manipulation, respectively.

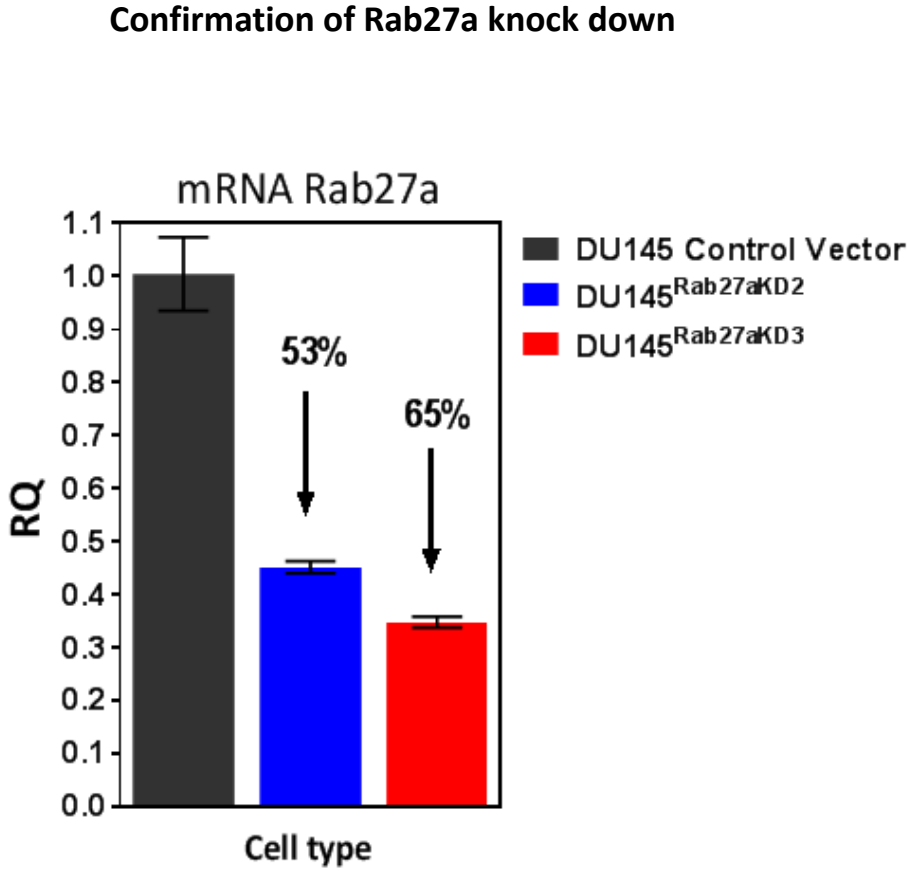

Figure 5.4: Ribozyme silencing method of Rab27a^{KD} cells have reduced Rab27a mRNA expression. Relative quantitation (RQ) of Rab27a mRNA among the low passage of DU145$^{Control\ Vector}$, DU145^{Rab27aKD2} and DU145^{Rab27aKD3} were evaluated using qPCR with GAPDH marker as the internal control (housekeeping gene).

Location of EEA1 and LAMP-2 within the DU145 control vector and RAB27a^{KD} cells

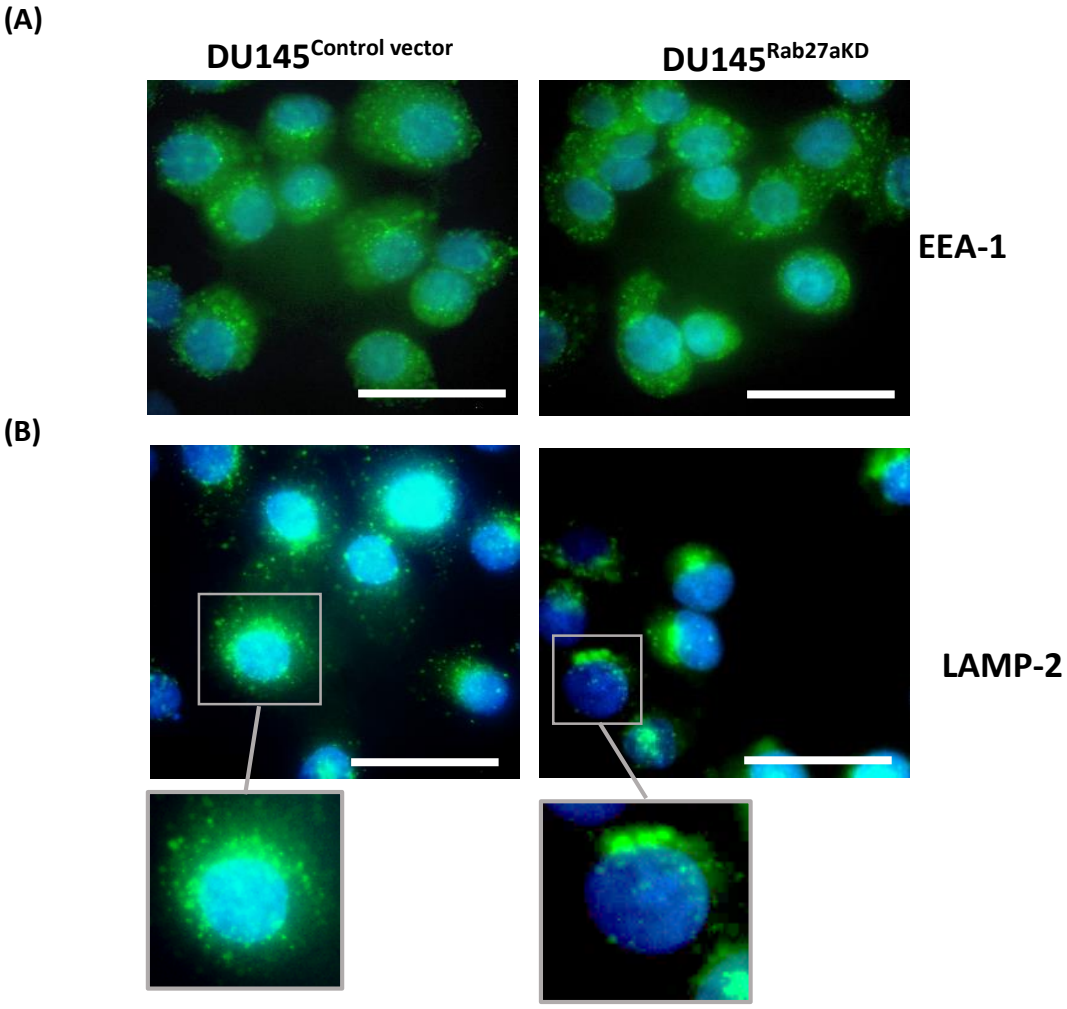

Figure 5.5: RAB27a^{KD} does not affect the location of EEA-1 but affects the location of LAMP-2. DU145$^{control\ vector}$ and DU145^{Rab27aKD3} cells were fixed and expression of EEA-1 (green) (A) and LAMP-2 (green) (B) were assessed by immunohistochemistry. DAPI (blue) was used to stain nuclei. The spread-out and concentrated location of LAMP-2, in the DU145$^{Control\ vector}$ and DU145^{Rab27aKD} are shown, respectively in the grey box. Scale bar 100µm.

RAB27a knock down attenuates exosome secretion

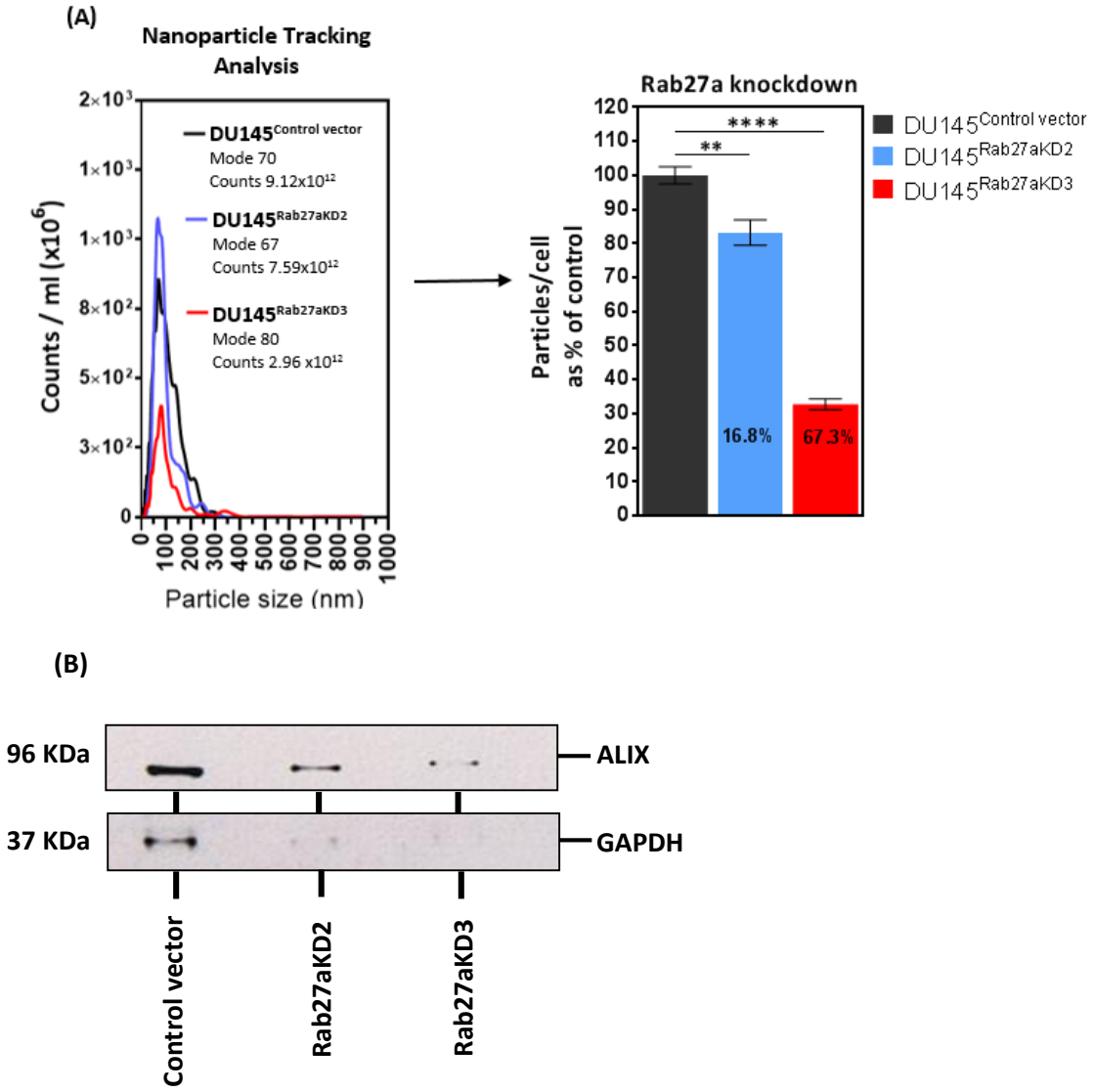

Figure 5.6: RAB27a^{KD} attenuate exosome secretion.
Conditioned media from the DU145$^{Control\ Vector}$, DU145^{Rab27aKD2} and DU145^{Rab27aKD3} cells were collected, normalised to cell count and particle count was measured using Nanoparticle Tracking Analysis and percentage of particle concentration by the different cells plotted as a bar graph. 6 measurements were taken per sample. One-way ANOVA with Tukey's post-test **P≤0.01, ***P≤0.001 and ****P≤0.0001 (A). Exosome pellet from the different cell types were stained for the antibodies against ALIX and GAPDH and evaluated by western blotting blot (B).

High speed ultracentrifugation removes exosomes

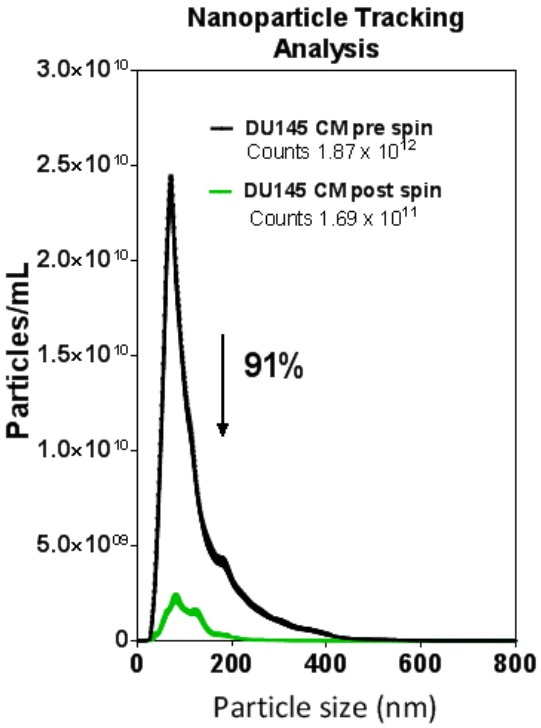

Figure 5.7: Exosomes can be removed by high speed ultracentrifugation.
Normal DU145 conditioned media pre-spin (black) and post-spinning (green) by high speed ultracentrifugation were subjected to Nanoparticle Tracking Analysis for quantifying exosome particle concentration. Six measurements were obtained from each sample. One-way ANOVA with Tukey's post-test * P<0.05, **P<0.01 and ***P<0.001.

5.2.2 MSC cultured in exosomes depleted DU145 culture media do not differentiate into myofibroblasts

To investigate whether BM-MSC differentiation was solely dependent on prostate cancer exosomes, BM-MSCs were cultured in culture media (CM) from exosome-proficient and exosome-deficient DU145 cells. DU145 cancer cells had been rendered exosome-deficient by Rab27a knockdown, or alternatively the exosomes were depleted from the CM using ultracentrifugation at 120,000 x g. In addition, the exosome containing pellet generated by the spin was resuspended in the original volume and used to culture the BM-MSCs. After 14 days, α-SMA expression was assessed by immunohistochemistry and the proportion of α-SMA positive cells were examined.

Untreated BM-MSCs exhibited negligible levels of α-SMA positive cells, as expected and in the presence of non-manipulated DU145 CM, the majority of BM-MSCs differentiated into α-SMA positive myofibroblasts (figure 5.8 A,B). This myofibroblastic differentiation failed to occur when the BM-MSCs were cultured with exosome-depleted DU145 CM, in which the $DU145^{Rab27aKD}$ CM or exosome depleted DU145 CM post-spin revealed a 6-fold and 5-fold reduction in α-SMA positive cells, respectively (figure 5.8B), akin to the findings with untreated BM-MSCs in standard media. The exosome containing pellet however was sufficient to fully restore myofibroblastic differentiation to that of the DU145 control CM. Therefore our data show that cancer exosomes and not other soluble factors within the cancer cell secretome are chiefly responsible for controlling the differentiation of BM-MSCs into myofibroblasts.

Myofibroblastic differentiation of BM-MSCs is dependent on PCa-derived exosomes

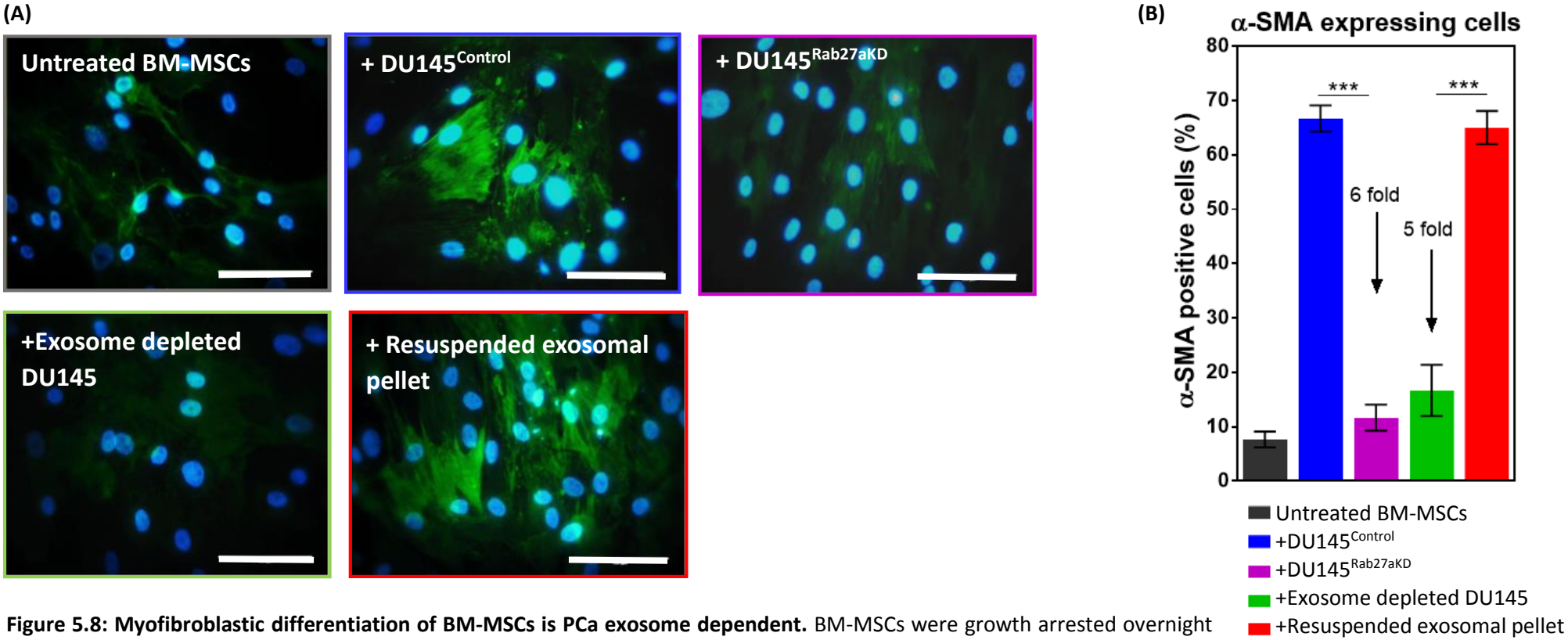

Figure 5.8: Myofibroblastic differentiation of BM-MSCs is PCa exosome dependent. BM-MSCs were growth arrested overnight and thereafter cultured in standard media (DMEM 1% FBS) alone or with DU145 culture media (CM) at a 1:1 ratio. CM used was normalised for cell number and was taken from $DU145^{Control}$ or $DU145^{Rab27aKD}$ cells, or from $DU145^{Control}$ cells following ultracentrifugation to pellet exosomes (120,000g supernatant), or the exosome containing pellet from this spin (120,000g pellet) which was resuspended in the original volume. After 14 days, cells were assessed for the expression of α-SMA (green) and DAPI (blue) by immunohistochemistry. Scale bar 200µm (A). Quantification of the proportion of α-SMA positive cells from a total of 6 microscopic fields were examined in duplicate wells per treatment, and mean (±SD) proportion of α-SMA positive cells are shown. Representative of two experiments (B). Students T-test ***P≤0.001.

5.3 The role of exosomal TGF-β1 in MSC differentiation

The mechanism by which exosomes trigger alterations in recipient cells are not well understood. PCa exosomes have been shown to express TGF-β1 in the previous chapter and is hypothesised to be chiefly responsible for BM-MSC differentiation into myofibroblast-like cells.

5.3.1 Blocking exosomal TGF-β1 partially inhibits α-SMA expression

To test the role of exosomal TGF-β1 on BM-MSC differentiation, TGFβ signalling was blocked using either an inhibitor of the ALK5 TGFβ-receptor I, SB431542 (10μM) or using a neutralising antibody (10μg/ml) against TGF-β that will bind to and inhibit exosomally-delivered TGF-β1 as described by others (Webber *et al.* 2010; Webber *et al.* 2014). The proportion of α-SMA positive cells, arising following stimulation was assessed by immunohistochemistry and quantified, revealing a 6 fold increase in α-SMA positive cells forming stress fibres, in the presence of exosomes. However, exosomes added with either inhibitors, failed to trigger differentiation into α-SMA positive cells, as the percentage α-SMA positive cells remained low, similar to that of the untreated or sTGF-β1 treated BM-MSCs (figure 5.9 A,B). Therefore, the mechanism by which prostate cancer cells modulate BM-MSC fate requires exosomes and exosomally-delivered TGF-β1.

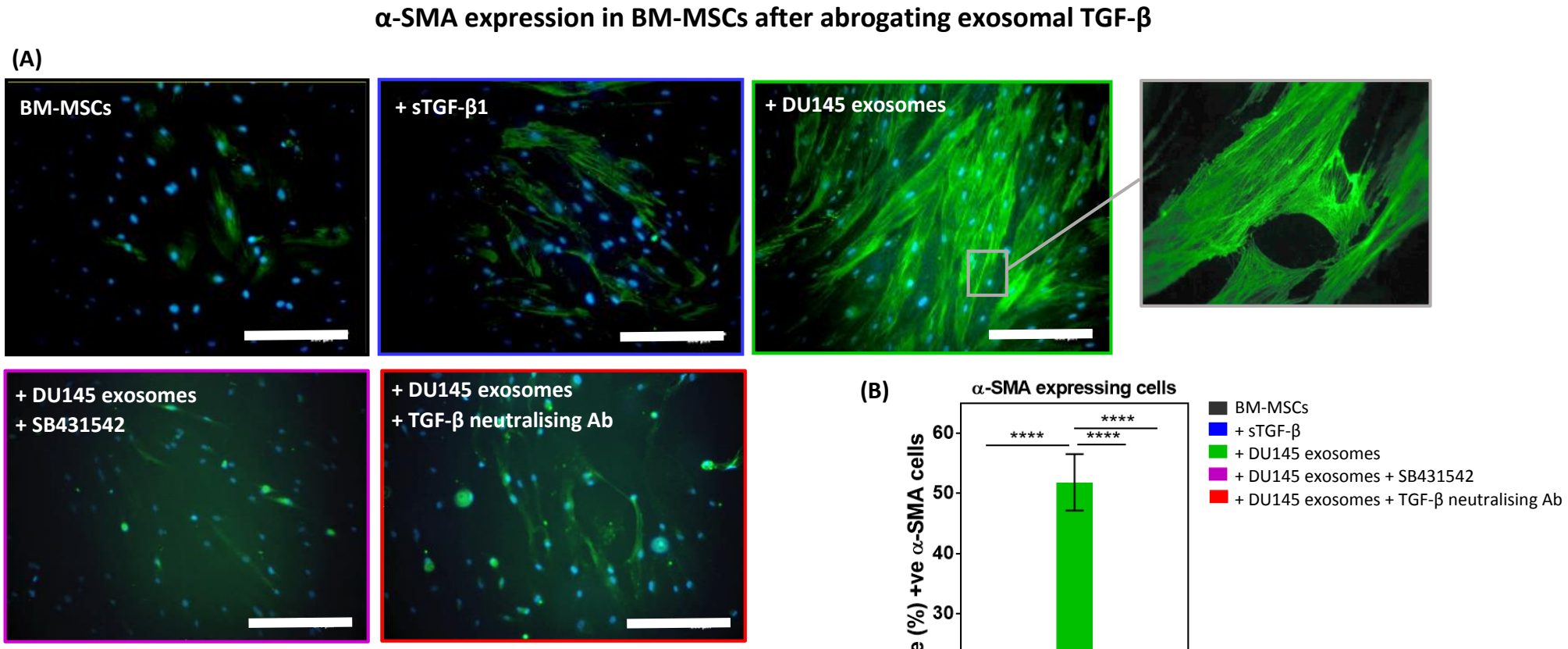

Figure 5.9: Myofibroblastic differentiation of MSC is DU145 exosome dependent.
BM-MSCs were growth arrested for 24h and then cultured in standard media (DMEM 1% FBS) alone or with sTGFβ (1ng/ml), or DU145 exosome (150µg/ml) in the absence or presence of the Alk-5 inhibitor SB431542 (10µM) or neutralising antibody against TGFβ (10µg/ml). At day 14, the cells were assessed for the expression of α-SMA (green) and DAPI (blue) by immunohistochemistry. Filamentous stress fibres are observed with exosome treatment (grey box). Scale bar; 200µm (A). Quantification of the proportion of α-SMA positive cells from a total of 6 microscopic fields were examined in duplicate wells per treatment are shown (B). Bars, Mean ±SD. One-Way ANOVA with Tukey's post test ***P≤0.001 and ****P≤0.0001.

5.4 Discussion

Soluble TGF-β1 is a well-known cytokine involved in the myofibroblastic differentiation of fibroblasts (Thannickal *et al.* 2003; Midgley *et al.* 2013). In this chapter, the phenotype of BM-MSCs differentiated by sTGF-β1 or TGF-β1 positive PCa exosomes was shown to differ. Treatment with sTGF-β1 resulted in low levels of α-SMA positive cells and VEGF-A secretion, similar to that of the untreated BM-MSCs and a decreased level of HGF secretion. Therefore, unlike with fibroblasts, sTGF-β1 fails to differentiate BM-MSCs into myofibroblast-like cells and the reasons for this are not well understood. However, MSCs can clearly respond to sTGF-β1 as they have the TGF-β receptor and intracellular signalling machinery to do so (Shangguan *et al.* 2012) and sTGF-β1 is known to play an important role in directing fate decisions for MSCs. For example, sTGF-β1 is a key requirement for stimulating the initial stages of chondrogenic differentiation of MSCs (Tuli *et al.* 2003; Niger *et al*. 2013), by supporting MSC condensation, chondrocyte proliferation, extracellular matrix deposition of type II collagen and aggrecan, and finally terminal differentiation which is required for chondrogenesis. For example, MSC condensation is strongly stimulated by TGF-β1 induced elevation of N-cadherin expression, which in turn enhances cell adhesion. TGF-β1 signalling via Smad 1/5/8 is required for chondrocyte hypertrophy, a part of the differentiation process (Tuli *et al.* 2003; Song *et al.* 2007). Likewise, TGF-β1 can provide support for osteoblast (Zhou, 2011) and smooth muscle cell differentiation (Alimperti *et al.* 2014), but inhibits adipogenesis (Choy *et al.* 2003) and myogenesis (Liu *et al.* 2001). Therefore, under the influence of sTGF-β1, MSCs maybe more prone to differentiate into cell types other than myofibroblasts.

In contrast, PCa exosomes had the potent capacity to differentiate BM-MSCs into myofibroblasts, as noted by the onset of α-SMA stress-fibres. This finding agrees with recent observations in umbilical cord and adipose tissue derived MSCs using gastric cancer and breast cancer exosome, respectively (Gu *et al.* 2012; Cho *et al.* 2012). Furthermore, we have shown that exosome treated BM-MSCs secrete elevated levels of the pro-angiogenic factors; VEGF and HGF, which are consistent with features of prostate cancer-associated myofibroblasts, as shown by previous studies (Webber *et al.* 2014). Our data demonstrates the response to exosome treatment is dose and time-dependent, where exosomes had a remarkable effect on BM-MSCs with a single treatment of 150μg/ml, giving a dramatic

differentiation towards α-SMA stress fibres myofibroblasts-like cells at day 14. This differed to Gu *et al.* (2012) study, where umbilical cord-MSCs required 800μg/ml gastric cancer-exosomes, with repetitive exposure every 3 days over a 14 day period. The difference may be because the expression of TGF-β1 from PCa exosomes may significantly differ from exosomes of gastric cancer cells. Also, these studies isolate exosomes using crude pelleting with no sucrose cushion, which results in pelleting exosomes along with a lot of contaminants as shown by Webber *et al. (*2012). These contaminants which contribute to the dose of exosomes used may have no effect on BM-MSCs. Unlike these studies, I have isolated exosomes using the sucrose cushion, which obtains exosomes with much less contaminates as shown by Webber (2012). Thus it is likely that the exosomes isolated from the sucrose cushion are more pure, and so a much more apparent effect is seen with lower dose of exosomes.

The kinetics of α-SMA in MSCs takes longer, up to 14 days, in comparison to fibroblasts (Webber *et al.* 2010) in which α-SMA peaks at around 72h post exosome stimulation. In general, BM-MSCs take longer to differentiate, for example 21 days are required for differentiation into adipocytes and chondrocytes and osteoblasts to occur (Pittenger *et al.* 1999; Solchaga *et al.* 2011; Birmingham *et al.* 2012).

Next, in this chapter, we investigated whether BM-MSC differentiation was solely dependent on cancer exosomes and to address this, exosome-deficient cancer cells were used by knock down of Rab27a. This manipulation attenuated exosome secretion from the cells, significantly as shown by loss of exosome associated protein (ALIX) within the exosome containing pellet and a reduction in particle concentration, in agreement with the similar reduction of Rab27a mRNA. Knock down of Rab27a also accumulated LAMP-2 around the nuclei, suggesting an accumulation of exosomes in the cell. This observation agreed with previous studies (Webber *et al.* 2014; Ostrowski *et al.* 2010) and additionally Ostrowski (2010) noted $Rab27a^{KD}$ to result in an enlarged MVE, most possibly from the accumulation of exosomes. Inhibition of Rab27a, however, for assessing exosome function is flawed as inhibition of Rab27a also effects secretion of soluble factors such as placenta growth factor and platelet-derived growth factors in melanoma cells (Peinado *et al.* 2012). Similarly, in breast cancer cells, secretion of other non-exosome associated proteins such as MMP-9 was decreased, with Rab27a knock

down (Bobrie *et al.* 2012). This makes the Rab27a^{KD} approach inadequate for the purpose intended as it is not entirely exosome-specific and evaluation must be taken with caution. We used high speed ultracentrifugation as another approach to remove exosomes and our data demonstrated BM-MSCs failed to differentiate into α-SMA positive myofibroblast-like cells, when cultured in exosome-deficient cancer CM, by either the genetic manipulation or the biophysical approach. Furthermore, the addition of the resuspended exosome rich pellet restored the generation of α-SMA positive-myofibroblasts. Therefore, myofibroblastic differentiation is predominantly an exosome-mediated effect and not governed by other factors derived from the cancer cells.

Lastly, in this chapter, we tried to touch upon the mechanism of interaction between the BM-MSCs and PCa exosomes, involved in the myofibroblastic differentiation. Previous studies have reported fibroblasts and umbilical cord derived MSCs differentiation into myofibroblasts to be exosomal TGF-β1 dependent (Webber *et al.* 2010; Gu *et al.* 2012). Here, we interfered with TGF-β1 signalling by using the ALK5 inhibitor (SB431542), revealing the myofibroblastic differentiation of BM-MSCs to be dependent on TGF-β receptor 1 (TGF-βRI). However, other factors also bind to TGF-βRI, such as activin (Goumans *et al.* 2003). Thus the neutralising antibody against TGF-β1 was used as a blocking experiment to show that the TGF-β1 and TGF-βRI interaction is required for BM-MSC differentiation into myofibroblast-like cells. In addition, studies have demonstrated exosomal TGF-β1 to trigger phosphorylation of SMAD2/3 signalling pathway and inhibition of TGF-β1 on exosomes attenuated SMAD2/3 phosphorylation and the subsequent differentiation of cells into α-SMA positive myofibroblasts (Webber *et al.* 2010; Gu *et al.* 2012). Therefore the myofibroblastic differentiation of BM-MSCs induced by exosomally expressed TGF-β1 may be SMAD-dependent, but this has not been investigated here.

The myofibroblastic differentiation cannot be reproduced using a matched-dose of sTGF-β1 and the reason for this difference may be due to the differences in the interaction between the sTGF-β1 and exosome expressing TGF-β1. TGF-β1 is tethered to the exosome surface by the transmembrane proteoglycan betaglycan and inhibiting the expression of betaglycan using siRNA or releasing betaglycan from exosome surface using pervanadate reagent, both reduced exosome TGF-β1 levels. This in turn, reduced the onset of α-SMA stress fibres in

fibroblasts (Webber *et al.* 2010), indicating that betaglycan aids the delivery of exosomal TGF-β1 to the recipient cell. Furthermore, generating myofibroblasts from fibroblasts using exosomes was dependent on herparan sulphate (HS) side chains. Cleavage of HS side chains from the exosome surface, resulted in the attenuation of SMAD-dependent signalling, therefore the HS side chains are important in delivering efficient SMAD 2/3 signalling to the fibroblasts, and the same may occur to BM-MSCs. In contrast, soluble TGF-β1 is known to induce SMAD 1/5/8 and the Wnt signalling pathway which drive MSC differentiation towards chondrogenesis (Tuli *et al.* 2003). Whether exosomal TGF-β1 drive SMAD-independent pathways such as the Wnt signalling have not been explored. Furthermore exosomes are complex vesicles containing various growth factors, mRNA, miRNA (Valadi *et al.* 2007) which can be taken up by recipient cells (Escrevente *et al.* 2011). Therefore, as well as the interaction with exosomal TGF-β1, the possible co-delivery of other growth factors, mRNA and miRNA from the cancer exosomes may influence differentiation of BM-MSCs into myofibroblasts. Further investigation of the phenotype of exosome-differentiated BM-MSCs may provide us with an insight of the potential function of these myofibroblast-like cells.

Chapter 6: The phenotype of exosome-differentiated BM-MSCs

Phenotype of exosome-differentiated BM-MSCs

The cellular and molecular mechanisms found active in wounds are also found in cancer and so these observations led Harold Dvorak in 1986, to postulate that "tumours are wounds that do not heal" (Dvorak 1986). These include the presence of αSMA positive myofibroblasts (Gabbiani 2003; Orimo *et al.* 2005; Ueno *et al.* 2004) and an increase in proliferation and invasion of epithelial cells (Sternlicht *et al.* 1999). In healing wounds, myofibroblasts are generated from fibroblasts, by TGF-β signalling and other factors, which allows efficient re-epithelialization of the injured site and the myofibroblasts are terminated via apoptosis when the wound is fully covered by a new epidermis (Gabbiani 2003). In carcinoma, however, this process is not self-limiting, and is more akin to chronic wounds, resulting in uncontrollable tumour growth and eventually metastasis (Schäfer and Werner, 2008).

A key step in prostate cancer (PCa) metastasis is the degradation of the extracellular matrix (ECM). Matrix metalloproteinases (MMPs), such as MMP-1 and MMP-13, have been found to be expressed by invasive PCa epithelial cells (PC3 cell line) which help break down collagen type I and type II within the ECM, respectively (Wu *et al.* 1991; Daja *et al.* 2003). MMPs and other proteolytic enzymes are also produced by stromal cells, such as fibroblasts within breast cancer stroma (Witty *et al.* 1995) which degrade the ECM, allowing the migration and invasion of the cells. We know α-SMA is increased in exosome treated BM-MSCs but a more in-depth exploration of the phenotype has not been done before. Since the control of the matrix is a major function of stromal cells and because this is perturbed in cancer, we predicted that we would discover several alterations in relation to this following exosome-mediated differentiation.

To do this, exosome treated BM-MSCs were analysed using a human fibrosis Prolifer™ PCR array. The array covers transcripts of key genes encoding ECM remodelling enzymes, TGF-β signalling molecules and inflammatory cytokines, as well as additional genes important for a chronic wound setting. This would give us a focused read-out and allow us to rapidly assess their validated factors of release.

6.1 Changes in mRNA profile of exosome-differentiated BM-MSCs

The untreated BM-MSCs, sTGFβ treated and exosome treated BM-MSCs were analysed using the PCR fibrosis array to identify any characteristic features of the exosome-generated myofibroblasts.

6.1.1 RT-qPCR fibrosis array analysis of BM-MSCs and differentiated BM-MSCs

From the previous chapter, we know that HGF and VEGF-A secreted by exosome treated BM-MSCs was elevated at a time point earlier than 14 days. Hence we predicted day 4 to be the time point most likely to see changes in growth factors such as VEGF and HGF as well as other proteins involved in fibrosis. Thus BM-MSCs after 4 days of treatment with sTGF-β1 or DU145 exosomes were analysed using the PCR fibrosis array, which contained 84 transcripts of known involvement in fibrosis. The mean fold-change of the transcripts compared to untreated BM-MSCs are shown in table 6.1 with bold highlights to indicate changes considered differentially expressed based on the criteria of ± 3 fold change compared to the untreated BM-MSC with a p-value ≤0.05. In addition the mean fold change of exosome treated and TGF-β treated BM-MSCs were compared to highlight changes unique to the exosome-generated phenotype and the data are presented as volcano plots. Treatment with sTGF-β1 was not inert, as we saw elevated mRNA for IL-1A and INHBE, whilst there was a decrease in SMAD3, SMAD6, CCL2, IL5, ITGB8 and HGF compared to the untreated BM-MSC (figure 6.1, blue circles). Treatment with exosomes also elevated INHBE and IL-1A, whilst decreasing ITGB8, but otherwise the alterations were dissimilar to those mediated by sTGF-β1. Exosomes strongly elevated MMP-3, MMP-13 and SerpinA-1 and less strongly ITGA2, ITGB6 and MMP1 compared to the untreated BM-MSCs. Exosome treatment also triggered a decrease in AGT and BCL2 (figure 6.1, red circles). Unexpectedly, in comparison to the untreated BM-MSCs, HGF are found to be down-regulated in exosome-differentiated BM-MSCs (fold change ratio of 0.43), which does not agree with our protein data (in the previous chapter). The mRNA for VEGF-A was up-regulated in exosome-treated BM-MSCs but was not greater than the 3 fold change boundary. In addition there was no change in the αSMA expression, but we know the αSMA protein to increase at day 9 or more. Thus the array data cannot always be in total agreement with our known protein data. The transcripts that could discriminate sTGF-β1 treated BM-MSCs from exosome-treated

BM-MSCs are HGF, IL5, CCL2, which were significantly declined by sTGF-β1 treatment. Whereas, mRNA for TGF-β3 and metalloproteinase's such as MMP-1, -3 and -13 were significantly up-regulated by exosome treatment (figure 6.1, green circles). Therefore, both sTGF-β1 and exosome stimulation of BM-MSCs change the mRNA for various fibrosis-related transcripts in comparison to the BM-MSCs. However, it is the exosome-treated BM-MSCs that have features consistent with matrix turnover and inflammation.

PCR-Fibrosis Profiler Array

	Exosome vs Untreated		TGFβ vs Untreated		Exosome vs TGFβ	
mRNA	**FOLD Change**	**p Value**	**FOLD Change**	**p Value**	**FOLD Change**	**p Value**
ACTA2	0.9834	0.9930	1.9776	0.0123	0.4973	0.0183
AGT	**0.2326**	**0.0318**	0.4236	0.0572	0.5492	0.1434
AKT1	0.8463	0.2831	0.7163	0.2052	1.1815	0.5812
BCL2	**0.3112**	**0.0042**	0.3901	0.0003	0.7978	0.6274
BMP7	1.0990	0.6299	1.4227	0.2531	0.7725	0.6699
CAV1	0.5660	0.0144	0.8912	0.5112	0.6351	0.0334
CCL11	0.4747	0.1508	0.3332	0.2757	1.4245	0.8367
CCL2	1.6428	0.1743	**0.2161**	**0.0070**	**7.6032**	**0.0185**
CCL3	1.4448	0.4934	0.6953	0.4092	2.0781	0.3863
CCR2	0.7085	0.5419	0.8021	0.5720	0.8833	0.8901
CEBPB	1.4727	0.0269	0.5894	0.1547	2.4988	0.0238
COL1A2	1.4808	0.0005	1.9265	0.0023	0.7686	0.0250
COL3A1	1.7498	0.0160	1.8150	0.0056	0.9641	0.7933
CTGF	1.0502	0.6893	1.3088	0.0480	0.8024	0.0813
CXCR4	2.6848	0.2667	2.5817	0.3556	1.0399	0.8841
DCN	1.3845	0.1447	0.6306	0.0127	2.1953	0.0196
EDN1	0.8315	0.0207	1.0616	0.3456	0.7833	0.0137
EGF	1.6083	0.0991	2.4336	0.0250	0.6609	0.1004
ENG	1.0461	0.7206	0.6580	0.0692	1.5899	0.1135
FASLG	0.9232	0.8077	2.2583	0.3459	0.4088	0.3389
GREM1	1.1101	0.1362	0.7078	0.0145	1.5684	0.0098
HGF	0.4372	0.0009	**0.1219**	**0.0000**	**3.5852**	**0.0125**
IFNG	0.9232	0.8077	1.4227	0.2531	0.6489	0.2473
IL10	0.6114	0.9924	0.4446	0.1992	1.3751	0.4786
IL13	1.6605	0.4195	1.5333	0.0908	1.0830	0.5322
IL13RA2	0.5018	0.0323	0.6284	0.1111	0.7985	0.2892
IL1A	**9.1426**	**0.0250**	**22.2091**	**0.0307**	0.4117	0.1334
IL1B	0.8149	0.6342	0.9906	0.8526	0.8226	0.6590
IL4	1.6118	0.7286	3.0142	0.3439	0.5347	0.4425
IL5	0.7856	0.3181	**0.1545**	**0.0124**	**5.0844**	**0.0331**
ILK	0.7063	0.0178	0.8300	0.3770	0.8510	0.4203
INHBE	**10.9874**	**0.0161**	**26.8968**	**0.0220**	0.4085	0.0848
ITGA1	8.7288	0.7019	0.8786	0.7089	9.9350	0.3637
ITGA2	**3.9709**	**0.0024**	2.5603	0.0469	1.5509	0.1547
ITGA3	0.5088	0.0172	0.7562	0.3628	0.6728	0.2717
ITGAV	0.9610	0.7879	0.8673	0.6429	1.1080	0.7745
ITGB1	1.4364	0.0299	1.2772	0.0998	1.1246	0.3636
ITGB3	0.6096	0.0200	0.9124	0.4853	0.6682	0.0716
ITGB5	1.0796	0.5151	0.9136	0.6991	1.1818	0.4560
ITGB6	**6.5460**	**0.0017**	7.4509	0.2202	0.8786	0.5316
ITGB8	**0.1929**	**0.0145**	**0.1179**	**0.0102**	1.6359	0.3754
JUN	1.0620	0.6512	1.0433	0.7437	1.0179	0.9078

Table 6.1: The Human Fibrosis RT² Profiler™ PCR Array profiles the expression of 84 key genes involved in fibrosis, depicting differentially expressed transcripts

Untreated BM-MSCs or treatment of BM-MSCs with sTGF-β1 or DU145 exosomes (over 4 days) were compared using the RT²-Profiler™ Fibrosis array. Bold text highlights mRNA considered differentially expressed according to the criteria of ±3 x fold change and a p-value of ≤0.05 (t-test based on biological triplicates per treatment).

PCR-Fibrosis Profiler Array

	Exosome vs Untreated		TGFβ vs Untreated		Exosome vs TGFβ	
mRNA	**FOLD Change**	**p Value**	**FOLD Change**	**p Value**	**FOLD Change**	**p Value**
LOX	0.9665	0.8121	1.1998	0.1474	0.8056	0.1798
LTBP1	1.1981	0.1146	1.1053	0.4087	1.0839	0.4323
MMP1	**3.361**	**0.0161**	0.7416	0.5907	**4.5322**	**0.0147**
MMP13	**14.3312**	**0.0013**	1.8575	0.0864	**7.7155**	**0.0018**
MMP14	1.3842	0.1216	0.7739	0.6900	1.7885	0.1908
MMP2	1.6081	0.0662	1.0982	0.5897	1.4643	0.1878
MMP3	**42.4110**	**0.0096**	0.5927	0.0992	**71.5576**	**0.0093**
MMP8	0.7126	0.2574	1.4758	1.4758	0.4829	0.0273
MMP9	3.2356	0.3071	0.8412	0.5845	3.8469	0.2139
MYC	1.8240	0.0150	2.3413	0.0015	0.7791	0.0976
NFKB1	0.9104	0.5020	0.7172	0.0188	1.2694	0.1947
PDGFA	0.6840	0.0546	1.1063	0.5935	0.6183	0.1044
PDGFB	0.9232	0.8077	1.4227	0.2531	0.6489	0.2473
PLAT	0.9863	0.9482	0.7119	0.1616	1.3854	0.1979
PLAU	1.2081	0.3322	1.2233	0.2320	0.9876	0.9912
PLG	0.7913	0.3020	0.4363	0.0443	1.8134	0.0568
SERPINA1	**13.2713**	**0.0147**	0.9513	0.8363	**13.005**	**0.0155**
SERPINE1	1.0189	0.8402	1.7801	0.0849	0.5724	0.0936
SERPINH1	1.4507	0.0088	2.6688	0.0013	0.5436	0.0039
SMAD2	0.7627	0.0502	0.8805	0.2932	0.8662	0.3487
SMAD3	0.3752	0.0483	**0.1604**	**0.0098**	2.3392	0.1149
SMAD4	0.8963	0.5901	0.7615	0.0187	1.1771	0.3504
SMAD6	0.6809	0.2149	**0.3109**	**0.0045**	2.1899	0.0892
SMAD7	1.3734	0.1058	0.7495	0.3231	1.8326	0.0555
SNAI1	2.1055	0.0627	0.9437	0.8715	2.2312	0.1779
SP1	0.9925	0.8698	0.6750	0.3475	1.4703	0.2878
STAT1	1.5344	0.0957	0.7639	0.2424	2.0086	0.0086
STAT2	0.6487	0.0662	1.4970	0.8734	0.4334	0.5621
TGFB1	1.5107	0.0941	1.6242	0.1965	0.9301	0.6896
TGFB2	1.2627	0.0088	1.9774	0.0003	0.6386	0.0011
TGFB3	1.0061	0.9888	0.3261	0.0265	**3.0848**	**0.018**
TGFBR1	1.0905	0.6675	0.5638	0.0919	1.9341	0.0711
TGFBR2	0.6924	0.1494	0.4326	0.0233	1.6007	0.0762
TGIF1	1.5901	0.0037	1.4112	0.0296	1.1268	0.2588
THBS1	0.7754	0.0959	0.8742	0.5876	0.8870	0.5287
THBS2	0.9094	0.6834	0.8009	0.6788	1.1354	0.8971
TIMP1	2.2392	0.0012	2.7349	0.0000	0.8188	0.0391
TIMP2	0.5663	0.2508	0.5551	0.2430	1.0201	0.9224
TIMP3	0.6663	0.1198	1.0161	0.9549	0.6557	0.0841
TIMP4	0.8829	0.5808	1.2689	0.0813	0.6958	0.0986
TNF	0.5817	0.3729	2.5033	0.3031	0.2324	0.1517
VEGFA	1.81	0.0716	2.0893	0.0411	0.8663	0.6159

Table 6.1 continued: The Human Fibrosis RT^2 Profiler^{TM} PCR Array profiles the expression of 84 key genes involved in fibrosis, depicting differentially expressed transcripts

Untreated BM-MSCs or treatment of BM-MSCs with sTGFβ or DU145 exosomes (over 4 days) were compared using the RT^2-Profiler^{TM} Fibrosis array. Bold text highlights mRNA considered differentially expressed according to the criteria of ±3 x fold change and a p-value of $\leq$0.05 (t-test based on biological triplicates per treatment)

PCR fibrosis array of untreated, TGF-β1 or exosome treated BM-MSCs

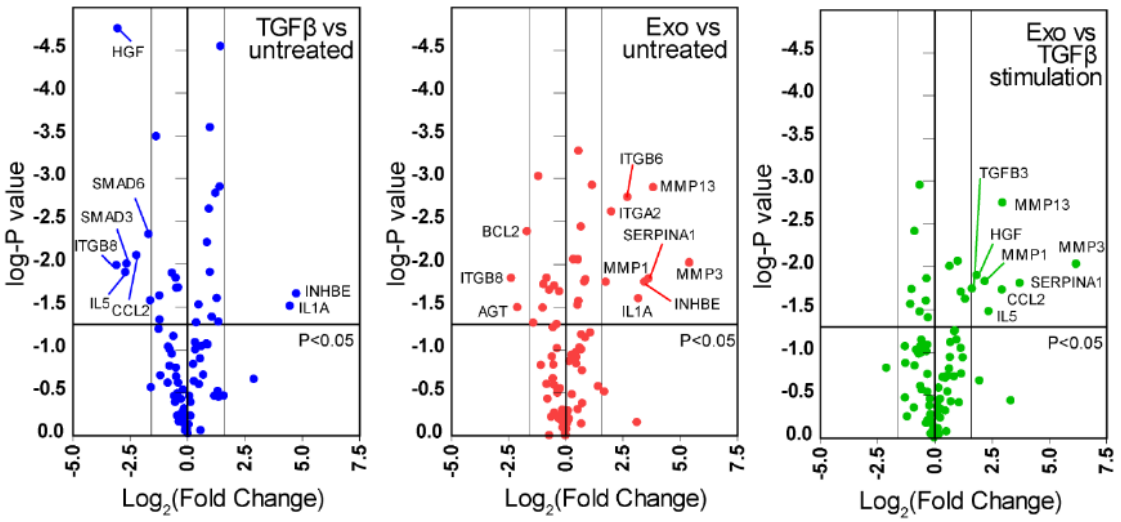

Figure 6.1: MP-1, MMP-3, MMP-13 and serpinA-1 are highly expressed in exosome-stimulated BM-MSCs

Volcano plot, depicting results from RT^2-Profiler™ fibrosis array comparing day 4 untreated BM-MSC with sTGF-β1 treated (1ng/ml) (left) or with exosome-treated (150µg/ml) BM-MSC (middle) or exosome-treatment vs sTGF-β1 treatment (right). Applied thresholds were a fold change of ±3 and a p-value of $\leq$0.05 (t-test based on biological triplicates per treatment).

6.1.2 Verification of mRNA gene expression changes

The PCR array revealed transcripts for MMP-1, -3, -13, SerpinA-1 and AGT to significantly distinguish exosome-treated BM-MSCs from the other BM-MSCs. Thus these transcripts were verified among the BM-MSCs using individual primers against these genes using TaqMan PCR array. In agreement with the array data, there was a particularly strong ($p \leq 0.001$) elevation in MMP-3 and also elevated MMP-13 ($p \leq 0.001$), MMP-1 ($P \leq 0.05$) and SerpinA-1 ($p \leq 0.05$), with decreased mRNA for AGT ($P \leq 0.001$). However sTGF-β1 was also shown to decrease AGT (figure 6.2), which differed from the PCR array. Together the data show that exosomes impart a phenotype that has some overlap with that of sTGF-β1 stimulus, but points some unique features, particularly, the heightened matrix regulating proteases such as MMP's and SerpinA-1.

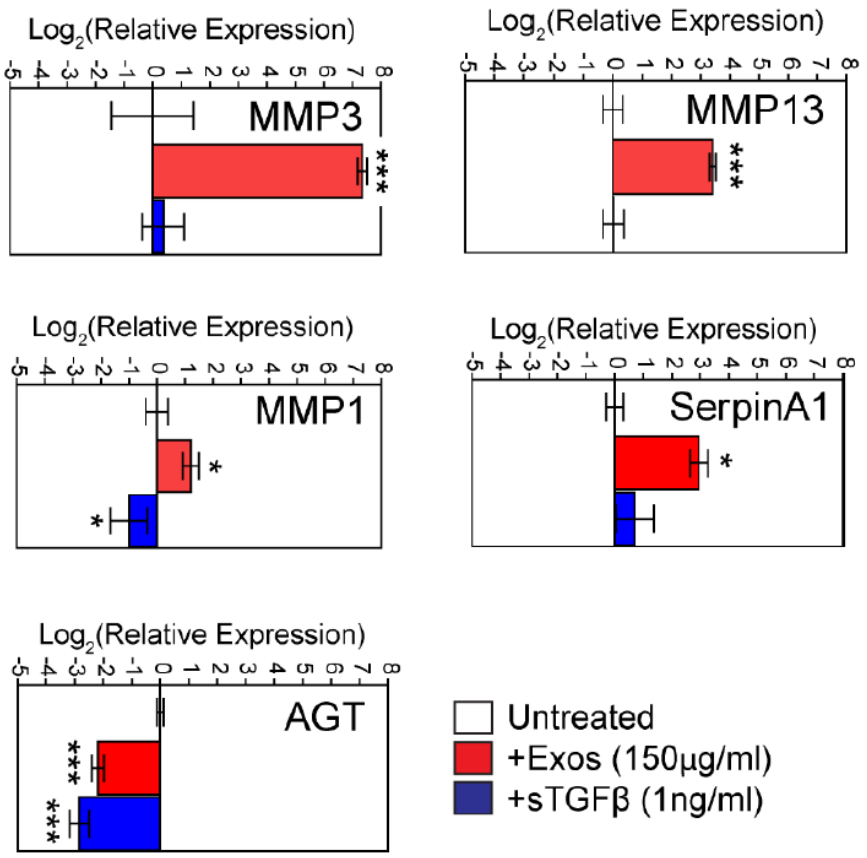

Figure 6.2: MMP-1, MMP-3, MMP-13 and SerpinA-1 are highly expressed in exosome-stimulated BM-MSCs

TaqMan-PCR verification of selected transcripts identified by the array (MMP-1, MMP-3, MMP-13, SerpinA-1 and AGT), revealing reproducible and significant changes in relative mRNA with GAPDH as an internal standard, at day 4. Columns represent Log_2 (relative expression) ±SD, compared to untreated BM-MSC (based on biological triplicates).

6.2 Changes in exosome-differentiated BM-MSCs at protein level

Since, mRNA of MMPs and SerpinA-1 were up-regulated in exosome-treated BM-MSCs, the protein of these matrix remodelling enzymes was assessed.

6.2.1 Protein analysis using immunohistochemistry

For protein detection, the untreated, sTGF-β1 treated or exosome treated BM-MSCs after 6 days of stimulation were fixed-permeabilised and then subjected to intracellular staining using the antibodies against MMP-1, -3, -13, SerpinA-1 and visualised by immunohistochemistry (figure 6.3). MMP-1 was not stained in all three types of BM-MSCs, whereas, MMP-3 and MMP-13 were positively stained in exosome treated BM-MSCs, with little or no staining in untreated and sTGF-β1 treated BM-MSCs. SerpinA-1, however, was highly elevated in exosome treated BM-MSCs. Therefore, unlike the MMP-1 which was not detected under these conditions in BM-MSCs, MMP-3, -13 and SerpinA-1 are elevated in exosome-treated BM-MSCs, and may play an important role in the function of exosome-treated BM-MSCs.

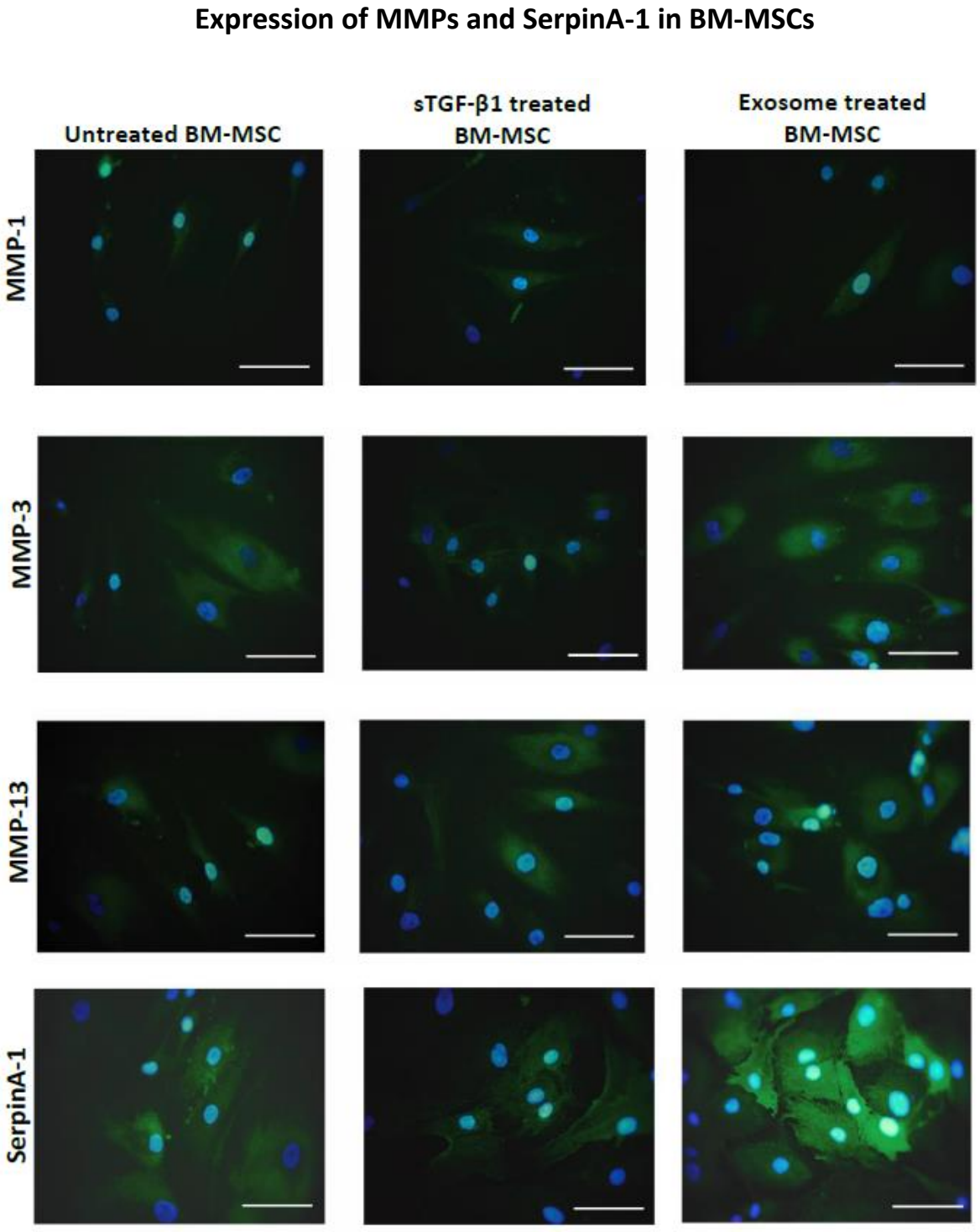

Figure 6.3: Exosome-treated BM-MSCs are highly positive for SerpinA-1 and to a lesser extent positive for MMP-3 and MMP-13

BM MSCs were cultured in untreated DMEM 1% MSC-FBS or with the addition of sTGFβ (1ng/ml) or DU154 exosomes (150µg/ml) over 6 days. The cells were then fixed-permeabilised and stained with monoclonal antibodies against MMP-1, MMP-3, MMP-13 and SerpinA-1 (green) and DAPI (blue). Scale, 200µm.

6.3 Discussion

mRNA expression in BM-MSCs

The tumour microenvironment is known to resemble that of the chronic wound or a fibrotic diseased organ (Ueno *et al.* 2004). Thus, using a fibrosis PCR array, we explored the consequence of exosome stimulation on BM-MSCs arising which may resemble myofibroblast-like cells found within carcinoma and chronic wound healing sites. For analyses of phenotypic differences among the BM-MSCs, an arbitrary threshold of ± 3 fold change was used. A lower threshold would have given us more candidates, but our confidence that these changes can be validated will be reduced. Here the selected threshold will help us to find the more extreme changes, which may be easier to validate and potentially have a bigger biological effect, with regard to the function of differentiated BM-MSCs.

Exosome treated BM-MSCs had some overlapping features to that of sTGFβ-1 treated BM-MSCs as they both had elevated INHBE and IL1-A. INHBE is a member of the activin beta family, required for the production of activin which was initially described as a protein that stimulates the release of follicle stimulating hormone from the pituitary (Aroua *et al.* 2012). In recent years, INHBE has been identified to be overexpressed at wound healing sites and skin carcinomas (Antsiferova and Werner 2012). Moreover, clinical data showed that circulating levels of INHBE, measured by ELISA, was found to correlate with invasive breast cancer and prostate cancer patients with bone metastasis, whilst INHBE remained low among normal controls (Incorvaia *et al.* 2007; Leto *et al.* 2006). In addition, the pro-inflammatory cytokine, IL-1A was previously found to be highly expressed in prostate cancer tissues, compared to normal prostate or benign prostate hyperplasia (BPH), as shown by immunohistochemistry and western blot (Ricote *et al.* 2004). Furthermore, IL-1A knock out mice with melanoma had a much lower tumour development in comparison to the wild type mice and in the absence of IL-1A, the carcinoma cells were shown to have a low migration rate in matrigel plugs (Voronov *et al.* 2003). Therefore INHBE and IL-1A from sTGF-β1 treated or exosome treated BM-MSCs may support tumour progression. Other similarities between sTGF-β1 treated and exosome treated BM-MSCs is the decreased mRNA levels of integrin beta-8 (ITGB8). High mRNA of ITGB8 are found in breast cancer patients with lung metastasis,

making ITGB8 gene a predictor for lung metastasis in breast cancer patients (Culhane and Quackenbush 2009; Hedenfalk *et al.* 2001). However, ITGB8 expression was not observed by sTGF-β1 or exosome treated BM-MSCs. Apart from these similarities, sTGF-β1 treated and exosome treated BM-MSCs are dissimilar, in which the sTGF-β1 treated BM-MSCs have a significant decrease in CCL2, IL5, and HGF. These components are required for tumour progression. For example, the monocyte chemoattractant, CCL2 is overexpressed in prostate cancer in correlation with the advanced stages (Lu *et al.* 2006) and CCL2 is found to mediate the proliferation and invasion of PCa cells *in vitro* (Loberg *et al.* 2006) and tumour growth *in vivo*, as shown using inhibitory experiments (Loberg *et al.* 2007). IL-5 and HGF has also been found to enhance the invasion of bladder cancer cells and squamous cell carcinomas, respectively (Lee *et al.* 2012; Ren *et al.* 2005). In addition, HGF is known to promote tumour angiogenesis (Ren *et al.* 2005) and the decrease in this pro-angiogenic factor, here, by sTGF-β1 treated BM-MSCs agrees with the decrease in HGF secreted by the sTGF-β1 treated BM-MSCs, as shown in chapter 5. Therefore, unlike exosome treated BM-MSCs, the TGFβ treated BM-MSCs may be predicted as being less able to promote disease.

Exosome-treated BM-MSCs have strongly elevated mRNA for MMP-3, MMP-13 and SerpinA-1 and to a lesser extent MMP-1, as revealed by the PCR fibrosis array and verified by TaqMan qPCR analysis. Furthermore, the protein expression level of MMPs and SerpinA-1 in exosome-treated BM-MSCs analysed by immunohistochemistry correlated with their mRNA expression. These findings agree with published literature, where up-regulation of MMPs such as MMP-3 mRNA expression have been found in breast cancer (Witty *et al*. 1995; Sternlicht *et al.* 1999; Lochter *et al.* 1997), and prostate cancer (Daja *et al.* 2003). Most of the MMPs are found to be secreted by the stromal cells, rather than the epithelial cells (Witty *et al.* 1995), thus stromal cells secretion of MMPs are of critical importance in tumours. MMPs are well known to break down the ECM, by cleaving collagen II, IX, X and XI (Wu *et al.* 1991; Knäuper *et al.* 1996). MMP-3, in particular, can also disrupt cell-cell junction by cleaving E-cadherin, as shown by a marked decrease in E-cadherin by immunohistochemistry (Lochter *et al.* 1997; Sternlicht *et al.* 1999), allowing the epithelial cells to lose anchorage dependency and invade. MMPs are synthesised and secreted as a pro-enzyme and are activated by removal of

the N-terminal pro-domain (Becker *et al.* 1995). Activated MMP-3 are pro-invasive, as they have been shown to support migration of the cells through matrigel in a Boyden chamber assay and this invasion capacity induced by MMP-3 was abolished when MMP inhibitor was added (Lochter *et al.* 1997). Other than the direct pro-invasive property of MMP-3, they can also activate other MMPs, such as pro-MMP-1, pro-MMP-9 and pro-MMP-13 (Shapiro *et al.* 1995; Knäuper *et al.* 1996), by cleaving the N-terminal bond to generate fully active MMPs (Suzuki *et al.* 1990; Knäuper *et al.* 1993). Therefore MMPs, in particular, MMP-3 are important for the invasion of epithelial cells as they can initiate an MMP cascade that can further enhance tumour invasion. Additionally, exosome-treated BM-MSCs also have up-regulated SerpinA-1, which has been found in previous studies to be up-regulated by tumour epithelial cells, such as squamous cell carcinoma (SCC) (Farshchian *et al.* 2011) and gastric cancer cells (Shin *et al.* 2012). SerpinA-1 was found to correlate with poor prognosis both at mRNA and protein level. Additionally, gastric cancer cells which had been manipulated to overexpress SerpinA-1, enhanced the migration and invasion of gastric cancer cells in a transwell system (Kwon *et al.* 2014). Therefore SerpinA-1 may also play a role in tumour invasion in prostate cancer.

Exosome treatment also decreased the mRNA of B-cell lymphoma 2 (BCL2) and angiotensinogen (AGT) in BM-MSCs. BCL-2 may aid tumour progression via its anti-apoptotic function (Yip and Reed 2008). Whereas, AGT delays tumour angiogenesis by inhibiting the proliferation of endothelial cells. An *in vivo* experiment demonstrated mice of hepatocellular carcinoma overexpressing AGT had a longer survival in comparison to hepatocellular carcinoma control cells (Vincent *et al.* 2009). Thus, even though tumour-promoting BCL-2 is decreased in exosome treated BM-MSCs, a greater decrease in AGT may aid tumorigenesis. In summary, the fibrosis array revealed exosome treated BM-MSCs to impart a phenotype that has some overlap with sTGF-β1 treated BM-MSCs, but exosome stimulation results in some unique features which signify a more tumour-supporting function.

Chapter 7: Influence of exosome-differentiated BM-MSCs on endothelial cells

7.1 Possible influence of differentiated BM-MSCs on endothelial cell behaviour

Access to a disorganised vasculature offers a means of systemic dissemination of the tumour cells. Thus the new growth in the vascular network, the process of which is called angiogenesis, is important since the proliferation as well as metastatic spread of cancer cells depends on adequate supply of O_2 and nutrients and the removal of waste products. Various studies have shown angiogenesis to directly correlate with the incidence of tumour metastasis (Weidner *et al.* 1991; Macchiarini *et al.* 1992; Tanigawa *et al.* 1996; Graham *et al.* 1994). Thus angiogenesis is of critical importance for growth of primary neoplasm and provides an avenue for hematogenous metastasis. Angiogenesis is a multi-step, multi-cellular process involving the proliferation, migration and organisation of endothelial cells into vessel-like structures (Hoeben *et al.* 2004). Various growth factors secreted from cancer epithelial and stroma cells have been identified to promote angiogenesis. For example, the expression of vascular endothelial growth factor (VEGF) and its receptor, VEGFR-2 was significantly higher in metastatic than non-metastatic neoplasms and was found to directly correlate with vessel count in specimens from colon or gastric cancer patients (Takahashi *et al.* 1995, 1996). In addition, expression of interleukin (IL-8), basic fibroblast growth factor (bFGF) and plate-derived endothelial cell growth factor (PD-ECGF) were also observed to correlate with vessel count in gastric carcinomas (Kitadai *et al.* 1998; Tanimoto *et al.* 1991; Takahashi *et al.* 1998). These components may therefore be involved in supporting vessel formation but the source of these factors have not been thoroughly investigated. Immunohistochemical staining, however, showed that the growth factors are released from epithelial cells and stromal cells such as fibroblasts as well as infiltrating stromal cells such as macrophages (Kitadai *et al.* 1998; Tanimoto *et al.* 1991).

Tumour-associated myofibroblasts are pro-angiogenic as demonstrated in many studies. For example, breast cancer cells admixed with tumour myofibroblasts revealed extensive vascular formation in a xenograft model (Orimo *et al.* 2005). In contrast capillaries were far less developed when cancer cells were admixed with non-cancerous fibroblasts. Likewise, myofibroblasts from gastric cancer enhanced endothelial cell tube formation *in vitro* (Guo *et al.* 2008). It should be noted, however, that not all

myofibroblasts are pro-angiogenic. Recent studies have shown α-SMA positive myofibroblasts generated from sTGF-β1 induced fibroblasts did not have elevated angiogenic growth factors (Webber *et al.* 2014). In contrast, prostate cancer (PCa) exosome induced fibroblasts differentiated into myofibroblasts which were pro-angiogenic, as observed by elevated growth factors and their ability to promote endothelial vessel-like structure formation *in vitro* (Webber *et al.* 2014). Additionally PCa myofibroblasts (tumour educated *in vivo*) were pro-angiogenic unlike the normal non-myofibroblastic stroma. However the normal non-myofibroblastic stroma became pro-angiogenic myofibroblasts after PCa exosome stimulation. Therefore, only some forms of myofibroblasts exhibit a pro-angiogenic influence, possibly through the production of VEGF-A, HGF and other factors.

I have shown PCa exosomes, to be a vital factor for BM-MSC differentiation into myofibroblast-like cells. Whether these exosome-differentiated MSCs exert tumour promoting functions akin to myofibroblasts at tumour sites has yet to be explored. In this chapter, I will explore the effects exosome-differentiated BM-MSCs have on endothelial cells. The hypothesis is that exosome-differentiated BM-MSC and their secreted factors drive the angiogenesis behaviour of endothelial cells.

7.1.1 The effects of exosome-differentiated BM-MSCs on endothelial cell proliferation and survival

Whether or not exosome-differentiated BM-MSCs exhibit a pro-angiogenic function was explored in this chapter. To do this several aspects of endothelial cell behaviour, such as their proliferation, migration and organisation into vessel-like structures *in vitro*, in response to exosome-differentiated BM-MSCs was investigated. Angiogenesis studies requires an appropriate endothelial cell source, such as the human umbilical vein endothelial cell line (HUVECs). HUVECs are the most commonly studied endothelial cell type in angiogenesis as they are well characterised and conveniently accessible and so HUVECs were used for the experiments.

The proliferation and survival properties of HUVECs were examined by equally seeding the cells ($1x10^4$) *in vitro* in the presence of BM-MSC conditioned medium (CM) which had been normalised for cell number. The CM was collected from BM-MSCs untreated or pre-treated for 4 days with sTGF-β1 (1ng/ml) or DU145 exosomes (150µg/ml) and added to the HUVECs in the absence of exogenous endothelial-cell growth factors. After 6 days of culture, cell number and cell viability was determined by flow cytometry using the ViaCount reagent. The ViaCount assay distinguishes viable and non-viable cells based on differential permeabilities of two DNA-binding dyes within the ViaCount reagent; the nuclear dye which stains only nucleated cells and the viability dye, which brightly stains dying cells. The data shows the endothelial cell numbers poorly expanded with CM from the untreated BM-MSCs, whilst there was a higher proliferative response to CM from sTGF-β1 treated BM-MSC (figure 7.1A). This was significantly stronger, however following exosome-treated BM-MSC CM which resulted in a > 4-fold elevation of endothelial cell numbers at day 6. Exosome-differentiated BM-MSCs must therefore produce factors which support endothelial cell expansion. The viability of the endothelial cells grown in untreated BM-MSC CM was >75%, but there was a small increase using CM from either sTGF-β1 or exosome treated BM-MSCs (Figure 7.1B). Therefore survival of endothelial cells is supported by CM from exosome treated BM-MSCs and to a lesser extent from sTGF-β1 treated BM-MSCs CM.

Viability of endothelial cells when cultured in untreated or exosome treated BM-MSC conditioned medium

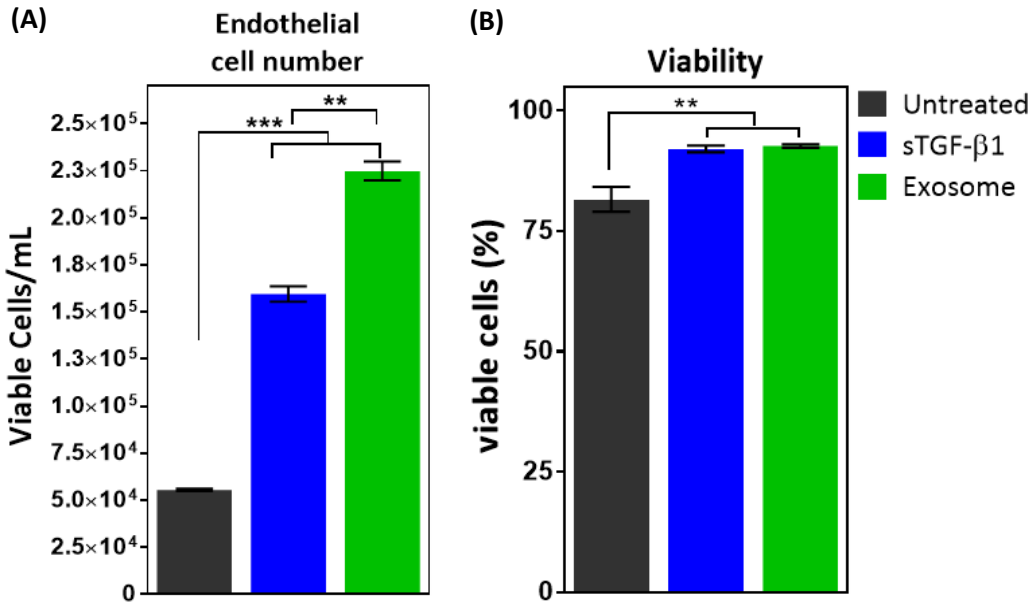

Figure 7.1: Exosome-treated BM-MSC CM increase HUVEC cell proliferation
$1x10^4$ primary HUVEC were cultured with conditioned media normalised for cell number from BM-MSC pre-treated for 4 days by sTGFβ or DU145 exosomes. Following 6 days in culture, HUVECs were harvested and total viable cell number (A) and percentage viability (B) were measured using the ViaCount system on a GUAVA flow cytometer. (Bars, mean ± SD, of triplicates, One-way ANOVA with Tukey's multiple comparison post-test, **$p \leq 0.01$, ***$p \leq 0.001$.

7.1.2 The effect of conditioned medium from exosome-differentiated BM-MSCs on endothelial migration

For angiogenesis to occur, endothelial migration is essential. Hence the influence of exosome-differentiated BM-MSCs on endothelial cell migration using an endothelial monolayer scratch assay was examined. One of the major advantages of this simple scratch assay is that it mimics to some extent the migration of the cells *in vivo*. For example, the removal of part of the endothelium in blood vessels will induce migration of endothelial cells into the denuded area close to the wound (Liang *et al.* 2007). So, by creating an empty space in a monolayer of endothelial cells, the cells should be able to migrate to cover the scratch created, in response to particular stimulus.

The confluent monolayer of endothelial cells was growth arrested overnight, followed by removal of the media and then a scratch was created using a 200µL pipette tip as mentioned in materials and methods. The endothelial cells were then cultured in 1:1 ratio of EBM-2 media to conditioned media from BM-MSCs, which had been untreated or pre-treated with TGF-β1 or DU145 exosomes (150µg/ml) over 4 days. Images of scratch closure were taken over 24h and the distance between the wound margins was measured. Conditioned media, from exosome-treated BM-MSCs accelerated scratch closure, with full closure occurring by 24h (figure 7.2A,B). In contrast the scratch exposed to sTGF-β1 treated BM-MSC conditioned media was only 50% closed by 24h (figure 7.2B). At this time point, the endothelial cells were alive but poorly adherent in the presence of CM from untreated BM-MSC, and as such it was not possible to determine the position of the scratch margins at 24h. Nevertheless, scratch closure for this treatment was clearly less complete at 6, 12 and 18h compared to the other treatments and this phenomenon of loss of plastic adherence was apparent in three independent experiments. Therefore, exosome-treated BM-MSCs exhibit heightened capacity to encourage endothelial cell motility.

Motility of endothelial cells in the presence of BM-MSC conditioned medium

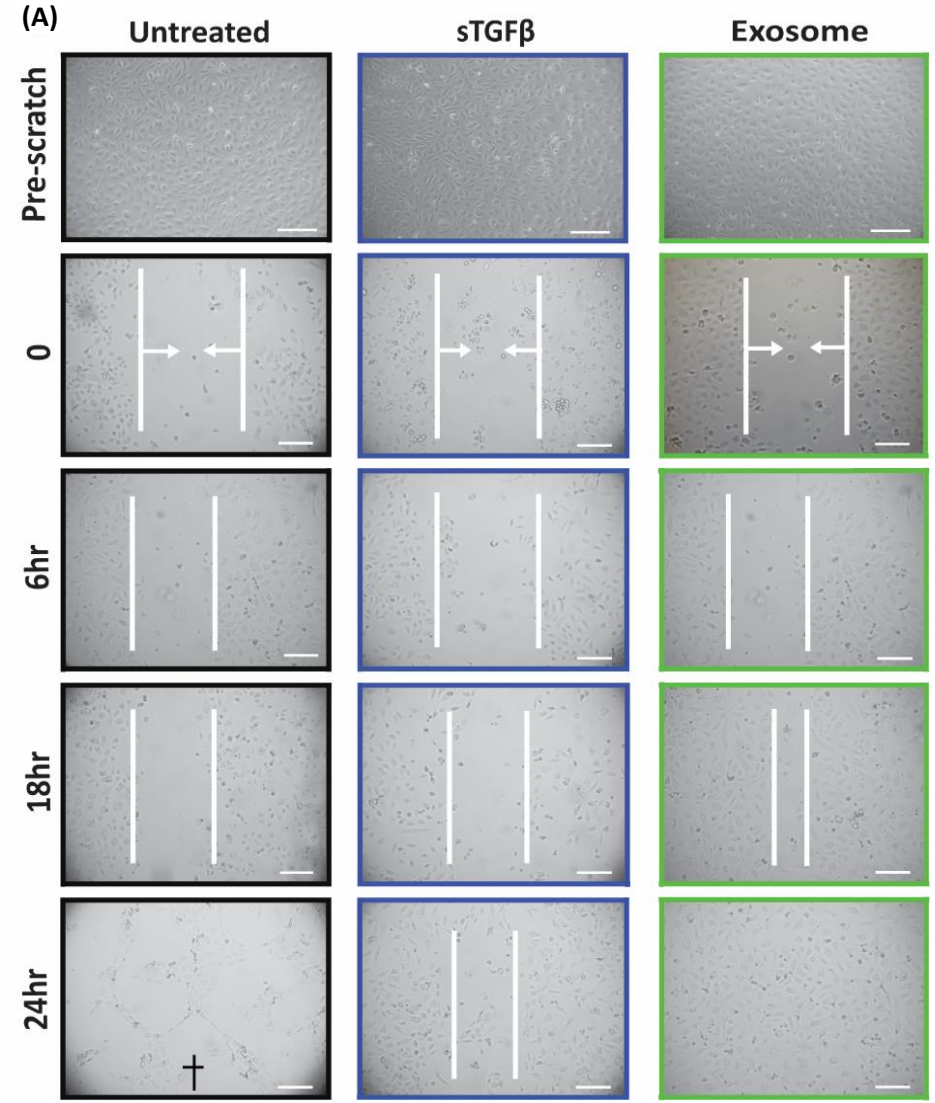

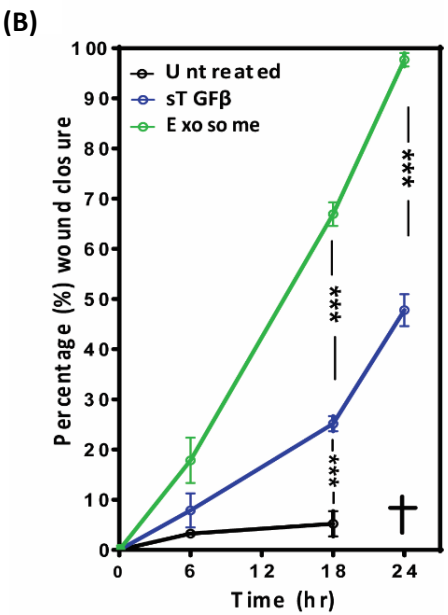

Figure 7.2: Conditioned media from exosome-differentiated MSCs accelerate endothelial migration.

Monolayer of HUVEC was scrapped using a 200µl pipette tip to create a single vertical scratch. CM normalised for cell number from BM-MSCs pre-treated with sTGFβ (1ng/ml) or DU145 exosomes (150µg/ml), were added, and the distance between two sides of the scratch, highlighted by vertical white lines and arrows, was monitored at specified time points microscopically up to 24 hr. Scale bar 200µM (A). The distance of scratch closure was measured using Image J. The symbol † depicts a loss of HUVEC adhesion at 24h, hence scratch width could not be measured (B). (Graph shows Mean ± SD, of duplicate wells per treatment. Data are representative of three such experiments. One-Way ANOVA with Tukey's multiple comparison test *$p \leq 0.05$, **$p \leq 0.01$, ***$p \leq 0.001$).

7.1.3 The effect of exosome-differentiated BM-MSCs on the formation of vessel-like structures

The process of angiogenesis, resulting in a highly ordered network of blood vessels, requires proliferation and precise control over the migration and branching of endothelial cells (Aase *et al.* 2007). To measure proliferation, migration and cell organisation, an *in vitro* tubule-formation assay was performed, through co-culture of pre-treated BM-MSCs monolayers with endothelial cells as described by Sheldon *et al* (2010). BM-MSCs were left untreated or treated with sTGF-β1 or DU145 exosomes with or without anti-TGFβ neutralising antibody (10μg/ml) for 4 days prior to the drop-wise and scattered addition of endothelial cells to the wells. After a further 6 days of culture, cells were fixed and stained for the endothelial marker CD31. In wells containing either the untreated or sTGF-β1 treated BM-MSCs, some clusters of CD31-positive cells formed on top of the BM-MSC monolayer, but these were relatively rare, forming short structures with no evidence of branching (figure 7.3A). In contrast, exosome-treated BM-MSCs allowed the support of multiple branched, long and wide structures consistent with supporting more elaborate vessel-like structures. Additionally, these CD31 positive vessel-like structures occupied a significant area of the well they were cultured in (figure 7.3B). However, the addition of anti-TGF-β1 neutralising antibody, along with the exosomes, generated rare vessel-like structures which were short and thin with very little branching and did not occupy a large area of the culture system (figure 7.3A,B). Therefore, exosome-differentiated BM-MSCs support the proliferation, motility and organisation of endothelial cells and is consistent with a pro-angiogenic function. Even though sTGF-β1 had no effect on the formation of multi-branched vessel-like structures, blockage of exosomal TGF-β1 attenuated the ability of the BM-MSCs to support endothelial vessel-like structure formation.

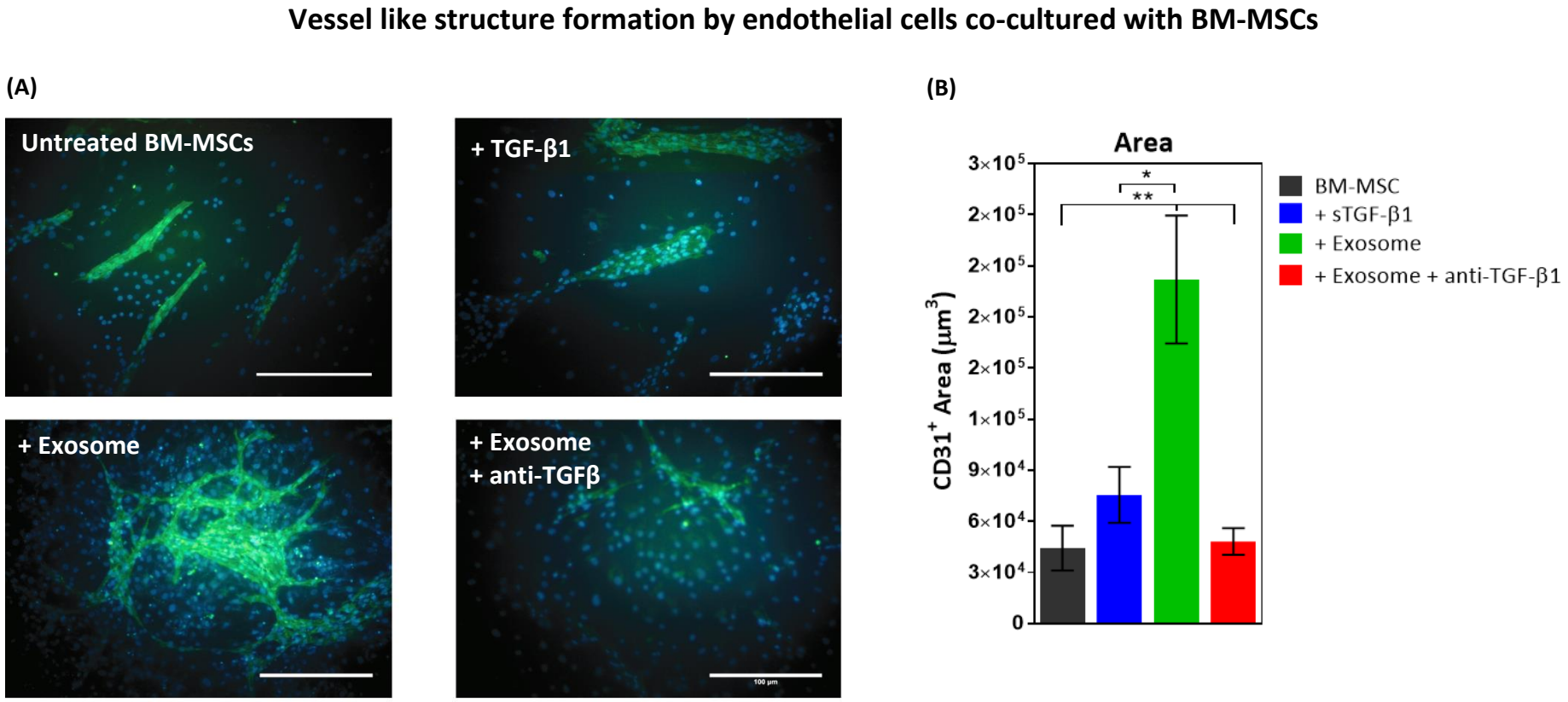

Figure 7.3: Exosome-differentiated MSCs support endothelial cells to form vessel-like structures.
Monolayers of BM-MSCs were pre-treated with sTGFβ (1ng/ml) or DU145 exosomes (150µg/ml) with or without anti-TGFβ neutralising antibody (10µg/ml) for 4 days, at which 50% of the culture medium was removed, and replaced by the same volume of EBM-2 endothelial cell culture medium lacking growth factors, containing 20,000 HUVEC per well. After 6 day incubation, the co-cultures were fixed and immunofluorescently stained for CD31 (green) and DAPI (blue). Scale 400µm (A). Quantification of surface area of the CD31-positive structures was performed using Image J (B). (Bars, Mean±SD of triplicate well per condition. One-way ANOVA with Tukey's post-test *p≤0.05 and **p≤0.01. Representative of three such experiments).

7.2 Discussion

Angiogenesis is a multistep and multi-cellular process that involves proteolytic degradation of the extracellular matrix, followed by migration, proliferation and organisation of endothelial cells (Hoeben *et al.* 2004). In this chapter, I have shown that conditioned medium (CM) from exosome-differentiated BM-MSCs can strikingly elevate endothelial proliferation as well as survival *in vitro*, in comparison to the untreated BM-MSC CM. This proliferative effect were also observed by myofibroblasts in various cancers (Orimo *et al.* 2001, 2005; Sobral *et al.* 2011), suggesting exosome-differentiated BM-MSCs have characteristics consistent with tumour-associated myofibroblasts. The CM from sTGF-β1 differentiated BM-MSCs, had a much weaker influence on endothelial proliferation and survival and so these BM-MSCs were not completely inert. Similar observations were reported using sTGF-β1 and exosome-treated fibroblasts, where exosome-treated fibroblasts had the greatest proliferative effect upon endothelial cells (Webber *et al.* 2014). Therefore myofibroblasts generated by tumour exosomes have characteristics that are consistent with tumour-associated myofibroblasts.

A monolayer scratch assay is a commonly used method by many researchers to examine the motility of endothelial cells (Pin *et al.* 2012; Chim *et al.* 2011; Chrzanowska-Wodnicka *et al.* 2008). The scratch assay, however, does not establish a chemical gradient and thus does not replace well-established methods for chemotaxis such as the Boyden chamber assays. Nevertheless, the monolayer scratch assay is the simplest and an inexpensive method to study cell motility *in vitro* (Reinhart-King 2008). Using this method, my data showed that endothelial cells cultured in CM from untreated BM-MSCs were very poorly motile and in fact a good proportion became non-adherent under these conditions at 24h, although the cells remained alive. The reason behind this has not been investigated thoroughly, but there are however, some studies showing BM-MSCs to express BMP-9 (Liu *et al.* 2013) which can inhibit migration of breast cancer cells (Ren *et al.* 2014). Additionally, studies report BM-MSCs to secrete anti-tumorigenic factors such as TIMP-1 and TIMP-2, which also inhibit the migration of breast cancer cells, in a transwell assay (Clarke *et al.* 2014). Thus, similar factors may also negatively impact endothelial cells motility. In contrast to the untreated BM-MSC CM, my experiment showed that the CM from exosome treated BM-MSCs were able to complete

endothelial migration by 24h. Similar results was observed using fibroblasts by our group, where unlike the untreated or sTGF-β1 treated fibroblasts, the exosome differentiated fibroblasts accelerated endothelial cell motility (Webber *et al.* 2014). Thus exosome differentiated BM-MSCs exhibit a clear pro-motility function and may again mimic this property of tumour- associated myofibroblasts.

There is currently no gold standard method to study angiogenesis *in vitro*. Since angiogenesis is the formation of blood vessel from pre-existing blood vessels, the use of a 3-dimentional *ex-vivo* mouse aortic ring assay would have been a more physiologically relevant assay to use, in comparison to the traditional cell-based assays (Baker *et al.* 2011). However, this *ex-vivo* method has limitations which include the requirement for fresh mouse tissue, the lack of non-aortic tissues and the regression of vessels over time, giving a limited window for analysis (Baker *et al.* 2011). In addition, unlike endothelial cells from aortic vessels, endothelial cells from veins such as HUVECs are more appropriate for studying angiogenesis, as they are prone to generating capillaries, akin to ones found at tumour sites. Here, using the co-culturing method, my data revealed exosome-differentiated BM-MSCs to be pro-angiogenic as their interaction with the endothelial cells were essential for the formation of long and thin multi-branched vessels. Furthermore, matrigel™ was not used and so vessel formation was purely due to cell-cell interaction between the endothelial cells and the BM-MSCs and not due to matrix components. The pro-angiogenic function of exosome-differentiated BM-MSCs are similar to tumour-associated myofibroblasts. For example, gastric cancer derived myofibroblasts promoted angiogenesis in mice (Guo *et al.* 2008). Similarly, myofibroblasts from prostate cancer or myofibroblasts generated from cancer exosome-induced fibroblasts were pro-angiogenic, as observed by endothelial cells forming vessel-like structures *in vitro*. In contrast, myofibroblasts generated using sTGF-β1- induced fibroblasts failed to support angiogenesis (Webber *et al.* 2014), indicating that not all myofibroblasts are tumour promoting. Here, my experiments demonstrated PCa exosomes drive BM-MSCs to differentiate into myofibroblasts which have a pro-angiogenic phenotype consistent with tumour-associated myofibroblasts. Earlier chapters demonstrated the myofibroblastic differentiation of BM-MSCs were dependent on exosomes expressing TGF-β1. Likewise, blockage of TGF-β1 here,

abrogated the pro-angiogenic function of the differentiated BM-MSCs, suggesting the dependence of TGF-β1 bearing exosomes in driving BM-MSCs into pro-angiogenic myofibroblast-like cells.

The pro-angiogenic feature of exosome differentiated BM-MSCs may be driven by the enhanced secretion of VEGF-A and HGF (shown in previous chapters). Even though the role of these growth factors in angiogenesis has not been explored here, various studies show that VEGF-A and HGF stimulate angiogenesis (Hoeben *et al* 2004). The HGF receptor, cMET is found on endothelial cells (Takahashi *et al.* 1995) and activation of the receptor induces angiogenesis through the up-regulation of VEGF-A, HGF and down regulation of thrombospondin-1 expression, a potent angiogenic inhibitor (Shojaei *et al.* 2010; Tomita *et al*. 2003). Activation of cMET also phosphorylates annexin-1 (ANXA1) which induces endothelial cell proliferation and migration (Pin *et al.* 2012). The microRNA, miR-196, represses ANXA1 induced angiogenesis (Luthra *et al.* 2008), but VEGF-A declines the expression of miR-196 (Pin *et al.* 2012), suggesting that VEGF and HGF are both required for angiogenesis. Furthermore, binding of VEGF-A to its receptor on endothelial cells, results in activation of various signalling pathways such as the extracellular regulated kinase (Erk) pathway which induces proliferation, migration and increases vascular permeability (Murphy *et al.* 2006). Activation of VEGF receptor also leads to the production of nitric oxide by the endothelial cells (Arsham *et al.* 2002; Gerber *et al.* 1998), resulting in endothelial migration and increased vascular permeability (Fulton *et al.* 1999). Therefore, both VEGF and HGF are pro-angiogenic and these factors secreted from differentiated BM-MSCs may stimulate angiogenesis. Matrix-metalloproteinase enzymes (MMP-1, MMP-3 and MMP13) are also up-regulated by exosome-differentiated BM-MSCs (previous chapter) which may be involved in the degradation of the ECM, thus aiding endothelial migration. Additionally, pro-angiogenic growth factors can be bound to the ECM matrix via ECM-binding domain (Park *et al.* 1993) and studies demonstrate a subset of MMPs (including MMP-1 and MMP-3) to cleave the matrix-bound growth factors such as VEGF-A (Lee *et al.* 2005), thus amplifying the pro-angiogenic effect. Taken together, in this chapter, I have shown exosome-differentiated BM-MSCs to support the proliferation, motility and organisation of

endothelial cells into forming vessel-like structures. The data are consistent with a pro-angiogenic phenotype and function of tumour-associated myofibroblasts.

Chapter 8: Influence of exosome-differentiated BM-MSCs on tumour cells

8.1 Influence of exosome-differentiated BM-MSCs on prostate cancer cell behaviour

The progression of tumours requires the cancer cells to be proliferative, motile and invasive and myofibroblasts are believed to play an essential role in these properties of carcinoma cells. For example, myofibroblasts or fibroblasts isolated from invasive breast cancer or non-cancerous stroma from the same patients were administered with the breast carcinoma cells in mice. Unlike the fibroblasts, the presence of myofibroblasts enhanced tumour growth the most, by promoting tumour cell proliferation (Orimo *et al.* 2005). Furthermore, tumour-associated myofibroblasts may direct the invasion of cancer cells, as myofibroblasts are found to be concentrated at the invasive front of the tumours (Gaggioli *et al.* 2007; Conti *et al*. 2011). Additionally, the conditioned media (CM) containing HGF from tumour-associated myofibroblasts or sTGF-β1 generated myofibroblasts, promoted the invasive capacity of carcinoma cells through a Matrigel (a mixture of basement membrane proteins). In contrast, the CM from carcinoma cells alone did not provide a pro-invasive effect to such an extent (Lewis *et al.* 2004; Cat *el al.* 2006; Conti and Thomas 2011; Dimanche-Boitrel *et al.* 1994). Therefore myofibroblasts are an important element in tumour progression.

Even though myofibroblasts derived from BM-MSCs are known to recruit to the prostate cancer stroma (Luo *et al.* 2014), the functions of myofibroblasts-derived from BM-MSCs has not been widely explored. In earlier chapters, my data revealed that unlike sTGF-β1, prostate cancer exosomes differentiate BM-MSCs into α-SMA positive myofibroblasts-like cells with heightened production of VEGF-A, HGF, MMPs and SerpinA-1. Whether myofibroblastic-differentiation of BM-MSCs driven by exosomes possess pro-tumorigenic function, similar to that of diseased prostate stroma has not been investigated. In this chapter, the effects of exosome-differentiated BM-MSCs upon prostate cancer cell lines will be investigated. The hypothesis is that exosome-differentiated BM-MSCs alter the behaviour of tumour cells towards a more aggressive phenotype.

8.1.1 The effect of conditioned media from exosome-differentiated BM-MSCs on prostate cancer cell proliferation and survival

Cancer-associated myofibroblasts promote tumour growth by up-regulating the proliferation of cancer epithelial cells (Orimo *et al.* 2005). In this chapter, I examined the impact of exosome-differentiated BM-MSCs on DU145 prostate cancer cell proliferation and survival. To do this, 1 x 10^4 DU145 epithelial cells were cultured in the presence of BM-MSC conditioned medium (CM) which were normalised for cell number. The CM was collected from untreated BM-MSCs or BM-MSCs pre-treated for 4 days with sTGF-β1 or exosomes. After 3 days of culture, cell number and viability was determined by flow cytometry using the ViaCount reagent. In comparison to the untreated CM, a 3.5 fold and 7 fold increase ($P \leq 0.001$) in the proportion of live cells was observed with sTGF-β1 or exosome treated BM-MSC CM respectively (figure 8.1). When examining the percentage of viable cells, a higher percentage of viable tumour cells was observed with CM from sTGF-β1 treated BM-MSCs in comparison to the untreated BM-MSC CM ($P \leq 0.05$). However, an even greater viability was noted with the exosome BM-MSC CM ($P \leq 0.01$) where 90% of the cells were viable. Therefore BM-MSCs do produce factors which support prostate cancer cell expansion, with exosome-differentiated BM-MSCs having the greatest effect.

Proliferation of another PCa cell line, PC3, in response to the same conditions was also assessed, with a similar positive effect on proliferation. Whereby, exosome treated BM-MSC CM resulted in a 5-fold increase in the total PC3 viable cells ($P \leq 0.0001$), in comparison to the untreated BM-MSC CM (figure 8.2). sTGF-β1 treated BM-MSC CM also increased the cell number, but only double the amount to that of the untreated BM-MSC CM ($P \leq 0.05$). Thus exosome-differentiated BM-MSC CM again resulted in the greatest degree of cell expansion. There was no difference in cell survival of the tumour cells cultured in the presence of the untreated or sTGF-β1 treated BM-MSC CM. In contrast, exosome-treated BM-MSC CM gave a small but significantly increased tumour survival ($P \leq 0.01$), where the tumour cell viability was more than 80%. Hence, exosome-differentiated BM-MSCs supported proliferation and survival of both the DU145 and PC3 cells.

Proliferation and survival of DU145 cells when cultured in the different BM-MSC CM

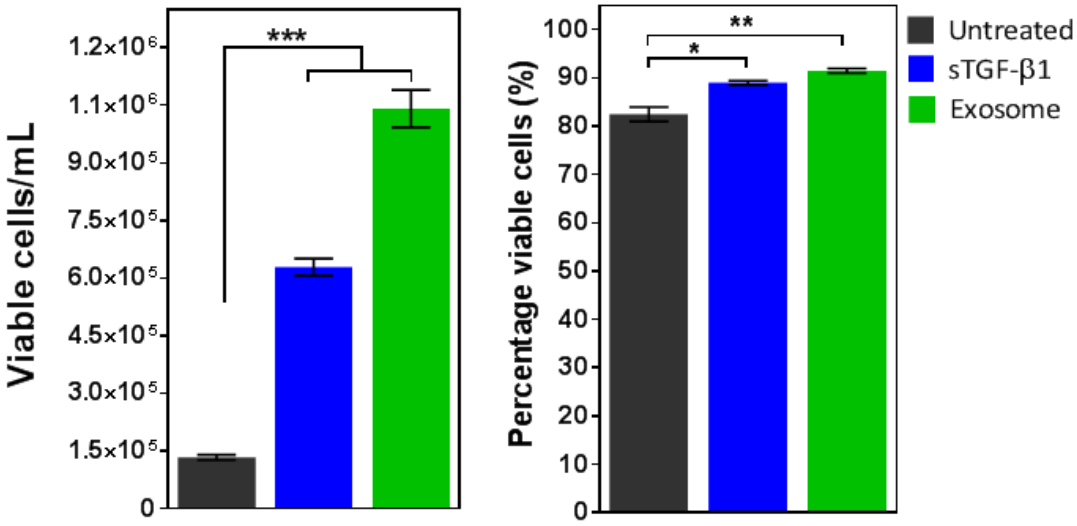

Figure 8.1: Exosome-treated MSC CM promote the proliferation of DU145 cells.
$1x10^4$ DU145 tumour cells were cultured in 1:1 ratio of RPMI media and CM from equally seeded BM-MSCs (untreated or pre-treated for 4 days with sTGFβ1 at 1ng/ml or DU145 exosomes at 150µg/ml). Following 3 days in culture, DU145 cells were harvested and viability and cell counts performed using the ViaCount system on a Guava flow cytometer (Bars, mean±SD, of triplicates, One-way ANOVA with Tukey's multiple comparison test *p≤0.05, **p≤0.01, ***p≤0.001). Representative of three such experiments with the DU145 cell line.

Proliferation and survival of PC3 cells when cultured in the different BM-MSC CM

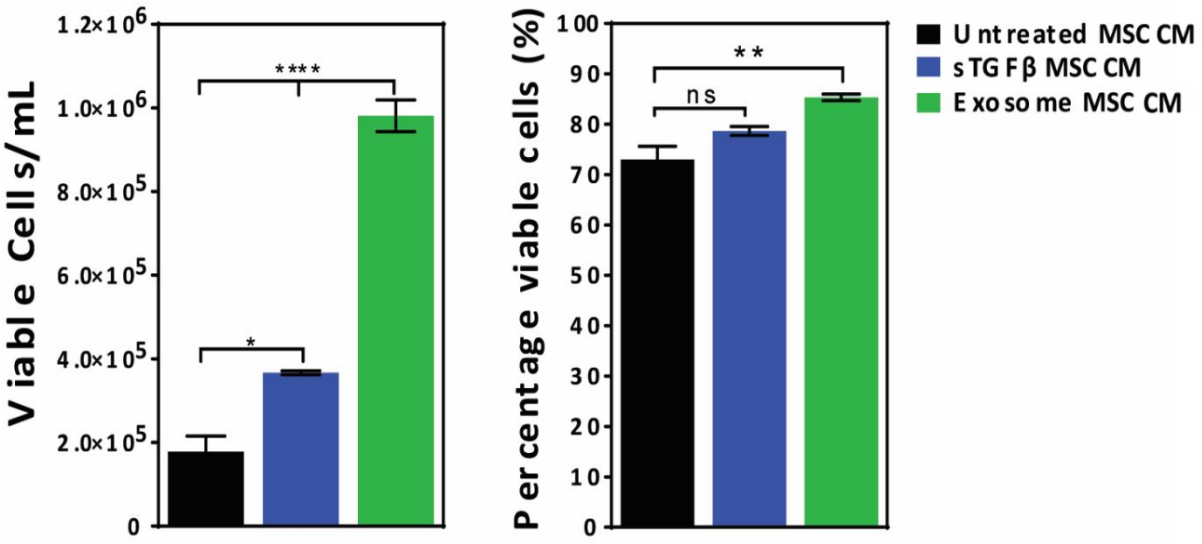

Figure 8.2: Exosome-treated MSC CM promote the proliferation of PC3 cells.
1x10^4 PC3 tumour cells were cultured in 1:1 ratio of RPMI media and CM from equally seeded BM-MSCs (untreated or pre-treated for 4 days with sTGFβ1 at 1ng/ml or DU145 exosomes at 75µg/ml). Following 3 days in culture, PC3 cells were harvested and viability and cell counts performed using the ViaCount system on a Guava flow cytometer (Bars, mean±SD, of triplicates, One-way ANOVA with Tukey's multiple comparison test *p≤0.05, **p≤0.01, ***p≤0.001, ****p≤0.0001). Representative of three such experiments with the PC3 cell line.

8.1.2 The effect of conditioned media from exosome-differentiated MSC on prostate cancer cell motility

To investigate if exosome-differentiated BM-MSCs possess tumour-promoting functions which can aid metastasis, the effects of CM from exosome-differentiated BM-MSCs on the motility of PCa cells were examined using a monolayer scratch assay. To do this, a monolayer of DU145 cells was growth arrested overnight, followed by a vertical scratch using a pipette tip. The media was replaced with CM normalised for cell number from untreated, sTGF-β1 or exosome-treated BM-MSCs and tumour cell motility in response to the different BM-MSC CM was then examined by imaging and measuring scratch closure over 24h. From an early time point of 6h, the epithelial scratch closure in response to the untreated or sTGF-β1 treated BM-MSC CM was less than 50% (figure 8.3A,B). Whereas, the epithelial response to exosome-differentiated BM-MSC CM was much faster, as noted by the scratch closure of more than 60% ($P \leq 0.001$) and was almost completed after 10h (95%) ($P \leq 0.001$). In contrast, untreated or sTGF-β1 treated BM-MSC CM were extremely slow (<70%) at this time point. Therefore, soluble factors from exosome-differentiated BM-MSCs enhance the motility of tumour cells.

The pro-motility effect was also examined on PC3 cells in the same way. Similar to DU145 cells, the PC3 cancer cell scratch closure in response to exosome-differentiated BM-MSC CM was more than 60% at 6h and closure almost completed at 10h (figure 8.4 A,B). In contrast, the motility of PC3 cells was much slower in response to the untreated or sTGF-β1 treated BM-MSC CM with complete closure observed at 24hr. Therefore, soluble factors from exosome-treated BM-MSCs also accelerated the motility of PC3 prostate cancer cells.

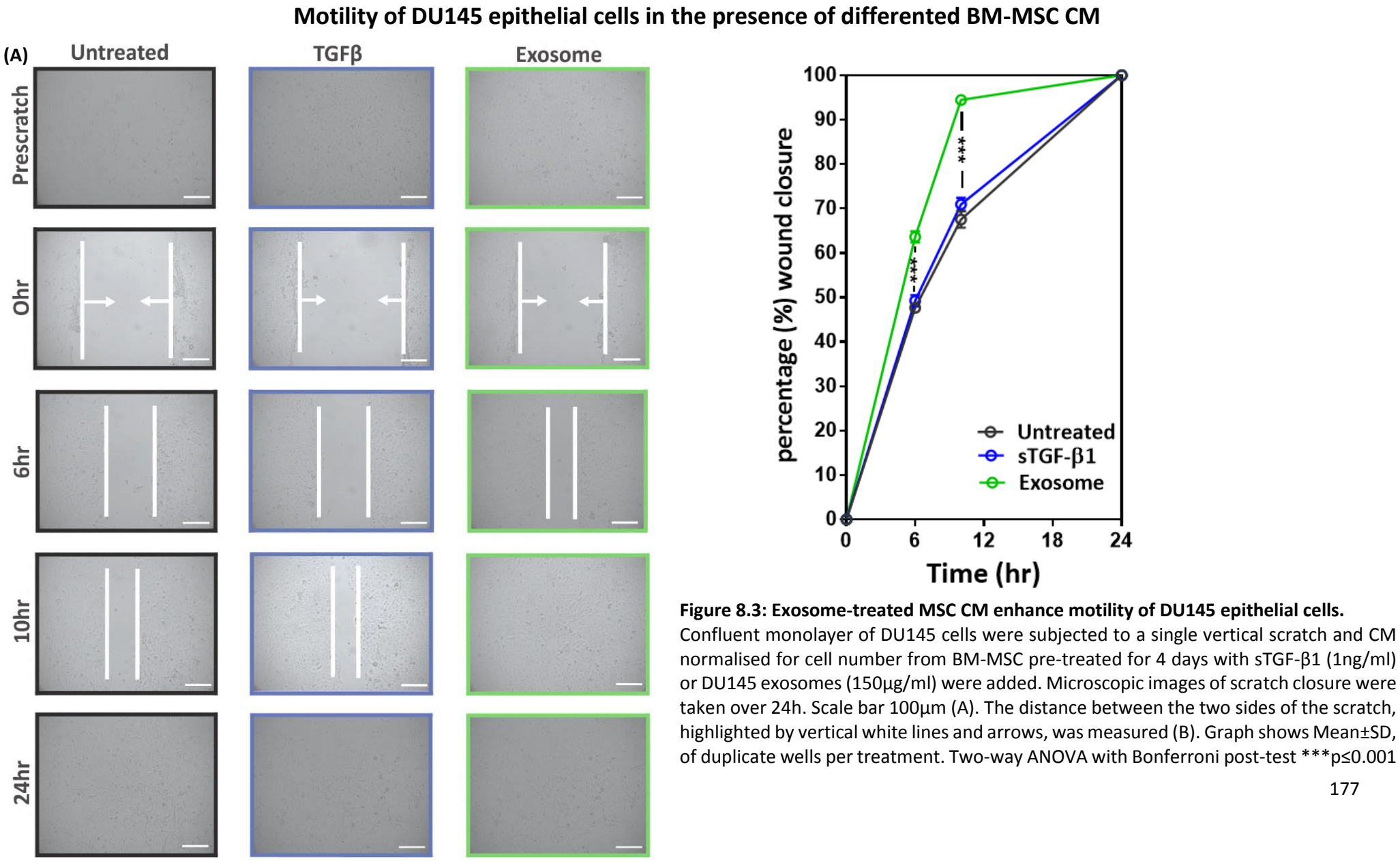

Figure 8.3: Exosome-treated MSC CM enhance motility of DU145 epithelial cells. Confluent monolayer of DU145 cells were subjected to a single vertical scratch and CM normalised for cell number from BM-MSC pre-treated for 4 days with sTGF-β1 (1ng/ml) or DU145 exosomes (150µg/ml) were added. Microscopic images of scratch closure were taken over 24h. Scale bar 100µm (A). The distance between the two sides of the scratch, highlighted by vertical white lines and arrows, was measured (B). Graph shows Mean±SD, of duplicate wells per treatment. Two-way ANOVA with Bonferroni post-test ***p≤0.001

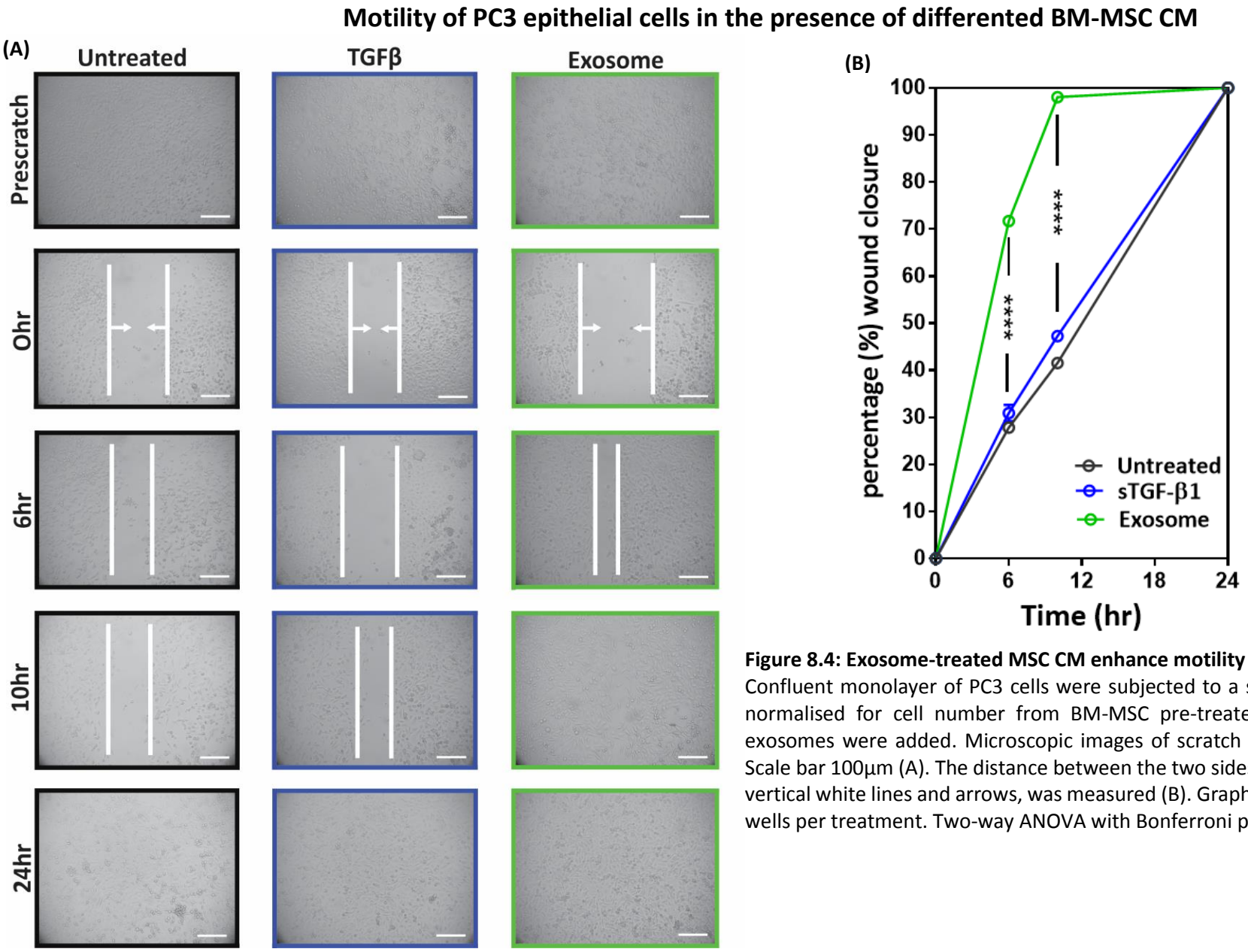

Figure 8.4: Exosome-treated MSC CM enhance motility of PC3 epithelial cells. Confluent monolayer of PC3 cells were subjected to a single vertical scratch and CM normalised for cell number from BM-MSC pre-treated for 4 days with sTGFβ or exosomes were added. Microscopic images of scratch closure were taken over 24h. Scale bar 100µm (A). The distance between the two sides of the scratch, highlighted by vertical white lines and arrows, was measured (B). Graph shows Mean±SD, of duplicate wells per treatment. Two-way ANOVA with Bonferroni post-test ****p≤0.0001.

8.1.3 The effect of BM-MSCs on tumour growth in a 3D spheroid model

3D-multicellular tumour spheroids mimic growth characteristics of *in vivo* tumour more closely than *in vitro* 2-D (monolayer) culture, as spheroids exhibit natural cell-cell attachments, elevated cell survival and proliferation in their outer layers, whilst the inner hypoxic core have reduced proliferation (due to diffusion gradient) (Pistollato *et al.* 2010). Thus, heterotypic spheroids were used to assess the effects BM-MSCs have on tumour growth, under the presence or absence of cancer exosomes.

Exosome-deficient DU145 cells were established by shRNA lentiviral knockdown of Rab27a (carried out by Dr Jason Webber). The DU145 non mammalian shRNA control ($DU145^{NM\ Control}$) or $DU145^{Rab27aKD}$ were used in this experiment as exosome-proficient or exosome- deficient cancer cells, respectively. The $DU145^{NM\ Control}$ or $DU145^{Rab27aKD}$ were incubated alone or together with BM-MSC at a ratio of 4 tumour cells: 1 MSC, in Poly-hema coated 96-well "u"- bottom plates. The spheroids were cultured in a 1:1 ratio of RPMI: DMEM 10% FBS and every other day, 50% of the culture media was replaced by fresh media, similar to other protocols used to generate spheroids (Vinci *et al.* 2012). The spheroids were fully established at day 4 (figure 8.5A) with some cellular debris around the spheroid. From an early time point of day 4, all the way to day 20, the centre of the spheroids containing BM-MSCs was darker in comparison to spheroids with no BM-MSCs. This may be because light has to travel through more thickness, indicating the presence of a greater number of cells within the inner core of the spheroids.

Spheroid growth was measured over a 20 day period and the free hand tool on image J was used to measure the radius of the spheroid which was then used to estimate the spheroid volume using the formula; $(4/3)\pi\ r_1r_2r_3$ (Wapnir *et al.* 1996). At an early time point of day 4, the spheroid volume in the absence of BM-MSCs was smaller in comparison to spheroids containing BM-MSCs. By day 8, the spheroid volume of all spheroids declined (figure 8.5B), indicating some contraction of the spheroids, resulting in a more compact sphere. In the absence of BM-MSCs however, there was a significant decline in tumour size from day 4 to day 20, by 40% and 44% in the $DU145^{NM}$ and $DU145^{Rab27aKD}$ spheroids, respectively ($P<0.0001$). In contrast, spheroids containing BM-MSCs remained the same size, with only a small decline in volume in spheroids

containing exosome-deficient tumour cells with BM-MSCs ($P<0.001$). Collectively, the data shows no spheroid growth over a 20 day period, among the different conditions, but the absence of BM-MSCs reduced the spheroid size immensely. However the presence of BM-MSCs maintained spheroid size, with the availability of PCa exosomes providing the greatest spheroid size stability. This suggests that BM-MSCs promote cell proliferation, and under the influence of PCa exosomes, the BM-MSCs have a stronger proliferative effect.

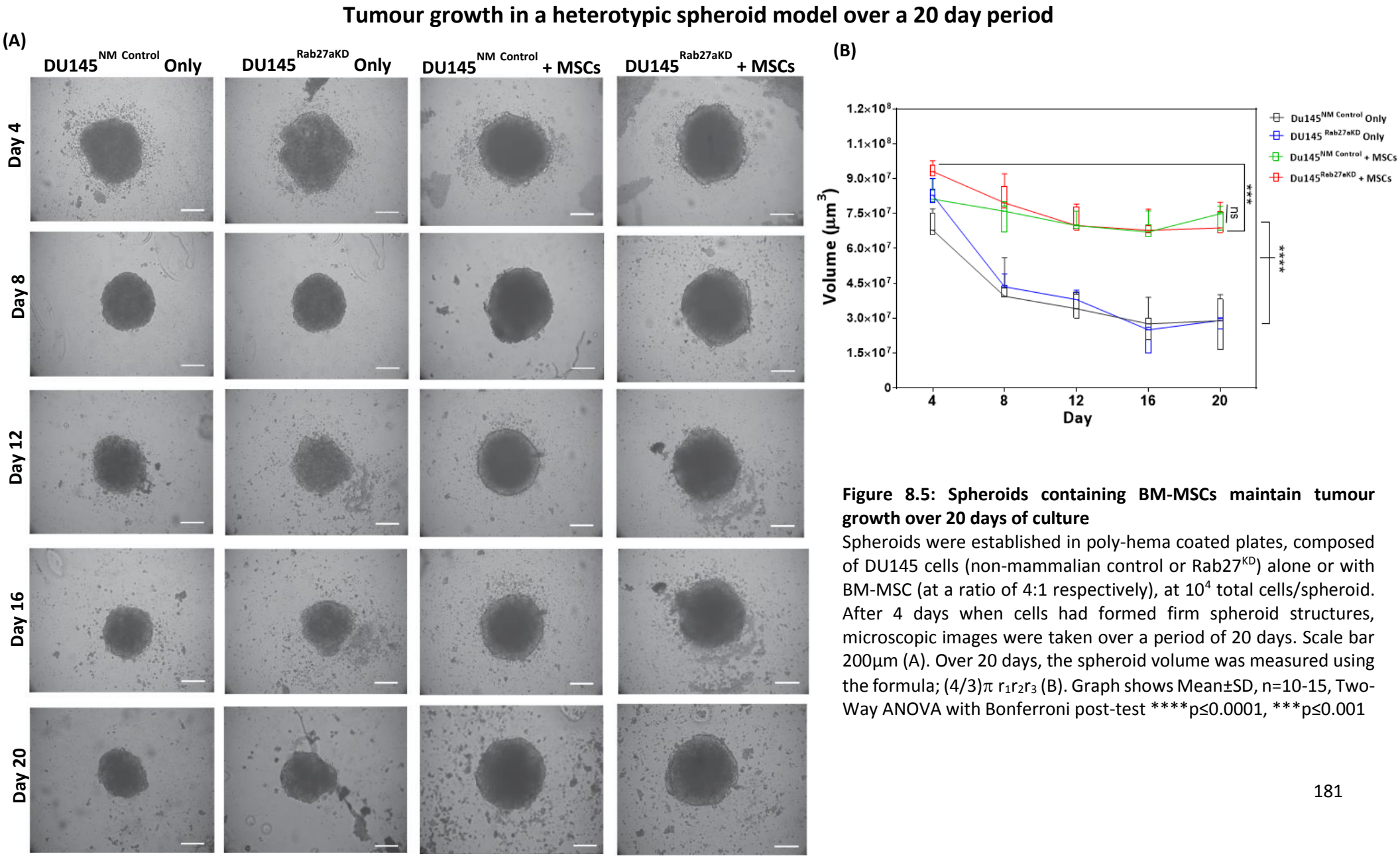

Figure 8.5: Spheroids containing BM-MSCs maintain tumour growth over 20 days of culture

Spheroids were established in poly-hema coated plates, composed of DU145 cells (non-mammalian control or Rab27^{KD}) alone or with BM-MSC (at a ratio of 4:1 respectively), at 10^4 total cells/spheroid. After 4 days when cells had formed firm spheroid structures, microscopic images were taken over a period of 20 days. Scale bar 200µm (A). Over 20 days, the spheroid volume was measured using the formula; $(4/3)\pi\ r_1r_2r_3$ (B). Graph shows Mean±SD, n=10-15, Two-Way ANOVA with Bonferroni post-test ****p≤0.0001, ***p≤0.001

8.1.4 The effect of BM-MSCs on prostate cancer cell invasion

Myofibroblasts can remodel the extracellular matrix through enzymes, rendering the tumour microenvironment more supportive for tumour cell invasion (Kessenbrock *et al.* 2010; Levental *et al.* 2009). To test if BM-MSCs under the influence of PCa exosomes promote the invasion of prostate cancer cells, an invasion assay was carried out using heterotypic spheroids. Like before, $DU145^{NM\ Control}$ or $DU145^{Rab27aKD}$ cells were used in this experiment as exosome-proficient or exosome- deficient cancer cells, respectively.

Once the 3D tumour spheroids with or without BM-MSCs were established at day 4, they were transferred to fresh wells and Matrigel^{TM} was added burying the spheroids in a 3D basement membrane (figure 8.6A). On top of the Matrigel^{TM} was the media which consisted of 1:1 (v/v) of RPMI and DMEM in 10% FBS. Each spheroid was microscopically examined for 96h, and the area of the outgrowth was measured to ascertain whether or not there was any effect on escape of cells out from the spheroid, into the surrounding matrix. Both the $DU145^{NM\ Control}$ and $DU145^{Rab27aKD}$ alone showed a paucity of cell outgrowth even at 96 hours (figure 8.6B). In marked contrast, combining BM-MSCs with the $DU145^{NM}$ cells revealed outgrowth as early as 24hr, and growing beyond the field of view at x10 microscope objective at 48 hours. By tiling multiple images, I was able to continue to assess invasion for up to 96 hours demonstrating a highly significant increase in the matrigel area occupied by extra-spheroidal cells ($p \leq 0.0001$) (figure 8.6C). Spheroids comprising BM-MSCs and exosome deficient tumour cells resulted in outgrowths at a later time point of 48h and outgrowths were drastically less extensive by 96 hours, with a clear attenuation of invasion capacity in the absence of an intact exosome secretion pathway. In summary, BM-MSCs under the influence of PCa exosomes is required to trigger the matrix invasion characteristics of the 3D-spheroid model, and attenuating exosome secretion, strongly attenuates tumour invasion.

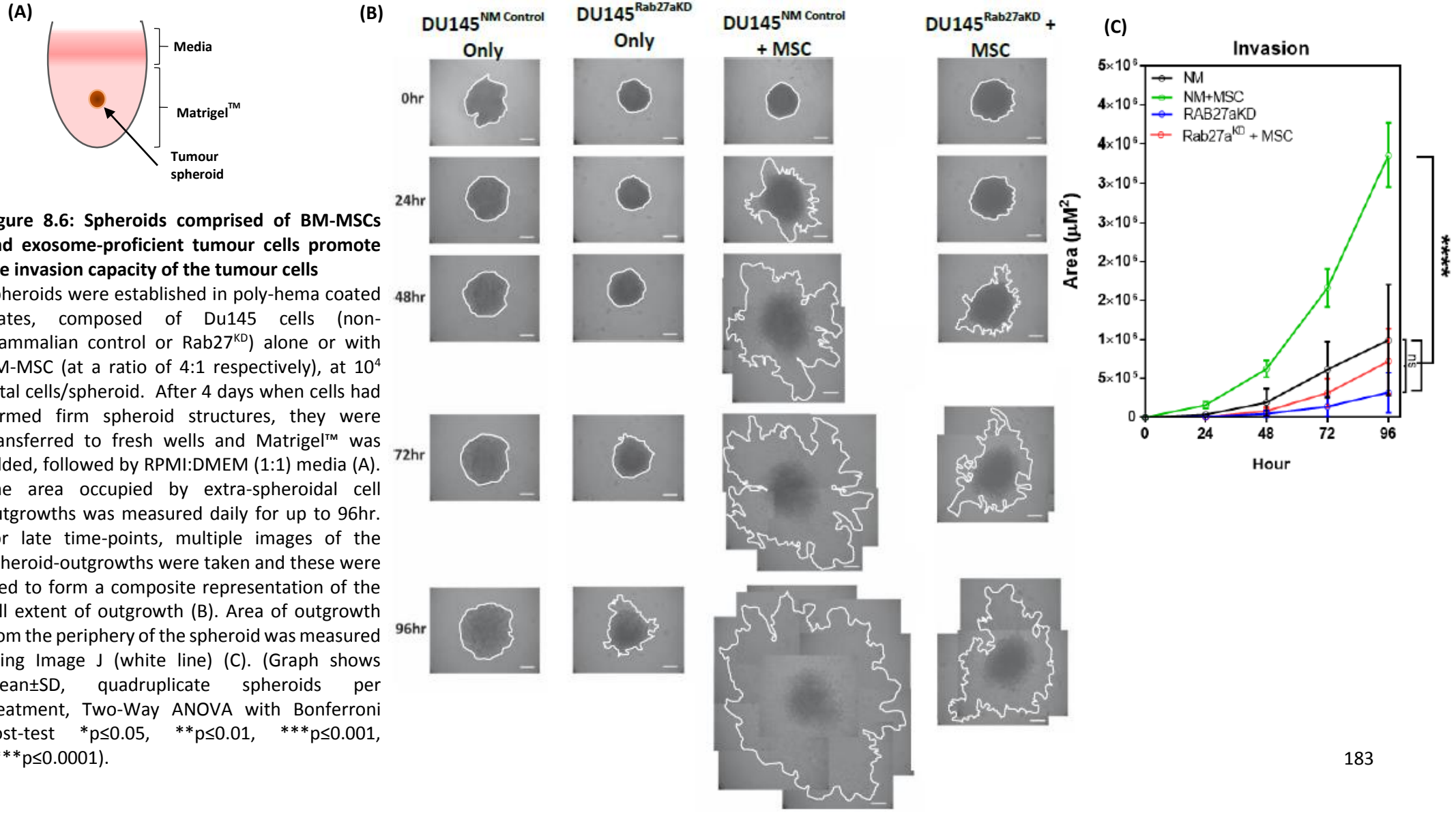

Figure 8.6: Spheroids comprised of BM-MSCs and exosome-proficient tumour cells promote the invasion capacity of the tumour cells

Spheroids were established in poly-hema coated plates, composed of Du145 cells (non-mammalian control or Rab27^{KD}) alone or with BM-MSC (at a ratio of 4:1 respectively), at 10^4 total cells/spheroid. After 4 days when cells had formed firm spheroid structures, they were transferred to fresh wells and Matrigel™ was added, followed by RPMI:DMEM (1:1) media (A). The area occupied by extra-spheroidal cell outgrowths was measured daily for up to 96hr. For late time-points, multiple images of the spheroid-outgrowths were taken and these were tiled to form a composite representation of the full extent of outgrowth (B). Area of outgrowth from the periphery of the spheroid was measured using Image J (white line) (C). (Graph shows Mean±SD, quadruplicate spheroids per treatment, Two-Way ANOVA with Bonferroni post-test *p≤0.05, **p≤0.01, ***p≤0.001, ****p≤0.0001).

8.1.5 RT-qPCR analysis MMP-3 and SerpinA-1 in the spheroids

The RT-qPCR fibrosis array performed in chapter 6 revealed exosome-treated BM-MSCs express high levels of matrix-metalloproteinase (MMP-3) and serpinA-1 in comparison to the untreated and sTGFβ-treated BM-MSCs. MMP-3 and serpinA-1 are known to be involved in the degradation of the extracellular matrix and thus have the capacity to support cellular invasion (Sternlicht *et al.* 1999; Daja *et al.* 2003; Tahara *et al.* 1984). For this reason, the level of these transcripts were evaluated in these tumour cell and BM-MSC heterotypic spheroids used for my experiments. The $DU145^{NM\ Control}$ and $DU145^{Rab27aKD}$ spheroids alone or with MSCs were collected and RNA was isolated using Tri Reagent as described in materials and methods. The relative levels of mRNA for MMP-3 or SerpinA-1 were compared among the different spheroids using TaqMan PCR assay. Relative quantification using the $2^{-\Delta\Delta Ct}$ method was used to observe differences in the gene expression of the MMP-3 or SerpinA-1 among the different spheroids relative to the $DU145^{NM\ Control}$ spheroids. The mRNA for MMP-3 and SerpinA-1 was significantly up-regulated by 70% and 74% respectively in $DU145^{NM\ Control}$ with BM-MSCs (figure 8.7). In contrast, exosome deficient cells with or without BM-MSCs showed no increase in MMP-3 or SerpinA-1. Overall, in agreement with the PCR fibrosis array data in chapter 6, MMP-3 and SerpinA-1 are confirmed to be highly expressed in tumour spheroids containing PCa exosome and BM-MSCs, and the invasive capacity of the tumour cells were also elevated in this group the most. Hence MMP-3 and SerpinA-1 may be involved in supporting the invasion of the tumour cells.

mRNA level for matrix-metalloproteinase-3 and Serpina-1

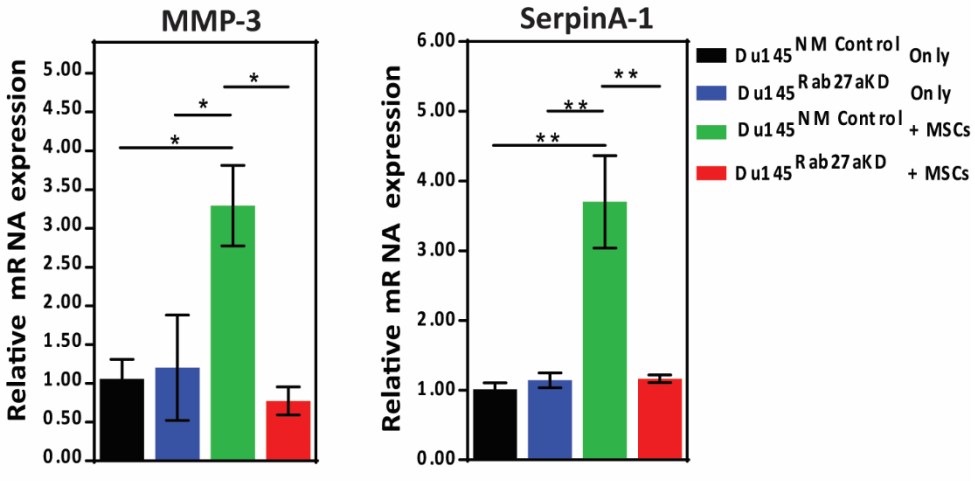

Figure 8.7: Tumour spheroids containing PCa exosomes and BM-MSCs have heightened transcripts for MMP-3 and SerpinA-1.
RNA was isolated from the DU145$^{NM\ Control}$ and DU145^{Rab27aKD} spheroids with or without BM-MSCs at day 23. Quantification of mRNA expression levels for MMP-3 and serpinA-1 in the different spheroids were measured relative to the DU145$^{NM\ Control}$ using qPCR. (Bars, Mean±SD, technical replicates. One-way ANOVA with Tukey's multiple comparison test, *p≤0.05, **p≤0.01, ***p≤0.001)

8.1.6 The effect of BM-MSCs on tumour growth in a xenograft model

Tumour growth in the presence of BM-MSCs with exosome proficient ($DU145^{Control\ Vector}$) or exosome-deficient ($DU145^{Rab27aKD}$) PCa cells was assessed in mice. Exosome-deficient cancer cells were generated using ribozyme targets of Rab27a. This experiment was carried out before we had received the more efficient and reliable lentiviral delivery of shRNA for Rab27a knock down in DU145 cells. Nevertheless, the ribozyme knockdown approach has been used by Dr Jason Webber for many years successfully in xenograft model systems *in vivo*. Our group showed that administration of exosome-proficient DU145 ($DU145^{Control\ vector}$) cells with fibroblasts accelerated tumour growth in mice, whereas exosome-deficient DU145 ($DU145^{Rab27aKD}$) cells with the fibroblasts failed to do this. Therefore cancer exosomes are suggested to be required to educate stromal cells to become tumour-promoting.

Since BM-MSCs are also precursors of myofibroblasts, we chose to repeat the above mentioned experiment, but substituting fibroblasts for BM-MSCs. In collaboration with Prof Wen Jiang and his group, $DU145^{control\ vector}$ or $DU145^{Rab27aKD}$ cells alone or with BM-MSCs were injected into immune-deficient mice, at a 4 tumour: 1 MSC ratio. As a negative control BM-MSCs alone were also administered. Tumour growth was assessed over a 28 day period by the current standard technique for volume determination by using an external caliper to measure the height and width of the tumour. These measurements were then used to calculate tumour volume using the formula; 0.523 x $width^2$ x length, as described previously (Escudero-Esparza *et al.* 2012).

Throughout the 28 day period, BM-MSCs administered alone did not cause any tumours, as expected. At an early time point of day 8, there was no significant difference in tumour volume among the different conditions (figure 8.8). By day 15, however, mice containing BM-MSCs with PCa cells resulted in a greater tumour volume, which where almost double the size in comparison to the tumours in the absence of BM-MSCs. By day 28, mice with BM-MSCs and $DU145^{Control\ vector}$ cells had significantly larger tumours ($P \leq 0.001$) to that of $DU145^{Control\ vector}$ cells alone. In contrast, there was no difference between BM-MSCs with $DU145^{Rab27aKD}$ cells and $DU145^{Rab27aKD}$ cells alone. Thus, at the end point of day 28, it may seem that BM-MSCs with exosome-proficient PCa cells

promote tumour growth. However, since there was a very heterogeneous range of tumour growth across the different conditions, the effect of BM-MSCs under the influence of exosomes on tumour growth is inconclusive. Collectively, the data shows that adding BM-MSCs with tumour cells enhances growth *in vivo*, regardless of the exosome-secretion status of the tumour cells. We were disappointed not to have revealed a clear cut role of exosomes in this experiment and wanted to explore potential reasons why this may have happened.

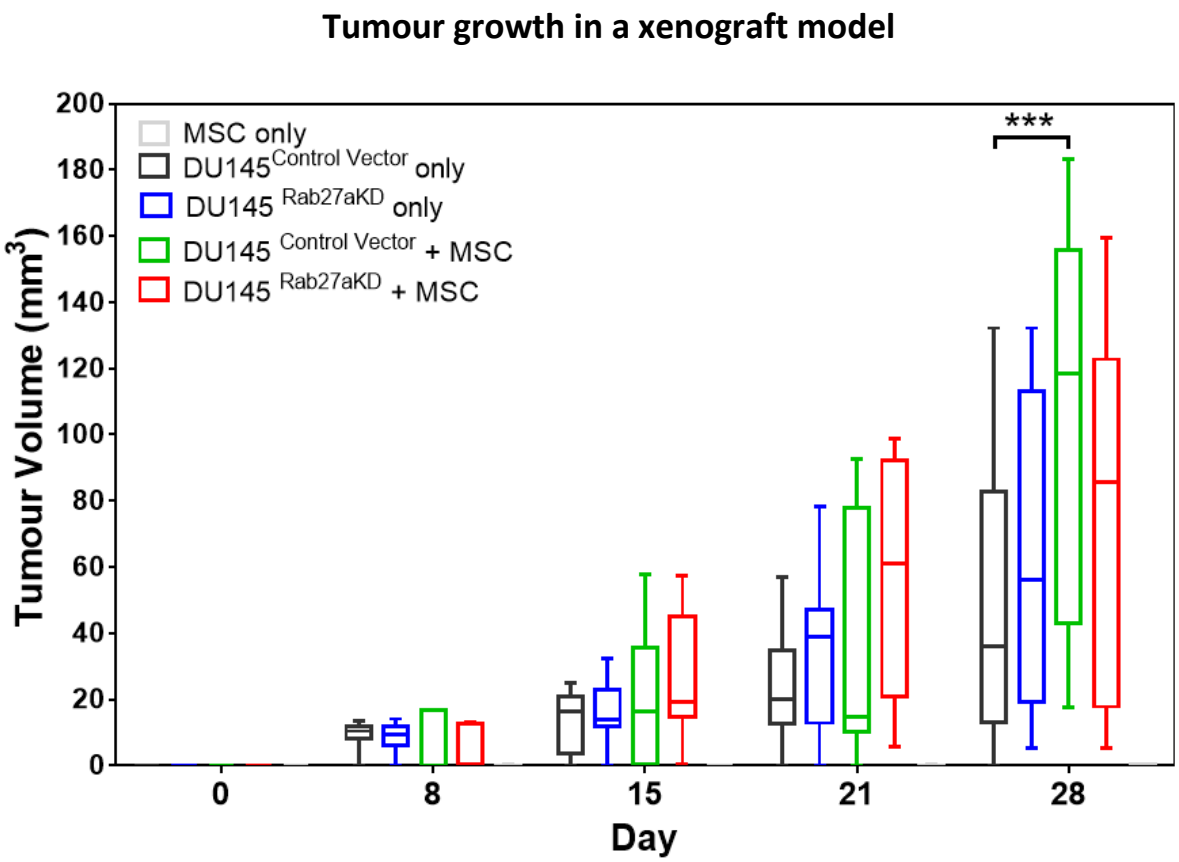

Figure 8.8: BM-MSCs with exosome-proficient PCa cancer cells accelerates tumour growth after 28 days post injection into mice.
DU145$^{\text{Control Vector}}$ or DU145 $^{\text{Rab27aKD}}$ cells were administered alone or with BM-MSCs in a 4:1 ratio respectively, into the hindlimbs of immunodeficient mice. BM-MSCs alone were also administered into the mice. Tumour height and width was measured using an external caliper and used to calculate tumour volume over 28 days. (Graph shows Mean±SD, n=12, except for BM-MSC alone control which has an n=6. Two-Way ANOVA with Bonferroni post-test ***p≤0.001)

8.1.7 Instability of Rab27a knock down

Since there was no significant difference between the DU145$^{Control\ vector}$ with BM-MSCs and DU145^{Rab27aKD} with BM-MSCs, this raised the question if the knock down of Rab27a using the ribozyme silencing method was stable enough to sustain this exosome-deficient property of the cancer cells over time. To test this, DU145$^{Control\ vector}$ and DU145^{Rab27aKD} cells were cultured in T75 flasks and RNA was sequentially collected over 8 weeks of culture. mRNA for Rab27a was assessed using qPCR. After 2 weeks of cell culture, there was a decrease in Rab27a gene expression in DU145^{Rab27aKD} cells by 64% ($P \leq 0.0001$) in comparison to the DU145$^{Control\ vector}$ cells (figure 8.8). By 4th and the 6th week of culture, there was only ~30% loss of Rab27a gene expression in the DU145^{Rab27aKD} cells in comparison to the DU145$^{Control\ vector}$. The knock down of Rab27a was further declined to 7% at 8 weeks of cell culture. Therefore, knock down of Rab27a was lost with time, suggesting that exosome secretion is no longer blocked. The instability of Rab27a knock down could explain why there was no drastic difference amongst the exosome-deficient tumour cells with BM-MSCs to that of exosome-proficient tumour cells with BM-MSCs. Furthermore, the Rab27a status of DU145 cells used for the *in vivo* work was not confirmed prior to the experiment, thus the cells injected into the mice may have already lost the knockdown. This may have allowed BM-MSCs to differentiate into myofibroblasts under the influence of exosomes and thus promote tumour growth in mice containing DU145^{Rab27aKD} with BM-MSCs.

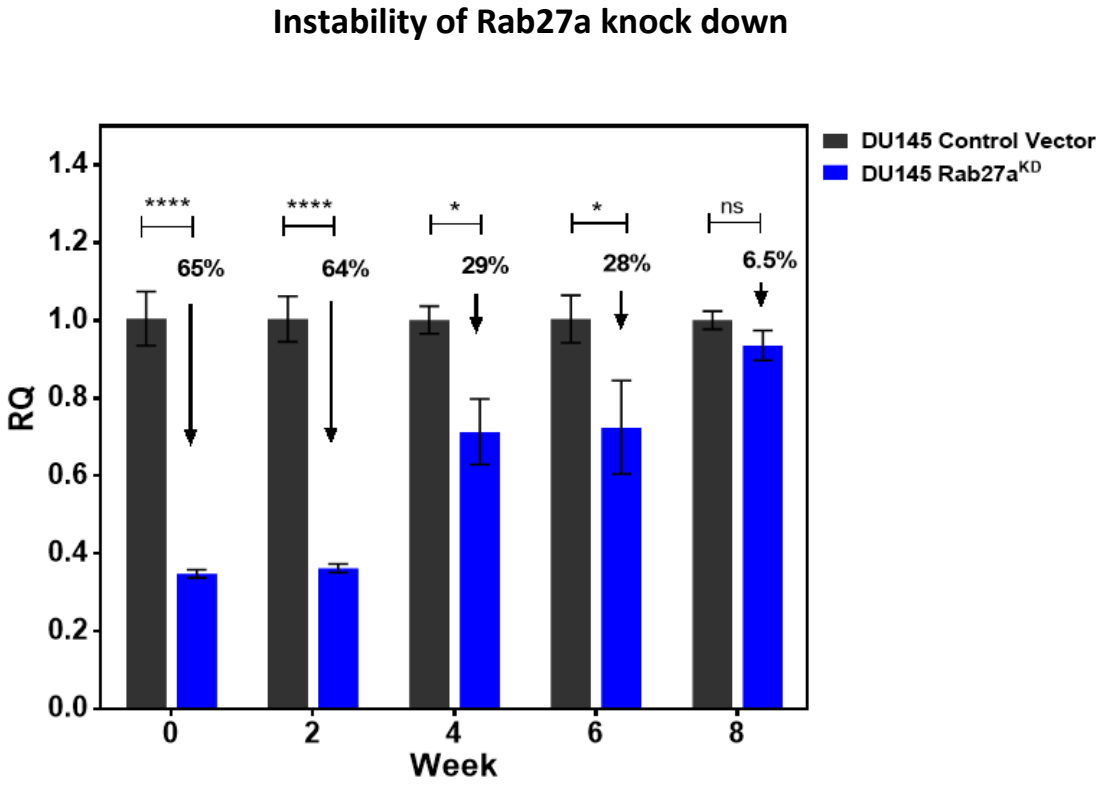

Figure 8.9: Stability of Rab27a^{KD} declines over time
RNA was isolated from DU145 $^{Control\ Vector}$ and DU145^{Rab27aKD} cells over 8 weeks of cell culture. Relative quantification (RQ) of mRNA for Rab27a were evaluated using qPCR, using GAPDH as the housekeeping gene. (Bar Mean±SD, n=3, Two-Way ANOVA with Benforri post-test, *p≤0.05, ****p≤0.0001)

8.2 Discussion

Exosome-differentiated BM-MSCs increase tumour cell proliferation and motility

Cancer associated myofibroblasts are important determinants of tumour cell behaviour, as the stromal cells act to condition the tumour microenvironment, favouring tumour growth and metastasis (Orimo *et al.* 2005; Webber *et al.* 2014). I have shown that CM from exosome-differentiated BM-MSCs strikingly elevates the proliferation of prostate cancer cells (DU145 and PC3 cell lines). CM from sTGF-β1 treated BM-MSCs also increased the proliferation of PCa cells but to a much lesser extent to that of exosome-differentiated BM-MSCs. Metastasis is a key consequence of tumour progression, which requires carcinoma cells to be motile and invade the ECM, in order to enter the circulation and reach a distant organ. In the presence of soluble factors from exosome-differentiated BM-MSCs there was a heightened motility of PCa cells in a scratch assay, almost completing scratch closure by 10 hours. The mechanism behind the pro-proliferative and pro-motility effect has not been explored here, but published literature reports HGF secreted from cancer stroma cells promotes the proliferation and motility of carcinoma cells in liver cancer and colon cancer (Jia *et al.* 2013; Kermorgant *et al.* 2001). Moreover, VEGF has been revealed to enhance the proliferation of breast cancer cells by inducing the anti-apoptotic protein BCL-2 (Liang *et al.* 2006). Thus the enhanced secretion of VEGF-A and HGF from exosome-differentiated BM-MSCs may also be involved and by selectively blocking VEGF-A or HGF, we can determine their relative importance in tumour proliferation and motility.

BM-MSCs and tumour growth in vitro

Spheroids generated with DU145$^{\text{NM Control}}$, DU145$^{\text{Rab27aKD}}$ cells alone or with BM-MSCs were cultured over 20 days. During growth of the spheroids, a dense core was observed, suggestive of a necrotic core from other studies. Such studies have reported cells in the inner core to be deprived of oxygen, glucose, ATP and other nutrients, whereas metabolic waste accumulates, resulting in a necrotic core (Bertuzzi *et al.* 2010). Analysis of tumour spheroid growth revealed a rapid decline of tumour only spheroids, similar to other reports, attaining a limiting size, regardless of how often new media was provided or how much open space was made available for growth (Folkman and Holchberg 1973). In contrast, the presence of PCa exosomes and BM-MSCs, maintained a consistent

tumour size over 20 days. Similar was observed with BM-MSCs with exosome-deficient tumour cells but to a lesser extent. The overall shrinkage of the spheroids may have been due to the organisation of the cells and cellular contraction (Nyga *et al*. 2013; Sodek *et al.* 2009), but the presence of BM-MSCs possibly promoted tumour cell proliferation and hence the maintenance of tumour cell size.

The presence BM-MSCs with prostate cancer exosomes did not seem to cause an immense spheroid growth in comparison to BM-MSCs with exosome-deficient cancer cells. However, the measurement of tumour volume may have been a hindrance of observing any differences which may have existed. The estimation of tumour volume was based on spheroid surface measurement in 2D, which is not a good representative of tumour growth, as we are assuming that the spheroids are all perfect spheres but the depth of the spheroids may actually be different. Thus, spheroids which look small on the surface, may have been greater in depth, but would not be noted based on this measurement.

BM-MSCs and tumour invasion in vitro

Using 3D spheroids in a matrigel invasion assay, the control DU145 cells along with BM-MSCs drastically supported the invasion of tumour cells through the Matrigel^{TM}. Whereas Rab27a^{KD} DU145 cells along with BM-MSCs, did not support tumour invasion as well. This suggests that the presence of PCa exosomes, may have generated myofibroblasts using the BM-MSCs which are an important element in controlling the invasion of cancer cells.

The mechanism behind the pro-invasive property of exosome-differentiated BM-MSCs has not been investigated before. Like with proliferation and motility, elevated factors from exosome-treated BM-MSCs, such as VEGF-A and HGF (shown in chapter 5) may be involved in the invasion of PCa cells. Studies have reported the requirement of VEGF-A and HGF secreted by myofibroblasts for supporting the invasion of squamous cell carcinoma cells in a transwell matrigel assay (Cat *et al.* 2006). HGF stimulated invasiveness of cancer cells has been associated with the increased secretion of the protease, urokinase-plasminogen activator (uPA) and its receptor, uPAR by the cancer

cells (Jedeszko *et al.* 2009). The receptor bound uPA generates a proteolytic cascade that contributes to the degradation of the basement membrane and ECM (Kobayashi, 1996). Similarly, an up-regulation of uPA are also observed by prostate cancer stromal cells and exosome-differentiated fibroblasts (Webber *et al.* 2014), and so high uPA is secreted by both cancer epithelial and stromal cells. Therefore HGF secreted from exosome-differentiated BM-MSCs may also trigger a proteolytic cascade for ECM breakdown.

RT-qPCR analysis revealed mRNA for MMP-3 and SerpinA-1 was highly expressed in tumour spheroids containing BM-MSCs with PCa exosome proficient cell. This agreed with the high mRNA levels of MMP-3 and SerpinA-1 found in exosome-treated BM-MSCs (shown in chapter 6). Therefore, MMP-3 and SerpinA-1 may be involved in promoting invasion of tumour cells. By blocking the MMPs and SerpinA-1 selectively, the relative importance they have in the spheroid culture for invasion can be determined. MMP-3 has been shown to promote breast cancer cell invasion *in vitro*, in a dose-dependent manner (Phromnoi *et al.* 2009), by degrading numerous ECM substrates such as collagens, laminins, fibronectin and ECM proteoglycans (Lu *et al.* 2011; Sternlicht *et al*. 1999). Thus inhibiting MMP-3 attenuated the invasion capacity of the tumour cells (Phromnoi *et al.* 2009). Furthermore, SerpinA-1 is up-regulated and correlated with poor prognosis in adenocarcinoma (Tahara *et al.* 1984) and gastric cancer (Shin *et al.* 2012). Immunohistochemical staining of serpinA-1 was shown to increase with increasing gastric tumour size and knock down of serpinA-1 decreased invasion and migration of the cancer cells (Shin *et al.* 2012). SerpinA-1 was found to up-regulate mRNA level and release of MMP-8 by gastric cancer cells (Kwon *et al.* 2014). In addition MMP-3 can cleave the precursors of MMP-8 to activate them (Page- McCaw *et al.* 2007), which can further break down the ECM. Therefore spheroids comprising of BM-MSCs with exosome-proficient PCa cells can up-regulate matrix remodelling proteins which can degrade the ECM and support the invasive nature of the tumour.

The data in this chapter revealed exosome-differentiated BM-MSCs to have a pro-proliferative and pro-motility effect on prostate cancer cell lines. Furthermore, co-culture of BM-MSCs and exosome proficient PCa cells, maintain growth and promote

the tumour cell invasion *in vitro.* Therefore BM-MSCs under the influence of PCa exosomes are tumour promoting.

BM-MSCs and tumour growth in vivo

An attempt to examine the dependency of cancer exosomes and BM-MSCs on tumour growth in a xenograft model was carried out. DU145 cells, whether exosome-proficient ($DU145^{Control\ Vector}$) or exosome-deficient ($DU145^{Rab27aKD}$), had accelerated tumour growth over 28 days in the presence of BM-MSCs, but there was no difference in growth between the $DU145^{Control\ Vector}$ cells with BM-MSCs vs the $DU145^{Rab27aKD}$ cells with BM-MSCs. From the *in vitro* experiments, we know that exosome-differentiated BM-MSCs support tumour progression by substantially increasing tumour cell proliferation. But here, it is only at a later stage, of day 28 that tumour volume was the largest in the presence of $DU145^{Control\ Vector}$ with BM-MSCs. After seeing no difference between the $DU145^{Control\ Vector}$ cells with BM-MSCs vs the $DU145^{Rab27aKD}$ cells with BM-MSCs at earlier time point, the *in vivo* experiment was ended at day 28, but that was when the tumour promoting effects of exosome-differentiated BM-MSCs started to become noticeable. Therefore tumour growth may be dependent on both the cancer exosomes and BM-MSCs and hence the exosome-generated myofibroblasts from BM-MSCs.

In comparison to previous studies by our group, the $DU145^{Control\ Vector}$ cells showed accelerated growth in the presence of normal fibroblasts over 32 days, whereas $DU145^{Rab27aKD}$ cells with fibroblasts showed no growth enhancement and these differences were seen from an earlier time point of day 20 (Webber *et al.* 2014). But it is known that myofibroblastic differentiation of fibroblasts only takes 72hr (Webber *et al.* 2010), whereas I have shown α-SMA myofibroblastic differentiation of BM-MSCs to take up to 14 days. Therefore a bigger difference in tumour growth between the $DU145^{Control\ Vector}$ with BM-MSCs and $DU145^{RAB27aKD}$ with BM-MSCs may have been appeared at a later date.

Furthermore, tumour volume was measured using an external caliper which is the current gold standard for volumetric measurements of xenograft tumours, but this method is often affected by errors such as variability of tumour shape and subcutaneous

fat layer thickness. Other techniques such as the microCT has been found to be more accurate (Jensen *et al.* 2008), as it measures the depth of the tumour more accurately than the external caliper which assumes the depth of the tumour is same as the outgrowth of tumour measured. This means, that the tumour-promoting effect of exosome-differentiated BM-MSCs may be underestimated if the tumour grew inwardly. However the most likely reason as to why there was no big difference between the $DU145^{Control\ Vector}$ with BM-MSCs and $Du145^{Rab27aKD}$ with BM-MSCs is due to the instability of the Rab27aKD using the ribozyme silencing method, as the mRNA level for Rab27a was seen to increase with time of cell culture. Thus, there may have been enough exosomes secreted by the cancer cell to generate myofibroblast-like cells from BM-MSCs which may in turn accelerate tumour growth. A better approach would have been to use lentiviral shRNA knock down of Rab27a, which has been used in my spheroid model. However, exosome-deficient DU145 cells using such method was not available during the mice studies.

Alternatively, the administration of BM-MSCs that had already been differentiated by PCa exosomes *in vitro*, may have been a better approach to observe a bigger response of accelerated tumour growth by the exosome-differentiated BM-MSCs, in comparison to the untreated or sTGF-β1 treated BM-MSCs. This would have allowed BM-MSCs to have had a head-start on differentiating into myofibroblast-like cells. Nevertheless, the *in vitro* experiments in this thesis revealed exosome-differentiated BM-MSCs to be essential for the increase in PCa cell proliferation, motility, invasion and maintenance of tumour growth all of which are required for the tumour to progress.

Chapter 9: General Discussion

9.1 General Discussion

9.1.1 Summarising Discussion

Prostate Cancer (PCa) is the most common cancer in men in the UK (NICE 2009) and a lot of therapies for PCa are targeted towards the prostatic cancer cells. However, it should not be forgotten that the cancer cells exist in close and symbiotic relationship with the reactive stromal compartment. Recently there has been a renewed interest in the cross-talk between the cancer cells and the stromal cells, with increasing evidence for a profound influence of fibroblastic stromal cells in driving disease progression, dictating treatment response and ultimately relating to poor clinical outcome (Yamashita *et al.* 2012; Tomas *et al.* 2010). Several studies have identified common characteristics of cancer associated stromal cells across diverse solid cancer types. These include the molecular traits of myofibroblasts, which promote tumour cell growth directly and stimulate angiogenesis, by providing various growth factors such as PDGF, VEGF, FGF and uPA (Webber *et al.* 2014; Tuxhorn *et al.* 2002; Orimo *et al.* 2005; Galie *et al.* 2005; Liang *et al.* 2005). However, there are some recent reports in pancreatic carcinoma where myofibroblasts play a protective role and limits the tumour growth (Rhim *et al.* 2014; Gore *et al.* 2014). Whilst, such data has not been shown for other cancer types, the main paradigm is that cancer associated myofibroblasts promotes tumour growth and can be used as an indicator of a poor prognosis. Therefore the cancer associated myofibroblasts may represent new potential therapeutic targets. However, there remains an incomplete understanding about the stroma, the generation of cancer associated myofibroblasts, their cellular and molecular nature and their consequence in terms of disease outcome.

There are multiple origins of myofibroblasts and although soluble TGF-β1 secreted by cancer cells has remained the principle culprit driving myofibroblastic differentiation, studies have shown TGF-β1 expressed on the surface of cancer exosomes to also drive this differentiation pathway (Clayton *et al.* 2007; Webber *et al.* 2010). Studies by our group (Webber *et al.* 2010) have recently highlighted a role of exosome vesicles in delivering TGF-β1 to differentiate fibroblasts into α-SMA positive myofibroblasts, which in turn promote cancer growth *in vivo* (Webber *et al.* 2014). Additionally, others have shown cancer derived exosomes to differentiate MSCs from umbilical cord or adipose

tissue into myofibroblasts (Gu *et al.* 2012; Cho *et al.* 2011; Cho *et al.* 2012). However, most studies have shown bone marrow-derived MSCs (BM-MSCs) to migrate to the tumour sites (Shinagawa *et al.* 2010; Teo *et al.* 2012), but the effect that the BM-MSCs have in cancer, under the influence of cancer exosomes has not been explored before and is the main focus in this thesis.

MSCs exhibit cellular plasticity, capable of differentiating into multi-lineage cell types, under appropriate hormonal or growth factor stimulants applied sequentially, often over long time periods such as a month. MSCs can differentiate into adipocytes when cultured under appropriate adipogenic stimulants (Pittenger *et al.* 1999). However, the addition of sTGF-β1 or the equivalent dose of exosomal TGF-β1 inhibited the adipogenic differentiation of BM-MSCs. sTGF-β1 in the presence of adipogenic stimulants, including dexamethasone and insulin along with other growth factors may halt MSC differentiation towards adipocytes and drive them to differentiate into other cell types. For example, sTGF-β1 along with dexamethasone is known to differentiate MSCs into osteoblasts (Bruder *et al.* 1997; Jaiswal *et al.* 1997). Similarly, MSCs placed in aggregate cultured with sTGF-β1, along with dexamethasone, insulin and other factors will undergo chondrogenic differentiation (Johnstone *et al.* 1998; Mackay *et al.* 1998; Lee *et al.* 2004b). Therefore sTGF-β1 has the capacity to differentiate MSCs into various cell types. Interestingly however, exosome associated TGF-β1 and not sTGF-β1 was able to skew MSC differentiation away from adipocytes and instead towards α-SMA positive myofibroblasts. What is equally remarkable is that a single stimulation with exosomes (at 150µg/ml) over 14 days was sufficient to trigger the onset of α-SMA stress fibres, suggesting a myofibroblast-like differentiation. My data suggests, cancer exosomes may be capable of overriding the natural control of MSC differentiation *in vitro*, away from self-renewal or reparative phenotypes, towards undesirable disease promoting myofibroblasts.

Previous studies have shown fibroblasts to exhibit the capacity to differentiate into myofibroblasts under the influence of sTGF-β1, and this requires additional factors such as endogenous hyaluronic acid production and the interaction between CD44 and the EGF receptor (Midgley *et al.* 2013). However, the detailed myofibroblastic phenotype

arising from sTGF-β1 treatement appears to differ from cancer associated stromal cells, as it is not pro-angiogenic and fails to enhance PCa growth in xenograft models (Webber *et al.* 2014). In contrast, stimulating the fibroblasts (same stromal cell source) with TGF-β1 bearing PCa exosomes generated myofibroblasts that mimic those extracted from cancerous tissues, such as driving angiogenesis and promoting tumour growth *in vivo* (Webber *et al.* 2014). In this thesis, the phenotypic differences between sTGF-β1 treated and exosomal TGF-β1 treated MSCs have been explored. PCa exosomes differentiated BM-MSCs towards a myofibroblastic phenotype exhibiting heightened VEGF and HGF secretion. The cell arising, therefore represent those above-mentioned traits of cancer associated stroma even though the originating cell source is different. This suggests that it is the nature of the trigger (i.e. exosomes), rather than the originating cell type, that is the most important for the phenotype and function of the myofibroblast arising. In contrast, sTGF-β1 stimulation of BM-MSCs gave a drastically different response that lacked the onset of αSMA-stress fibres or elevated VEGF and reduced constitutive HGF secretion. Comparing the direct effect of exosomal TGF-β1 and sTGF-β1 highlighted the profound difference in the cell response arising, with the exosomal TGF-β1 treated BM-MSCs being more akin to the stromal cells naturally arising at the site of prostate cancer (Webber *et al.* 2014). A detailed mechanistic explanation for this difference is lacking and given the molecular complexity of exosomes secreted by the cancer cell, makes it significantly challenging.

It is clear that unlike sTGF-β1, exosome-mediated generation of myofibroblasts from BM-MSCs exhibit the characteristic traits of cancer associated stromal cells and these myofibroblastic features are dependent on TGF-β1 as shown by blocking TGF-β1 signalling. This agrees with previous findings using fibroblasts and DU145 exosomes, where blocking TGF-β signalling attenuated the differentiation of fibroblasts into α-SMA expressing myofibroblasts and the pro-angiogenic function of these differentiated stromal cells (Webber *et al.* 2014). A key difference between sTGF-β and exosomal TGF-β1 delivery is that exosomes have TGF-β receptor III (a heparan sulphate proteoglycan called betaglycan) on their surface which aids the delivery of TGFβ1 to the stromal cells for their differentiation into myofibroblasts (Webber *et al.* 2014). The presence of heparan sulphate proteoglycan (HSPG) on exosomes, however only shows the

differences between the sTGF-β1 and the exosomal TGF-β1 and not necessarily their behavioural differences. Nevertheless, it has been revealed that intact HSPG is required for functional delivery of vesicular TGF-β1 (Webber *et al.* 2014). In the case of fibroblasts, cleavage of the heparan sulphate side chains by heparinase III, still maintained the tethering of TGF-β1 to the exosome surface (no impact on TGFβ levels), however exosome-induced SMAD-3 dependent TGF-β1 signalling was attenuated, resulting in the loss of α-SMA expression and the pro-angiogenic function of the differentiated fibroblasts. Thus the heparan sulphate side chains appear to have functions that control the behaviour of exosomal TGF-β1 and similar interactions may apply with BM-MSCs, as precursor cells of myofibroblasts. It should be noted, however that cells also express HSPG which can aid the delivery of the TGF-β1 ligand to the TGF-βR I and TGF-βR II (Lopez-Casillas *et al.* 1993). Thus this feature alone cannot explain the differences in phenotype and function observed between sTGFβ treated and the exosomal TGF-β1 treated BM-MSCs. Some studies have shown active sTGF-β1 in culture to have a short half-life (Rollins *et al.* 1989; Coffey *et al.* 1987) in comparison to the latent form of TGF- β1 (Wakefield *et al.* 1990). The reason behind this is unknown, but TGF-β1 expressed on the exosome surface is predominantly in the latent form (Webber *et al.* 2010) therefore exosomal TGF-β1 may exhibit a longer time of bioavailability, a facet likely to be very relevant for the slow-differentiation process of MSCs. Still, this does not explain the phenotypic and functional differences between the sTGFβ-induced and exosome-induced myofibroblasts generated. Exosomes are complex vesicles, consisting of various mRNA and miRNA, growth factors, enzymes and molecules associated with the biogenesis and secretion of exosomes. The possible co-delivery of these contents from exosomes along with TGFβ delivery may influence BM-MSC differentiation and is an area of interest for future investigation.

By interfering with the exosome secretion pathway via Rab27a silencing, my data clarifies that cancer exosomes are the dominant factor in mediating myofibroblastic differentiation. It is acknowledged that the specificity of the Rab27a silencing approach for selective inhibition of exosome secretion and not other factors by the cells is somewhat controversial (Bobrie *et al.* 2012) and so reliance on Rab27a knockdown as the exclusive approach for evaluating the role of exosomes must be taken with caution.

Another approach of reducing the level of exosomes in cancer cell conditioned media, is by high speed centrifugation, which generates cell conditioned media that is poor in driving myofibroblast differentiation. From this, the differentiation was observed to reside in the 120,000 g pelletable fraction, strongly implicating exosomes as mechanistically central to cancer mediated control of MSC. It should be noted, however, the pellets containing exosomes may also contain other factors. Thus, treating MSCs with different density fractions from a continuous sucrose gradient containing exosomes, may definitively show that myofibroblastic differentiation of MSCs is exclusively focused on exosomal vesicles and not co-pelleted material. But this has yet to be tested. Nevertheless, the use of pellets containing exosomes and the Rab27a silencing approach collectively provide data supporting these conclusions.

The functional properties of exosome-generated myofibroblasts support the premise that cancer exosomes have a disease-promoting influence. Although the direct effect of cancer exosomes on angiogenesis has been well documented (Sheldon *et al.* 2010; Al-Nedawi *et al.* 2009), the impact of exosome-differentiated BM-MSCs on this process has not to our knowledge been studied. Endothelial cells exhibited enhanced proliferation and migration in the presence of soluble factors produced by the exosome-differentiated BM-MSCs. The endothelial cells have also been documented to form complex vessel-like structures in the presence of exosome-differentiated BM-MSCs. These structure were akin to those produced using PCa derived stroma cells (Webber *et al.* 2014). Growth factors such as VEGF-A and HGF which are found to be highly secreted by exosome differentiation MSCs may be involved in this pro-angiogenic function. To investigate this, blocking antibodies against HGF and VEGF can be used to examine if the angiogenic influence is abolished.

In a similar fashion, exosome-differentiated MSCs have a direct positive effect on tumour cell proliferation and migration, and provide an enhanced tendency for cells to invade into the extracellular matrix using a 3D spheroid model. Whether the invading cells are principally epithelial or mesenchymal in nature are unknown, but given the predominance of tumour cells (4:1) in the spheroids, and the pro-proliferative influence of BM-MSC on tumour cells, the invading cells are most likely to be epithelial cells as

suggested by their cobblestone appearance. The extensive invasion property was abrogated when targeting exosome secretion by Rab27a silencing. Additionally, the invasion of the cancer cells were absent when BM-MSCs were left out of the spheroids highlighting the role of this stromal cells and exosomes in directing the invasion behaviour. This high invasive capacity of the system agrees with additional evidence showing exosome-driven elevation of metalloproteinases in BM-MSCs, a feature found specifically from exosome treatment and not observed when using sTGF-β1. Such factors, which include the collagenases MMP-1 and MMP-13 and the stromelysin MMP-3, have well documented roles in disease progression and can in particular aid cell penetration through the extracellular matrices, supporting invasion and metastasis in several types of cancer (Ala-aho *et al.* 2005). Notably a recent study highlighted BM-derived myofibroblasts found at the primary tumour site in a skin cancer model as the principal source of MMP-13 *in situ* (Lecomte *et al.* 2012) and that this MMP was required for subsequent invasive behaviour (Lecomte *et al.* 2012; Zigrino *et al.* 2009). Furthermore, a recent study has demonstrated that down-regulation of MMP-3 in cancer associated fibroblasts subsequently attenuated PCa cell invasion (Slavin *et al.* 2014). Other transcripts modulated by exosomes were ITGB6 and ITGB8 encoding for components of the integrin αvβ6 and αvβ8, respectively, which are implicated in the conversion of latent-TGFβ to bioactive TGF-β in several systems (Minagawa *et al.* 2014; Aluwihare *et al.* 2009). The importance of these exosome mediated changes in BM-MSCs for TFG-β1 activation and adhesive functions has not yet been investigated but is an area of interest for future investigation. The outcome of my experiments indicates that the onset of αSMA stress fibres in stromal cells are not directly coupled to their tumour modulating function and therefore a better alternative indicator of stromal functionality may be the secretion of certain factors including MMPs, VEGF and HGF. However, we don't know yet if the exosome differentiated BM-MSCs enhanced secretion of MMPs is relevant to the heightened invasion that is observed. One way to investigate this would be to inhibit specific MMPs such as MMP-1, MMP-3 and MMP-13 using blocking antibodies or generating specific MMP deficient cell model using siRNA targets of MMPs (Jiang *et al.* 2005; Gencer *et al.* 2011; Hayami *et al.* 2008). This will allow us to examine the function of the secreted factors from the stromal cell. One should be aware that exosomes themselves may also contain matrix remodelling molecules which may also

be responsible for the invasion property of the cancer cells. Exosomes from melanoma cells carry the active form of MMP-14 which was able to activate latent MMP-2 and degrade collagen type I and gelatin, suggesting exosomal MMP-14 was functionally active (Hakulinen *et al.* 2008). Lastly, exosomes from the differentiated BM-MSCs may also contribute the breakdown of the matrix and so the role exosomes play in the invasive property of PC is worth investigating in the future.

The spheroid models revealed the tumour size to decline gradually as the inner core became necrotic. Other studies have also reported a reduction in tumour growth in spheroid models (Folkman *et al.* 1973) and this was due to the degradation of cells within the inner core. However, it was noted that the presence of exosomes and BM-MSCs maintains the spheroid growth over time, perhaps by enhancing tumour cell proliferation. Additionally, exosome-deficient tumours with BM-MSCs also maintains tumour growth, but to a much lesser extent. Since the knock down of Rab27a reduces exosome secretion and hence an attenuation of exosome generated myofibroblasts from BM-MSCs, tumour growth was expected to be attenuated *in vivo*, similar to previous observations using fibroblasts (Webber *et al.* 2014). However, there was no significant difference in tumour size in the presence of BM-MSCs along with exosome proficient or exosome-deficient tumour cells after 28 day period. This may have been due to the poor stability of the ribozyme method used for silencing Rab27a in DU145 cells for the *in vivo* assessment of tumour growth and hence the tumour cells were not truly exosome-deficient. Knock down of Rab27a using lentiviral would have been a more stable method and thus a better model for evaluation of exosome-dependence on tumour growth *in vivo*. Since BM-MSCs take longer to differentiate into tumour promoting myofibroblasts in comparison to fibroblasts, which take only 3 days (Webber *et al.* 2014), the use of pre-differentiated BM-MSCs injected along with tumour cells may be a better approach to observe an earlier response and to ensure BM-MSCs had time to differentiate. Nevertheless, the collective functional data, such as the pro-invasive and pro-angiogenic properties of the differentiated BM-MSCs correlate well with the phenotypic alterations induced by exosome stimulation. These changes emphasise the profound role of MSCs with tumour cells in driving distinct aspects of disease

progression, and that a functional cancer exosome secretion pathway is essential for this influence.

In conclusion my study identifies PCa exosomes as potent factors for controlling the phenotypic and functional differentiation of BM-MSCs towards pro-angiogenic and pro-invasive myofibroblasts. The phenotype is similar to that reported for cancer associated stromal cells, with exosomes and not other soluble factors required to generate this dominant form of differentiation. Therefore molecular targeting of this cancer exosome driven process in a clinical setting is likely to attenuate tumour-manipulation of the local microenvironment, and slow disease progression.

9.1.2 Future Directions

Cancer exosomes have been demonstrated to be strong drivers of myofibroblastic differentiation and hence aid tumour to progress. Further understanding of the role of exosomes may provide avenues for inhibiting exosome secretion by the cell or lowering their effect, and thus slowing tumour progression.

Are the responses to cancer exosomes specific to a sub-population of BM-MSCs?

The nature of the BM-MSCs response to exosome stimulation in terms of the cell population has not been addressed, and it is currently unclear as to whether the response is homogenous or whether it is a sub-population of MSCs which differentiate into myofibroblasts that subsequently proliferate to take over the population. My studies have shown around 60-70% of MSCs exhibit αSMA positivity after around 2 weeks which is quite different from stimulating fibroblasts where almost ~100% of the cell population differentiate into αSMA positive myofibroblasts by 3 days (Webber *et al.* 2010). Such observations suggest a more heterogeneous response with BM-MSCs as a stromal cell source. The question may have *in vivo* relevance, as the infiltration of the cancer microenvironment by a few BM-MSCs may be sufficient to generate a growing population of myofibroblastic cells *in situ*. Addressing such questions will enable us to gain a greater insight into such exosome mediated changes in subpopulations of stem cells.

The in-depth mechanism of exosome induced myofibroblast differentiation

The full mechanism involved in the generation of myofibroblasts by cancer exosomes is still incomplete. Recent studies have demonstrated internalisation of exosomes by recipient cells in which the exosomes can incorporate components such as miRNA and mRNA into the recipient cells (Valadi *et al.* 2007; Batagov and Kurochkin 2013). Among these molecules found in exosomes, miRNAs have attracted most attention, due to their regulatory roles in gene expression. However, there are limitations to the current functional studies with exosome associated miRNAs. Firstly, there are numerous methods for isolating exosomes, which can result in slight variation in exosomal content, including proteins and miRNAs (Rekker *et al.* 2014; Tauro *et al.* 2012; Taylor *et al.* 2011). The variability of miRNAs may regulate different signalling pathways, resulting in different result outcomes on recipient cells. This makes it challenging to fully understand the functions of exosomal miRNAs. Secondly, some studies use RNAse to examine the function of miRNA, but one should remember that exosomes can prevent RNAse from damaging miRNA held within the vesicle (Koga *et al.* 2011). Hence in these studies, researchers may not be examining exosome-associated miRNA, but instead are examining the effects of free miRNAs (extracellular soluble miRNAs). Hence the functional results from some studies may not be due to the exosomal associated miRNAs.

Identifying miRNAs highly abundant in cancer exosomes and utilising knock down experiments of candidate genes may identify those involved in generating tumour-associated myofibroblastic phenotype. In collaboration with an Australian group, our group profiled the miRNAs in DU145 cell derived exosomes, revealing some highly abundant miRNA with *in silico* predicted association with the TGF-β signalling pathways. Theoretically, this would implicate miRNA delivery by exosomes as relevant. However, following treatment of fibroblasts with exosomes, qPCR primers against miRNAs showed no changes in these exosomally carried miRNA species, or indeed any changes in several of the top-predicted miRNA targets. Nevertheless differentiation into myofibroblasts still occurred (unpublished data, personal communication by Dr Aled Clayton). Thus exosomal miRNA are probably not incorporated into the recipient stromal cells machinery for controlling mRNA translation or the miRNAs may be degraded rapidly by

the cells. Therefore, the exosome-induced myofibroblastic differentiation seems to be RNA independent but the data however, requires further investigation. Lastly, a recent study obtained exosomes from different sources (including the plasma, seminal fluid, dendritic cells, mast cells and ovarian cancer cells) and quantified exosomes using the Nanosight Tracking Analysis and the number of miRNA molecules in the exosome preparations using qPCR, revealing that on average, exosomes do not contain enough miRNAs to have a functional effect (Chevillet *et al.* 2014). Taken together, this leads us to question the emphasis made in the exosome field on miRNA. There is a possibility that exosomes do not exert functions via miRNAs and the functional outcomes observed in some studies may be due to free miRNAs and not ones associated with exosomes.

Cancer exosome-mediated recruitment of cells

Several studies have revealed the migration of BM-MSCs into various tumour sites (Quante *et al.* 2011; Shinagawa *et al.* 2010; Jung *et al.* 2013). However, the recruitment signals involved are poorly understood. In a recent study, mouse-derived bone marrow macrophages secreted heightened levels of chemokines following treatment with exosomes from *M. tuberculosis*-infected macrophage, whereas the uninfected macrophages secreted low levels of chemokines. The resultant *M. tuberculosis*-infected macrophages possessed the capacity to induce cellular recruitment of immune cells such as myeloid cells, neutrophils, macrophages and splenocytes both *in vitro* and *in vivo* (Singh *et al.* 2012). Thus exosomes can direct the recruitment of cells. Whether or not PCa cells can also generate pro-recruiting exosomes is an open question of considerable interest. Additionally, melanoma derived exosomes have been documented to play a role in long-distance communication to the bone and mobilise BM-progenitor cells into the blood, to influence disease progression. This mobilisation is speculated to be driven by the exosomal transfer of MET receptor as noted by elevated levels of MET receptors on circulating BM progenitor cells in patients with advanced melanoma. Furthermore, in a murine model, the knock down of MET levels in exosomes using shRNA lowered the metastasis capacity of the BM progenitor cells. Additionally, the inhibition of exosome secretion by knockdown of Rab27a attenuated metastasis (Peinado *et al.* 2012). Therefore mobilisation of BM progenitor cells are exosomal MET-dependent. Whether PCa exosomes are capable recruiting BM-MSCs to the prostate in a similar fashion, is in

an area of great interest for future investigation, and if so, when along this mobilisation route, do BM-MSCs differentiate into myofibroblasts is an open question of considerable interest.

Function of exosomes produced by exosome differentiated MSCs

The function of exosomes released from cancer-associated myofibroblasts have not been investigated thoroughly. A recent study demonstrated Wnt11 tethered to CD81 positive exosomes from myofibroblasts to be internalised by breast cancer cells, which in turn promoted breast cancer cell motility and metastasis *in vivo* (Luga *et al.* 2012; Hoffman *et al.* 2013). The Wnt 11 ligand was associated with the enhanced motility and metastasis of breast cancer cells by signalling through the Frizzled (Fzd) receptors, indicating that exosomes from myofibroblasts allow cross-talks between the stromal and cancer cells to promote metastasis. Furthermore, a recent study reported exosomes from MSCs to increase VEGF expression in tumour cells, resulting in enhanced angiogenesis which promoted tumour growth *in vivo* (Zhu *et al.* 2012). However, the function of exosomes from BM-MSCs differed depending on the phenotype of the BM-MSCs. For example, exosomes released by BM-MSCs from multiple melanoma patients had higher levels of oncogenic proteins, cytokines and adhesion molecules in comparison to exosomes from BM-MSCs of healthy individuals (Roccaro *et al.* 2013). Furthermore, in a xenograft model, the exosomes from BM-MSCs of multiple melanoma patients promoted disease progression whereas exosomes from BM-MSCs of healthy individuals inhibited tumour growth *in vivo* (Roccaro *et al.* 2013). This indicates that exosomes from stromal cells such as BM-MSCs under disease conditions can be tumour-promoting. Similar observations were reported by other researchers (Bruno *et al.* 2013). In a similar manner, exosomes released from PCa exosomes-differentiated BM-MSCs may also promote tumour growth. Since BM-MSCs in general are immunosuppressive (Ringden *et al*. 2006; Figueroa *et al.* 2012) their secreted exosome may also exhibit an immunosuppressive property which may in turn help cancer cells evade the immune surveillance. Investigating the role of exosomes from PCa exosomes-differentiated BM-MSCs will further our knowledge in the function of exosome generated myofibroblasts in tumour progression.

Targeting exosomes as a therapeutic approach

Since my data emphasises the disease promoting nature of cancer exosomes, targeting exosomes as a new therapeutic approach may help slow down tumour progression. A negative feedback system has been revealed for regulating exosome release by the cells, in which the exosomes secreted by normal mammary epithelial cells into the extracellular space inhibits any further release of exosomes from the cells (Riches *et al.* 2014). The same negative feedback is observed between breast cancer cells and their exosomes. Furthermore, when exosomes from normal epithelial cells were added to breast cancer cells, there was a marked inhibition in exosome release. The level of exosome secretion was actually much lower than that of the untreated normal epithelial cells used as a control (Riches *et al.* 2014). Fluorescently labelled normal epithelial cell derived exosomes were internalised into the tumour cells, suggesting a dynamic equilibrium and thus implicating a mechanism for negative feedback control. This approach of adding exosomes from healthy cells to cancer cells may be applicable in controlling exosome release by prostate cancer cells.

Exosomes have been identified to aid cellular chemoresistance by exporting drugs out from the cells, attenuating the beneficial effect of chemotherapy. Instead drugs which interfere with the stability of the cytoskeletal components involved in directing the exocytosis pathway such as taxanes and vinca alkaloids, may be able to inhibit the secretion of exosomal vesicles and hence hindering chemoresistance of the cells (Iero *et al*. 2008). Furthermore, methods involved in altering the exosome composition that are tumour promoting may also be a good approach to lower the detrimental effect of exosomes. One such example, is the dietary component, curcumin which was found to reduce the immunosuppressive activities of breast cancer exosomes against NKs cells. Curcumin was speculated to alter the cargo sorting of exosomes during their biogenesis into MVBs (Zhang *et al.* 2007). Thus there are numerous pharmacological approaches open for further investigation for blocking the tumour promoting effects of exosomes.

The use of blood filtration is an attractive strategy which could be used to remove exosomes from circulation. An adaptive dialysis-like affinity platform technology (ADAPT^{TM}) has been developed by Aethlon Medical (Aethlon Medical Inc, San Diego,

USA) which can separate particles based on their size and phenotype. This device is composed of an outer compartment containing immobilised affinity agents and the compartment integrates with a standard renal dialysis machine. As the patient's blood is passed through the dialysis, only particles less than 200nm will pass through the porous fibres to the outer compartment and interact with the immobilised affinity agents to which exosomes can be selectively attached to. White blood cells and non-bound serum components, on the other hand, will carry on passing through the dialysis and so the blood is free from selected exosomes (reviewed by Marleau *et al.* 2012). This strategy can therefore be used to capture tumour-derived exosomes. For example in HER2 positive breast cancer, anti-HER2 antibodies in combination with antibodies against exosome associated proteins may enable the entrapment of breast cancer exosomes. In a similar manner, this ADAPT^{TM} machine should be able to isolate PCa exosomes from the patient's blood. The safety and efficacy of this ADAPT^{TM} machine for exosome removal, however, has yet to be clinically tested. Taken together, recent reports highlights some therapeutic approaches which may control the deleterious effects of tumour exosomes.

Concluding Remarks

My studies show for the first time, that prostate cancer exosomes educate BM-MSCs into tumour-promoting cells. This emphasises along with literature that cancer exosomes are an essential factor for generating a tumour promoting microenvironment and thus targeting exosomes is likely to be a valuable therapeutic approach for attenuating tumour progression.

Bibliography

Aase, K., Ernkvist, M., Ebarasi, L., Jakobsson, L., Majumdar, A., Yi, C., Birot, O. *et al.* 2007. Angiomotin regulates endothelial cell migration during embryonic angiogenesis. *Genes Development.* **21** (16): 2055-2068.

Abe, R., Donnelly, S., Peng, T., Bucala, R and Metz, C. 2001. Peripheral blood fibrocytes: differentiation pathway and migration to wound sites. *Journal of immunology* **166** (12)**:**7556-7562.

Abusamra, A., Zhong, Z., Zheng, X., Li, M., Ichim, T., Chin, J. and Min, W. 2005. Tumor exosomes expressing Fas ligand mediate CD8(+) T-cell apoptosis. *Blood Cells, Molecules and Diseases* **35** (2)**:**169-173.

Abusamra, A., Zhong, Z., Zheng, X., Li, M., Ichim, T., Chin, J., Min, W., 2005. Tumor exosomes expressing Fas ligand mediate CD8(+) T-cell apoptosis. *Blood Cells, Molecules and Diseaases* **35** (2):169-173.

Admyre, C., Grunewald, J., Thyberg, J., Gripenbäck, S., Tornling, G., Eklund, A., Scheynius, A and Gabrielsson, S. 2003. Exosomes with major histocompatibility complex class II and co-stimulatory molecules are present in human BAL fluid. *The European Respiratory Journal* **22** (4):578-583.

Aggarwal, S and Pittenger, M. 2005. Human mesenchymal stem cells modulate allogeneic immune cell responses. . *Blood* **105** (4)**:**1815-1822.

Ala-aho, R and Kähäri, VM. 2005. Collagenases in cancer. *Biochimie* **87** (3-4)**:**273-286.

Alimirah, F., Chen, J., Basrawala, Z., Xin, H.and Choubey, D. 2006. DU-145 and PC-3 human prostate cancer cell lines express androgen receptor: implications for the androgen receptor functions and regulation. *FEBS Letters*. **580** (9): 2294-2300.

Alimperti, S., You, H., George, T., Agarwal, S and Andreadis, S. 2014. Cadherin-11 regulates both mesenchymal stem cell differentiation into smooth muscle cells and the development of contractile function in vivo. *Journal of Cell Science* **127** (12)**:**2627-2638.

Al-Nedawi, K., Meehan, B., Kerbel, R.S., Allison, A.C., Rak, J. 2009. Endothelial expression of autocrine VEGF upon the uptake of tumor-derived microvesicles containing oncogenic EGFR. *Proceedings of the National Acedamy of Sciences of the USA* **106** (10):3794-3799.

Alt, E., Yan, Y., Gehmert, S., Song, Y., Altman,, A. Gehmert, S., Vykoukal, D *et al.* 2011. Fibroblasts share mesenchymal phenotypes with stem cells, but lack their differentiation and colony-forming potential. *Biology of the cell* **103** (4)**:**197-208.

Altekruse SF., Kosary, CL., Krapcho, M et al. 2010. SEER Cancer Statistics Review 1975-2007. *National Cancer Institute*.

Aluwihare, P., Mu, Z., Zhao, Z., Yu, D., Weinreb, P. H., Horan, G. S., Violette, S. M. *et al.* 2009. Mice that lack activity of αvβ6- and αvβ8-integrins reproduce the abnormalities of Tgfb1- and Tgfb3-null mice. *Journal of Cell Science* **122** (2)**:**227-232.

Andre, F., Schartz, NE., Movassagh, M., Flament, C., Pautier, P., Morice, P., Pomel, C. *et al.* 2002. Malignant effusions and immunogenic tumour-derived exosomes. *Lancet* **360** (9829)**:**295-305.

Andreola, G., Rivoltini, L., Castelli, C., Huber, V., Perego, P., Deho, P., Squarcina, P., Accornero, P., Lozupone, F., Lugini, L., Stringaro, A., Molinari, A., Arancia, G., Gentile, M., Parmiani, G., Fais, S. 2002. Induction of Lymphocyte Apoptosis by Tumor Cell Secretion of FasL-bearing Microvesicles. *The Journal of Experimental Medicine* **195** (10): 1303-1316.

Annes, J., Munger, J and Rifkin, D. 2003. Making sense of latent TGFbeta activation. *Journal of Cell Science* **116** (2)**:**217-224.

Antsiferova, M and Werner, S. 2012. The bright and the dark sides of activin in wound healing and cancer. *Journal of Cell Science.* **125** (17)**:**3929-3937.

Aroua, S., Maugars, G., Jeng, S., Chang, C., Weltzien, F., Rousseau, K and Dufour, S. 2012. Pituitary gonadotropins FSH and LH are oppositely regulated by the activin/follistatin system in a basal teleost, the eel. *General and Comparative Endocrinology.* **175** (1)**:**82-91.

Arsham, A., Plas, D., Thompson, C. a. and Simon, M. 2002. Phosphatidylinositol 3-kinase/Akt signaling is neither required for hypoxic stabilization of HIF-1 alpha nor sufficient for HIF-1-dependent target gene transcription. *J Biol Chem.* **277** (17)**:**15162-15170.

Aubin, J. 2001. Regulation of osteoblast formation and function. *Reviews in endocrine and metabolic disorders* **2** (1)**:**81-94.

Augello, A., Tasso, R., Negrini, S., Amateis, A., Indiveri, F., Cancedda, R and Pennesi, G. 2005. Bone marrow mesenchymal progenitor cells inhibit lymphocyte proliferation by activation of the programmed death 1 pathway. *European journal of immunology* **35** (5)**:**1482-1490.

Azab, S., Osama, A and Rafaat, M. 2012. Does normalizing PSA after successful treatment of chronic prostatitis with high PSA value exclude prostatic biopsy? *Translational Andrology and Urology* **3** (1)**:**148-152.

Azoulay, L., Yin, H., Benayoun, S., Renoux, C., Boivin, J and Suissa, S. 2011. Androgen-Deprivation Therapy and the Risk of Stroke in Patients With Prostate Cancer. *European Urology.* **60** (6)**:**1244-1250.

Babst, M. 2011. MVB vesicle formation: ESCRT-dependent, ESCRT-independent and everything in between. *Current Opinion in Cell Biology* **23** (4): 452-457.

Babst, M., Katzmann, D., Snyder, W., Wendland, B and Emr, S. 2002. Endosome-associated complex, ESCRT-II, recruits transport machinery for protein sorting at the multivesicular body. *Developmental Cell* **3** (2): 283-289.

Bahl, A., Oudard, S., Tombal, B., Ozgüroglu, M., Hansen, S., Kocak, I., Gravis, G. *et al.* 2013. Impact of cabazitaxel on 2-year survival and palliation of tumour-related pain in men with metastatic castration-resistant prostate cancer treated in the TROPIC trial. *Annals of Oncology* **24** (9)**:**2402-2408.

Baietti, M., Zhang, Z., Mortier E, Melchior, A., Degeest, G., Geeraerts, A., Ivarsson, Y., Depoortere, F., Coomans, C., Vermeiren, E., Zimmermann, P and David, G. 2012. Syndecan-syntenin-ALIX regulates the biogenesis of exosomes. *Nature Cell Biology* **14** (7): 677-685.

Baker, M., Robinson, S., Lechertier, T., Barber, P., Tavora, B., D'Amico, G., Jones, D. *et al.* 2011. Use of the mouse aortic ring assay to study angiogenesis. *Nature Protocols* **7** (1)**:**89-104.

Bargão Santos, P and Patel, HR. 2014. Prostate stem cell antigen - novel biomarker and therapeutic target? *Expert Rev Anticancer Therapy.* **14** (1)**:**5-7.

Barnes, S. 2001. Role of phytochemicals in prevention and treatment of prostate cancer. *Epidemiology Reviews* **23** (1)**:**102-105.

Barrett-Lee, P., Travers, M., Luqmani, Y and Coombes, R. 1990. Transcripts for transforming growth factors in human breast cancer: clinical correlates. *British Journal of Cancer* **61** (4)**:**612-617.

Barry, F., Boynton, R., Haynesworth, S., Murphy, JM and Zaia, J. 1999. The monoclonal antibody SH-2, raised against human mesenchymal stem cells, recognizes an epitope on endoglin (CD105). *Biochemical Biophysical Research Community.* **265** (1)**:**134-139.

Barry, F., Boynton, R., Liu, B and Murphy, J. 2001. Chondrogenic differentiation of mesenchymal stem cells from bone marrow: differentiation-dependent gene expression of matrix components. *Experimental Cell Research* **268** (12)**:**189-200.

Bartholomew, A., Sturgeon, C., Siatskas, M., Ferrer, K., McIntosh, K., Patil, S., Hardy, W. *et al.* 2002. Mesenchymal stem cells suppress lymphocyte proliferation in vitro and prolong skin graft survival in vivo. *Experimental Hematology* **30** (1)**:**42-48.

Batagov, A and Kurochkin, I. 2013. Exosomes secreted by human cells transport largely mRNA fragments that are enriched in the 3'-untranslated regions. *Biological Direct* **8** (12) doi: 10.1186/1745-6150-1188-1112.

Becker, J., Marcy, A., Rokosz, L., Axel, M., Burbaum, J., Fitzgerald, P., Cameron, P. *et al.* 1995. Stromelysin-1: three-dimensional structure of the inhibited catalytic domain and of the C-truncated proenzyme. *Protein Science* **4** (95)**:**1966-1976.

Bertuzzi, A., Fasano, A., Gandolfi, A and Sinisgalli, C. 2010. Necrotic core in EMT6/Ro tumour spheroids: Is it caused by an ATP deficit? *Journal of Theoretical Biology.* **262** (1)**:**142-150.

Bharathiraja, C., Sukirtha, R., Heifetz, Y., Achiraman, S., Krishnan, M. and and Kamalakkannan, S. 2014. Nanovesicles Mediated Tumor Tolerance in Dalton's Ascites Lymphoma Mice. *Stem Cell Research & Therapy* **4** (11).

Bieback, K., Kern, S., Klüter, H and Eichler, H. 2004. Critical parameters for the isolation of mesenchymal stem cells from umbilical cord blood. *Stem cells* **22** (4)**:**625-634.

Birmingham, E., Niebur, G., McHugh, P., Shaw, G., Barry, F and McNamara, L. 2012. Osteogenic differentiation of mesenchymal stem cells is regulated by osteocyte and osteoblast cells in a simplified bone niche. *European cells & materials*. **12** (13):13-27.

Blanchard, N., Lankar, D., Faure, F., Regnault, A., Dumont, C., Raposo, G., Hivroz, C. 2002. TCR Activation of Human T Cells Induces the Production of Exosomes Bearing the TCR/CD3/{zeta} Complex. *Journal of Immunology* **168** (7): 3235-3241.

Blott, E and Griffiths, G. 2002. Secretory lysosomes. *Nat Rev Mol Cell Biol.* **3** (2)**:**122-131.

Bobrie, A., Krumeich, S., Reyal, F., Recchi, C., Moita, L. F., Seabra, M. C., Ostrowski, M. *et al.* 2012. Rab27a Supports Exosome-Dependent and -Independent Mechanisms That Modify the Tumor Microenvironment and Can Promote Tumor Progression. *Cancer Research* **72** (19)**:**4920-4930.

Böing, A., van der Pol, E., Grootemaat, A., Coumans, F., Sturk, A and Nieuwland, R. 2014. Single-step isolation of extracellular vesicles by size-exclusion chromatography. *Journal of Extracellular Vesicles* doi: 10.3402/jev.v3403.23430.

Boire, A., Covic, L., Agarwal, A., Jacques, S., Sherifi, S and Kuliopulos, A. 2005. PAR1 is a matrix metalloprotease-1 receptor that promotes invasion and tumorigenesis of breast cancer cells. *Cell* **120** (3)**:**303-313.

Booth, AM., Fang, Y., Fallon, JK., Yang, JM., Hildreth, JEK., Gould, S.J. 2006. Exosomes and HIV Gag bud from endosome-like domains of the T cell plasma membrane. *Journal of Cell Biology* **172** (6): 923-935.

Bouïs, D., Kusumanto, Y., Meijer, C., Mulder, N and Hospers, G. 2006. A review on pro- and anti-angiogenic factors as targets of clinical intervention. *Pharmacological research* **53** (2)**:**89-103.

Brayman, M., Thathiah, A and Carson, D. 2004. MUC1: a multifunctional cell surface component of reproductive tissue epithelia. *Reprod Biol Endocrinol.* **2** (4).

Bretton, P. 1994. Prostate-specific antigen and digital rectal examination in screening for prostate cancer: a community-based study. . *South Med J.* **87** (7)**:**720.

Brimble, S., Sherrer, E., Uhl, E., Wang, E., Kelly, S., Merrill, A., Robins, A *et al.* 2007. The cell surface glycosphingolipids SSEA-3 and SSEA-4 are not essential for human ESC pluripotency. *Stem Cells.* **25** (1)**:**54-62.

Bruder, S., Jaiswal, N and Haynesworth, S. 1997. Growth kinetics, self-renewal, and the osteogenic potential of purified human mesenchymal stem cells during extensive subcultivation and following cryopreservation. *J Cell Biochem.* **64** (2)**:**278-294.

Bruno, S., Collino, F., Deregibus, M., Grange, C., Tetta, C and Camussi, G., 2013. Microvesicles derived from human bone marrow mesenchymal stem cells inhibit tumor growth. *Stem Cells and Development* **22** (5):758-771.

Bunker, C., Patrick, A., Konety, B., Dhir, R., Brufsky, A., Vivas, C., Becich, M. *et al.* 2002. High prevalence of screening-detected prostate cancer among Afro-Caribbeans: the Tobago Prostate Cancer Survey. *Cancer Epidemiology, Biomarkers & Prevention* **11** (8)**:**726-729.

Burridge, K and Chrzanowska-Wodnicka, M. 1996. Focal adhesions, contractility, and signaling. *Annual review of cell and developmental biology* **12:**463-518.

Caby, M., Lankar, D., Vincendeau-Scherrer, C., Raposo, G and Bonnerot, C. 2005. Exosomal-like vesicles are present in human blood plasma. *Int Immunol.* **17** (7)**:**879-887.

Cai, Z., Zhang, W., Yang, F., Yu, L., Yu, Z., Pan, J., Wang, L. *et al.* 2012. Immunosuppressive exosomes from TGF-β1 gene-modified dendritic cells attenuate Th17-mediated inflammatory autoimmune disease by inducing regulatory T cells. *Cell Research* **22** (3)**:**607-610.

Cannon, L. B., DT. Skolnick, M., et al. 1982. Genetic epidemiology of prostate cancer in the Utah Mormon genealogy. *Cancer Survey* **1** (2)**:**47-69.

Carroll, P. Coley, C., McLeod, D. Schellhammer, P. Sweat, G. Wasson, J. Zietman, A. Thompson, I. 2001. Prostate-specific antigen best practice policy--part I: early detection and diagnosis of prostate cancer. *Urology* **57** (2)**:**217-224.

Carter, B., Beaty, T., Steinberg, G., Childs, B and Walsh, P. 1992. Mendelian inheritance of familial prostate cancer. *Proceedings of the National Academy of Sciences* **89** (8)**:**3367-3371.

Cat, B., Stuhlmann, D., Steinbrenner, H., Alili, L., Holtkötter, O., Sies and Brenneisen, P. 2006. Enhancement of tumor invasion depends on transdifferentiation of skin fibroblasts mediated by reactive oxygen species. *Journal of cell science* **119** (13)**:**2727-2738.

Catalona, W. R., JP. Ahmann, FR. Hudson, MA. Scardino, PT. Flanigan, RC. De Kernion, JB. Ratliff, TL. Kavoussi, LR and Dalkin, BL. 1994. Comparison of digital rectal examination and serum prostate specific antigen in the early detection of prostate cancer: results of a multicenter clinical trial of 6,630 men. *Journal of Urology.* **151** (5)**:**1283-1290.

Catalona, W. S., DS. Ratliff, TL. Dodds, KM. Coplen, DE. Yuan, JJ. Petros, JA and Andriole GL. 1991. Measurement of prostate-specific antigen in serum as a screening test for prostate cancer. . *New England Journal of Medicine.* **324** (17)**:**1156-1561.

Cavarretta, I., Altanerova, V., Matuskova, M., Kucerova, L., Culig, Z and Altaner, C. 2010. Adipose tissue-derived mesenchymal stem cells expressing prodrug-converting enzyme inhibit human prostate tumor growth. *Molecular Therapy.* **18** (1)**:**223-231.

Chen, A., D'Amico, A., Neville, B and Earle, C. 2006. Patient and treatment factors associated with complications after prostate brachytherapy. *Journal of clinical oncology* **24** (3)**:**5298-5304.

Chen, S., Fang, W., Ye, F., Liu, Y., Qian, J., Shan, S., Zhang, J. *et al.* 2004. Effect on left ventricular function of intracoronary transplantation of autologous bone marrow mesenchymal stem cell in patients with acute myocardial infarction. *American journal of cardiology* **94** (1)**:**92-95.

Chen, W., Liu, X., Lv, M., Chen, L., Zhao, J., Zhong, S., Ji, M. *et al.* 2014. Exosomes from drug-resistant breast cancer cells transmit chemoresistance by a horizontal transfer of microRNAs. *PLoS One* **9** (4)**:** doi: 10.1371/journal.pone.0095240.

Chevillet, J., Kang, Q., Ruf, I., Briggs, H., Vojtech, L., Hughes, S., Cheng, H., Arroyo, J., Meredith, E., Gallichotte, E., Pogosova-Agadjanyan, E., Morrissey, C., Stirewalt, D., Hladik, F., Yu, E., Higano, C and Tewari, M., 2014. Quantitative and stoichiometric analysis of the microRNA content of exosomes. *Proceedings of the National Academy of Sciences of USA* **111** (41):14888-14893.

Chim, S., Qin, A., Tickner, J., Pavlos, N., Davey, T., Wang, H., Guo, Y. *et al.* 2011. EGFL6 promotes endothelial cell migration and angiogenesis through the activation of extracellular signal-regulated kinase. *The Journal of Biological Chemistry* **286** (25)**:**22035-22046.

Cho, H., Hyun, J., Kim, J., Jeong, H., Park, H., You, D.and Jung, H. 2013. Measurement of ice thickness on vitreous ice embedded cryo-EM grids: investigation of optimizing condition for visualizing macromolecules. *Journal of Analytical Science and Technology.* **4** (7)

Cho, J. A., Park, H., Lim, E. H and Lee, K. W. 2012. Exosomes from breast cancer cells can convert adipose tissue derived mesenchymal stem cells into myofibroblast-like cells. *International Journal of Oncology* **40** (1)**:**130-138.

Cho, J., Park, H., Lim, E., Kim, K., Choi, J., Lee, J., Shin, J and Lee, K., 2011. Exosomes from ovarian cancer cells induce adipose tissue-derived mesenchymal stem cells to acquire the physical and functional characteristics of tumor-supporting myofibroblasts. *Gynecology Oncology* **123** (2):379-386.

Choi, D., Lee, J., Park, G., Lim, H., Bang, J., Kim, Y., Kwon, K., Kwon, H., Kim, K and Gho, Y. 2007. Proteomic analysis of microvesicles derived from human colorectal cancer cells. *Journal of Proteome Research* **6** (12): 4646-4655.

Choy, L and Derynck, R. 2003. Transforming growth factor-beta inhibits adipocyte differentiation by Smad3 interacting with CCAAT/enhancer-binding protein (C/EBP) and repressing C/EBP transactivation function. *The Journal of Biological Chemistry* **278** (11).

Chrzanowska-Wodnicka, M., Kraus, A., Gale, D., White, G and Vansluys, J. 2008. Defective angiogenesis, endothelial migration, proliferation, and MAPK signaling in Rap1b-deficient mice. *Blood* **111** (5)**:**2647-2656.

Cimitan, M., Evangelista, L., Hodolič, M., Mariani, G., Baseric, T., Bodanza, V., Saladini, G. *et al.* 2015. Gleason Score at Diagnosis Predicts the Rate of Detection of 18F-Choline PET/CT Performed When Biochemical Evidence Indicates Recurrence of Prostate Cancer: Experience with 1,000 Patients. *Journal of Nuclear Medicine* **56** (2)**:**209-215.

Clarke, M., Imhoff, F and Baird, S. 2014. Mesenchymal Stem Cells Inhibit Breast Cancer Cell Migration and Invasion Through Secretion of Tissue Inhibitor of Metalloproteinase-1 and -2. *Molecular Carcinogenesis* doi: 10.1002/mc.22178.

Clayton, A., Court, J., Navabi, H., Adams, M., Mason, M. D., Hobot, J. A., Newman, G. R. *et al.* 2001. Analysis of antigen presenting cell derived exosomes, based on immuno-magnetic isolation and flow cytometry. *Journal of Immunological Methods* **247** (1-2)**:**163-174.

Clayton, A., Mitchell, J. P., Court, J., Mason, M. D. and Tabi, Z. 2007. Human tumor-derived exosomes selectively impair lymphocyte responses to interleukin-2. *Cancer Res* **67** (15)**:**7458-7466.

Coffey, R., Kost, L., Lyons, R., Moses, H and LaRusso, N. 1987. Hepatic processing of transforming growth factor beta in the rat. Uptake, metabolism, and biliary excretion. *Journal of Clinical Investigation.* **80** (3)**:**750–757.

Coffey, R., Shipley, G. and and Moses, H. 1986. Production of Transforming Growth Factors by Human Colon Cancer Lines1. *Cancer Research* **46:**1916-1930.

Collins, R., Trowman, R., Norman, G., Light, K., Birtle, A., Fenwick, E., Palmer, S. *et al.* 2006. A systematic review of the effectiveness of docetaxel and mitoxantrone for the treatment of metastatic hormone-refractory prostate cancer. *British Journal of Cancer* **95** (4)**:**457-462.

Colloca, G., Venturino, A and Checcaglini, F. 2010. Patient-reported outcomes after cytotoxic chemotherapy in metastatic castration-resistant prostate cancer: a systematic review. *Cabcer Treatment Reviews* **36** (6)**:**501-506.

Colombo, M., Moita, C., van Niel, G., Kowal, J., Vigneron, J., Benaroch, P., Manel, N., Moita, L., Théry, C and Raposo, G., 2013. Analysis of ESCRT functions in exosome biogenesis, composition and secretion highlights the heterogeneity of extracellular vesicles. *Journal of cell science* **126** (24): 5553-6555.

Craig, W., Kay, R., Cutler, R and Lansdorp, P. 1993. Expression of Thy-1 on human hematopoietic progenitor cells. *Journal of Experimental Medicine.* **1777** (3)**:**1331-1342.

Culhane, A and Quackenbush, J. 2009. Confounding effects in "A six-gene signature predicting breast cancer lung metastasis". *Cancer Research.* **69** (18)**:**7480-7485.

Daja, M., Niu, X., Zhao, Z., Brown, J. and Russell, P. 2003. Characterization of expression of matrix metalloproteinases and tissue inhibitors of metalloproteinases in prostate cancer cell lines. *Prostate Cancer Prostatic Disease.* **6** (1) **:**15-26.

Darby, I., Skalli, O and Gabbiani, G. 1990. Alpha-smooth muscle actin is transiently expressed by myofibroblasts during experimental wound healing. *Labouratory Investigation; a journal of technical methods and pathology* **63** (1)**:**21-29.

Darby, JA., Laverdet, B., Bonte, R and Desmoliére, A. 2014. *Clinical, Cosmetics and Investigational Dermatology* **7:**301–311.

Davis, G and Senger, D. 2005. Endothelial extracellular matrix: biosynthesis, remodeling, and functions during vascular morphogenesis and neovessel stabilization. *Circulation Research* **97** (11)**:**1093-1107.

De Crescenzo, G., Pham, P., Durocher, Y and O'Connor-McCourt, M. 2003. Transforming growth factor-beta (TGF-beta) binding to the extracellular domain of the type II TGF-beta receptor: receptor capture on a biosensor surface using a new coiled-coil capture system demonstrates that avidity contributes significantly to high affinity binding. *Journal of Molecular Medicine* **328** (5)**:**1173-1183.

De Monte, L., Reni, M., Tassi, E., Clavenna, D., Papa, I., Recalde, H., Braga, M., Di Carlo, V., Doglioni, C.a., Protti, M. 2011. Intratumor T helper type 2 cell infiltrate correlates with cancer-associated fibroblast thymic stromal lymphopoietin production and reduced survival in pancreatic cancer. *The Journal of Experimental Medicine* **208** (3): 469-478.

De Wever, O., Westbroek, W., Verloes, A., Bloemen, N., Bracke, M., Gespach, C., Bruyneel, E *et al.* 2004. Critical role of N-cadherin in myofibroblast invasion and migration in vitro stimulated by colon-cancer-cell-derived TGF-beta or wounding. *Journal of Cell Science* **117** (20)**:**4691-4703.

Denzer, K., Kleijmeer, M. J., Heijnen, H. F., Stoorvogel, W. and Geuze, H. J. 2000. Exosome: from internal vesicle of the multivesicular body to intercellular signaling device. *Journal of Cell Science* **113** (Pt 19):3365-3374.

Desmoulière, A., Geinoz, A., Gabbiani, F and Gabbiani, G. 1993. Transforming growth factor-beta 1 induces alpha-smooth muscle actin expression in granulation tissue myofibroblasts and in quiescent and growing cultured fibroblasts. *Journal of Cell Biology* **122** (1)**:**103-111.

Di Nicola, M., Carlo-Stella, C., Magni, M., Milanesi, M., Longoni, PD., Matteucci *et al.* 2002. Human bone marrow stromal cells suppress T-lymphocyte proliferation induced by cellular or nonspecific mitogenic stimuli. *Blood* **99** (10)**:**3838-3843.

Direkze, N., Forbes, S., Brittan, M., Hunt, T., Jeffery, R., Preston, S., Poulsom, R. *et al.* 2003. Multiple organ engraftment by bone-marrow-derived myofibroblasts and fibroblasts in bone-marrow-transplanted mice. *Stem cells* **21** (5)**:**514-520.

Direkze, N., Hodivala-Dilke, K., Jeffery, R., Hunt, T., Poulsom, R., Oukrif, D., Alison, M *et al.* 2004. Bone marrow contribution to tumor-associated myofibroblasts and fibroblasts. *Cancer Research* **64** (23)**:**8492-8495.

Djouad, F., Bony, C., Häupl, T., Uzé, G., Lahlou, N., Louis-Plence, P., Apparailly, F. *et al.* 2005. Transcriptional profiles discriminate bone marrow-derived and synovium-derived mesenchymal stem cells. *Arthritis Research & Therapy* **7** (6)**:**1304–1315.

Djouad, F., Plence, P., Bony, C., Tropel, P., Apparailly, F., Sany, J., Noël, D. *et al.* 2003. Immunosuppressive effect of mesenchymal stem cells favors tumor growth in allogeneic animals. *Blood* **102** (10)**:**3837-3844.

Dominici, M., Le Blanc, K., Mueller, I., Slaper-Cortenbach, I., Marini, F. C., Krause, D. S., Deans, R. J. *et al.* 2006. Minimal criteria for defining multipotent mesenchymal stromal cells. The International Society for Cellular Therapy position statement. *Cytotherapy* **8** (4)**:**315-317.

Dorsett, Y and Tuschl, T. 2004. siRNAs: applications in functional genomics and potential as therapeutics. *Nat Rev Drug Discov.* **3** (4)**:**318-329.

Doyle-Lindrud, S. (2012). Managing side effects of the novel taxane cabazitaxel in castrate-resistant prostate cancer. *Clinical journal of oncology nursing* **16** (3)**:**286-291.

Dugina, V., Fontao, L., Chaponnier, C., Vasiliev, J and Gabbiani, G. 2001. Focal adhesion features during myofibroblastic differentiation are controlled by intracellular and extracellular factors. *Journal of Cell Science* **114** (18)**:**3285-3296.

Dvorak, H. 1986. Tumors: wounds that do not heal. Similarities between tumor stroma generation and wound healing. *New England of Journal Medicine.* **315** (26)**:**1650-1659.

Eastham, J., Truong, L., Rogers, E., Kattan, M., Flanders, K., Scardino, P and Thompson, T. 1995. Transforming growth factor-beta 1: comparative immunohistochemical localization in human primary and metastatic prostate cancer. *Labouratory Investigation.* **73** (5)**:**628-635.

Eliceiri, B and Cheresh, D. 2001. Adhesion events in angiogenesis. *Current Opinion in Cell Biology* **13** (5):563-368.

Escola, J., Kleijmeer, M., Stoorvogel, W., Griffith, J., Yoshie, O and Geuze, H. 1998. Selective Enrichment of Tetraspan Proteins on the Internal Vesicles of Multivesicular Endosomes and on Exosomes Secreted by Human B-lymphocytes. *Journal of Biological Chemistry* **273** (32)**:**20121-20127.

Escrevente, C., Keller, S., Altevogt, P and Costa, J. 2011. Interaction and uptake of exosomes by ovarian cancer cells. *BMC Cancer.* **11:**108.

Escudero-Esparza, A., Jiang, W and Martin, T. 2012. Claudin-5 is involved in breast cancer cell motility through the N-WASP and ROCK signalling pathways. *Journal of Experimental and Clinical Cancer Research.* **31:**31-43.

Espagnolle, N., Guilloton, F., Deschaseaux, F., Gadelorge, M., Sensébé, L and Bourin, P. 2014. CD146 expression on mesenchymal stem cells is associated with their vascular smooth muscle commitment. *Journal of Cellular and Molecular Medicine.* **18** (1)**:**104-114.

Fader, C., Sánchez, D., Mestre, M and Colombo, M. 2009. TI-VAMP/VAMP7 and VAMP3/cellubrevin: two v-SNARE proteins involved in specific steps of the autophagy/multivesicular body pathways. *Biochimica Biophysica Acta.* **1793** (12)**:**1901-1916.

Fang, B., Song, Y., Liao, L., Han, Q and Zhao, R. 2006. Treatment of severe therapy-resistant acute graft-versus-host disease with human adipose tissue-derived mesenchymal stem cells. . *Bone Marrow Transplant* **38:**389-390.

Farshchian, M., Kivisaari, A., Ala-Aho, R., Riihilä, P., Kallajoki, M., Grénman, R., Peltonen, J. *et al.* 2011. Serpin peptidase inhibitor clade A member 1 (SerpinA1) is a novel biomarker for progression of cutaneous squamous cell carcinoma. *American Journal of Pathology* **179** (3)**:**1110-1119.

Feldon, SE., O'loughlin, CW., Ray, DM., Landskroner-Eiger, S., Seweryniak, KE and Phipps, RP. 2006. Activated human T lymphocytes express cyclooxygenase-2 and produce proadipogenic prostaglandins that drive human orbital fibroblast differentiation to adipocytes. *The American Journal of Pathology* **169** (4): 1183-1193.

Figueroa, F., Carrión, F., Villanueva, S and Khoury, M. 2012. Mesenchymal stem cell treatment for autoimmune diseases: a critical review. *Biological Research.* **45** (3)**:**269-277.

Folkman, J. and Hochberg, M. 1973. Self-regulation of growth in three dimensions. *Journal of Experimental Medicine.* **138** (4)**:**745-753.

Fortier, L and Smith, R. 2008. Regenerative medicine for tendinous and ligamentous injuries of sport horses. *Veterinary Clinical North Americal Equine Practice.* **24** (1)**:**191-201.

Fraser, J., Wulur, I., Alfonso, Z and Hedrick, M. 2006. Fat tissue: an underappreciated source of stem cells for biotechnology. *Trends Biotechnol.* **24** (4)**:**150-154.

Friedenstein, A., Gorskaja, J and Kulagina, N. 1976. Fibroblast precursors in normal and irradiated mouse hematopoietic organs. *Experimental Hematology.* **4** (5)**:**267-274.

Frühbeis, C., Fröhlich, D., Kuo, W., Amphornrat, J., Thilemann, S., Saab, A., Kirchhoff, F., Möbius, W., Goebbels, S., Nave, K., Schneider, A., Simons, M., Klugmann, M., Trotter, J and Krämer-Albers, E. 2013. Neurotransmitter-triggered transfer of exosomes mediates oligodendrocyte-neuron communication. *PLoS Biology* **11** (7): doi: 10.1371/journal.pbio.

Fu, X., Han, B., Cai, S., Lei, Y., Sun, T and Sheng, Z. 2009. Migration of bone marrow-derived mesenchymal stem cells induced by tumor necrosis factor-alpha and its possible role in wound healing. *Wound Repair Regen.* **17** (2)**:**185-191.

Fujita, R., Tamai, K., Aikawa, E., Nimura, K., Ishino, S., Kikuchi, Y and Kaneda, Y. 2015. Endogenous Mesenchymal Stromal Cells in Bone Marrow Are Required to Preserve Muscle Function in mdx Mice. *Stem Cells.* **33** (3)**:**962-975.

Fulton, D., Gratton, J., McCabe, T., Fontana, J., Fujio, Y., Walsh, K., Franke, T. *et al.* 1999. Regulation of endothelium-derived nitric oxide production by the protein kinase Akt. *Nature* **399** (6736)**:**597-601.

Gabbiani, G. 2003. The myofibroblast in wound healing and fibrocontractive diseases. *Journal of Pathology* **200** (4)**:**500-503.

Galie, M., Sorrentino, C., Montani, M., Micossi, L., Di Carlo, E., D'Antuono, T., Calderan, L. *et al.* 2005. Mammary carcinoma provides highly tumourigenic and invasive reactive stromal cells. *Carcinogenesis* **26** (11)**:**1868-1878.

Gang, E., Bosnakovski, D., Figueiredo, C., Visser, J and Perlingeiro, R. 2007. SSEA-4 identifies mesenchymal stem cells from bone marrow. *Blood* **109** (4)**:**1743-1751.

Gao, P., Ding, Q., Wu, Z., Jiang, H and Fang, Z. 2010. Therapeutic potential of human mesenchymal stem cells producing IL-12 in a mouse xenograft model of renal cell carcinoma. *Cancer Lett.* **290** (2)**:**157-166.

Gao, X., Pang, J., Si-tu, J., Luo, Y., Zhang, H., Li, L and Zhang, Y. 2013. Single-port transvesical laparoscopic radical prostatectomy for organ-confined prostate cancer: technique and outcomes. *BJU international* **112** (7)**:**944-952.

Gastpar, R., Gehrmann, M., Bausero, M., Asea, A., Gross, C., Schroeder, J. and Multhoff, G. 2005. Heat shock protein 70 surface-positive tumor exosomes stimulate migratory and cytolytic activity of natural killer cells. *Cancer Res* **65** (12)**:**5238-5247.

Gencer, S., Cebeci, A and Irmak-Yazicioglu, M. 2011. Silencing of the MMP-3 gene by siRNA transfection in gastric cancer AGS cells. Journal of Gastrointestinal Liver Diseases **20** (1):19-26.

Gerber, H., McMurtrey, A., Kowalski, J., Yan, M., Keyt, B., Dixit, V and Ferrara, N. 1998. Vascular endothelial growth factor regulates endothelial cell survival through the phosphatidylinositol 3'-kinase/Akt signal transduction pathway. Requirement for Flk-1/KDR activation. *Journal of Biological Chemistry.* **273** (46)**:**30336-30343.

Gerdes, M., Larsen, M., McBride, L., Dang, T., Lu, B and Rowley, D. 1998. Localization of transforming growth factor-beta1 and type II receptor in developing normal human prostate and carcinoma tissues. *The journal of histochemistry and cytochemistry* **46** (3)**:**379-388.

Gesierich, S., Berezovskiy, I., Ryschich, E., Zoller, M. 2006. Systemic induction of the angiogenesis switch by the tetraspanin D6.1A/CO-029. *Cancer Research* **66** (14): 7083-7094.

Giannoni, E., Bianchini, F., Masieri, L., Serni, S., Torre, E., Calorini, L and Chiarugi, P. 2010. Reciprocal activation of prostate cancer cells and cancer-associated fibroblasts stimulates epithelial-mesenchymal transition and cancer stemness. *Cancer Research* **70** (17)**:**6945-6956.

Gingis-Velitski, S., Zetser, A., Kaplan, V., Ben-Zaken, O., Cohen, E., Levy-Adam, F., Bashenko, Y., Flugelman, M., Vlodavsky, I and Ilan, N. 2004. Heparanase uptake is mediated by cell membrane heparan sulfate proteoglycans. *The Journal of Biological Chemistry* **279** (42): 44084-44092.

Glennie, S., Soeiro, I., Dyson, P., Lam, E and Dazzi, F. 2005. Bone marrow mesenchymal stem cells induce division arrest anergy of activated T cells. *Blood* **105** (7)**:**2821-2827.

Goetzl, M., VanVeldhuizen, P and Thrasher, J., 2007. Effects of soy phytoestrogens on the prostate. *Prostate Cancer and Prostatic Diseases* **10**: 216–223.

Gonzales, P., Pisitkun, T., Hoffert, J., Tchapyjnikov, D., Star, R., Kleta, R., Wang, N and Knepper, M. 2009. Large-scale proteomics and phosphoproteomics of urinary exosomes. *Journal of American Society of Nephrology* **20** (2): 363-379.

Gore, J and Korc, M. 2014. Pancreatic Cancer Stroma: Friend or Foe? *Cancer Cell* **25** (6)**:**711-712.

Goumans, M., Valdimarsdottir, G., Itoh, S., Lebrin, F., Larsson, J., Mummery, C., Karlsson, S and Ten Dijke, P. 2003. Activin receptor-like kinase (ALK)1 is an antagonistic mediator of lateral TGFbeta/ALK5 signaling. *Moelcular Cell.* **12** (4): 817-828.

Graham, C., Rivers, J., Kerbel, R., Stankiewicz, K and White, W. 1994. Extent of vascularization as a prognostic indicator in thin (< 0.76 mm) malignant melanomas. *The American Journal of Pathology* **145** (3)**:**510-514.

Graner, MW., Alzate, O., Dechkovskaia, AM., Keene, JD., Sampson, JH., Mitchell, DA and Bigner, DD. 2009. Proteomic and immunologic analyses of brain tumor exosomes. *FASEB Journal* **23** (5):1541-1557.

Grange, C., Tapparo, M., Collino, F., Vitillo, L., Damasco, C., Deregibus, M.C., Tetta, C., Bussolati, B., Camussi, G. 2011. Microvesicles Released from Human Renal Cancer Stem Cells Stimulate Angiogenesis and Formation of Lung Premetastatic Niche. *Cancer Research* **71** (15):5346-5356.

Grassucci, R., Taylor, D and Frank, J. 2007. Preparation of macromolecular complexes for cryo-electron microscopy. *Nature Protocols*. **2** (12): 3239-3246.

Grossfeld, G., Hayward, S. W., Tlsty, T and Cunha, G. 1998. The role of stroma in prostatic carcinogenesis. *Endocrine-Related Cancer* **5:**253-270.

Gu, J., Qian, H., Shen, L., Zhang, X., Zhu, W., Huang, L., Yan, Y. *et al.* 2012. Gastric Cancer Exosomes Trigger Differentiation of Umbilical Cord Derived Mesenchymal Stem Cells to Carcinoma-Associated Fibroblasts through TGF-β/Smad Pathway. *PLoS One* **7** (12)**:**e52465.

Gu, L., Zhu, Y., Yang, X., Guo, Z., Xu, W. and Tian, X. 2007. Effect of TGF-beta/Smad signaling pathway on lung myofibroblast differentiation. *Acta Pharmacol Sin.* **28** (3)**:**382-391.

Guerrero, F., Herencia, C., Almadén, Y., Martínez-Moreno, J., Montes de Oca, A., Rodriguez-Ortiz, M., Diaz-Tocados, J. *et al.* 2014. TGF-β prevents phosphate-induced osteogenesis through inhibition of BMP and Wnt/β-catenin pathways. *PLoS One* **9** (12).

Guerrero-Esteo, M., Sanchez-Elsner, T., Letamendia, A and Bernabeu, C. 2002. Extracellular and cytoplasmic domains of endoglin interact with the transforming growth factor-beta receptors I and II. *The Journal of Biological Chemistry* **277:**29197-29209.

Guo, X., Oshima, H., Kitmura, T., Taketo, M and Oshima, M. 2008. Stromal fibroblasts activated by tumor cells promote angiogenesis in mouse gastric cancer. *The Journal of Biological Chemistry* **283** (28)**:**19864-19871.

Gupta, P., Das, A., Chullikana, A. and and Majumdar, A. 2012. Mesenchymal stem cells for cartilage repair in osteoarthritis. *Stem Cell Research & Therapy* **3** (4)**:**25.

Hakulinen, J., Sankkila, L., Sugiyama, N., Lehti, K., Keski-Oja, J. 2008. Secretion of active membrane type 1 matrix metalloproteinase (MMP-14) into extracellular space in microvesicular exosomes. *Journal of Cellular Biochemistry* **105** (5):1211-1218.

Harding, C., Heuser, J and Stahl, P. 1983. Receptor-mediated endocytosis of transferrin and recycling of the transferrin receptor in rat reticulocytes. *Journal of Cell Biology* **97** (2): 329-339.

Harding, C., Heuser, J and Stahl, P. 1984. Endocytosis and intracellular processing of transferrin and colloidal gold-transferrin in rat reticulocytes: demonstration of a pathway for receptor shedding. *European Journal of Cell Biology* **35** (2): 256-263.

Hashimoto, S., Gon, Y., Takeshita, I., Matsumoto, K., Maruoka, S and Horie, T. 2001. Transforming Growth Factor-b1 Induces Phenotypic Modulation of Human Lung Fibroblasts to Myofibroblast Through a c-Jun-NH 2 -Terminal Kinase-Dependent Pathway. *American Journal of Respiratory and Critical Care Medicine* **163**: 152-157

Hata, Y., Ishikawa, H., Ueki, T., Kajii, T., Tamaoki, S., Tsuruga, E., Sawa, Y *et al.* 2013. Quantitative evaluation of myofibroblast apoptosis during wound healing in rat palate after post-operative administration of basic fibroblast growth factor (bFGF). *Acta Odontologica Scandinavica* **71** (6)**:**1501-1507.

Hayami, T., Kapila, Y and Kapila, S., 2008. MMP-1 (collagenase-1) and MMP-13 (collagenase-3) differentially regulate markers of osteoblastic differentiation in osteogenic cells. *Matrix Biology* **27** (8):682-692.

Hayward, S., Wang, Y., Cao, M., Hom, Y., Zhang, B., Grossfeld, G., Sudilovsky, D. *et al.* 2001. Malignant transformation in a nontumorigenic human prostatic epithelial cell line. *Cancer Research* **61** (22)**:**8135-8142.

Hedenfalk, I., Duggan, D., Chen, Y., Radmacher, M., Bittner, M., Simon, R., Meltzer, P. *et al.* 2001. Gene-expression profiles in hereditary breast cancer. *New Englland Journal of Medicine.* **344** (8)**:**539-548.

Hegmans, J., Bard, M., Hemmes, A., Luider, T., Kleijmeer, M., Prins, J., Zitvogel, L., Burgers, S., Hoogsteden, H., Lambrecht, B. 2004. Proteomic analysis of exosomes secreted by human mesothelioma cells. *American Journal of Pathology* **164** (5): 1807 - 1815.

Heidenreich, A., Aus, G., Bolla, M., Joniau, S., Matveev, V., Schmid, H and Zattoni, F. 2008. EAU guidelines on prostate cancer. *European Urology* **53** (1)**:**68-80.

Heijnen, H., Schiel, A., Fijnheer, R., Geuze, H and Sixma, J. 1999. Activated platelets release two types of membrane vesicles: microvesicles by surface shedding and exosomes derived from exocytosis of multivesicular bodies and alpha-granules. *Blood* **94** (11)**:**3791-3799.

Hematti, P. 2012. Mesenchymal stromal cells and fibroblasts: a case of mistaken identity? *Cytotherapy.* **14** (5)**:**516-521.

Hinz, B. 2007. Formation and Function of the Myofibroblast during Tissue Repair. *Journal of Investigative Dermatology* **127** (6)**:**526-537.

Hinz, B., Celetta, G., Tomasek, J. J., Gabbiani, G. and Chaponnier, C. 2001. Alpha-Smooth Muscle Actin Expression Upregulates Fibroblast Contractile Activity. *Molecular Biology of the Cell* **12** (9)**:**2730-2741.

Hoeben, A., Landuyt, B., Highley, M., Wildiers, H., Van Oosterom, A and De Bruijn, E. 2004. Vascular endothelial growth factor and angiogenesis. *Pharmacological Reviews* **56** (4)**:**549-580.

Hoemann, C., El-Gabalawy, H and McKee, M. 2009. In vitro osteogenesis assays: influence of the primary cell source on alkaline phosphatase activity and mineralization. *Pathologie-biologie* **57** (4)**:**318-323.

Hoffman, R. 2013. Stromal-cell and cancer-cell exosomes leading the metastatic exodus for the promised niche. *Breast Cancer Research* **15** (3)**:**310.

Hong, B., Cho, J., Kim, H., Choi, E., Rho, S., Kim, J., Kim, J. *et al.* 2009. Colorectal cancer cell-derived microvesicles are enriched in cell cycle-related mRNAs that promote proliferation of endothelial cells. *BMC Genomics* **10** (556).

Hong, ZF., Huang, XJ and Yin, ZY. 2009. Immunocharacteristics of bone marrow mesenchymal stem cell. *Zhonghua Gan Zang Bing Za Zhi.* **17** (1): 53-58.

Hood, JL., San, RS., Wickline, SA. 2011. Exosomes Released by Melanoma Cells Prepare Sentinel Lymph Nodes for Tumor Metastasis. *Cancer Research* **71** (11):3792-3801.

Hoogendam, A., Buntinx, F., de Vet, HC. 1999. The diagnostic value of digital rectal examination in primary care screening for prostate cancer: a meta-analysis. *Family Practice* **16** (6)**:**621-626.

Horwitz, E., Prockop, D., Fitzpatrick, L., Koo, W., Gordon, P., Neel, M., Sussman, M. *et al.* 1999. Transplantability and therapeutic effects of bone marrow-derived mesenchymal cells in children with osteogenesis imperfecta. *Nature Medicine.* **5** (3)**:**309-313.

Hough, C., Radu, M and Doré, J. 2012. TGF-beta induced Erk phosphorylation of smad linker region regulates smad signaling. *PLoS One* **7** (8)**:**doi: 10.1371/journal.pone.0042513.

Hsing, A., Tsao, L and Devesa, S., 2000. International trends and patterns of prostate cancer incidence and mortality. *International Journal of cancer* **85** (1): 60-67

Hsu, C., Morohashi, Y., Yoshimura, S.-i., Manrique-Hoyos, N., Jung, S., Lauterbach, M. A., Bakhti, M. *et al.* 2010. Regulation of exosome secretion by Rab35 and its GTPase-activating proteins TBC1D10A–C. *The Journal of Cell Biology* **189** (2)**:**223-232.

Huang, Z., Nelson, E., Smith, R and Goodman, S. 2007. The sequential expression profiles of growth factors from osteoprogenitors [correction of osteroprogenitors] to osteoblasts in vitro. *Tissue Engineering* **13** (9)**:**2311-2320.

Huber, V., Fais, S., Iero, M., Lugini, L., Canese, P., Squarcina, P., Zaccheddu, A., Colone, M., Arancia, G., Gentile, M., Seregni, E., Valenti, R., Ballabio, G., Belli, F., Leo, E., Parmiani, G., Rivoltini, L. 2005. Human Colorectal Cancer Cells Induce T-Cell Death Through Release of Proapoptotic Microvesicles: Role in Immune Escape. *Gastroenterology* **128** (7):1796-1804.

Husain, M and Harrod, K. 2011. Enhanced acetylation of alpha-tubulin in influenza A virus infected epithelial cells. *FEBS Letters.* **385** (1)**:**128-132.

Husson, O., Mols, F and van de Poll-Franse, L. 2011. The relation between information provision and health-related quality of life, anxiety and depression among cancer survivors: a systematic review. . *Annals of Oncology.* **22** (4)**:**761-772.

Iero M, Valenti R, Huber V, Filipazzi P, Parmiani G, and, Fais, S and Rivoltini, L. 2008. Tumour-released exosomes and their implications in cancer immunity. *Cell death and differentiation* **15** (1):80-88.

Iguchi, H., Kosaka, N and Ochiya, T. 2010. Secretory microRNAs as a versatile communication tool. *Communicative and Integrative Biology* **3** (5): 478-481.

Incorvaia, L., Badalamenti, G., Rini, G., Arcara, C., Fricano, S., Sferrazza, C., Di Trapani, D. *et al.* 2007. MMP-2, MMP-9 and activin A blood levels in patients with breast cancer or prostate cancer metastatic to the bone. *Anticancer Research.* **27** (3B)**:**1519-1525.

Isaacs, J and Coffey, D. 1981. Adaptation versus selection as the mechanism responsible for the relapse of prostatic cancer to androgen ablation therapy as studied in the Dunning R-3327-H adenocarcinoma. *Cancer Research* **41** (12 pt.1): 5070-5075.

Ito, T., Williams, J., Fraser, D and Phillips, A. 2004. Hyaluronan regulates transforming growth factor-beta1 receptor compartmentalization. *Journal of Biological Chemistry* **279** (24)**:**25326-25332.

Jaiswal, N., Haynesworth, S., Caplan, A and Bruder, S. 1997. Osteogenic differentiation of purified, culture-expanded human mesenchymal stem cells in vitro. *Journal of Cellular Biochemistry* **64** (2)**:**295-312.

Jamadar, R. W., MJ. And Maki, PM. 2012. Cognitive changes associated with ADT: a review of the Literature. *Asian Journal of Andrology* **14** (2)**:**232–238.

Jedeszko, C., Victor, B., Podgorski, I and Sloane, B. 2009. Fibroblast hepatocyte growth factor promotes invasion of human mammary ductal carcinoma in situ. *Cancer Research* **69** (23)**:**9148-9155.

Jensen, M., Jørgensen, J., Binderup, T and Kjaer, A. 2008. Tumor volume in subcutaneous mouse xenografts measured by microCT is more accurate and reproducible than determined by 18F-FDG-microPET or external caliper. *BMC Medical Imaging* **8** (16)**:** doi: 10.1186/1471-2342-1188-1116.

Jester, J., Huang, J., Barry-Lane, P., Kao, W., Petroll, W. and Cavanagh, H. 1999. Transforming growth factor(beta)-mediated corneal myofibroblast differentiation requires actin and fibronectin assembly. *Investigative Ophthalmology and Visual Science.* **40** (9)**:**1959-1967.

Ji, H., Erfani, N., Tauro, B., Kapp, E., Zhu, H., Moritz, R., Lim, J and Simpson, R. 2008. Difference gel electrophoresis analysis of Ras-transformed fibroblast cell-derived exosomes. *Electrophoresis* **29** (12):2660-2671.

Jia, CC., Wang, TT., Liu, W., Fu, BS., Hua, X., Wang, GY., Li, TJ. *et al.* 2013. Cancer-Associated Fibroblasts from Hepatocellular Carcinoma Promote Malignant Cell Proliferation by HGF Secretion. *Plos One* **8** (2)**:**9.

Jiang, W., Davies, G., Martin, T., Kynaston, H., Mason, M and Fodstad, O. 2006. Com-1/p8 acts as a putative tumour suppressor in prostate cancer. *International Journal of Molecular Medicine* **18** (5)**:**981-986.

Jiang, X., Dutton, CM., Qi, WN., Block, JA., Garamszegi, N and Scully, SP. 2005. siRNA mediated inhibition of MMP-1 reduces invasive potential of a human chondrosarcoma cell line. *Journal of cellular physiology* **202** (3):723-730.

Johnstone, B., Hering, T., Caplan, A., Goldberg, V and Yoo, J. 1998. In vitro chondrogenesis of bone marrow-derived mesenchymal progenitor cells. *Experimental Cell Research*. **238** (1): 265-272.

Johnstone, R., Adam, M., Hammond, J., Orr, L., Turbide, C. 1987. Vesicle formation during reticulocyte maturation. Association of plasma membrane activities with released vesicles (exosomes). *Journal of Biological Chemistry* **262** (19): 9412-9420.

Joshi, M., Ahmad, R., Yin, L., Raina, D., Rajabi, H., Bubley, G., Kharbanda, S. *et al.* 2009. MUC1 oncoprotein is a druggable target in human prostate cancer cells. *Molecular Cancer Therapy.* **8:**3056-3065.

Jouvenet, N., Zhadina, M., Bieniasz, P and Simon, S. 2011. Dynamics of ESCRT protein recruitment during retroviral assembly. *Nature Cell Biology* **13** (4):394-401.

Jung, Y., Kim, J. K., Shiozawa, Y., Wang, J., Mishra, A., Joseph, J., Berry, J. E. *et al.* 2013. Recruitment of mesenchymal stem cells into prostate tumours promotes metastasis. *Nature Communications* **4** (11)**:**1795.

Kalluri, R and Zeisberg, M. 2006. Fibroblasts in cancer. *Nature Reviews in Cancer* **6** (5): 392-401.

Kalra, H., Adda, C., Liem, M., Ang, C., Mechler, A., Simpson, R., Hulett, M. *et al.* 2013. Comparative proteomics evaluation of plasma exosome isolation techniques and assessment of the stability of exosomes in normal human blood plasma. *Proteomics* **13** (22)**:**3354-3364.

Kamoun, W., Chae, S., Lacorre, D., Tyrrell, J., Mitre, M., Gillissen, M., Fukumura, D. *et al.* 2010. Simultaneous measurement of RBC velocity, flux, hematocrit and shear rate in vascular networks. *Nature Methods* **7** (8)**:**655-660.

Kapanci, Y., Ribaux, C., Chaponnier, C and Gabbiani, G. 1992. Cytoskeletal features of alveolar myofibroblasts and pericytes in normal human and rat lung. *The journal of histochemistry and cytochemistry* **40** (12)**:**1955-1963.

Karnoub, A. E., Dash, A. B., Vo, A. P., Sullivan, A., Brooks, M. W., Bell, G. W., Richardson, A. L. *et al.* 2007. Mesenchymal stem cells within tumour stroma promote breast cancer metastasis. *Nature* **449** (7162)**:**557-563.

Katzmann, D., Babst, M and Emr, S. 2001. Ubiquitin-dependent sorting into the multivesicular body pathway requires the function of a conserved endosomal protein sorting complex, ESCRT-I. *Cell* **106** (2): 145-155.

Katzmann, D., Stefan, C., Babst, M., Emr, S. 2003. Vps27 recruits ESCRT machinery to endosomes during MVB sorting. Journal of Cell Biology 162 (3):413 - 423.

Kawada, H., Fujita, J., Kinjo, K., Matsuzaki, Y., Tsuma, M., Miyatake, H., Muguruma, Y. *et al.* 2004. Nonhematopoietic mesenchymal stem cells can be mobilized and differentiate into cardiomyocytes after myocardial infarction. *Blood* **102** (12)**:**3581-3587.

Kermorgant, S., Aparicio, T., Dessirier, V., Lewin, M and Lehy, T. 2001. Hepatocyte growth factor induces colonic cancer cell invasiveness via enhanced motility and protease overproduction. Evidence for PI3 kinase and PKC involvement. *Carcinogenesis* **22** (7):1035-1042.

Kesimer, M., Scull, M., Brighton, B., DeMaria, G., Burns, K., O'Neal, W., Pickles, R. *et al.* 2009. Characterization of exosome-like vesicles released from human tracheobronchial ciliated epithelium: a possible role in innate defense. *FASEB journal* **23** (6)**:**1858-1868.

Kessenbrock, K., Plaks, V and Werb, Z. 2010. Matrix metalloproteinases: regulators of the tumor microenvironment. *Cell* **141** (1)**:**52-67.

Khakoo, A., Pati, S., Anderson, S., Reid, W., Elshal, M., Rovira, I., Nguyen, A. *et al.* 2006. Human mesenchymal stem cells exert potent antitumorigenic effects in a model of Kaposi's sarcoma. *Journal of Experimental Medicine.* **203** (5)**:**1235-1247.

Kiciński, M., Vangronsveld, J and Nawrot, T. 2011. An epidemiological reappraisal of the familial aggregation of prostate cancer: a meta-analysis. *PloS One* **6**(10)**:** doi:10.1371/journal. pone.0027130.

King, H., Michael, M and Gleadle, J. 2012. Hypoxic enhancement of exosome release by breast cancer cells. *BMC Cancer* **12** (1): 421

Kitadai, Y., Haruma, K., Sumii, K., Yamamoto, S., Ue, T., Yokozaki, H., Yasui, W. *et al.* 1998. Expression of interleukin-8 correlates with vascularity in human gastric carcinomas. *American Journal of Pathology* **152** (1)**:**93–100.

Kitagawa, Y., Toriyama, K., Kamei, Y and Torii, S. 2006. History of discovery of human adipose-derived stem cells and their clinical applications. *Japanese Journal of Plastic and Reconstructive Surgery* **49:**1097-1104.

Klopp, A., Speath, E., Dembinski, J., Woodward, W., Munshi, A., Meyn, R., Cox, J. *et al.* 2007. Tumor Irradiation Increases the Recruitment of Circulating Mesenchymal Stem Cells into the Tumor Microenvironment. *Cancer Research* **67** (24)**:**11687-11695.

Knäuper, V., Wilhelm, S., Seperack, P., DeClerck, Y., Langley, K., Osthues, A and Tschesche, H. 1993. Direct activation of human neutrophil procollagenase by recombinant stromelysin. *Biochemical Journal.* **295** (2)**:**581-586.

Knäuper, V., Will, H., López-Otin, C., Smith, B., Atkinson, S., Stanton, H., Hembry, R. *et al.* 1996. Cellular mechanisms for human procollagenase-3 (MMP-13) activation. Evidence that MT1-MMP (MMP-14) and gelatinase a (MMP-2) are able to generate active enzyme. *Journal of Biological Chemistry.* **271** (29)**:**17124-17131.

Kobayashi, H. 1996. Mechanism of tumor cell-induced extracellular matrix degradation--inhibition of cell-surface proteolytic activity might have a therapeutic effect on tumor cell invasion and metastasis. *Nihon Sanka Fujinka Gakkai Zasshi* **48:**623-632.

Koga, K., Matsumoto, K., Akiyoshi, T., Kubo, M., Yamanaka, N., Tasaki, A., Nakashima, H., Nakamura, M., Kuroki, S., Tanaka, M and Katano, M. 2005. Purification, characterization and biological significance of tumor-derived exosomes. *Anticancer Research* **25** (6A): 3703-3707.

Koga, Y., Yasunaga, M., Moriya, Y., Akasu, T., Fujita, S., Yamamoto, S.a., Matsumura, Y., 2011. Exosome can prevent RNase from degrading microRNA in feces. *Journal of Gastrointestinal Oncology* **2** (4):215-222.

Kosaka, N., Iguchi, H., Yoshioka, Y., Takeshita, F., Matsuki, Y and Ochiya, T. 2010. Secretory mechanisms and intercellular transfer of microRNAs in living cells. *The Journal of Biological Chemistry* **285** (23):17442-17452.

Kowal, J., Tkach, M and Théry, C. 2014. Biogenesis and secretion of exosomes. *Current Opinion in Cell Biology* **29**:116-125.

Krebsbach, P., Kuznetsov, S., Bianco, P and Robey, P. 1999. Bone marrow stromal cells: characterization and clinical application. *Critical Review or Oral Biological Medicine* **10** (2)**:**165-181.

Kucharzewska, P., Christianson, H., Welch, J., Svensson, K., Fredlund, E., Ringnér, M., Mörgelin, M., Bourseau-Guilmain, E., Bengzon, J and Belting, M. 2013. Exosomes reflect the hypoxic status of glioma cells and mediate hypoxia-dependent activation of vascular cells during tumor development. *Proceedings National Academy of Sciences* **110** (18):7312-7317.

Kundrotas, G. 2012. Surface markers distinguishing mesenchymal stem cells from fibroblasts. *Acta Medica Lituanica* **19** (2)**:**75-79.

Kupelian, P., Potters, L., Khuntia, D., Ciezki, J., Reddy, C., Reuther, A., Carlson, T. *et al.* 2004. Radical prostatectomy, external beam radiotherapy <72 Gy, external beam radiotherapy > or =72 Gy, permanent seed implantation, or combined seeds/external beam radiotherapy for stage T1-T2 prostate cancer. *International journal of radiation oncology, biology and physics* **58** (1)**:**25-33.

Kuriyan, AE., Woeller, CF., O'Loughlin, CW., Phipps, RP and Feldon, SE. 2013. Orbital fibroblasts from thyroid eye disease patients differ in proliferative and adipogenic responses depending on disease subtype. *Investigative Ophthalmology and Visual Science* **54** (12): 7370-7377.

Kwon, C., Park, H., Lee, J., Kim, H., Jeon, T., Jo, H., Kim, D. *et al.* 2014. Serpin peptidase inhibitor clade A member 1 is a biomarker of poor prognosis in gastric cancer. *British Journal of Cancer* **111** (10)**:**1993-2002.

Lacunza, E., Baudis, M., Colussi, A., Segal-Eiras, A., Croce, M and Abba, M. 2010. MUC1 oncogene amplification correlates with protein overexpression in invasive breast carcinoma cells. *Cancer Genet Cytogenet.* **201** (2)**:**102-110.

Lamalice, L., Le Boeuf, F and Huot, J. 2007. Endothelial cell migration during angiogenesis. *Circulation Research* **100** (30)**:**782-794.

Lamparski, H., Metha-Damani, A., Yao, J., Patel, S., Hsu, D., Ruegg, C. and Le Pecq, J. 2002. Production and characterization of clinical grade exosomes derived from dendritic cells. *Journal of Immunological Methods* **270** (2)**:**211-226.

Lang, S., Sharrard, R., Stark, M., Villette, J and Maitland, N. 2001. Prostate epithelial cell lines form spheroids with evidence of glandular differentiation in three-dimensional Matrigel cultures. *British Journal of Cancer*. **85** (4): 590-599.

Langley, S and Laing, R. 2004. Iodine seed prostate brachytherapy: an alternative first-line choice for early prostate cancer. *Prostate Cancer & Prostatic Diseases* **7** (3)**:**201-207.

Laulagnier, K., Motta, C., Hamdi, S., Roy, S., Fauvelle, F., Pageaux, J., Kobayashi, T., Salles, J., Perret, B., Bonnerot, C and Record, M. 2004. Mast cell- and dendritic cell-derived exosomes display a specific lipid composition and an unusual membrane organization. *The Biochemical Journal* **380** (1):161-171.

Le Blanc, K. 2003. Immunomodulatory effects of fetal and adult mesenchymal stem cells. *Cytotherapy* **5** (6):485-489.

Le Blanc, K., Frassoni, F., Ball, L., Locatelli, F., Roelofs, H., Lewis, I., Lanino, E. *et al.* 2008. Mesenchymal stem cells for treatment of steroid-resistant, severe, acute graft-versus-host disease: a phase II study. *Lancet* **371** (9624)**:**1579-1586.

Le Blanc, K., Rasmusson, I., Sundberg, B., Götherström, C., Hassan, M., Uzunel, M and Ringdén, O. 2004. Treatment of severe acute graft-versus-host disease with third party haploidentical mesenchymal stem cells. *Lancet* **363** (9419)**:**1439-1441.

Leask, A., Abraham, D., Finlay, D., Holmes, A., Pennington, D., Shi-Wen, X., Chen, Y. *et al.* 2002. Dysregulation of transforming growth factor beta signaling in scleroderma: overexpression of endoglin in cutaneous scleroderma fibroblasts. *Arthritis & Rheumatism* **46** (7)**:**1857-1865.

Lecomte, J., Masset, A., Blacher, S., Maertens, l., Gothot, A., Delgaudine, M., Bruyère, F. *et al.* 2012. Bone Marrow-derived Myofibroblasts Are the Providers of Pro-invasive Matrix Metalloproteinase 13 in Primary Tumor. *Neoplasia* **14** (10)**:**943-951.

Lee, E., Park, S., Kim, W and Moon, S. 2012. IL-5-induced migration via ERK1/2-mediated MMP-9 expression by inducing activation of NF-κB in HT1376 cells. *Oncology Reports* **28** (3)**:**1084-1090.

Lee, JC., Lee, KM., Kim, DW and Heo, DS. 2004a. Elevated TGF-{beta}1 Secretion and Down-Modulation of NKG2D Underlies Impaired NK Cytotoxicity in Cancer Patients. *Journal of Immunology* **172** (12)**:**7335-7340.

Lee, S., Jilani, S., Nikolova, G., Carpizo, D and Iruela-Arispe, M. 2005. Processing of VEGF-A by matrix metalloproteinases regulates bioavailability and vascular patterning in tumors. *The Journal of Cell Biology* **169** (4)**:**681-691.

Lee, WJ., Kim, YH., Kim, SH., Han, SH and Hahn, SB. 2004b. Chondrogenic Differentiation of Mesenchymal Stem Cells and its Clinical Applications. *Yonsei Medical Journal*. **45**: 41-47.

Leto, G., Incorvaia, L., Badalamenti, G., Tumminello, F., Gebbia, N., Flandina, C., Crescimanno, M. *et al.* 2006. Activin A circulating levels in patients with bone metastasis from breast or prostate cancer. *Clinical Experimental Metastasis.* **23** (2)**:**117-122.

Levchenko, A., Mehta, B., Niu, X., Kang, G., Villafania, L., Way, D., Polycarpe, D. *et al.* 2005. Intercellular transfer of P-glycoprotein mediates acquired multidrug resistance in tumor cells. *Proceedings of the National Academy of Sciences* **102** (6)**:**1933-1938.

Levental, K., Yu, H., Kass, L., Lakins, J., Egeblad, M., Erler, J., Fong, S. *et al.* 2009. Matrix crosslinking forces tumor progression by enhancing integrin signaling. *Cell* **139** (5)**:**:891-906.

Levy, S and Shoham, T. 2005. The tetraspanin web modulates immune-signalling complexes. *Nature reviews immunology* **5** (2): 136-148.

Lewis, M., Lygoe, K., Nystrom, M., Anderson, W., Speight, P., Marshall, J and Thomas, G. 2004. Tumour-derived TGF-beta1 modulates myofibroblast differentiation and promotes HGF/SF-dependent invasion of squamous carcinoma cells. *British Journal of Cancer* **90** (4)**:**822-832.

Li, W., Hu, Y., Jiang, T., Han, Y., Han, G., Chen, J. and Li, X. 2014. Rab27A regulates exosome secretion from lung adenocarcinoma cells A549: involvement of EPI64. *APMIS*.

Li, W., Zhong, S., Wu, Y., Xu, W., Xu, J., Tang, J and Zhao, J. 2013. Systematic expression analysis of genes related to multidrug-resistance in isogenic docetaxel- and adriamycin-resistant breast cancer cell lines. *Molecular Biology Reports.* **40** (11)**:**6143-6150.

Liang, C., Park, A and Guan, J. 2007. In vitro scratch assay: a convenient and inexpensive method for analysis of cell migration in vitro. *Nature Protocols* **2** (2)**:**329-333.

Liang, P. I. N., Hong, J.-W., Ubukata, H., Liu, G. E., Katano, M., Motohashi, G. Y. O., Kasuga, T. *et al.* 2005. Myofibroblasts Correlate with Lymphatic Microvessel Density and Lymph Node Metastasis in Early-stage Invasive Colorectal Carcinoma. *Anticancer Research* **25** (4)**:**2705-2712.

Liang, Y., Brekken, R and Hyder, S. 2006. Vascular endothelial growth factor induces proliferation of breast cancer cells and inhibits the anti-proliferative activity of anti-hormones. *Endocrine-Related Cancer* **13** (3):905-919.

Lijnen, P., Petrov, V and Fagard, R. 2003. Transforming growth factor-β1-mediated collagen gel contraction by cardiac fibroblasts. *Journal of the Renin Angiotensin Aldosterone System* **4** (2)**:**113-118.

Liu, A. 2000. Differential expression of cell surface molecules in prostate cancer cells. *Cancer Research* **60** (13)**:**3429-3434.

Liu, C., Yu, S., Zinn, K., Wang, J., Zhang, L., Jia, Y., Kappes, J. C. *et al.* 2006. Murine Mammary Carcinoma Exosomes Promote Tumor Growth by Suppression of NK Cell Function. *J Immunol* **176** (3)**:**1375-1385.

Liu, D., Black, B. and Derynck R. 2001. TGF-β inhibits muscle differentiation through functional repression of myogenic transcription factors by Smad3. *Genes and development* **15** (22)**:**2950-2966.

Liu, X., Qin, J., Luo, Q., Bi, Y., Zhu, G., Jiang, W., Kim, S. *et al.* 2013. Cross-talk between EGF and BMP9 signalling pathways regulates the osteogenic differentiation of mesenchymal stem cells. *Journal of Cellular and Molecular Medicine.* **17** (9)**:**1160-1172.

Loberg, R., Day, L., Harwood, J., Ying, C., St John, L., Giles, R., Neeley, C. *et al.* 2006. CCL2 is a potent regulator of prostate cancer cell migration and proliferation. *Neoplasia.* **8** (7)**:**578-586.

Loberg, R., Ying, C., Craig, M., Yan, L., Snyder, L and Pienta, K. 2007. CCL2 as an important mediator of prostate cancer growth in vivo through the regulation of macrophage infiltration. *Neoplasia* **9** (7)**:**556-562.

Lochter, A., Galosy, S., Muschler, J., Freedman, N., Werb, Z and Bissell, M. 1997. Matrix metalloproteinase stromelysin-1 triggers a cascade of molecular alterations that leads to stable epithelial-to-mesenchymal conversion and a premalignant phenotype in mammary epithelial cells. *Journal of Cell Biology* **139** (7)**:**1861-1872.

López-Casillas, F., Wrana, J.L., Massagué, J. 1993. Betaglycan presents ligand to the TGFβ signaling receptor. *Cell* **73** (7):1435-1444.

Lu, P., Takai, K., Weaver, V and Werb, Z. 2011. Extracellular matrix degradation and remodeling in development and disease. *Cold Spring Harbour Perspectives in Biology.* **3** (1) **:**doi: 10.1101/cshperspect.a005058.

Lu, Y., Cai, Z., Galson, D., Xiao, G., Liu, Y., George, D., Melhem, M. *et al.* 2006. Monocyte chemotactic protein-1 (MCP-1) acts as a paracrine and autocrine factor for prostate cancer growth and invasion. *Prostate* **66** (12)**:**1311-1318.

Luga, V., Zhang, L., Viloria-Petit, Alicia M., Ogunjimi, Abiodun A., Inanlou, Mohammad R., Chiu, E., Buchanan, M. *et al.* 2012. Exosomes Mediate Stromal Mobilization of Autocrine Wnt-PCP Signaling in Breast Cancer Cell Migration. *Cell* **151** (7)**:**1542-1556.

Luo, J., Ok, L., Liang, L., Huang, C., Li, L., Wen, S and Chang, C. 2014. Infiltrating bone marrow mesenchymal stem cells increase prostate cancer stem cell population and metastatic ability via secreting cytokines to suppress androgen receptor signaling. *Oncogene* **33** (21)**:**2768-2778.

Luthra, R., Singh, R., Luthra, M., Li, Y., Hannah, C., Romans, A., Barkoh, B. *et al.* 2008. MicroRNA-196a targets annexin A1: a microRNA-mediated mechanism of annexin A1 downregulation in cancers. *Oncogene* **27** (52)**:**6667-6678.

Lv, L., Wan, Y., Lin, Y., Zhang, W., Yang, M., Li, G., Lin, H. *et al.* 2012. Anticancer drugs cause release of exosomes with heat shock proteins from human hepatocellular carcinoma cells that elicit effective natural killer cell antitumor responses in vitro. *The Journal of Biological Chemistry* **287** (19)**:**15874-15885.

Lyons, R., Keski-Oja, J and Moses, H. 1988. Proteolytic activation of latent transforming growth factor-beta from fibroblast-conditioned medium. *Journal of Cell Biology* **106** (5)**:**1659-1665.

Maby-El Hajjami, H., Amé-Thomas, P., Pangault, C., Tribut, O., DeVos, J., Jean, R., Bescher, N. *et al.* 2009. Functional alteration of the lymphoma stromal cell niche by the cytokine context: role of indoleamine-2,3 dioxygenase. *Cancer Research* **69** (7)**:** doi: 10.1158/0008-5472.

Macchiarini, P., Fontanini, G., Hardin, M., Squartini, F and Angeletti, C. 1992. Relation of neovascularisation to metastasis of non-small-cell lung cancer. *Lancet* **340** (8812)**:**145–146.

Mackay, A., Beck, S., Murphy, J., Barry, F., Chichester, C and Pittenger, M. 1998. Chondrogenic differentiation of cultured human mesenchymal stem cells from marrow. *Tissue Engineering* **4** (4)**:**415-428.

Marleau, A., Chen, CS., Joyce, J., Tullis, R., 2012. Exosome removal as a therapeutic adjuvant in cancer. *Journal of Translational Medicine* **10** (1):134.

Marsh, D., Suchak, K., Moutasim, K., Vallath, S., Hopper, C., Jerjes, W., Upile, T., Kalavrezos, N., Violette, S., Weinreb, P., Chester, K., Chana, J., Marshall, J., Hart, I., Hackshaw, A., Piper, K.a., Thomas, G. 2011. Stromal features are predictive of disease mortality in oral cancer patients. *The Journal of Pathology* **223** (4): 470-481.

Martinez, C., Hofmann, T., Marino, R., Dominici, M and Horwitz, E. 2007. Human bone marrow mesenchymal stromal cells express the neural ganglioside GD2: a novel surface marker for the identification of MSCs. *Blood* **109** (10)**:**4245-4248.

Mathivanan, S., Fahner, C.J., Reid, G.E., Simpson, R.J. 2012. ExoCarta 2012: database of exosomal proteins, RNA and lipids. *Nucleic Acids Research* **40** (1): D1241-D1244.

Mathivanan, S., Lim, J., Tauro, B., Ji, H., Moritz, R and Simpson, R. 2010. Proteomics analysis of A33 immunoaffinity-purified exosomes released from the human colon tumor cell line LIM1215 reveals a tissue-specific protein signature. *Molecular & Cellular proteomics* **9** (2):197-208.

Matsushita, T., Kibayashi, T., Katayama, T., Yamashita, Y., Suzuki, S., Kawamata, J., Honmou, O. *et al.* 2011. Mesenchymal stem cells transmigrate across brain microvascular endothelial cell monolayers through transiently formed inter-endothelial gaps. *Neuroscience Letters.* **502** (41-45).

McAnulty, R. 2007. Fibroblasts and myofibroblasts: their source, function and role in disease. *The International Journal of Biochemistry and Cell Biology* **39** (4)**:**666-671.

McConnell, JD., Barry, ML., Bruskewitz RC, et al. 1994. Benign Prostatic Hyperplasia: Diagnosis and Treatment. Clinical Practice Guidelines. . *Agency for Health Care Policy and Research* AHCPR Publication no. 94-0582.

Mears, R., Craven, R., Hanrahan, S., Totty, N., Upton, C., Young, S., Patel, P., Selby, P., Banks, R. 2004. Proteomic analysis of melanoma-derived exosomes by two-dimensional polyacrylamide gel electrophoresis and mass spectrometry. *Proteomics* **12**:4019-4031.

Meisel, R., Zibert, A., Laryea, M., Göbel, U., Däubener, W and Dilloo, D. 2004. Human bone marrow stromal cells inhibit allogeneic T-cell responses by indoleamine 2,3-dioxygenase-mediated tryptophan degradation. *Blood* **103** (12)**:**4619-4621.

Menon, M and Walsh, P., 1979. Hormonal Therapy for Prostate Cancer. *Diagnosis, management and screening of early localised prostate cancer Health Technology Assessment 1:*1-96

Micallef, L., Vedrenne, N., Billet, F., Coulomb, B., Darby, I and Desmoulière, A. 2012. The myofibroblast, multiple origins for major roles in normal and pathological tissue repair. *Fibrogenesis & Tissue Repair* **5**.

Midgley, A., Rogers, M., Hallett, M., Clayton, A., Bowen, T. and Phillips, A., and Steadman, Robert. 2013. Transforming growth factor-β1 (TGF-β1)-stimulated fibroblast to myofibroblast differentiation is mediated by hyaluronan (HA)-facilitated epidermal growth factor receptor (EGFR) and CD44 co-localization in lipid rafts. *The Journal of Biological Chemistry* **288** (21)**:**14824-14838.

Miletic, H., Fischer, Y., Litwak, S., Giroglou, T., Waerzeggers, Y., Winkeler, A., Li, H. *et al.* 2007. Bystander killing of malignant glioma by bone marrow-derived tumor-infiltrating progenitor cells expressing a suicide gene. *Molecular Therapy.* **15** (7)**:**1373-1381.

Minagawa, S., Lou, J., Seed, RI., Cormier, A., Wu, S., Cheng, Y., Murray, L. *et al.* 2014. Selective Targeting of TGF-β Activation to Treat Fibroinflammatory Airway Disease. *Science Translational Medicine* **6** (241)**:**241-279.

Mishra, PJ., Mishra, PJ., Humeniuk, R., Medina, DJ., Alexe, G., Mesirov, JP., Ganesan, S. *et al.* 2008. Carcinoma-Associated Fibroblast–Like Differentiation of Human Mesenchymal Stem Cells. *Cancer Research* **68** (11)**:**4331-4339.

Mitchell, JP., Court, J., Mason, MD., Tabi, Z. and Clayton, A. 2008. Increased exosome production from tumour cell cultures using the Integra CELLine Culture System. *Journal of Immunological Methods* **335** (1-2)**:**98-105.

Moore, C., Guthrie, E., Huang, M and Taxman, D. 2010. Short hairpin RNA (shRNA): design, delivery, and assessment of gene knockdown. *Methods of Molecular Biology.* **629:**141-158.

Morizono, K., De Ugarte, D., Zhu, M., Zuk, P., Elbarbary, A., Ashjian, P., Benhaim, P. *et al.* 2003. Multilineage cells from adipose tissue as gene delivery vehicles. *Human Gene Therapy* **14** (1)**:**59-66.

Morse, M., Garst, J., Khan, S., Compagna, L., Hobeika, A., Colling, K., Ghanayem, M., Heck, R., Valente, N., Pecq, J and Clay, T. 2002. Preliminary results of a phase I/II study of active immunotherapy with autologous dexosomes loaded with MAGE peptides in HLA A2+ patients with stage III/IV non-small cell lung cancer. *American Society of Clinical Oncology* **21**

Motoyama, M., Deie, M., Kanaya, A., Nishimori, M., Miyamoto, A., Yanada, S., Adachi, N *et al.* 2010. In vitro cartilage formation using TGF-beta-immobilized magnetic beads and mesenchymal stem cell-magnetic bead complexes under magnetic field conditions. *Journal of Biomedical Material Research Part A.* **92** (1)**:**196-204.

Moul, J., Sesterhenn, I., Connelly, R., Douglas, T., Srivastava, S., Mostofi, F and McLeod, D. 1995. Prostate-specific antigen values at the time of prostate cancer diagnosis in African-American men. *JAMA* **274** (16)**:**1277-1281.

Murphy, D., Makonnen, S., Lassoued, W., Feldman, M., Carter, C and Lee, W. 2006. Inhibition of tumor endothelial ERK activation, angiogenesis, and tumor growth by sorafenib (BAY43-9006). *American Journal of Pathology.* **169** (5)**:**1875-1885.

Murphy, G., Mettlin, C., Menck, H., Winchester, D. a. and Davidson, A. 1994. National patterns of prostate cancer treatment by radical prostatectomy: results of a survey by the American College of Surgeons Commission on Cancer. *The Journal of Urology* **152** (2)**:**1817-1819.

Nagaya, N., Kangawa, K., Itoh, T., Iwase, T., Murakami, S., Miyahara, Y., Fujii, T. *et al.* 2005. Transplantation of mesenchymal stem cells improves cardiac function in a rat model of dilated cardiomyopathy. *Circulation* **112** (8)**:**1128-1135.

Nagle, R., Ahmann, F., McDaniel, K., Paquin, M., Clark, V and Celniker, A. 1987. Cytokeratin Characterization of Human Prostatic Carcinoma and Its Derived Cell Lines. *Cancer Research* **47:**281.

Nazarenko, I., Rana, S., Baumann, A., McAlear, J., Hellwig, A., Trendelenburg, M., Lochnit, G., Preissner, K.T., Zoller, M. 2010. Cell Surface Tetraspanin Tspan8 Contributes to Molecular Pathways of Exosome-Induced Endothelial Cell Activation. *Cancer Research* **70** (4):1668-1678.

Nelson, C., Lee, J., Gamboa, M and AJ., R. 2008. Cognitive effects of hormone therapy in men with prostate cancer: a review. *Cancer* **113** (5)**:**1097-1106.

Németh, K., Leelahavanichkul, A., Yuen, P., Mayer, B., Parmelee, A., Doi, K., Robey, P. *et al.* 2009. Bone marrow stromal cells attenuate sepsis via prostaglandin E(2)-dependent reprogramming of host macrophages to increase their interleukin-10 production. *Nature Medicine* **15** (1)**:**42-49.

NICE. 2009. Prostate Cancer: Diagnosis and Treatment. CG58. London:. *National Institute for Health and Clinical Excellence.*

Niger, C., Beazley, K and Nurminskaya, M. 2013. Induction of chondrogenic differentiation in mesenchymal stem cells by TGF-beta cross-linked to collagen-PLLA [poly(L-lactic acid)] scaffold by transglutaminase 2. *Biotechnology Letters.* **35** (12)**:**2193-2199.

Nilsson, J., Skog, J., Nordstrand, A., Baranov, V., Mincheva-Nilsson, L., Breakefield, O and Widmark, A. 2009. Prostate cancer-derived urine exosomes: a novel approach to biomarkers for prostate cancer. *British Journal of Cancer* **100** (10)**:**1603–1607.

Nyati, S., Schinske, K., Ray, D., Nyati, M., Ross, B. and Rehemtulla, A. 2011. Molecular imaging of TGFβ-induced Smad2/3 phosphorylation reveals a role for receptor tyrosine kinases in modulating TGFβ signaling. *Clinical Cancer Research* **17** (23)**:**7424-7439.

Nyga, A., Loizidou, M., Emberton, M and Cheema, U. 2013. A novel tissue engineered three-dimensional in vitro colorectal cancer model. *Acta Biomaterials* **9** (8):7917-7926.

Ode, A., Kopf, J., Kurtz, A., Schmidt-Bleek, K., Schrade, P., Kolar, P., Buttgereit, F. *et al.* 2011. CD73 and CD29 concurrently mediate the mechanically induced decrease of migratory capacity of mesenchymal stromal cells. *European Cell Material.* **22:**26-42.

Oesterling, J., Jacobsen, S., Chute, C., Guess, H., Girman, C., Panser, L and Lieber, M. 1993. Serum prostate-specific antigen in a community-based population of healthy men. Establishment of age-specific reference ranges. *JAMA* **270** (7)**:**860-864.

Ogura, N., Kawada, M., Chang, W.-J., Zhang, Q., Lee, S.-Y., Kondoh, T. and Abiko, Y. 2004. Differentiation of the human mesenchymal stem cellsderived from bone marrow and enhancement of cellattachment by fibronectin. *Journal of Oral Science* **46** (4)**:**207-213.

Olumi, AF., Grossfeld, GD., Hayward, SW., Carroll, PR., Tlsty, TD. and Cunha, GR. 1999. Carcinoma-associated Fibroblasts Direct Tumor Progression of Initiated Human Prostatic Epithelium. *Cancer Research* **59** (19)**:**5002-5011.

Onik, G., Cohen, J., Reyes, G., Rubinsky, B., Chang, Z and Baust, J. 1993. Transrectal ultrasound-guided percutaneous radical cryosurgical ablation of the prostate. *Cancer* **72** (4)**:**1291-1299.

Oosthuyzen, W., Sime, N., Ivy, J., Turtle, E., Street, J., Pound, J., Bath, L., Webb, D., Gregory, C., Bailey, M and Dear, J. 2013. Quantification of human urinary exosomes by nanoparticle tracking analysis. *The Journal of Physiology* **591** (23): 5833-5842.

Orbay, H., Tobita, M and Mizuno, H. 2012. Mesenchymal stem cells isolated from adipose and other tissues: basic biological properties and clinical applications. *Stem cells international* doi: 10.1155/2012/461718.

Orimo, A., Gupta, P., Sgroi, D., Arenzana-Seisdedos, F., Delaunay, T., Naeem, R., Carey, V. *et al.* 2005. Stromal fibroblasts present in invasive human breast carcinomas promote tumor growth and angiogenesis through elevated SDF-1/CXCL12 secretion. *Cell* **121** (3)**:**335-348.

Orimo, A., Tomioka, Y., Shimizu, Y., Sato, M., Oigawa, S., Kamata, K., Nogi, Y. *et al.* 2001. Cancer-associated myofibroblasts possess various factors to promote endometrial tumor progression. *Clinical Cancer Research* **7** (10)**:**3097-3105.

Ostman, A and Augsten, M. 2009. Cancer-associated fibroblasts and tumor growth--bystanders turning into key players. *Cuurent Opinion in Genetics and Development* **19** (1)**:**67-73.

Ostrowski, M., Carmo, N. B., Krumeich, S., Fanget, I., Raposo, G., Savina, A., Moita, CF. *et al.* 2010. Rab27a and Rab27b control different steps of the exosome secretion pathway. *Nature Cell Biology.* **12** (1)**:**19-30.

Otsu, K., Das, S., Houser, S., Quadri, S., Bhattacharya, S and Bhattacharya, J. 2009. Concentration-dependent inhibition of angiogenesis by mesenchymal stem cells. *Blood* **113** (18)**:**4197-4205.

Page-McCaw, A., Ewald, A and Werb, Z. 2007. Matrix metalloproteinases and the regulation of tissue remodelling. *Nature Reviews of Molecular Cell Biology.* **8** (3)**:**221-233.

Pan, B., Teng, K., Wu, C., Adam, M and Johnstone, R. 1985. Electron microscopic evidence for externalization of the transferrin receptor in vesicular form in sheep reticulocytes. *Journal of Cell Biology* **101** (3)**:**942-948.

Park, J., Keller, G and Ferrara, N. 1993. The vascular endothelial growth factor (VEGF) isoforms: differential deposition into the subepithelial extracellular matrix and bioactivity of extracellular matrix-bound VEGF. *Molecular biology of the cell* **4** (12)**:**1317–1326.

Peinado, H., Aleckovic, M., Lavotshkin, S., Matei, I., Costa-Silva, B., Moreno-Bueno, G., Hergueta-Redondo, M. *et al.* 2012. Melanoma exosomes educate bone marrow progenitor cells toward a pro-metastatic phenotype through MET. *Nature Medicine* **18** (16)**:**883-891.

Peinemann, F., Grouven, U., Hemkens, L., Bartel, C., Borchers, H., Pinkawa, M., Heidenreich, A *et al.* 2011. Low-dose rate brachytherapy for men with localized prostate cancer. *The Cochrane Database of Systematic Reviews* **6** (7)**:**doi: 10.1002/14651858.CD14008871.pub14651852.

Perez-Hernandez, D., Gutiérrez-Vázquez, C., Jorge, I., López-Martín, S., Ursa, A., Sánchez-Madrid, F., Vázquez, J and Yáñez-Mó, M. 2013. The intracellular interactome of tetraspanin-enriched microdomains reveals their function as sorting machineries toward exosomes. *Journal of Biological Chemistry* **288** (17):11649-11661.

Perkel, V., Mohan, S., Herring, S., Baylink, D and Linkhart, T. 1990. Human Prostatic Cancer Cells, PC3, Elaborate Mitogenic Activity Which Selectively Stimulates Human Bone Cells. Cancer Research. **75** (5): 6902-6907.

Peters, PJ., Borst, J., Oorschot, V., Fukuda, M., Krahenbuh, O., Tsxchopp, J., Slot, JW. *et al.* 1991. Cytotoxic T Lymphocyte Granules Are Secretory Lysosomes Containing Both Perforin and Granzymes. *Journal of Experimental Medicine* **173:**1099-1109.

Phromnoi, K., Yodkeeree, S., Anuchapreeda, S and Limtrakul, P. 2009. Inhibition of MMP-3 activity and invasion of the MDA-MB-231 human invasive breast carcinoma cell line by bioflavonoids. *Acta Pharmacologica Sinica.* **30** (8)**:**1169-1176.

Pin, A., Houle, F., Fournier, P., Guillonneau, M., Paquet, É., Simard, M., Royal, I. *et al.* 2012. Annexin-1-mediated endothelial cell migration and angiogenesis are regulated by vascular endothelial growth factor (VEGF)-induced inhibition of miR-196a expression. *Journal of Biological Chemistry* **287** (36)**:**30541-30551.

Pisitkun, T., Shen, R. and Knepper, M. 2004. Identification and proteomic profiling of exosomes in human urine. *PNAS* **101** (36)**:**13369-13373.

Pistollato, F., Abbadi, S., Rampazzo, E., Persano, L., Della Puppa, A., Frasson, C., Sarto, E., Scienza, R., D'avella, D and Basso, G. 2010. Intratumoral hypoxic gradient drives stem cells distribution and MGMT expression in glioblastoma. *Stem Cells* **28** (5):851-862.

Pittenger, M., Mackay, A., Beck, S., Jaiswal, R., Douglas, R., Mosca, J., Moorman, M. *et al.* 1999. Multilineage potential of adult human mesenchymal stem cells. *Science* **284** (5411)**:**143-147.

Powis, S., Soo, C., Zheng, Y., Campbell, E and Riches, A. 2011. Nanoparticle tracking analysis of cell exosome and nanovesicle secretion. *Microscopy and Analysis* **25** (6):7-9.

Proux-Gillardeauxc, V., Raposo, G., Irinopoulou, T and Galli, T. 2007. Expression of the Longin domain of TI-VAMP impairs lysosomal secretion and epithelial cell migration. *Biology of the Cell* **99** (5):261-271.

Punglia, R., D'Amico, A., Catalona, W., Roehl, K and Kuntz, K. 2003. Effect of verification bias on screening for prostate cancer by measurement of prostate-specific antigen. *The New England Journal of Medicine* **349** (4)**:**335-342.

Qian, SW., Li, X., Zhang, YY., Huang, HY., Liu, Y., Xia Sun, and Tang, QQ. 2010. Characterization of adipocyte differentiation from human mesenchymal stem cells in bone marrow. *BMC Developmental Biology* **10** (47)**:**1-11.

Qiao, L., Xu, Z., Zhao, T., Zhao, Z., Shi, M., Zhao, R., Ye, L. *et al.* 2008. Suppression of tumorigenesis by human mesenchymal stem cells in a hepatoma model. *Cell Research.* **18** (4)**:**500-507.

Quante, M., Tu, S., Tomita, H., Gonda, T., Wang, S., Takashi, S., Ho Baik, G. *et al.* 2011. Bone marrow-derived myofibroblasts contribute to the mesenchymal stem cell niche and promote tumor growth. *Cancer Cell* **19** (2)**:** 257–272.

Quarles, L., Yohay, D., Lever, L., Caton, R and Wenstrup, R. 1992. Distinct proliferative and differentiated stages of murine MC3T3-E1 cells in culture: an in vitro model of osteoblast development. *Journal of bone and mineral research* **7** (6)**:**683-692.

Rabesandratana, H., Toutant, J., Reggio, H and Vidal, M. 1998. Decay-accelerating factor (CD55) and membrane inhibitor of reactive lysis (CD59) are released within exosomes during In vitro maturation of reticulocytes. *Blood* **97** (7):2573-2580.

Rabinowits, G., Gerçel-Taylor, C., Day, J., Taylor, D and Kloecker, G. 2009. Exosomal microRNA: a diagnostic marker for lung cancer. *Clinical Lung Cancer* **10** (1)**:**42-46.

Rajkumar, V., Howell, K., Csiszar, K., Denton, C., Black, C and Abraham, D. 2005. Shared expression of phenotypic markers in systemic sclerosis indicates a convergence of pericytes and fibroblasts to a myofibroblast lineage in fibrosis. *Arthritis Research & Therapy* **7** (5)**:**1113-1123.

Rao, S., Huynh, C., Proux-Gillardeaux, V., Galli, T and Andrews, N. 2004. Identification of SNAREs involved in synaptotagmin VII-regulated lysosomal exocytosis. *The Journal of Biological Chemistry* **279** (19)**:**20471-20479.

Raposo, G., Nijman, H., Stoorvogel, W., Leijendekker, R., Harding, C., Melief, C. and Geuze, H. 1996. B Lymphocytes secrete Antigen-presenting Vesicles. *Journal of Experimental Medicine* **183:**1161-1172.

Reinhart-King, C. 2008. Endothelial cell adhesion and migration. *Methods in Enzymology* **443:**45-64.

Reis, C., Egea, V., Karow, M., Kolb, H., Jochum, M and Neth, P. 2007. MMP-2, MT1-MMP, and TIMP-2 are essential for the invasive capacity of human mesenchymal stem cells: differential regulation by inflammatory cytokines. *Blood* **109** (9)**:**4055-4063.

Reiter, R., Gu, Z., Watabe, T., Thomas, G., Szigeti, K., Davis, E., Wahl, M. *et al.* 1998. Prostate stem cell antigen: a cell surface marker overexpressed in prostate cancer. *Proceeding of National Academy of Science.* **95** (4)**:**1735-1740.

Rekker, K., Saare, M., Roost, A., Kubo, A., Zarovni, N., Chiesi, A., Salumets, A and Peters, M. 2014. Comparison of serum exosome isolation methods for microRNA profiling. *Clinical Biochemistry* **47** (1-2):135-138.

Ren, C., Kumar, S., Chanda, D., Chen, J., Mountz, J and Ponnazhagan, S. 2008. Therapeutic potential of mesenchymal stem cells producing IFN-α in a mouse melanoma lung metastasis model. *Stem Cells* **26** (21)**:**2332–2338.

Ren, W., Liu, Y., Wan, S., Fei, C., Wang, W., Chen, Y., Zhang, Z. *et al.* 2014. BMP9 inhibits proliferation and metastasis of HER2-positive SK-BR-3 breast cancer cells through ERK1/2 and PI3K/AKT pathways. *PLoS One* **9** (5)**:**doi: 10.1371/journal.pone.0096816.

Ren, Y., Cao, B., Law, S., Xie, Y., Lee, P., Cheung, L., Chen, Y. *et al.* 2005. Hepatocyte growth factor promotes cancer cell migration and angiogenic factors expression: a prognostic marker of human esophageal squamous cell carcinomas. *Clin Cancer Res.* **11** (17)**:**6190-6197.

Rhim, Andrew D., Oberstein, Paul E., Thomas, Dafydd H., Mirek, Emily T., Palermo, Carmine F., Sastra, Stephen A., Dekleva, Erin N. *et al.* 2014. Stromal Elements Act to Restrain, Rather Than Support, Pancreatic Ductal Adenocarcinoma. *Cancer Cell* **25** (6)**:**735-747.

Riches, A., Campbell, E., Borger, E and Powis, S. 2014. Regulation of exosome release from mammary epithelial and breast cancer cells - a new regulatory pathway. *European Journal of Cancer.* **50** (5)**:**1025-1034.

Ricote, M., García-Tuñón, I., Bethencourt, F., Fraile, B., Paniagua, R and Royuela, M. 2004. Interleukin-1 (IL-1alpha and IL-1beta) and its receptors (IL-1RI, IL-1RII, and IL-1Ra) in prostate carcinoma. *Cancer.* **100** (7)**:**1388-1396.

Ringdén, O., Uzunel, M., Rasmusson, I., Remberger, M., Sundberg, B., Lönnies, H., Marschall, H. *et al.* 2006. Mesenchymal stem cells for treatment of therapy-resistant graft-versus-host disease. *Transplantation* **81** (10)**:**1390-1397.

Ritter, G., Cohen, L., Nice, E., Catimel, B., Burgess, A., Moritz, R., Ji, H., Heath, J., White, S., Welt, S., Old, L and Simpson, R. 1997. Characterization of posttranslational modifications of human A33 antigen, a novel palmitoylated surface glycoprotein of human gastrointestinal epithelium. *Biochemical and Biophysical Research Communication* **236** (3):682-686.

Roberts, A. 1999. TGF-beta signaling from receptors to the nucleus. *Microbes and infection* **1** (15)**:**1265-1273.

Roccaro, AM., Sacco, A., Maiso, P., Azab, AK., Tai, YT., Reagan, M., Azab, F., Flores, LM., Campigotto, F., Weller, E., Anderson, KC., Scadden, DT., Ghobrial, IM. 2013. BM mesenchymal stromal cell–derived exosomes facilitate multiple myeloma progression. *The Journal of Clinical Investigation* **123** (4):1542-1555.

Rollins, B., O'Connell, T., Bennett, G., Burton, L., Stiles, C and Rheinwald, J. 1989. Environment-dependent growth inhibition of human epidermal keratinocytes by recombinant human transforming growth factor-beta. *Journal of Cellular Physiology.* **139** (3)**:**455-462.

Ronnov-Jessen, L and Peterson, OW. 1996. A Function for Filamentous a-Smooth Muscle Actin: Retardation of Motility in Fibroblasts. *The Journal of Cell Biology* **134** (1)**:**67-80.

Ross, R., Pike, M., Coetzee, G., Reichardt, J., Yu, M., Feigelson, H., Stanczyk, F. *et al.* 1998. Androgen metabolism and prostate cancer: establishing a model of genetic susceptibility. *Cancer Research* **58** (20)**:**4497-4504.

Rosu-Myles, M., McCully, J., Fair, J., Mehic, J., Menendez, P., Rodriguez, R and Westwood, C. 2013. The globoseries glycosphingolipid SSEA-4 is a marker of bone marrow-derived clonal multipotent stromal cells in vitro and in vivo. *Stem Cells Development.* **22** (9)**:**1387-1397.

Russell, K., Tucker, H., Bunnell, B., Andreeff, M., Schober, W., Gaynor, A., Strickler, K. *et al.* 2013. Cell-surface expression of neuron-glial antigen 2 (NG2) and melanoma cell adhesion molecule (CD146) in heterogeneous cultures of marrow-derived mesenchymal stem cells. *Tissue Engineering Part A.* **19:**2253-2266.

Safaei, R., Larson, B., Cheng, T., Gibson, M., Otani, S., Naerdemann, W. and Howell, S. 2005. Abnormal lysosomal trafficking and enhanced exosomal export of cisplatin in drug-resistant human ovarian carcinoma cells. *Molecular Cancer Therapetics* **4** (10)**:**1595-1604.

Saharinen, J., Taipale, J and Keski-Oja, J. 1996. Association of the small latent transforming growth factor-beta with an eight cysteine repeat of its binding protein LTBP-1. *EMBO J* **15** (2)**:**245-253.

Sakr, W. 1999. Prostatic intraepithelial neoplasia: a marker for high-risk groups and a potential target for chemoprevention. *European Urology.* **25** (5-6)**:**474-478.

Sakr, W., Grignon, D., Crissman, J., Heilbrun, L., Cassin, B., Pontes, J and Haas, G. 1994. High grade prostatic intraepithelial neoplasia (HGPIN) and prostatic adenocarcinoma between the ages of 20-69: an autopsy study of 249 cases. *In Vivo* **8** (3)**:**439-443.

Sato, K., Ozaki, K., Oh, I., Meguro, A., Hatanaka, K., Nagai, T., Muroi, K. *et al.* 2007. Nitric oxide plays a critical role in suppression of T-cell proliferation by mesenchymal stem cells. *Blood* **109** (1)**:**228-234.

Savina, A., Fader, C., Damiani, M and Colombo, M. 2005. Rab11 promotes docking and fusion of multivesicular bodies in a calcium-dependent manner. *Traffic* **6** (2)**:**131-143.

Savina, A., Furlán, M., Vidal, M.a., Colombo, M., 2003. Exosome release is regulated by a calcium-dependent mechanism in K562 cells. The Journal of Biological Chemistry 248, 20083-20090.

Schäfer, M. and Werner, S. 2008. Cancer as an overhealing wound: an old hypothesis revisited. *Nature Reviews of Molecular Cell Biology.* **9** (8)**:**628-638.

Schmidt, A., Ladage, D., Steingen, C., Brixius, K., Schinkothe, T., Klinz, F., Schwinger, R. *et al.* 2006. Mesenchymal stem cells transmigrate over the endothelial barrier. *European Journal of Cell Biology.* **85**: 1179-1188

Schmitt, B., Bennett, C., Seidenfeld, J., Samson, D and Wilt, T. 2000. Maximal androgen blockade for advanced prostate cancer. . *Cochrane Database of Systematic Reviews* **2**.

Seo, S., Kim, K., Park, S., Suh, Y., Kim, S., Jeun, S and Sung, Y. 2011. The effects of mesenchymal stem cells injected via different routes on modified IL-12-mediated antitumor activity. *Gene Therapy.* **18** (5)**:**488-495.

Serpa Neto, A., Tobias-Machado, M., Kaliks, R., Wroclawski, M., Pompeo, A and Del Giglio, A. 2011. Ten years of docetaxel-based therapies in prostate adenocarcinoma: a systematic review and meta-analysis of 2244 patients in 12 randomized clinical trials. *Clinical genitourinary cancer* **9** (2)**:**115-123.

Shangguan, L., Ti, X., Krause, U., Hai, B., Zhao, Y., Yang, Z and Liu, F. 2012. Inhibition of TGF-β/Smad signaling by BAMBI blocks differentiation of human mesenchymal stem cells to carcinoma-associated fibroblasts and abolishes their protumor effects. *Stem Cells*. **30** (12):2810-2819.

Shapiro, S., Fliszar, C., Broekelmann, T., Mecham, R., Senior, R and Welgus, H. 1995. Activation of the 92-kDa gelatinase by stromelysin and 4-aminophenylmercuric acetate. Differential processing and stabilization of the carboxyl-terminal domain by tissue inhibitor of metalloproteinases (TIMP). *Journal of Biological Chemistry.* **270** (11)**:**6351-6356.

Sharma, S., Rasool, H., Palanisamy, V., Mathisen, C., Schmidt, M., Wong, D. and Gimzewski, J. 2010. Structural-mechanical characterization of nanoparticle exosomes in human saliva, using correlative AFM, FESEM, and force spectroscopy. *ACS Nano* **4** (4)**:**1921-1926.

Sheldon, H., Heikamp, E., Turley, H., Dragovic, R., Thomas, P., Oon, CE., Leek, R. *et al.* 2010. New mechanism for Notch signaling to endothelium at a distance by Delta-like 4 incorporation into exosomes. *Blood* **116** (13)**:**2385-2394.

Shi, M., Zhu, J., Wang, R., Chen, X., Mi, L., Walz, T. and Springer, T. 2011. Latent TGF-β structure and activation. *Nature* **474** (7351)**:**343-349.

Shin, N., Jeong, E., Choi, C., Moon, H., Kwon, C., Chu, I., Kim, G. *et al.* 2012. Overexpression of Snail is associated with lymph node metastasis and poor prognosis in patients with gastric cancer. *BMC Cancer* **12** (521)**:**doi: 10.1186/1471-2407-1112-1521.

Shinagawa K, Kitadai Y, Tanaka M, Sumida T, Kodama M, Higashi Y, Tanaka S *et al.* 2010. Mesenchymal stem cells enhance growth and metastasis of colon cancer. *International Journal of Cancer* **127** (10)**:**2323-2333.

Shojaei, F., Lee, J., Simmons, B., Wong, A., Esparza, C., Plumlee, P., Feng, J. *et al.* 2010. HGF/c-Met acts as an alternative angiogenic pathway in sunitinib-resistant tumors. *Cancer Research* **70** (24)**:**10090-10100.

Shore, N., Abrahamsson, P., Anderson, J., Crawford, E and Lange, P. 2013. New considerations for ADT in advanced prostate cancer and the emerging role of GnRH antagonists. *Prostate Cancer Prostatic Diseases* **16** (1)**:**7–15.

Simpson, R., Jensen, S and Lim, J. 2008. Proteomic profiling of exosomes: current perspectives. *Proteomics* **8** (22):4083-4099.7

Singer, I., Kawka, D., Kazazis, D and Clark, R. 1984. In vivo co-distribution of fibronectin and actin fibers in granulation tissue: immunofluorescence and electron microscope studies of the fibronexus at the myofibroblast surface. *The Journal of Cell Biology* **98** (6)**:**2091-2106.

Singh, P., Smith, V., Karakousis, P and Schorey, J. 2012. Exosomes isolated from mycobacteria-infected mice or cultured macrophages can recruit and activate immune cells in vitro and in vivo. *Journal of Immunology* **189** (2):777-785.

Skog, J., Wurdinger, T., van Rijn, S., Meijer, D. H., Gainche, L., Curry, W. T., Carter, B. S. *et al.* 2008. Glioblastoma microvesicles transport RNA and proteins that promote tumour growth and provide diagnostic biomarkers. *Nature Cell Biology* **10** (12)**:**1470-1476.

Slavin, S., Yeh, C., Da, J., Yu, S., Miyamoto, H., Messing, E., Guancial, E. *et al.* 2014. Estrogen receptor α in cancer-associated fibroblasts suppresses prostate cancer invasion via modulation of thrombospondin 2 and matrix metalloproteinase 3. *Carcinogenesis* **35** (6)**:**1301-1309.

Sobral, L., Bufalino, A., Lopes, M., Graner, E., Salo, T and Coletta, R. 2011. Myofibroblasts in the stroma of oral cancer promote tumorigenesis via secretion of activin A. *Oral Oncology.* **47** (9)**:**840-846.

Sodek, K., Ringuette, M and Brown, T. 2009. Compact spheroid formation by ovarian cancer cells is associated with contractile behavior and an invasive phenotype. *International Journal of Cancer* **124** (9):2060-2070.

Sokolova, V., Ludwig, A., Hornung, S., Rotan, O., Horn, P., Epple, M. and Giebel, B. 2011. Characterisation of exosomes derived from human cells by nanoparticle tracking analysis and scanning electron microscopy. *Colloids and surfaces* **87** (9)**:**146-150.

Solchaga, L.A., Penick, K.J., Welter, J.F. 2011. Chondrogenic Differentiation of Bone Marrow-Derived Mesenchymal Stem Cells: Tips and Tricks. *Mesenchymal Stem Cell Assays and Applications*. **698**: 253-278.

Song, J., Aswad, R., Kanaan, R., Rico, M., Owen, T., Barbe, M., Safadi, F. *et al.* 2007. Connective tissue growth factor (CTGF) acts as a downstream mediator of TGF-beta1 to induce mesenchymal cell condensation. *Journal of Cellular Physiology* **210** (2)**:**398-410.

Soo, C., Song, Y., Zheng, Y., Campbell, E., Riches, A., Gunn-Moore, F and Powis, S. 2012. Nanoparticle tracking analysis monitors microvesicle and exosome secretion from immune cells. *Immunology* **136** (2):192-197.

Soucek, K., Kamaid, A., Phung, A., Kubala, L., Bulinski, J., Harper, R and Eiserich, J. 2006. Normal and prostate cancer cells display distinct molecular profiles of alpha-tubulin posttranslational modifications. *Prostate.* **66** (9)**:**954-965.

Spaeth, E., Labaff, A., Toole, B., Klopp, A., Andreeff, M and Marini, F. 2013. Mesenchymal CD44 expression contributes to the acquisition of an activated fibroblast phenotype via TWIST activation in the tumor microenvironment. *Cancer Research* **73** (17)**:**5347-5359.

Spaggiari, G., Abdelrazik, H., Becchetti, F and Moretta, L. 2009. MSCs inhibit monocyte-derived DC maturation and function by selectively interfering with the generation of immature DCs: central role of MSC-derived prostaglandin E2. *Blood* **113** (26)**:**6576-6583.

Stanford, J., Stephenson, R., Coyle, L., Kosary, C., Cerhan, J., Correa, R., Eley, J. *et al.* 1999. Prostate Cancer Trends 1973-1995, SEER Program. *National Cancer Institute*

Steiner, M and Barrack, E. 1992. Transforming growth factor-beta 1 overproduction in prostate cancer: effects on growth in vivo and in vitro. *Molecular Endocrinology.* **6** (1)**:**15-25.

Steingen, C., Brenig, F., Baumgartner, L., Schmidt, J., Schmidt, A and Bloch, W. 2008. Characterization of key mechanisms in transmigration and invasion of mesenchymal stem cells. *Journal of Molecular and Cellular Cardiology.* **44:**1072–1084.

Sternlicht, M and Werb, Z. 2001. How matrix metalloproteinases regulate cell behavior. *Annual Reviews of Cell and Developmental Biology* **17:**463-516.

Sternlicht, MD., Lochter, A., Sympson, CJ., Huey, B., Rougier, JP., Gray, JW., Pinkel, D. *et al.* 1999. The Stromal Proteinase MMP3/Stromelysin-1 Promotes Mammary Carcinogenesis. *Cell* **98** (2)**:**137-146.

Strauss, K., Goebel, C., Runz, H., Möbius, W., Weiss, S., Feussner, I., Simons, M and Schneider, A. 2010. Exosome secretion ameliorates lysosomal storage of cholesterol in Niemann-Pick type C disease. *The Journal of Biological Chemistry* **285** (34):26279-26288.

Studeny, M., Marini, F., Champlin, R., Zompetta, C., Fidler, I and Andreeff, M. 2002. Bone Marrow-derived Mesenchymal Stem Cells as Vehicles for Interferon-Delivery into Tumors. *Cancer Research* **62**.

Stuffers, S., Sem Wegner, C., Stenmark, H and Brech, A. 2009. Multivesicular endosome biogenesis in the absence of ESCRTs. *Traffic* **10** (7):925-937.

Subra, C., Laulagnier, K., Perret, B and Record, M. 2007. Exosome lipidomics unravels lipid sorting at the level of multivesicular bodies. *Biochimie* **89** (2):205-212.

Sun, Y., Niu, J and Huang, J. 2009. Neuroendocrine differentiation in prostate cancer. *American Journal of Translational Research* **1** (2)**:**148-162.

Surowiak, P., Murawa, D., Materna, V., Maciejczyk, A., Pudelko, M., Ciesla, S., Breborowicz, J., Murawa, P., Zabel, M., Dietel, M.a., Lage, H. 2007. Occurence of stromal myofibroblasts in the invasive ductal breast cancer tissue is an unfavourable prognostic factor. *Anticancer Research* **27** (4): 2917-2924.

Surowiak, P., Suchocki, S., Györffy, B., Gansukh, T., Wojnar, A., Maciejczyk, A., Pudełko, M. *et al.* 2006. Stromal myofibroblasts in breast cancer: relations between their occurrence, tumor grade and expression of some tumour markers. *Folio Histochemica et Cytobiologica* **44** (2)**:**111-116.

Suzuki, K., Enghild, J., Morodomi, T., Salvesen, G and Nagase, H. 1990. Mechanisms of activation of tissue procollagenase by matrix metalloproteinase 3 (stromelysin). *Biochemistry* **29** (44)**:**10261-10270.

Syvaranta, S., Helske, S., Laine, M., Lappalainen, J., Kupari, M., Mayranpaa, MI., Lindstedt, KA *et al.* 2010. Vascular Endothelial Growth Factor–Secreting Mast Cells and Myofibroblasts. *Arteriosclerosis, Thrombosis, and Vascular Biology* **30** (6)**:**1220-1227.

Szot, W., Kostkiewicz, M., Zając, J., Owoc, A and Bojar, I. 2014. Prostate cancer in patients from rural and suburban areas--PSA value, Gleason score and presence of metastases in bone scan. *Annals of agricultural and environmental medicine* **21** (4)**:**888-892.

Taeb, J., Asgari, M., Abolhasani, M., Farajollahi, M and Madjd, Z. 2014. Expression of prostate stem cell antigen (PSCA) in prostate cancer: a tissue microarray study of Iranian patients. *Pathology and Research Practice.* **210** (18-23).

Tahara, E., Ito, H., Taniyama, K., Yokozaki, H and Hata, J. 1984. Alpha 1-antitrypsin, alpha 1-antichymotrypsin, and alpha 2-macroglobulin in human gastric carcinomas: a retrospective immunohistochemical study. *Human Pathology* **15** (10)**:**957-964.

Tai, S., Sun, Y., Squires, J., Zhang, H., Oh, W., Liang, C and Huang, J. 2011. PC3 is a cell line characteristic of prostatic small cell carcinoma. *Prostate*. **71** (15): 1668-1679.

Takahashi, Y., Bucana, C., Akagi, Y., Liu, W., Cleary, K., Mai, M and Ellis, L. 1998. Significance of platelet-derived endothelial cell growth factor in the angiogenesis of human gastric cancer. *Clinical Cancer Research* **4** (2)**:**429-434.

Takahashi, Y., Cleary, K., Mai, M., Kitadai, Y., Bucana, C and Ellis, L. 1996. Significance of vessel count and vascular endothelial growth factor and its receptor (KDR) in intestinal-type gastric cancer. *Clinical Cancer Research* **2** (10)**:**1679-1684.

Takahashi, Y., Kitadai, Y., Bucana, C., Cleary, K and Ellis, L. 1995. Expression of vascular endothelial growth factor and its receptor, KDR, correlates with vascularity, metastasis, and proliferation of human colon cancer. *Cancer Research* **55** (18)**:**3964-3968.

Tanigawa, N., Amaya, H., Matsumura, M., Shimomatsuya, T., Horiuchi, T., Muraoka, R and Iki, M. 1996. Extent of tumor vascularization correlates with prognosis and hematogenous metastasis in gastric carcinomas. *Cancer Research* **56** (11)**:**2671-2676.

Tanimoto, H., Yoshida, K., Yokozaki, H., Yasui, W., Nakayama, H., Ito, H., Ohama, K. *et al.* 1991. Expression of basic fibroblast growth factor in human gastric carcinomas. *Virchows Archiv. B, Cell Pathology including molecular pathology* **61** (4)**:**263-267.

Tarrant, J., Robb, L., van Spriel, A and Wright, M. 2003. Tetraspanins: molecular organisers of the leukocyte surface. *Trends in Immunology*. **24** (11):610-617.

Tauro, B., Greening, D., Mathias, R., Ji, H., Mathivanan, S., Scott, A and Simpson, R. 2012. Comparison of ultracentrifugation, density gradient separation, and immunoaffinity capture methods for isolating human colon cancer cell line LIM1863-derived exosomes. *Methods* **56** (12):293-304.

Taylor, D and Gercel-Taylor, C. 2008. MicroRNA signatures of tumor-derived exosomes as diagnostic biomarkers of ovarian cancer. *Gynecology Oncology* **110** (1):1-2.

Taylor, D., Zacharias, W and Gercel-Taylor, C.,2011. Exosome isolation for proteomic analyses and RNA profiling. *Methods in Molecular Biology* **728**: 235-246

Teo, G., Ankrum, J., Martinelli, R., Boetto, S., Simms, K., Sciuto, T., Dvorak, A. *et al.* 2012. Mesenchymal stem cells transmigrate between and directly through tumor necrosis factor-α-activated endothelial cells via both leukocyte-like and novel mechanisms. *Stem Cells* **30** (11)**:**2472-2486.

Thannickal, V., Lee, D., White, E., Zongbin, C., Larios, J., Chacon, R., Horowitz, J. *et al.* 2003. Myofibroblast Differentiation by Transforming Growth Factor- 1 Is Dependent on Cell Adhesion and Integrin Signaling via Focal Adhesion Kinase*. *The Journal of Biological Chemistry* **278** (13)**:**2384–12389.

Théry, C., Amigorena, S., Raposo, G. and Clayton, A. 2006. Isolation and characterization of exosomes from cell culture supernatants and biological fluids. *Current Protocols in Cell Biology* **3**.

Théry, C., Boussac, M., Veron, P., Ricciardi_Castagnoli, P., Raposo, G., Garin, J. and Amigorena, S. 2001. Proteomic analysis of dendritic cell-derived exosomes: a secreted subcellular compartment distinct from apoptotic vesicles. *Journal of Immunology* **166** (12)**:**7309-7318.

Théry, C., Regnault, A., Garin, J., Wolfers, J., Zitvogel, L., Ricciardi-Castagnoli, P., Raposo, G. *et al.* 1999. Molecular Characterisation of Dendritic Cell-derived exosomes: Selective Accumulation of the Heat Shock Protein hsc73. *Journal of Cell Biology* **147** (3)**:**599-610.

Théry, C., Zitvogel, L., Amigorena, S. 2002. Exosomes: composition, biogenesis and function. *Nature Reviews Immunology* **2** (8):569-579.

Thompson, C., Purushothaman, A., Ramani, V., Vlodavsky, I.a., Sanderson, R., 2013. Heparanase regulates secretion, composition, and function of tumor cell-derived exosomes. *The Journal of Biological Chemistry* **288** (14):10093-10099.

Thompson, I.M., Pauler, D.K., Goodman, P.J., Tangen, C.M., Lucia, M.S., Parnes, H.L., Minasian, L.M., Ford, L.G., Lippman, S.M., Crawford, E.D., Crowley, J.J., Coltman, C.A. 2004. Prevalence of Prostate Cancer among Men with a Prostate-Specific Antigen Level ≤4.0 ng per Milliliter. *New England Journal of Medicine* **350** (22): 2239-2246.

Tipton, J., McDaniel, R., Barbour, L., Johnston, M., Kayne, M., LeRoy, P and Ripple, M. 2007. Putting evidence into practice: evidence-based interventions to prevent, manage, and treat chemotherapy-induced nausea and vomiting. *Clinical journal of oncology nursing* **11** (1)**:**69-78.

Tomas, D., Spajic, B., Milosevic, M., Demirovic, A., Marusic, Z., Kruslin, B., 2010. Intensity of stromal changes predicts biochemical recurrence-free survival in prostatic carcinoma. *Scandinavian Journal of Urology and Nephrology* **44** (5): 284-290.

Tomasek, J., Gabbiani, G., Hinz, B., Chaponnier, C and Brown, R. 2002. Myofibroblasts and mechano-regulation of connective tissue remodelling. *Nature Reviews of Molecular Cell Biology* **3:**349-363.

Tomita, N., Morishita, R., Taniyama, Y., Koike, H., Aoki, M., Shimizu, H., Matsumoto, K. *et al.* 2003. Angiogenic property of hepatocyte growth factor is dependent on upregulation of essential transcription factor for angiogenesis, ets-1. *Circulation* **107** (10)**:**1411-1417.

Tormin, A., Li, O., Brune, J., Walsh, S., Schütz, B., Ehinger, M., Ditzel, N. *et al.* 2011. CD146 expression on primary nonhematopoietic bone marrow stem cells is correlated with in situ localization. *Blood.* **117** (19)**:**5067-5077.

Trajkovic, K., Hsu, C., Chiantia, S., Rajendran, L., Wenzel, D., Wieland, F., Schwille, P., Brugger, B., Simons, M. 2008. Ceramide Triggers Budding of Exosome Vesicles into Multivesicular Endosomes. *Science* **319** (5867):1244-1247.

Tsujino, T., Seshimo, I., Yamamoto, H., Ngan, C., Ezumi, K., Takemasa, I., Ikeda, M., Sekimoto, M., Matsuura, N.a., Monden, M. 2007. Stromal myofibroblasts predict disease recurrence for colorectal cancer. *Clinical Cancer Research* **13** (7): 2082-2090.

Tuli R, Tuli S, Nandi S, Huang X, Manner PA, Hozack WJ, Danielson KG *et al.* 2003. Transforming growth factor-beta-mediated chondrogenesis of human mesenchymal progenitor cells involves N-cadherin and mitogen-activated protein kinase and Wnt signaling cross-talk. *The Journal of Biological Chemistry* **278** (42)**:**41227-41236.

Tuxhorn, JA., Ayala, GE., Smith, MJ., Smith, VC., Dang, TD. and Rowley, DR. 2002. Reactive Stroma in Human Prostate Cancer. *Clinical Cancer Research* **8** (9)**:**2912-2923.

Ueno, H., Jones, A., Wilkinson, K., Jass, J and Talbot, I. 2004. Histological categorisation of fibrotic cancer stroma in advanced rectal cancer. *Gut.* **53** (4)**:**581-586.

Umezu, T., Ohyashiki, K., Kuroda, M., Ohyashiki, J.H. 2013. Leukemia cell to endothelial cell communication via exosomal miRNAs. *Oncogene* **32** (22):2747-2755.

Underwood, T., Hayden, A., Derouet, M., Garcia, E., Noble, F., White, M., Thirdborough, S., Mead, A., Clemons, N., Mellone, M., Uzoho, C., Primrose, J., Blaydes, J and Thomas, G. 2015. Cancer-associated fibroblasts predict poor outcome and promote periostin-dependent invasion in oesophageal adenocarcinoma. *The Journal of Pathology* **235** (3): 466-477.

Valadi, H., Ekström, K., Bossios, A., Sjöstrand, M., Lee, JJ. and Lötvall, JO. 2007. Exosome-mediated transfer of mRNAs and microRNAs is a novel mechanism of genetic exchange between cells. *nature Cell Biology* **9:**654 - 659.

Valenti, R., Huber, V., Filipazzi, P., Pilla, L., Sovena, G., Villa, A., Corbelli, A., Fais, S., Parmiani, G., Rivoltini, L. 2006. Human Tumor-Released Microvesicles Promote the Differentiation of Myeloid Cells with Transforming Growth Factor-{beta}-Mediated Suppressive Activity on T Lymphocytes. *Cancer Research* **66** (18):9290-9298.

van Niel, G., Charrin, S., Simoes, S., Romao, M., Rochin, L., Saftig, P., Marks, M., Rubinstein, E and Raposo, G. 2011. The Tetraspanin CD63 Regulates ESCRT-Independent and -Dependent Endosomal Sorting during Melanogenesis. *Developmental Cell* **21** (4):708-721.

van Niel, G., Raposo, G., Candalh, C., Boussac, M., Hershberg, R., Cerf-Bensussan, N. and Heyman, M. 2001. Intestinal epithelial cells secrete exosome-like vesicles. *Gastroenterology* **121** (2)**:**337-349.

Vianello, F and Dazzi, F. 2008. Mesenchymal stem cells for graft-versus-host disease: a double edged sword? *Leukemia.* **22** (3)**:**463-465.

Vincent, F., Bonnin, P., Clemessy, M., Contrerès, J., Lamandé, N., Gasc, J., Vilar, J. *et al.* 2009. Angiotensinogen delays angiogenesis and tumor growth of hepatocarcinoma in transgenic mice. *Cancer Research* **69** (7)**:**2853-2860.

Vinci, M., Gowan, S., Boxall, F., Patterson, L., Zimmermann, M., Court, W., Lomas, C. *et al.* 2012. Advances in establishment and analysis of three-dimensional tumor spheroid-based functional assays for target validation and drug evaluation. *BMC Biology.* **10** (29)**:**doi: 10.1186/1741-7007-1110-1129.

Voronov, E., Shouval, D., Krelin, Y., Cagnano, E., Benharroch, D., Iwakura, Y., Dinarello, C *et al.* 2003. IL-1 is required for tumor invasiveness and angiogenesis. *Proceedings National Academy Science* **100** (5)**:**2645-2650.

Wakefield, L., Winokur, T., Hollands, R., Christopherson, K., Levinson, A and Sporn, M. 1990. Recombinant latent transforming growth factor beta 1 has a longer plasma half-life in rats than active transforming growth factor beta 1, and a different tissue distribution. *Journal Clinical Investigation.* **86** (6)**:**1976-1984.

Wang, CH., Cherng, WJ., Yang, NI., Kuo, LT., Hsu, CM., Yeh, HI., Lan, YJ., Yeh, CH and Stanford, WL., 2008. Late-outgrowth endothelial cells attenuate intimal hyperplasia contributed by mesenchymal stem cells after vascular injury. *Arteriosclerosis, Thrombosis, and Vascular Biology* **28** (1):54-60.

Wang, H., Cao, F., De, A., Cao, Y., Contag, C., Gambhir, S., Wu, J. *et al.* 2009. Trafficking mesenchymal stem cell engraftment and differentiation in tumor-bearing mice by bioluminescence imaging. *Stem Cells.* **27** (7)**:**1548-1558.

Wang, Y., Hayward, S., Cao, M., Thayer, K and Cunha, G. 2001. Cell differentiation lineage in the prostate. *Differentiation*. **68** (4-5), 270-279.

Webber, J. and Clayton, A. 2013. How pure are your vesicles? *Journal of Extracellular Vesicles* **2** (10).

Webber, J., Meran, S., Steadman, R. and Phillips, A. 2009. Hyaluronan orchestrates TGF-beta1 dependent maintenance of the myofibroblast phenotype. *Journal of Biological Chemistry* **284** (14)**:**9083-9092.

Webber, J., Steadman, R., Mason, MD., Tabi, Z. and Clayton, A. 2010. Cancer exosomes trigger fibroblast to myofibroblast differentiation. *Cancer Research* **70** (23)**:**9621-9630.

Webber, JP., Spary, LK., Sanders, AJ., Chowdhury, R., Jiang, WG., Steadman, R., Wymant, J. *et al.* 2014. Differentiation of tumour-promoting stromal myofibroblasts by cancer exosomes. *Oncogene* **10:** 290-302

Weidner, N., Semple, J., Welch, W and Folkman, J. 1991. Tumor angiogenesis and metastasis--correlation in invasive breast carcinoma. *The New England Journal of Medicine* **324** (1)**:**1-8.

Welton JL, Khanna S, Giles PJ, Brennan P, Brewis IA, Staffurth J, Mason MD *et al.* 2010. Proteomics analysis of bladder cancer exosomes. *Molecular & Cellular proteomics* **9** (6)**:**1324-1338.

Wipff, P and Hinz, B. 2008. Integrins and the activation of latent transforming growth factor beta1 - an intimate relationship. *European Journal of Cell Biology* **87** (8-9)**:**601-615.

Witty, J., Wright, J and Matrisian, L. 1995. Matrix metalloproteinases are expressed during ductal and alveolar mammary morphogenesis, and misregulation of stromelysin-1 in transgenic mice induces unscheduled alveolar development. *Molecular Biology Cell.* **6** (10)**:**1287-1303.

Wolfers, J., Lozier, A., Raposo, G., Regnault, A., Thery, C., Masurier, C., Flament, C. *et al.* 2001. Tumor-derived exosomes are a source of shared tumor rejection antigens for CTL cross-priming. *Nature Medicine* **7** (3)**:**297-303.

Wright, M., Moseley, G.a., van Spriel, A. 2004. Tetraspanin microdomains in immune cell signalling and malignant disease. *Tissue Antigens* **64** (5):533-542.

Wu, J., Lark, M., Chun, L and Eyre, D. 1991. Sites of stromelysin cleavage in collagen types II, IX, X, and XI of cartilage. *Journal of Biological Chemistry.* **266** (9)**:**5625-5628.

Wu, K., Chan, C., Tsai, C., Chang, Y., Sieber, M., Chiu, T., Ho, M. *et al.* 2011. Effective treatment of severe steroid-resistant acute graft-versus-host disease with umbilical cord-derived mesenchymal stem cells. *Transplantation.* **91** (12)**:**1412-1416.

Wu, Y., Chen, L., Scott, P and Tredget, E. 2007. Mesenchymal stem cells enhance wound healing through differentiation and angiogenesis. *Stem cells* **25** (10)**:**2648-2659.

Wubbolts, R., Leckie, R.S., Veenhuizen, P.T., Schwarzmann, G., Mobius, W., Hoernschemeyer, J., Slot, J.W., Geuze, H.J., Stoorvogel, W. 2003. Proteomic and biochemical analyses of human B cell-derived exosomes. Potential implications for their function and multivesicular body formation. *Journal of Biological Chemistry* **278** (13):10963-10972.

Xiang, X. Poliakov, A. Liu, C., Liu. Y,. Deng, ZB., Wang, J., Zhang, L., Grizzle, WE., Mobley, J and Zhang, HG. 2009. Induction of myeloid-derived suppressor cells by tumor exosomes. *International Journal of Cancer* **124** (11)**:**2621-2633.

Xiao, W., Zhang, Q., Jiang, F., Pins, M., Kozlowski, J and Wang, Z. 2003. Suppression of Prostate Tumor Growth by U19, a Novel Testosterone-regulated Apoptosis Inducer. *Cancer Research* **63:**4698.

Xie, Y., Chen, X and Wagner, T. 1997. A ribozyme-mediated, gene "knockdown" strategy for the identification of gene function in zebrafish. *Proceeding National Academy of Science.* **94** (25)**:**13777-13781.

Xue, D., Zhou, C., Shi, Y., Lu, H and He, X. 2015. MD-miniRNA could be a more accurate biomarker for prostate cancer screening compared with serum prostate-specific antigen level. *Tumour Biology* [Epub ahead of print].

Yamashita, M., Ogawa, T., Zhang, X., Hanamura, N., Kashikura, Y., Takamura, M., Yoneda, M. *et al.* 2012. Role of stromal myofibroblasts in invasive breast cancer: stromal expression of alpha-smooth muscle actin correlates with worse clinical outcome. *Breast Cancer* **19** (2)**:**170-176.

Yang, F., Tuxhorn, J., Ressler, S., McAlhany, S. J., Dang, T and Rowley, D. 2005. Stromal expression of connective tissue growth factor promotes angiogenesis and prostate cancer tumorigenesis. *Cancer Research* **65** (19)**:**8887-8895.

Yang, Z., Zhang, F., Ma, W., Chen, B., Zhou, F., Xu, Z., Zhang, Y. *et al.* 2010. A novel approach to transplanting bone marrow stem cells to repair human myocardial infarction: delivery via a noninfarct-relative artery. *Cardiovascular therapeutics* **28** (1)**:**doi:10.1111/j.1755-5922.2009.00116.

Yao, M., Zhang, W., Zhang, Q., Xing, L., Xu, A., Liu, Q. and Cui, B. 2011. Overexpression of MUC1 enhances proangiogenic activity of non-small-cell lung cancer cells through activation of Akt and extracellular signal-regulated kinase pathways. *Lung* **189** (6)**:**453-460.

Yip, K and Reed, J. 2008. Bcl-2 family proteins and cancer. *Oncogene* **27** (50)**:**6398-6406.

Yu, S., Liu, C., Su, K., Wang, J., Liu, Y., Zhang, L., Li, C. *et al.* 2007. Tumor Exosomes Inhibit Differentiation of Bone Marrow Dendritic Cells. *The Journal of Immunology* **178** (11)**:**6867-6875.

Yu, X., Harris, S and Levine, A. 2006. The regulation of exosome secretion: a novel function of the p53 protein. *Cancer Research* **66** (9)**:**4795-4801.

Zeegers, M., Jellema, A and Ostrer, H. 2003. Empiric risk of prostate carcinoma for relatives of patients with prostate carcinoma: a meta-analysis. *Cancer* **97** (8)**:**1894-1903.

Zelefsky, M. F., Z. Hunt, M. Yamada, Y. Marion, C. Ling, CC. Amols, H. Venkatraman, ES and Leibel, SA. 2002. High-dose intensity modulated radiation therapy for prostate cancer: early toxicity and biochemical outcome in 772 patients. *International Journal of Radiation Oncology Biology Physics.* **53** (5)**:**1111-1116.

Zelefsky, M. L., SA. Gaudin, PB. Kutcher, GJ. Fleshner, NE. Venkatramen, ES. Reuter, VE. Fair, WR. Ling, CC and Fuks, Z. 1998. Dose escalation with three-dimensional conformal radiation therapy affects the outcome in prostate cancer. *International Journal of Radiation Oncology Biology Physics.* **41** (3)**:**491-500.

Zhang, H., Kim, H., Liu, C., Yu, S., Wang, J., Grizzle, W., Kimberly, R and Barnes, S. 2007. Curcumin reverses breast tumor exosomes mediated immune suppression of NK cell tumor cytotoxicity. *Biochim Biophys Acta* **1773** (7):1116-1123.

Zhang, HG., Liu, C., Su, K., Yu, S., Zhang, L., Zhang, S., Wang, J. *et al.* 2006. A Membrane Form of TNF-{alpha} Presented by Exosomes Delays T Cell Activation-Induced Cell Death. *Journal of Immunology* **176** (12)**:**7385-7393.

Zheng, Y., Campbell, E., Lucocq, J., Riches, A and Powis, S. 2013. Monitoring the Rab27 associated exosome pathway using nanoparticle tracking analysis. *Experimental Cell Research* 319 (12):1706-1713.

Zhou, S. 2011. TGF-β regulates β-catenin signaling and osteoblast differentiation in human mesenchymal stem cells. *Journal of Cell Biochemistry.* **112** (6)**:**1651-1660.

Zhu, W., Huang, L., Li, Y., Zhang, X., Gu, J., Yan, Y., Xu, X., Wang, M., Qian, H., Xu, W., 2012. Exosomes derived from human bone marrow mesenchymal stem cells promote tumor growth in vivo. *Cancer Letters* **315** (1):28-37.

Zhu, W., Xu, W., Jiang, R., Qian, H., Chen, M., Hu, J., Cao, W. *et al.* 2006. Mesenchymal stem cells derived from bone marrow favor tumor cell growth in vivo. *Experimental Molecular Pathology.* **80** (3)**:**267-274.

Zigrino, P., Kuhn, I., Bauerle, T., Zamek, J., Fox, JW., Neumann, S., Licht, A. *et al.* 2009. Stromal Expression of MMP-13 Is Required for Melanoma Invasion and Metastasis. *Journal of Investigative Dermatology* **129** (11)**:**2686-2693.

Zitvogel, L., Regnault, A., Lozier, A., Wolfers, J., Filament, C., Tenza, D., Ricciardi-Castagnoli *et al.* 1998. Eradication of established murine tumours using a novel cell-free vaccine: dendritic cell-derived exosomes. *Nature Medicine* **4** (5)**:**594-600.

Zvereff, V., Wang, J., Shun, K., Lacoste, J and Chevrette, M. 2007. Colocalisation of CD9 and mortalin in CD9-induced mitotic catastrophe in human prostate cancer cells. *British Journal of Cancer.* **97** (7)**:**941-948.

Appendix: Peer-reviewed publications arising from the study